Treatment of mine water using a combination of coal fly ash and flocculants in a jet loop reactor system

Final Report

to the

Water Research Commission

by

L.F. Petrik[1], O.O. Fatoba[1], R. Missengue[1], R.M. Kalombe[2], S. Nyale[1,3], G. Madzivire[1,3]

[1] Environmental and Nano Sciences Research Group, Chemistry Department, University of the Western Cape, Bellville, South Africa

[2] Chemical Engineering Department, Cape Peninsula University of Technology

[3]Council for Geo Sciences

WRC Report No.2129/1/18

ISBN 978-0-6392-0040-8

April 2017

WATER RESEARCH COMMISSION

Obtainable from:

Water Research Commission
Private Bag X03
Gezina, 0031
Republic of South Africa

orders@wrc.org.za or download from www.wrc.org.za

Printed in the Republic of South Africa

EXECUTIVE SUMMARY

The generation of contaminated, sulphate-rich mine water and waste coal fly ash are undesired by-products in coal mining and coal-fired power stations respectively. Acid mine drainage (AMD) has been highlighted as a major problem in South Africa, especially where mines are abandoned and ownerless. AMD also prevents the closure of affected mines. Mining operations generate very acidic AMD, highly contaminated with iron, aluminium and sulphate. AMD will form spontaneously in the presence of air and water over the long term until all the pyrite in the associated geology is exhausted, which makes mine closure very difficult especially given stricter environmental protection legislation in South Africa. Many sources of contaminated mine waters may be less acidic, having lower concentrations of iron and aluminium (unlike AMD), but the waters may still be highly contaminated with calcium, magnesium, sodium and sulphate ions. The flows of AMD and sulphate-rich mine waters into South Africa's surface and ground water systems are causing long-term impairment to waterways and biodiversity. At the same time, significant environmental problems are also caused by the improper disposal of coal fly ash (FA) generated from coal-fired power plants.

Both coal FA and mine water are environmental liabilities. The need to remediate these problems has inspired the use of FA for the treatment of AMD. Several studies (see publication list below) have shown that when FA is used to treat AMD, 80–98% of sulphate ions and most other pollutants can be removed in one step. This study demonstrates the process at 1000 L scale.

SUMMARY OF PRIOR WORK

Extensive prior work has been carried out on the FA neutralisation process, showing the high-water quality that can be recovered and the stability of solid residues formed during neutralisation (WRC Research Report No.1242/1/05; WRC Research Report No.1546/1/07; SA Patent no.: ZA 2008/01062). A team at the University of the Western Cape has successfully demonstrated the utilisation of waste coal FA to treat mine water (acid or neutral mine drainage) using a jet loop reactor at an 80-litre pilot scale. Most of the contaminants were removed to acceptable levels in one simple procedure by contacting the AMD with FA in suitable ratios. The process produces water of sufficiently good quality for both agricultural and industrial applications, compliant with Department of Water and Sanitation standard guidelines for industrial and agricultural water (1996), category 4. This FA-AMD technology can be applied for the remediation of AMD resulting from coal or gold mining operations. For zero effluent during mining operations, it is necessary to prevent the formation of AMD; thus, it is necessary to fill the voids created by the mining operation, in which pyrite-bearing rock is exposed to air and water. The insoluble FA solid residue (SR) which remains after this primary treatment has been investigated as a suitable mine backfill material. Prior studies demonstrated that this SR develops strength and is suitable for filling the mine void to prevent the ingress of air and water and thus to seal off the pyrite from further reactions. The integrated FA-AMD process will lead to mines being able to achieve zero effluent discharge.

This treatment technology thus offers a cradle-to-cradle solution, since after active treatment of AMD with FA, the SR from the primary process can be placed back in the mine void from which it originated and thus stop

the generation of AMD. This FA-AMD technology is the only available technology to offer a means to treat and prevent formation of AMD. Hence, it is not an end-of-pipe technology but offers the possibility to treat the mine water and also prevent its future formation. This process is a serious contender for low-cost mine water treatment and recovery.

The efficiency of a patented jet loop reactor was studied at 80 L scale in industry-funded studies carried out by Madzivire and Petrik (2010 & 2011), and the jet loop reactor was shown to be a low-cost, efficient way of mixing FA and mine water slurry for rapid and effective neutralisation. Studies at 80 L capacity (Table A1) proved that the sulphate ion concentration could be reduced to less than 500 ppm both in neutral mine water collected from coal mines, and in highly contaminated acidic mine water (Madzivire, 2010).

Table A1: Physicochemical parameters of acid mine drainage and the product water produced after treatment with fly ash and $AlOH_3$ at 80 L scale, compared to the WHO limits for potable water

Parameter	Acid mine drainage	Treated water	Potable limit
pH	**2.65 ± 0.81**	**11.02**	6-9
EC	**2000 ± 27**	**1900**	700
sulphate	**2562.41 ± 6.85**	417.58 ± 4.93	500
Fe	**201.05 ± 0.55**	0.015 ± 0.001	0.1
Al	**26.63 ± 0.29**	0.071 ± 0.0002	0.15
Ca	**360.15 ± 4.25**	**209.85 ± 0.75**	32
Mg	**153 ± 0.7**	0.02 ± 0.003	30
Mn	**60.16 ± 0.17**	$9.6 \times 10^{-4} \pm 1 \times 10^{-4}$	0.05
Ni	2.11 ± 0.0043	$3.96 \times 10^{-3} \pm 2.9 \times 10^{-4}$	NV
Zn	1.93 ± 0.013	$4.99 \times 10^{-4} \pm 2.3 \times 10^{-4}$	0.5
Sr	0.45 ± 0.0034	23.75 ± 0.45	NV
Cu	0.28 ± 0.0033	$6.63 \times 10^{-5} \pm 6.63 \times 10^{-5}$	1
U	**0.28 ± 0.001**	$2.4 \times 10^{-4} \pm 2.98 \times 10^{-5}$	0.07
Li	$0.069 \pm 2.9 \times 10^{-4}$	1.34 ± 0.006	NV
Se	**0.061 ± 0.0023**	0.014 ± 0.001	0.04
Ba	$0.026 \pm 4.3 \times 10^{-4}$	0.082 ± 0.001	0.7
Cr	$0.023 \pm 2.9 \times 10^{-4}$	**0.12 ± 0.0062**	0.05
Pb	$7.5 \times 10^{-3} \pm 1.73 \times 10^{-5}$	$2.6 \times 10^{-4} \pm 2.82 \times 10^{-5}$	0.01
Cd	**$6.76 \times 10^{-3} \pm 1.22 \times 10^{-5}$**	$2.50 \times 10^{-5} \pm 5.09 \times 10^{-6}$	0.005
As	**$5.6 \times 10^{-3} \pm 2.49 \times 10^{-5}$**	**$1.4 \times 10^{-3} \pm 5.64 \times 10^{-5}$**	0.001
Be	$3.90 \times 10^{-3} \pm 4.17 \times 10^{-5}$	$8.31 \times 10^{-6} \pm 2.56 \times 10^{-6}$	0.012
Th	$1.8 \times 10^{-3} \pm 3.06 \times 10^{-5}$	$2.17 \times 10^{-6} \pm 1.86 \times 10^{-7}$	NV
V	$1.2 \times 10^{-2} \pm 7.6 \times 10^{-5}$	0.024 ± 0.0011	0.01
Mo	$5.3 \times 10^{-4} \pm 2.4 \times 10^{-5}$	**$0.16 \pm 3.7 \times 10^{-4}$**	0.07
B	$2.3 \times 10^{-3} \pm 4 \times 10^{-5}$	$0.0018 \pm 3 \times 10^{-5}$	2.4
Hg	$3.93 \times 10^{-5} \pm 1.18 \times 10^{-5}$	$4.65 \times 10^{-4} \pm 1.79 \times 10^{-5}$	0.001

All units are mg/L except that of EC (µS/cm) and pH. NV means no value mentioned in the WHO and DWAF guidelines for potable water.

A design for rapid mixing of FA/mine-water slurry with a jet loop reactor has shown that the energy input and mixing efficiency of the jet loop system is excellent compared to studies done with turbulators. The coal FA and jet loop reactor technology for AMD remediation was thus ready for scaling up to a 1000 L capacity.

OUTCOMES OF 1000 L STUDY

The primary aim of this research was to demonstrate 1000 L-scale pilot treatment of AMD and circumneutral mine water to produce cleaner water that is suitable for drinking, agricultural or industrial purposes. Building on the prior small-scale work, this study demonstrated the treatment of AMD with coal FA using a jet loop reactor system at 1000 L scale, which demonstrates the potential to use FA for remediation of AMD in an industrial and mining environment.

Coal FA was obtained from Matla coal power station in Mpumalanga province. Prior to treatment, the coal FA was characterised. The characterisation showed that the FA was Class F, with the sum of SiO_2, Fe_2O_3 and Al_2O_3 greater than 70%. Class F FA has pozzolanic properties, that is, it hardens when reacted with $Ca(OH)_2$ and water. The feedstock FA had a pH of 11.93, as revealed by analysis of the pore water extracted from the FA. Minor and trace element analysis of Matla FA showed that it contained about 34 elements. These elements included 16 (Ce, La, Nd, Y, Sc, Pr, Sm, Gd, Dy, Er, Eu, Ho, Tb, Tm and Lu) of the rare earth elements (REE), excluding promethium (Pm). The concentration of REE was found to be much higher than the normal concentration in the soil. Naturally occurring radionuclide materials (NORM) were also detected, which were U, Th, Ra, Pb and K. The gross alpha (3440 ± 210 $Bq.kg^{-1}$) and beta (1200 ± 20 $Bq.kg^{-1}$) radioactivity of the different radioisotopes in Matla coal FA could be attributed mainly to ^{238}U, ^{234}U, ^{235}U, ^{232}Th, ^{228}Th, ^{228}Ra, ^{226}Ra, ^{210}Pb, and ^{40}K. The activity concentration index for Matla coal FA was 2.96 mSv. This activity concentration index was three times the upper limit of 1 mSv. This means that coal FA from power stations in South Africa should be evaluated for its final activity concentration index prior to use in commercial applications. Matla FA was also found to contain trace levels of potentially toxic elements such as Cr, Pb, Ba, Cu, Zn, V, etc., that could leach into surface or ground water if the FA is subjected to acidification that may mobilise these elements.

Three mine waters were characterised, namely mine waters sourced from Rand Uranium mine, Matla coal mine and Lancaster dam. Lancaster dam water was sourced at site from a decant site in the Krugersdorp area. Rand Uranium water was collected from after the decant site but before the river enters the Hippo dam, in Randfontein, in the West Rand basin of the Witwatersrand Goldfields. These waters might vary but not that much since they come from the same geological area. The Matla mine water sample was collected from underground water pumping during coal mining at Matla coal mine in Mpumalanga. The google map in Figure A2 below shows the sites for Lancaster dam and Rand Uranium water.

Figure A2: Sampling sites for Lancaster dam and Rand Uranium mine.

The mine waters were all contaminated significantly with sulphates and numerous toxic elements but the water quality varied between sites and highlights the need to adjust the process to suit the requirements of the targeted water quality. For instance, the raw AMD from Lancaster gold mine dam had a pH of 2.26 and contained high sulphate levels but very low concentrations of Fe, Al and Mn. The mine waters were also contaminated with radionuclides such as U and Th.

As an example, Rand Uranium mine water was analysed for radioactivity using alpha and gamma spectrometry. Apart from the sulphate and other contaminants present in the raw mine water effluent, the results obtained indicated that the gross alpha and beta radioactivity of the mine water was 12 and 6 times more, respectively, than the required limit for potable water. Radioisotopes that contributed to the radioactivity of Rand Uranium mine water were; ^{238}U, ^{234}U, ^{230}Th, ^{226}Ra, ^{235}U, ^{227}Th, ^{229}Ra, ^{232}Th, ^{228}Th, and ^{224}Ra. The activities of radioisotopes that were greater than the allowed limit for potable water were ^{234}U, ^{235}U and ^{228Th}. Total U concentration in Rand Uranium mine water was about 256 µg/L. This was well above the allowed limit for total U concentration set by the WHO in 2011, which is 30 µg/L.

The Act2 program of the Geochemist's Workbench (GWB) software was used to calculate the aqueous species distribution and the saturation indices of the different minerals in Rand Uranium mine water and Matla mine water as well as any stable mineral phases that may form during precipitation of potentially toxic elements/ions. The GWB Act2 program predicted that if Matla mine water or Rand Uranium mine water were to be treated with coal FA, removal of the potentially toxic elements depended on the pH end point of the treatment process as well as the concentration of Ca ions in the mine water.

For example, the GWB Act2 program predicted that treatment of Rand Uranium mine water with coal FA could remove sulphate ions as alunite or gypsum. Removal of alunite and gypsum from Rand Uranium mine water was found to be $\log_a Ca^{2+}$ and/or pH dependent. If sulphate ions were to be removed in the form of alunite, the pH of the mixture would need to be maintained between 3.5 and 5 and $\log_a Ca^{2+}$ less than -1. If the sulphate ions were to be removed in the form of gypsum the $\log_a Ca^{2+}$ of the mixture would have to be increased to greater than -2.5. From the Act2 results, if Rand Uranium mine water was to be treated with Matla coal FA, it was predicted that U could precipitate in the form of uraninite (UO_2). The formation of UO_2 was found to be pH dependent if the $\log_a Ca^{2+}$ was less than -2.7. When $\log_a Ca^{2+}$ was less than -2.7, precipitation of UO_2 would occur when the pH of mine water was increased to greater than 3. If $\log_a Ca^{2+}$ of the mine water was to be increased from -2.7 to 0, the pH at which UO_2 could start precipitating would decrease from 3 to 2 as more Ca ions were added to the mixture. At a pH less than 3 and $\log_a Ca^{2+}$ less than about -0.3, U will exist as $U(SO_4)_2$ in solution. If $\log_a Ca^{2+}$ was increased to greater than about -0.3 and the pH kept below 3, U will exist as USO_4^{2+}, UOH^{3+} and $U(OH)_2^{2+}$. The Act2 program predicted that if Rand Uranium mine water was to be treated with Matla coal FA, Th could be removed as thorianite (ThO_2). The formation of ThO_2 was found to be pH dependent, when $\log_a Ca^{2+}$ was less than -2.3. When $\log_a Ca^{2+}$ was less than -2.3, ThO_2 could form if the pH of the mine water was increased to greater than 5. Increasing $\log_a Ca^{2+}$ from -2.3 to 0 would result in a decrease in the pH at which ThO_2 would precipitate from about 5 to about 4. Thus mineral formation is predicted to occur due to the pH and transient concentration gradients that evolve during jet loop mixing of mine water with FA which cause supersaturated conditions to arise for a limited period during which minerals precipitate that sequester the problem elements.

The information from the Act2 modelling can be used in deciding on the treatment technology and budgeting of the treatment process. It is advisable that scientists employ software packages such as GWB so that they can reduce the amount of time and the number of experiments they need to carry out during research and development of the treatment technology and remediation techniques at a particular mine.

In the 1000 L-scale process for the treatment of AMD with FA, the addition of lime and chemical flocculants was considered necessary because of the low Al and Fe content of the Lancaster dam AMD. Modelling showed that sulphate is removed through gypsum and ettringite mineral phase formation at a pH above 9–11. In cases where the mine waters were high in Fe and Al, the previous studies had shown that the FA on its own purified the AMD without additional lime or chemical flocculants through the formation of gypsum and oxyhydroxides. Since Lancaster dam AMD had low pH, low Fe and low Al but high sulphate content, it was deemed necessary to add lime to raise the pH above 11 and, at that pH, dosing of $Al(OH)_3$ was deemed necessary to precipitate sulphate in the form of ettringite.

An engineering design was prepared for the scaled-up (1000 L) jet loop pilot plant, and piping and instrumentation diagrams (P&ID) were developed. Construction of the scaled-up 1000 L pilot plant was successfully completed in Blackheath, Cape Town, thanks to Technology Innovation Agency (TIA) funding. Apart from electronic control software and hardware including automated control valves, the jet loop reactor system comprises only two moving parts, namely the slurry pump and a small impeller used to initiate blending upon the addition of FA or lime. The auxiliary parts are holding tanks and pipes.

In the 1000 L-scale pilot treatment of AMD, the application of basic engineering concepts such as mass and energy balance, and heat and mass transfer, was investigated and reported. A test run of the plant was performed and samples taken over the reaction time were analysed. In the test run, the inputs for the experiment consisted of 1000 L of raw AMD from Lancaster gold mine, 167 kg of Matla FA, 2.1 kg of lime and 3.6 kg of aluminium hydroxide. The 167 kg of FA was added while the AMD was circulating through the jet loop, and simultaneously the small impeller was activated to ensure initial blending. Following AMD and FA mixing, 2.1 kg of lime was added to the 1000 L AMD + FA mixture. The pH of the mixture was constantly monitored from the electronic display of the automated system for controlling and monitoring the AMD treatment process. When the pH was greater than 11, after 30 minutes and before 60 minutes, 3.6 kg of aluminium hydroxide was added to the AMD + fly ash + lime mixture. The subsequent AMD + FA + lime + Al $(OH)_3$ mixture was circulated through the jet loop for 150 minutes.

After the AMD had been treated, it was found that the concentration of most toxic elements was reduced to within target water quality range. Elements such as sulphate were reduced from 5680.33 mg/L to 87.27 mg/L. The pH of the mine water was raised from 2.26 to 8.8 and the electrical conductivity was reduced from 6880 µS/cm to 14 µS/cm. The slurry mixture was allowed to settle for an hour before the clear solution was decanted to another tank for carbonation. The concentration of the various elements in the water before and after treatment was determined using ICP-OES analytical technique (Table A3).

In the raw AMD, the concentration of sulphate, Al, Ca, Fe, Ta, Mg, Si, Na, Mn and Zn ions was 5680.33, 1862.51, 1694.55, 1377.74, 1013.41, 765.62, 482.22, 463.35, 224.44 and 154.59 mg/L respectively, while the

concentration of sulphate, Al, Ca, Fe, Ta, Mg, Si, Na and Mn ions in the treated AMD, after 180 minutes of treatment, was 87.27, 13.37, 242.77, 0.54, 54.60, 0.05, 16.60, 86.46 and 0.05 mg/L respectively. The mass transfer was determined to be the difference in concentration of the elements in the AMD and in the treated water, for example, sulphate concentration was reduced from 5680.33 mg/L to 87.27 mg/L and the difference was 5593 06 mg/L.

The composition of the raw intake AMD was compared with the treated water (prior to carbonation for pH correction and Ca removal) and with potable as well as irrigation standards published by the Department of Water and Sanitation, as shown in Table A3 below. The addition of $Al(OH)_3$ commenced after the 30 min sample was drawn.

Table A3: Composition of raw Lancaster dam AMD and treated AMD (treatment at 1000 L capacity, using 167 kg of Matla coal fly ash and 2.1 kg of lime up to 30 min; at 30 min, 3.6 kg of aluminium hydroxide was added and mixed up to 180 min)

Parameter	Raw AMD	Treated AMD						DWS Guidelines	
		30 min	60 min	90 min	120 min	150 min	180 min	Pot-able	Irrigat-ion
pH	2.26	10.1	9.9	9.9	9.7	10.5	8.8	6-9	6.5-8.4
EC (µS/cm)	6880.00	14	14	14	14	14	14		
Element (mg/L)	**Raw AMD**	**30 min**	**60 min**	**90 min**	**120 min**	**150 min**	**180 min**		
Sulphate	5680.33	92.77	90.99	85.01	92.28	83.37	87.27	0-200	
Al	1862.51	26.07	21.20	10.18	2.68	1.30	13.37	0-0.15	0-5
Ca	1694.55	305.13	250.56	228.48	253.02	248.77	242.77	0-32	
Fe	1377.74	1.38	0.43	0.77	0.11	0.08	0.54	0-0.1	0-5
Ta	1013.41	34.07	67.91	7.73	nd	30.66	54.60		
Mg	765.62	0.33	0.04	0.07	0.07	0.27	0.05	0-30	
Si	482.22	16.96	17.03	17.53	17.54	21.26	16.60		
Na	463.35	73.07	70.02	71.46	71.94	71.26	86.46	0-100	70.00
Mn	224.44	0.01	nd	0.01	0.06	0.07	0.05	0-0.05	0-0.2
Zn	154.59	0.57	0.08	0.18	nd	nd	nd	0-3	0-1
Ni	79.62	0.64	0.47	0.48	0.89	0.39	nd		0-0.20
K	51.27	3.49	nd	nd	nd	nd	nd	0-50	
Co	30.55	nd	nd	nd	nd	nd	nd		0-0.05
Cu	23.74	nd	nd	nd	nd	nd	nd	0-1	0-0.2
Pb	16.55	1.18	0.70	1.07	0.34	1.66	1.49	0-0.01	0-0.2
Ti	4.80	nd	nd	nd	nd	nd	nd	0-0.01	
Sr	3.43	4.90	4.08	6.33	7.52	9.04	7.16		
Cd	1.50	0.07	0.06	0.08	0.04	0.08	0.03	0-5	0-10
Cr	1.03	1.01	1.78	0.98	1.28	1.12	1.27	0-0.05	0-0.1
As	nd	0.36	0.48	1.41	0.11	0.93	0.55		0-0.1
Mo	nd	1.26	0.35	0.63	1.31	1.16	0.84		
Se	nd	nd	nd	nd	nd	0.80	nd	0-0.02	0-0.20
P	nd	1.39	1.16	0.36	0.46	0.01	0.66		
Li	nd	0.82	0.61	0.67	0.69	0.56	nd		0-2.5
Be	nd	0.00	nd	nd	nd	nd	nd		0-0.1
U	2.36	0.23	0.37	0.38	0.37	0.30	nd		
Th	0.23	0.01	nd	nd	nd	0.01	nd		

It is noteworthy that even after only 30 minutes of treatment with FA and lime, the sulphate level was reduced to 94 mg/L, prior to the addition of $Al(OH)_3$, and the concentration of most elements including U and Th in the treated AMD was already very significantly lower compared to the raw AMD. Thus $Al(OH)_3$ addition was not strictly necessary and lime addition could be minimised, depending upon the desired target water quality. Low traces of Sr (7.16 mg/L), As (0.55 mg/L) and Mo (0.84 mg/L) were the only elements that leached from the FA during treatment of AMD.

Table A4 shows the activity of the mine water before and after treatment.

Table A4: Activity of mine water before and after treatment (determined by gamma spectroscopy)

Sample	^{238}U	^{232}Th	^{40}K
	A (Bq/l)	**A (Bq/l)**	**A (Bq/l)**
AMD before treatment	33 ± 5	5 ± 3	32 ± 6
30 min treatment	6 ± 4	6 ± 5	31 ± 5
90 min treatment	10 ± 5	6 ± 3	35 ± 6
120 min treatment	11 ± 2	5 ± 4	35 ± 6
150 min treatment	5 ± 4	5 ± 4	29 ± 5
180 min treatment	4 ± 3	5 ± 2	18 ± 5

Uncertainties are at 1σ

The activity of the water after treatment, as tested by gamma spectroscopy, was found to be significantly lower than the raw water, even after 30 min, in the case of ^{238}U and ^{232}Th, but ^{40}K levels remained unchanged until 150 min. Hence the treatment with FA significantly reduced the activity of the treated water.

After separating the recovered water from the SR by gravity settling for one hour, CO_2 was sparged into the water for pH correction and to remove Ca as calcite. The carbonation step was stopped when the pH was brought to between 6 and 8, and the treated water was then recovered. At the end of the settling period of an hour, the calculated amount of treated water recovered was 720 L (72% of the initial raw AMD). The mass of SR recovered, after decanting the clear water after an hour settling, was found to be 479.02 kg, of which 64% was moisture content, The mass of the water was found to be 306.29 kg and the mass of the solids was found to be 172.33 kg. The SR could be pumped to a backfill placement as a slurry or paste, depending on the required pumping conditions, and then dewatered completely.

Separate pipe tests were performed in order to determine the slurry densities and pipe diameters most suited to pumping the partially dewatered slurry to the placement site. Previous trials with Lethabo ash showed that it was the intermediate range of particles, between 20 and 100 µm, that affected the rheological parameters most (Vadapalli et al., 2013). In this study, pseudo-shear data was obtained using 9 mm, 13 mm and 16 mm diameter pipe tests. Several concentrations of the slurry were prepared, and it was possible to obtain relative densities of 1.347 RD with this slurry. The slurries showed typical Bingham plastic behaviour. The yield stress for the maximum concentration was ~9 Pa. Laminar and turbulent flows were tested. The pressure drop per meter length was measured over a range of velocities from 0.2 to 5 m/s. The pressure drop in the 13.16 mm pipe did not exceed 4 kPa/m at approximately 2 m/s, after which turbulent flow ensued. At a velocity of approximately 5 m/s the pressure drop increased to ~20 kPa. In order to obtain the viscous properties of the slurries, the shear stresses were calculated at various pseudo-shear rates. The shear stresses increased for

each slurry with increasing density of the slurry. The viscous properties of slurries tested prior to CO_2 sparging were higher than those tested after CO_2 sparging for pH correction and Ca removal. The yield stresses ranged from 0.94 to 3.6 Pa.

The electrical power used during the 1000 L treatment for 180 min was 16.7 kW using an assumed flow rate which still needs to be determined; with the calculated energy evolved by the fluid and shaft work being 4.3 kw and 14.9 kw respectively. The supplied electrical power was only calculated for power supplied to the main pump, which was oversized. The temperature of the slurry increased over time due to friction caused by the velocity of the flow of slurry pumped through the jet loop orifices, which passively raised the temperature of the mixture of AMD+FA+lime+$Al(OH)_3$ from 25˚C to 80˚C without external heat input. Heat flux was equal to the difference between the energy of the shaft and that of the fluid, being equivalent to 10.6 kW of evolved heat, and this evolved heat may be recovered, thus making it possible to reduce the energy consumption considerably. Using the correct sized pump in future would also make the process more energy efficient as the pump was donated and oversized. Moreover, as the quality of the recovered water was excellent even after 30 min, it should be possible to run the pump for a much shorter period in future tests, saving a considerable amount of energy.

Regarding the environmental impact assessment licence, water use licence and waste licence, a consortium drawn from the coal mining industry, Eskom, academia and other relevant parties is currently in the process of clarifying the legislative requirements in order to obtain an exemption for specific waste management activities from the requirements of a waste management licence in terms of the National Environmental Management: Waste Act (NEM:WA GN R.634). The focus is currently on completing Regulation 9 requirements. The legal application is being made under Eskom's name although the focus is on industry-wide applications. Eskom was willing to do this for the benefit of the industry. Industry and key stakeholders have been requested to support the Eskom effort by providing information, knowledge, support and advice. The main aims are to demonstrate that the use of coal fly ash is safe for human health and the environment when used in specific exempted applications such as mine back-filling, brick and block making, road construction, and agricultural use. A detailed analysis of Regulation 9 requirements, the potential requirements in terms of the National Water Act (Act No. 36 of 1998), and the requirements in terms of SANS 10234 was performed. The preliminary motivation document was presented to the Department of Environmental Affairs (DEA) in April, 2016. Regulation 9(1) requirements are extensive in terms of the information to be provided. Currently, engagement with DEA on providing missing information is ongoing and Eskom and stakeholders will continue this engagement.

The treatment of AMD with FA at 1000 L pilot scale was successful, with 98.5% sulphate removal and water quality remediated to within Department of Water and Sanitation guidelines in one simple step, using jet loop reactor equipment with few moving parts. The treated water quality was suitable for agricultural and industrial purposes, or the water can be further treated to be make it potable by correcting its pH with CO_2 sparging which removes residual Ca in the form of calcite. The residual sodium and trace elements can be easily removed from the recovered water by ion-exchange resins or zeolite adsorption which would bring the recovered water to potable quality. This process circumvents the need for expensive membrane processes such as reverse osmosis. Based on the high quality of the treated water recovered after the process, it could

be concluded that the 1000 L scaled-up pilot plant process for AMD treatment is suited to low-cost AMD treatment. Many mining companies that are facing the problem of mine water disposal may find benefit using this FA-based treatment system to treat polluted mine water in one simple step. Residues produced from the process can be used to backfill mine voids in an integrated system which can prevent further AMD formation, offering a cradle-to-cradle solution. Void filling with SR will also prevent collapse of mine workings, prevent spontaneous combustion, enable better resource extraction and allow mine closure without long-term liabilities.

FUTURE WORK

The pilot plant has been reconfigured according to ESKOM safety specifications (See appendix for engineering drawings) and the reconfigured pilot plant will be transported to ESKOM Rocherville for further trials and demonstration using different sources of fly ash and minewaters.

PRIOR WORK BY THE AUTHORS

A summary of prior work is provided at the end of Ch 2.

For further reading, publications emanating from this and prior related research include:

SA Patent no.: ZA 2008/01062; Title: Fly Ash and Its Derivatives; Status: Grant date: 24/06/2009. Inventors: Leslie Felicia PETRIK, Wilson Mugera GITARI, Viswanath Ravi Kumar VADAPALLI, Olivier Christian Albert ETCHEBERS, Annabelle Anne Marie ELLENDT, Kelley Anne REYNOLDS, Damini SURENDER, Nicolette Rebecca HENDRICKS, Michael John KLINK, Vernon Sydwill SOMERSET, Colleen Lucie BURGERS

GITARI, W.M., PETRIK, L.F. AND MUSYOKA, N.M. (2016). Passive treatment of acid mine drainage in backfilled mine voids using coal fly ash-ordinary portland cement derivatives: Effluent chemistry and strength development. BOOK TITLE: *Coal Fly Ash Beneficiation - Treatment of Acid Mine Drainage with Coal Fly Ash.* InTECH Open Access

MADZIVIRE, G., GITARI, W.M., VADAPALLI, V.R.K. AND PETRIK, L.F. (2015). Jet loop reactor application for mine water treatment using fly ash, lime and aluminium hydroxide. *Int. J. Environ. Sci. Technology*, 12, pp. 173–182.

BÖKE, N., GRANT, D.B., NYALE, S. AND PETRIK, L.F. (2015). New synthesis method for the production of coal fly ash-based foamed geopolymers. *Construction & Building Materials*, 75, pp. 189–199. DOI: 10.1016/j.conbuildmat.2014.07.041.

MADZIVIRE, G., MALEKA, P.P., VADAPALLI, V.R.K., GITARI, W.M., LINDSAY, R., PETRIK, L.F. (2014). Fate of the naturally occurring radioactive materials during treatment of acid mine drainage with coal fly ash and aluminium hydroxide. *Journal of Environmental Management* 133, pp. 12–17. http://dx.doi.org/10.1016/j.jenvman.2013.11.041.

EZE, C.P., FATOBA, O., MADZIVIRE, G., OSTROVNAYA, T.M., PETRIK, L.F., FRONTASYEVA, M.V., NECHAEV, A.N. (2014). Elemental composition of fly ash: A comparative study using nuclear and related analytical techniques. *Chem Didact Ecol Metrol*, pp. 19–29.

MADZIVIRE, G., MALEKA, P., LINDSAY R., PETRIK. L.F. (2013). Radioactivity of mine water from a gold mine in South Africa, Water and Society II WIT eLibrary, WIT *Transactions on Ecology and the Environment*, 178, pp. 147–157.

GITARI, W.M., PETRIK, L.F., KEY, D.L., OKUJENI, C. (2013). Inorganic contaminants attenuation in acid mine drainage by fly ash and its derivatives: Column experiments. *International Journal of Environment and Pollution*, 51(1-2), pp. 32–56.

MUSYOKA, N.M., PETRIK, L.F., FATOBA, O.O., HUMS, E. (2013). Synthesis of zeolites from coal fly ash using mine waters. *Minerals Engineering*, 53, pp. 9–15. http://dx.doi.org/10.1016/j.mineng.2013.06.019.

VADAPALLI, V.R.K., FESTER, V., PETRIK, L., SLATTER. P. (2013). Effect of fly ash size fraction on the potential to neutralise acid mine drainage and rheological properties of sludge. *Desalination and Water Treatment*, pp. 6947–6955. DOI: 10.1080/19443994.2013.823355O

VADAPALLI, V.R.K., GITARI, M.W., PETRIK, L.F., ETCHEBERS, O., ELLENDT, A. (2012). Integrated acid mine drainage management using fly ash. *Journal of Environmental Science and Health*, Part A, 47(1), pp. 60-69.

MADZIVIRE, G., GITARI, W.M., VADAPALLI, V.R.K., OJUMU, T.V. AND PETRIK, L.F. (2011). Fate of sulphate removed during the treatment of circumneutral mine water and acid mine drainage with coal fly ash: Modelling and experimental approach; *Minerals Engineering*, 24, pp. 1467–1477.

MADZIVIRE, G., PETRIK, L.F., GITARI, W.M., OJUMU, T.V. AND BALFOUR, G. (2010). Application of coal fly ash to circumneutral mine waters for the removal of sulphates as gypsum and ettringite. Minerals Engineering. MINE3396. *Minerals Engineering*, 23, pp. 252–257.

MISHEER, N., MADZIVIRE, G., GITARI, W.M., OJUMU, T.V., BALFOUR, G. AND PETRIK, L.F. (2010). Removal of sulphates from South African mine water using coal fly ash. – In: Wolkersdorfer, Ch. & Freund, A. *Mine Water & Innovative Thinking*, pp. 151–155. Sydney, Nova Scotia (CBU Press).

GITARI, W. M., PETRIK, L.F., KEY, D.L. AND OKUJENI, C. (2010). Partitioning of major and trace inorganic contaminants in fly ash-acid mine drainage derived solid residues. *Int. J. Environ. Sci. Tech.*, 7(3), pp. 519–534.

GITARI, W.M., PETRIK, L. KEY, D., AND OKUJENI, C. (2010). Inorganic contaminants attenuation in acid mine drainage by fly ash and its derivatives: Column Experiments. – In: Wolkersdorfer, Ch. & Freund, A. *Mine Water & Innovative Thinking*, pp. 233–237. Sydney, Nova Scotia (CBU Press).

VADAPALLI, V.R.K., GITARI, W.M., ELLENDT, A., PETRIK, L.F. AND BALFOUR, G. (2010). Synthesis of zeolite-P from coal fly ash derivative and its utilisation in mine-water remediation. *South African Journal of Science*, 106(5/6), pp. 1-7. DOI: 10.4102/sajs.v106i5/6.231.

FESTER, V.G., SLATTER, P.T., VADAPALLI, V.R.K. and PETRIK, L. (2008). Use of fly ash to treat AMD before use in backfill operations, Paste 2008, International Seminar on Paste and Thickened Tailings, Kasane.

GITARI, W.M., PETRIK, L.F., ETCHEBERS, O., KEY, D.L., IWUOHA, E. AND OKUJENI, C. (2008). Utilization of fly ash for treatment of coal mines waste water: Solubility controls on major inorganic contaminants. *Fuel*, 87, pp. 2450–2462.

GITARI, W.M., PETRIK, L.F., ETCHEBERS, O., KEY, D.L., IWUOHA, E. AND OKUJENI, C. (2008). Passive neutralisation of acid mine drainage by fly ash and its derivatives: A column leaching study. *Fuel,* 87, pp. 1637–1650.

VADAPALLI, V.R.K., KLINK, M.J., ETCHEBERS, O., PETRIK, L.F. GITARI, W., WHITE, R.A., KEY D. AND IWUOHA, E. (2008). Neutralization of acid mine drainage using fly ash and strength development of the resulting solid residues. *South African Journal of Science*, 104, pp. 316–322.

COWAN, D.A., SHITANDI, A., VAN IJPEREN, C., KUHN, E., MUSARINGIMI, W. AND PETRIK, L.F. (2007). Impact of microbiology on fly ash-acid mine drainage co-disposal and remediation systems. WRC report No.:1549/1/07, ISBN: 978-1-77005-610-7

PETRIK, L.F., HENDRICKS, N., ELLENDT, A. AND BURGERS, C. (2007). Toxic element removal from water using zeolite adsorbents made from solid waste residues: 2007/02/01; WRC Research Report No.1546/1/07; ISBN No: 978-1-77005-464-6.

GITARI, M.W., PETRIK, L.F., ETCHEBERS, O., KEY, D.L., IWUOHA, E. AND OKUJENI, C. (2006). Treatment of acid mine drainage with fly ash: Removal of major contaminants and trace elements. *Journal of Environmental Science and Health-Part A*, A41(8), pp. 1729–47.

PETRIK, L.F., WHITE, R., KLINK, M., SOMERSET, V., KEY, D., BURGERS, C., IWUOHA, E. FEY, M.V. (2005). Utilization of fly ash for acid mine drainage remediation: 2005/01/07; WRC Research Report No.1242/1/05; ISBN No: 1-77005-316-6

SOMERSET, V., PETRIK, L. AND IWUOHA, E. (2005). Alkaline hydrothermal conversion of fly ash filtrates into zeolites 2: Utilization in wastewater treatment. *Journal of Environmental Science and Health*, 40 (8), pp. 1627–1636.

SOMERSET, V., PETRIK, L., KLINK, M., ETCHEBERS, O., WHITE, R., KEY, D. AND IWUOHA, E. (2005). Acid mine drainage transformation of fly ash into Zeolitic crystalline phases. *Fresenius Environmental Bulletin*, 14 (11), pp. 1074–1076.

SOMERSET, V.S. PETRIK, L., WHITE, R.A., KLINK, M.J. KEY, D. AND IWUOHA, E. (2004). The use of X-ray fluorescence (XRF) analysis in predicting the alkaline hydrothermal conversion of fly ash precipitates into zeolites. Talanta-special issue: Southern and Eastern Africa Network for Analytical Chemists, 64 (1), pp. 109–114.

TECHNICAL REPORTS:

PETRIK L.F., HENDRICKS N., ELLENDT A., BURGERS C. 2007. Toxic element removal from water using zeolite adsorbents made from solid residues. WRC Research Report No.1546/1/07 ISBN No:978-1-77005-464-6 - Published
http://www.wrc.org.za/Pages/DisplayItem.aspx?ItemID=3792&FromURL=%2fPages%2fKH_AdvancedSearch.aspx%3fdt%3d%26ms%3d%26d%3dToxic+element+removal+from+water+using+zeolite+adsorbents+made+from+solid+waste+residues%26start%3d1

PETRIK, L.F., BURGERS, C., GITARI, W., SURENDER, D., REYNOLDS, K., ELLENDT, A., ETCHEBERS, O., VADAPALLI V.R.K., KEY D., IWUOHA E.I. (2006). Stability and neutralisation capacity of potential mine backfill material formed by neutralisation of fly ash and acid mine drainage: WRC Research Report No.1458/1/06. 2006/12/01 . ISBN No: 1-77005-460-X– Published: http:// www.wrc.org.za/Pages/DisplayItem.aspx?ItemID=3791&FromURL=%2fPages%2fKH_AdvancedSearch.aspx%3fdt%3d%26ms%3d%26d%3dStability+and+neutralisation+capacity+of+potential+mine+backfill+material+formed+by+neutralisation+of+fly+ash+and+acid+mine+drainage%26start%3d1

PETRIK, L.F. (2007). Stability and neutralization capacity of potential mine backfill material formed by co-disposal of fly ash and acid mine drainage. COALTECH 2020 (Task 6.1.6): This is the same as K5/1458 above, but also published by Coaltech:
http://www.wrc.org.za/Pages/DisplayItem.aspx?ItemID=11296&FromURL=%2fPages%2fKH_AdvancedSearch.aspx%3fdt%3d%26ms%3d%26d%3dLarge+scale+stability+and+Neutralisation+capacity+of+Potential+mine+backfill+material+Formed+by+neutralisation+of+fly+ash+And+acid+mine+drainage%26start%3d1

PETRIK, L.F., MADZIVIRE, G. (2012). The role of flocculants and fly ash in sulphate removal from mine waters. ESKOM REPORT NO:RES/RR/11/34026</MR; ACTIVITY NO: PRJ08-00008300-3377. ORGANISATION: Eskom RD&T, contract no: 4600011734

PETRIK, L.F., BALFOUR, G., MADZIVIRE, G., NIEUWOUDT, O. (2010). Circumneutral mine water treatment. ESKOM Contract No. 4600011860

PETRIK, L.F. (2009). Utilisation of fly ash to neutralise and remediate acid mine drainage at a pilot scale demonstration unit, ESKOM Contract no: 4600011391

PETRIK, L.F., SURENDER, D. (2004–7): Development of a site specific co-disposal protocol for the neutralisation and amelioration of Arnot AMD and fly ash. The co-disposal and neutralisation of AMD with fly ash. Eskom Resources & Strategy-Research Development and Demonstration. ESKOM.Project No: R1263. RES/RR/03/21911, Eskom Contract numbers: 4600004797; 4600007902

ACKNOWLEDGEMENTS

The project team wishes to thank the following people for their contributions to the project.

Reference Group	Affiliation
Dr. J.E. Burgess	Water Research Commission (Chairperson)
Mrs. K. Slatter-Christie	Independent Consultant
Dr. C. Sheridan	University of the Witwatersrand
Dr. T. Harck	Solution [H+]
Mr. A. Wurster	Independent Consultant
Dr. M. Rodriguez Pascual	University of Cape Town
Scientific inputs	
Dr Peane Maleka	iThembaLABs
Dr Tunde Ojumu	Cape Peninsula University of Technology (CPUT)
Prof. Veruscha Fester	Cape Peninsula University of Technology (CPUT)

CONTENTS

LIST OF FIGURES

LIST OF TABLES

ACRONYMS & ABBREVIATIONS

AMD	Acid mine drainage
DEA	Department of Environmental Affairs
DWAF	Department of Water and Forestry
DWS	Department of Water and Sanitation
EC	Electrical conductivity
FA	Fly ash
GWB	Geochemist's Workbench
HMI	Human-machine interface
XRD	X-ray diffraction
XRF	X-ray fluorescence
ICP-OES	Inductively-coupled plasma-optical emission spectroscopy
IC	Ion chromatography
LA-ICP-MS	Laser ablation inductively-coupled plasma mass spectroscopy
NEM:WA	National Environmental Management: Waste Act
NMD	Neutral mine drainage
NWA	National Water Act
P&ID	Piping and instrumentation diagram
REE	Rare earth elements
SCADA	Supervisory control and data acquisition
SR	Solid residue
TWQR	Target water quality range
WHO	World Health Organization

CHAPTER 1: BACKGROUND

1.1 INTRODUCTION

Mine water and coal fly ash (FA) are waste materials produced by mines and coal power stations respectively. Mine water can be acidic, neutral or alkaline depending on the geological location of the mine (Lottermoser, 2007). Acid mine water, often termed acid mine drainage (AMD) is produced when the rock that was disturbed during mining contains more acid-producing minerals such as pyrite (FeS_2) than acid-neutralising minerals such as dolomite ($CaMg(CO_3)_2$) or calcite ($CaCO_3$). Mining exposes the FeS_2 to oxidation by oxygen in the presence of water resulting in the formation of sulphuric acid. The sulphuric acid generated can cause chemical weathering of the surrounding rocks, thereby causing the leaching of potentially toxic metals and radioactive elements into the water. Mine water from gold and uranium mines is usually acidic and may contain radioactive elements such as U (Winde, 2010). Neutral mine drainage (NMD) is produced when the rock that is disturbed during mining contains stoichiometrically equal proportions of acid-producing minerals and acid-neutralising minerals such as dolomite. Therefore, the acidity produced from the oxidation of FeS_2 is neutralized by the acid-neutralising minerals. AMD is mainly composed of Fe, Al and Mn cations and sulphate ions, while NMD contains Na, Ca, Mg, sulphate and carbonate ions.

In the Republic of South Africa, mining has been taking place for over 100 years and this has led to the creation of mine voids. The mine voids in the Witwatersrand Gold Fields, for example, are filling up at a rate of 0.59 m/day. As of November, 2010, the level of AMD was 510 m below the surface. At that rate, if decant prevention and management were not put into place, the water was predicted to reach the surface in March, 2013, resulting in AMD flowing in the streets of Johannesburg central business district and the popular tourist attraction, Gold Reef City (Coetzee et al., 2010). The problem of mine water in South Africa is not only confined to the Witwatersrand Gold Fields. It is also a huge problem in the Mpumalanga Coal Fields. Mine water containing high concentrations of Fe, Al, Mn and sulphate ions, from the Mpumalanga coal fields, is threatening the freshwater resources of the Vaal and Olifants River ecosystems. Due to the aforementioned problems, mine water in South Africa needs proper management. Some of the mine water management schemes proposed by the Acid Mine Drainage Inter-ministerial Committee, under the coordination of the Council for Geoscience of South Africa include: (1) Decant prevention and management (2) Controlling ingress of clean water (rainfall) into mine voids (3) Water quality management, (Coetzee et al., 2010). Decant prevention can be achieved by pumping the water out of the mine voids. The pumped water needs to be treated to remove potential toxic elements and sulphate ions before the water can be discharged into freshwater resources. Many treatment options are available to treat the contaminated mine water to the required standards for potable, industrial and agricultural purposes, but are too costly and unsustainable. Cheaper treatment technologies are continually being investigated.

Mine water usually comes from pumping underground water in order for miners to access the mine's minerals, but it can also leach from mine tailings. The composition of mine water differs from mine to mine

depending on the exploited geology. Types of mine water are classified according to their chemical composition. Mine water composition depends on the mined ore and the chemical additives used in the mineral and hydrometallurgical processing. This means that there is no typical composition of mine waters, and as a result, the classification of mine water based on its composition is very complex. A number of classification schemes for mine water have been proposed, using one or several water parameters (Lottermoser, 2007; Morin & Hutt, 1997). These include classification based on the major cations and anions; classification based on pH; and classification based on alkalinity vs acidity.

As mentioned earlier, mine water is mainly composed of Fe, Al, and Mn cations (for AMD) or Ca and Mg cations (for NMD), together with other potentially toxic elements depending on the geology that is mined. Sulphate is the major anion found in mine water and ranges from around 1 000 to 30 000 mg/L. Due to vast differences in the chemistry of mine waters and the variety of physical, chemical and biological methods to separate metals from mine water, a wide range of treatment technologies for mine water treatment exist. Treatment of mine drainage can be achieved through passive or active processes (Neculita et al., 2007).

Passive treatment schemes take advantage of naturally occurring geochemical and biological processes to improve the quality of the influent waters, with minimal operation and maintenance requirements. Passive treatments can be broadly classified as chemical or biological systems depending on the processes that occur to ameliorate the mine water (Neculita et al., 2007). Although passive treatment of mine water may be cheaper in the short term, it is limited by lack of space to set up a proper facility. Also, the quality of the product water is not guaranteed and may deteriorate over time.

Active treatment technologies improve water quality through processes which require the continuous input of artificial energy, biochemical or chemical reagents. Active treatment methods are recognised by the presence of a water treatment plant that is monitored by a skilled workforce who operate and maintain the equipment. Active treatment technologies are broadly classified as biological, chemical and membrane methods. Biological methods involve the use of sulphate-reducing bacteria (Johnson, 2000). Chemical treatment includes the precipitation of contaminants from mine water using chemicals such as lime/limestone, $BaCO_3$, BaS, $Ba(OH)_2$, $Mg(OH)_2$, $MgCO_3$ and $Al(OH)_3$ (Geldenhuys et al., 2001; Bosman, 1983, Smit, 1999; Adlem, 1997; Bosman et al., 1990). Membrane methods for the treatment of mine water include nano filtration, reverse osmosis and electrodialysis (Kentish & Stevens, 2001; Del Pino & Durham, 1999; Matsuura, 2001; Valerdi-Perez et al., 2001; Schoeman & Steyn, 2001). Mine water can also be treated using ion exchange (Kitchener, 1957).

The major advantage of active treatment is the capability to respond to any changes in mine water quality and quantity. This is because of the precise process control that is possible. Also, active treatment is a preferred technique to passive treatment if land availability is a limiting factor. The major disadvantages of the active treatment method are the brines and sludges that are produced as wastes, which are more expensive to handle and dispose of than the water purification process itself. Also, the continuous input of energy, reagents and the need of human resources to run and maintain the treatment plant makes active treatment expensive.

The choice of a suitable treatment technology depends on the mine water quality, the mine water quantity, the treated water quality, the storage options for any sludge produced and the cost of the treatment technique. In reality, there is no technical limit to the quality of the water which can be achieved using existing techniques; cost is the limiting factor. Therefore, the selection of treatment technique comes down to economic and environmental cost-benefit analysis. New, cheaper methods to remove contaminants from mine water are constantly sought. One method is the use of coal fly ash (FA) from coal power stations (Gitari et al., 2008). The advantage of this method is that FA is a waste material from coal combustion found close to coal mines. This means that FA treatment of mine water can be sustainable since coal FA is a waste material. South Africa produces about 80% of its electricity from coal and generates large amounts of coal FA. Disposing of FA has proved to be an environmental concern, and therefore recycling of coal FA for mine drainage treatment is important to achieve zero effluent discharge.

Treatment of AMD and NMD with coal FA was found to remove Fe, Al and Mn at pH 9. Sulphate ions were found to be removed to between 2000-3000 mg/L when AMD was treated with coal FA to pH 9 (Gitari et al., 2008, Surender, 2009). On the other hand, treatment of NMD with FA was found to remove an insignificant amount of sulphate when the pH was raised to 9. When the pH of NMD was raised to greater than 11, about 100% of Mg^{2+} was found to be removed and significant amounts of sulphate ions were found to precipitate out as gypsum (Madzivire, 2010). Addition of amorphous $Al(OH)_3$ to a mixture of FA and NMD at a pH greater than 11 resulted in sulphate concentration decreasing from 1500-2000 mg/L to 400-500 mg/L through ettringite precipitation (Madzivire et al., 2010). A summary of prior work is provided at the end of Chapter 2.

An upscale of the treatment of mine water with FA using turbulator systems was hindered by the fact that large amounts of FA may be required (2:1 and 3:1, using an overhead stirrer). Also, the time required to take the pH of 200 litres of mine water to greater than 11, using about 67 kg of FA in a tabulator aerator was about 44 hours (Surender, 2009). This made the treatment process not feasible industrially as large silos would be required to store the FA and very long stirring times would be required to neutralise the mine water.

A possible way to reduce the mixing time and the amount of FA that has to be used to treat mine water is by the development of a superior way of mixing mine water and FA to enhance the dissolution of lime from FA and speed up the reactions responsible for removal of impurities from mine water. A jet loop reactor system was tested at 80 L scale (Maleka, 2014), and was successful in requiring less ash and much shorter times. This current study would serve to demonstrate the jet loop process for mine water treatment with FA at 1000 L scale.

1.2 PROJECT AIMS

The following were the aims of the project:

1. The primary aim of this research project was to produce cleaner water suitable for drinking, agricultural or industrial purposes, from mining effluents such as acid mine drainage and circumneutral mine water.

2. To scale up the process to 1000 L by use of a jet loop reactor for low-energy, high-volume mixing of slurries.
3. To optimise sulphate removal from circumneutral mine water and acid mine drainage to levels below the requirements of the Department of Water and Sanitation (DWS, formerly DWA), using fly ash, with minimum processing steps, at 1000 L scale, in a jet loop reactor system.
4. To develop low-cost, industrially viable protocols for the bulk treatment of various qualities of mine water, ranging from highly acidic mine water, rich in sulphate, Al and Fe, to circumneutral mine water rich in sulphate, Ca, Mg, and Na.
5. To optimise the application of bulk fly ash and low-cost flocculants for achieving these aims.
6. To recover acid mine drainage and circumneutral water and polish it of any remaining cations, anions and toxic elements to bring it to within DWS standards.
7. To model the reaction mechanisms involved in the removal of contaminants.

CHAPTER 2: LITERATURE REVIEW

2.1 INTRODUCTION

This section reviews literature on fly ash and acid mine drainage (AMD) generation, disposal and treatment. The chemical composition, including the radionuclides present in fly ash and AMD, was also reviewed.

2.2 ACID MINE DRAINAGE

Mine water and coal fly ash are waste materials produced by coal mines and coal power stations respectively. Coal mines produce mine water that is acid, neutral or alkaline depending on the geology of the mine (Lottermoser, 2007). Acid mine water, or AMD, is produced when the rock that was disturbed during mining contains more acid-producing minerals such as pyrite (FeS_2) than acid-neutralising minerals such as dolomite ($CaMg(CO_3)_2$) or calcite ($CaCO_3$). Mining exposes the FeS_2 to oxidation in the presence of water and oxygen, according to Equation 2.1, resulting in the formation of sulphuric acid and Fe^{3+}. The reaction is catalyzed by bacteria called *Acidobacillus sp*.

$$FeS_2 + \tfrac{7}{2}O_2 + H_2O \xrightarrow{bacteria} Fe^{3+} + 2H^+ + 2SO_4^{2-} \quad \text{.....2.1}$$

Sulphuric acid causes chemical weathering of the surrounding rocks, causing the leaching of potential toxic metals such Al and Mn into the water. Mine water from gold and uranium mines is usually acidic and may contain radioactive elements such as U (Wade, 2010).

Neutral mine drainage (NMD) is produced when the rock disturbed during mining contains stoichiometrically equal proportions of acid-producing minerals and acid-neutralising minerals such as dolomite. Alkaline mine water is produced when acid-producing minerals are fewer than the acid-neutralising minerals (Equation 2.2).

$$FeS_2 + CaMg(CO_3)_2 + \tfrac{15}{4}O_2 + \tfrac{3}{2}H_2O \rightarrow Fe(OH)_3 + Ca^{2+} + Mg^{2+} + 2SO_4^{2-} + 2CO_2 \quad \text{.....2.2}$$

AMD is mainly contaminated with Fe, Al and Mn cations, and sulphate as the major anion. NMD and alkaline mine water contain Na, Ca or Mg cations and the major anions are sulphate and carbonate ions.

Mining has taken place for over 100 years in South Africa. It has left undesirable legacies of empty space underground called mine voids. The mine voids in the Witwatersrand Gold Fields are filling up at a rate of 0.59 m/day. As at November 2010 the level of AMD was 510 m below the surface. At that rate, if decant prevention and management were not put into place, the water was predicted to reach the surface in March 2013 resulting in AMD flowing in the streets of Johannesburg central business district and the popular tourist

attraction Gold Reef City (Coetzee et al., 2010). Although this prediction has not been realised to date (2016), the problem of mine water in South Africa remains a crisis and it is not only confined to the Witwatersrand Gold Fields. It is also a huge problem in the Mpumalanga Coal Fields. Mine water from the Mpumalanga coal fields contains high concentrations of Fe, Al, Mn and sulphate ions, and is threatening the freshwater resources of the Vaal and Olifants River ecosystems. Due to the aforementioned problems facing the environment of South Africa, mine water needs to be managed urgently and in an efficient way. Some of the mine water management schemes proposed by the Acid Mine Drainage Inter-ministerial Committee under the coordination of the Council for Geoscience of South Africa include (Coetzee et al., 2010):

- Decant prevention and management
- Controlling ingress of clean water (rainfall) into mine voids
- Water quality management

Decant prevention can be achieved by pumping the water out of the mine voids. Pumped water needs to be treated to remove potential toxic heavy metals and sulphate ions before the water can be discharged into freshwater resources. Many treatment options are available to treat the contaminated mine water to the required standards for potable, industrial and agricultural purposes, but are mostly too costly and unsustainable. Inexpensive treatment technologies are continually being investigated and the use of coal FA is one of them.

2.3 COAL FLY ASH

Coal fly ash (FA) is the mineral matter that remains after coal has been thermally altered through a combustion process to produce electricity. It is collected from flue gas using electrostatic precipitators or filter bags (Adriano et al., 1980). The major constituents of coal are C, O, H, N and S, which are thermally oxidised during coal combustion to produce electricity. Coal also contains trace elements such as As, Hg, B, Pb, Ni, Se, Sr, V and Zn, in association with different types of inorganic minerals such as aluminosilicates (clay minerals), carbonates (calcite and dolomite), sulphides (pyrites), and silica (quartz). The inorganic minerals make up between 5 and 40% of coal. South African power stations burn low-quality coal with very high inorganic content, containing up to 40% inorganic material (Pinetown et al., 2007).

It is these incombustible materials that form the ash that remains after combustion of coal. The chemical composition of FA is made up of Si, Ca, Al, Fe, Mg and S oxides, along with residual C and various trace elements. The silica, in the form of mineral quartz, passes through the combustion process and remains as quartz in the FA. The clay minerals transform into crystalline and non-crystalline (amorphous) aluminosilicate materials during combustion. Elements such as Fe, Ca, and Mg are oxidized to form oxide minerals such as magnetite (Fe_3O_4), hematite (Fe_2O_3), lime (CaO) and periclase (MgO) (Mattigod et al., 1990). The constituents and mineralogy of FA mainly depend on the chemical composition of the coal burnt and the combustion technology employed (Roy et. al., 1985). The amount of crystalline material and glass phase material depends largely on the combustion and gasification (cooling of the ash) process used at a particular power plant.

Fly ash contains elevated amounts of radioactive elements and rare earth elements when compared to the coal burnt during the combustion process (Senior et al., 2000; Depoi et al., 2008; Zielinski and Budahn, 1998). Fly ash contains relatively high amounts of radioactive elements such as U, Th and Ra when compared with bottom ash. Therefore, products from reuse of FA need to be evaluated for radioactivity before they can be channelled to the market.

2.4 RADIOACTIVITY IN COAL FLY ASH

The growing world population, coupled with an exponential depletion of natural resources, has resulted in much research and development focusing on recycling to promote sustainability of industrial processes. The use of FA in construction, agriculture and AMD treatment showed opportunities for recycling this waste material (Kovler, 2012; Madzivire et al., 2010; Gitari et al., 2008). FA is known to accumulate the incombustible constituents of coal in the combustion cycle during the production of electricity. About 550 MT per year of FA are produced by coal-fired powered stations worldwide. After China, the USA and India, South Africa is the fourth largest producer of FA. The radioactivity of most FA all over the world was found to be orders of magnitude higher than the parent coal. The concentration of U and Th in coal in American FA ranges between 1–4 mg/kg (USGS, 1997; Turhan et al., 2010; Papastefanou, 2010; Baykal and Saygılı, 2011; Peppas et al., 2010). As such, there is a great need to evaluate the radioactivity of South African FA and products produced from reuse of coal FA. During coal combustion to produce electricity in power stations, most of the U and Th, and their decay products, is released from the coal and partitioned between the gas phase and solid phase of the combustion products. The partitioning between the gas and solid phase is controlled by the volatility and chemistry of the individual elements. Virtually 100% of the radon gas present in the feed coal is transferred to the gas phase and is lost in stack emissions. In contrast, less volatile elements such as Th, U, and the majority of their decay products, are almost entirely retained in the solid combustion wastes (USGS, 1997). The concentration of most radioactive elements in the solid combustion wastes is approximately ten times the concentration in the original coal (USGS, 1997). The reuse of FA from South African coal power stations for construction depends mostly on its level of radioactivity. The leachability of radionuclides in FA needs to be evaluated in terms of establishing to what extent the radioactivity is transferred into the product water if used for treating AMD. Also, the use of FA in construction needs to be managed in such a way that the final structure is not a radioactive-emitting entity nor an environmental or health hazard.

2.5 RADIOACTIVITY OF MINE WATER

The geology that contains pyrite (FeS_2), together with radioactive elements such as U and Th, could form mine drainage contaminated with radioactive materials. This is because when FeS_2 is oxidized in the presence of H_2O and O_2, it forms acidic water that dissolves the radionuclide-containing minerals. Gold ores in the Witwatersrand basin contain about 3% FeS_2, U, Th, Ra and Pb (Scott, 1995; Durand, 2012). Mining of Au in the Witwatersrand basin leaves FeS_2 exposed to H_2O and O_2 in mine tailing and mine voids. Therefore, the mine waters from the mine voids and mine tailings in the basin are acidic and contain elevated concentrations of radioactive elements such as U, Th, Ra and Pb, in addition to Ca, Al and Mg, and heavy metals such as Fe, Mn, etc.

Radioactivity is the disintegration of the nucleus of an unstable atom by emitting particles containing ionization energy. Three types of radiation are alpha, beta and gamma particles. Alpha particles are produced when the nucleus of an unstable atom loses two protons and two neutrons (He-nucleus), while beta radiation occurs when a nucleus of an unstable atom loses either a positron or an electron. Gamma radiation is produced when the nucleus that was left in an excited state after alpha or beta decay loses excess energy to attain a stable state. An alpha particle is positively charged (+2), the beta particle (electron) or positive (positron) while the gamma photons (rays of electromagnetic radiation) have no charge (0). Different radioactive particles have different penetrating potential. An alpha particle can be stopped by a sheet of paper, while a beta particle may penetrate a thin sheet of aluminium foil. A gamma particle can pass through aluminium foil but can be reduced significantly by a thick block of lead or concrete.

Mine water from Au and U mines is usually contaminated with radioactive elements such as U, and its decay products such as Ra and Th. Naturally, the most abundant isotope is ^{238}U (99.27%) with a half-life of 4.5×10^9 years. Other isotopes that exist in nature are ^{235}U (0.72%) and ^{234}U (0.006%). The half-life of ^{235}U and ^{234}U are 7.04×10^8 and 2.46×10^5 years respectively (Bonotto et al., 2009). Uranium exists in various oxidation states of +2, +3, +4, +5 or +6. The most stable oxidation states are +4 and +6. The uranium (IV) state mainly exists as species which are highly insoluble in the natural environment and therefore are generally far less mobile than U(VI). In nature, Th exists mainly as ^{232}Th with a half-life of 1.4×10^{10} years (Paschoa and Steinhäusler, 2010). The radioactive decay series of U and Th forms various nuclides, and the end product is a stable ^{206}Pb isotope, as shown in Figure 2.1.

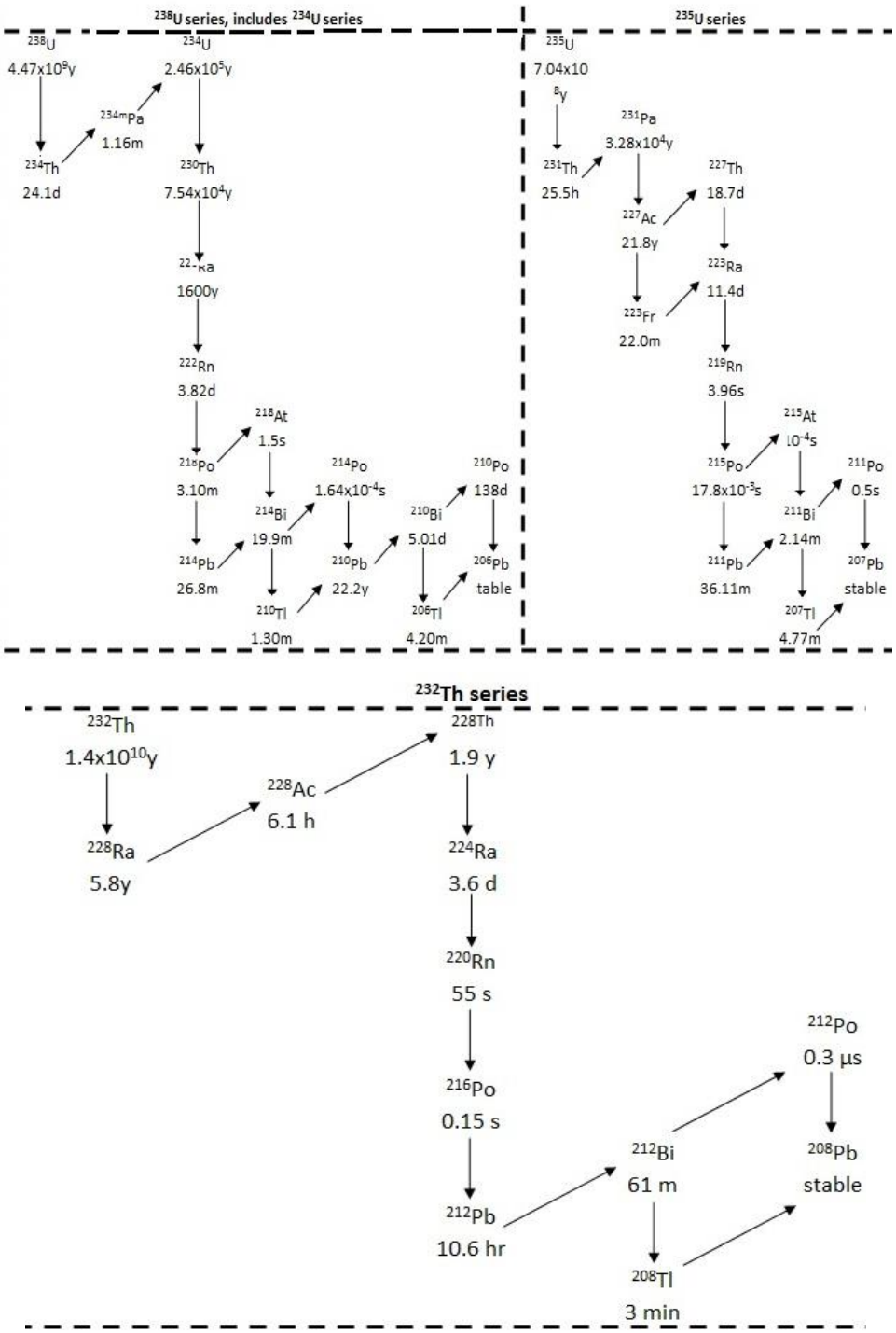

Figure 2.1: The radioactive decay series of 238U, 235U and 232Th (Arrows pointing downwards represent an alpha decay and arrows pointing upwards represent beta decay) (http://www.world nuclear.org/info/inf30.htmL).

The varied decay intermediates have different geochemical properties and therefore are fractionated into different geological environments. In acidic aqueous media, the chemistry of U and Th generally take the form of free cations. Each isotope in the ^{238}U, ^{235}U and ^{232}Th decay series has a unique fingerprint of alpha and gamma decay energies that can be used to identify and quantify each radioisotope, as shown in Table 2.1 and Table 2.2.

Table 2.1 Alpha energy particle (MeV) in the 238U, 235U and 232Th with absolute intensity greater than 5% (Bonotto et al., 2009)

^{238}U decay series			^{235}U decay series		
Nuclide	**Energy**	**Intensity**	**Nuclide**	**Energy**	**Intensity**
^{238}U	4.15	20.9	^{235}U	4.21	5.7
	4.2	79		4.37	17
^{234}U	4.72	28.4		4.4	55
	4.77	71.4		4.41	2.1
^{230}Th	4.62	23.4	^{231}Pa	4.74	8.4
	4.69	76.3		4.95	22.8
^{226}Ra	4.6	5.6		5.01	25.4
	4.78	94.4		5.03	20
^{222}Rn	5.49	99.9		5.06	11
^{218}Po	6	100	^{227}Th	5.76	20.4
^{214}Po	7.69	100		5.98	23.5
^{210}Po	5.3	100		6.04	24.2
^{232}Th decay series			^{223}Ra	5.61	25.7
Nuclide	**Energy**	**Intensity**		5.72	52.6
^{232}Th	3.95	21.7		5.75	9.2
	4.01	78.2	^{219}Rn	6.42	7.5
^{228}Th	5.34	27.2		6.55	12.9
	5.42	72.2		6.82	79.4
^{224}Ra	5.45	5.1	^{215}Po	7.39	100
	5.68	94.9	^{211}Bi	6.28	16.2
^{220}Rn	6.29	99.9		6.62	83.8
^{216}Po	6.78	100			
^{212}Bi	6.01	7.5			
	6.05	69.9			
	6.09	27.1			
	6.3	38.8			
	6.34	52.2			
^{212}Po	8.78	100			

Table 2.2: Gamma emissions (MeV) related to negative beta-emitting radioisotopes in the 238U, 235U and 232Th decay series with absolute intensity greater than 1% (Bonotto et al., 2009)

^{238}U decay series			^{232}Th decay series			^{235}U decay series		
Nuclide	**Energy**	**Intensity**	**Nuclide**	**Energy**	**Intensity**	**Nuclide**	**Energy**	**Intensity**
^{234Th}	0.063	4.8	^{228}Ra	0.014	1.6	^{231}Th	0.026	14.5
	0.092	2.8	^{228}Ac	0.099	1.3		0.084	6.6
	0.093	2.8		0.129	2.4	^{211}Pb	0.405	3.8
^{214}Pb	0.053	1.2		0.209	3.9		0.427	1.8
	0.242	7.4		0.27	3.5		0.837	3.5
	0.295	19.3		0.328	3			
	0.352	37.6		0.338	11.3			
	0.786	1.1		0.409	1.9			
^{214}Bi	0.609	46.1		0.463	4.4			
	0.665	1.5		0.772	1.5			
	0.768	4.9		0.794	4.2			
	0.806	1.2		0.836	1.6			
	0.934	3		0.911	25.8			
	1.12	15.1		0.965	5			
	1.155	1.6		0.969	15.8			
	1.238	5.8		1.588	3.2			
	1.281	1.4		1.631	1.5			
	1.378	4	^{212}Pb	0.239	43.3			
	1.402	1.3		0.3	3.3			
	1.408	2.2	^{212}Bi	0.04	1.1			
	1.509	2.1		0.727	6.6			
	1.661	1.2		0.785	1.1			
	1.73	2.9		1.62	1.5			
	1.764	15.4	^{208}Tl	0.277	6.3			
	1.847	2.1		0.511	22.6			
	2.118	1.1		0.583	84.5			
	2.204	5.1		0.763	1.8			
	2.448	1.6		0.86	12.4			
^{210}Pb	0.046	4.2		2.614	99			

The energies shown in Table 2.1 and Table 2.2 can be used to identify the respective radionuclides using alpha or gamma spectrometry respectively. The height of a peak with a particular energy can be used to quantify the radionuclides in the samples based on calibration with the known concentration of specific radionuclides.

2.6 GUIDANCE LEVELS FOR RADIOACTIVE NUCLIDES IN DRINKING WATER

Identification of radioactive species in drinking water is a very expensive and sophisticated process. The screening steps to identify if water is suitable for drinking purposes in terms of radioactivity are shown in Figure 2.3 below.

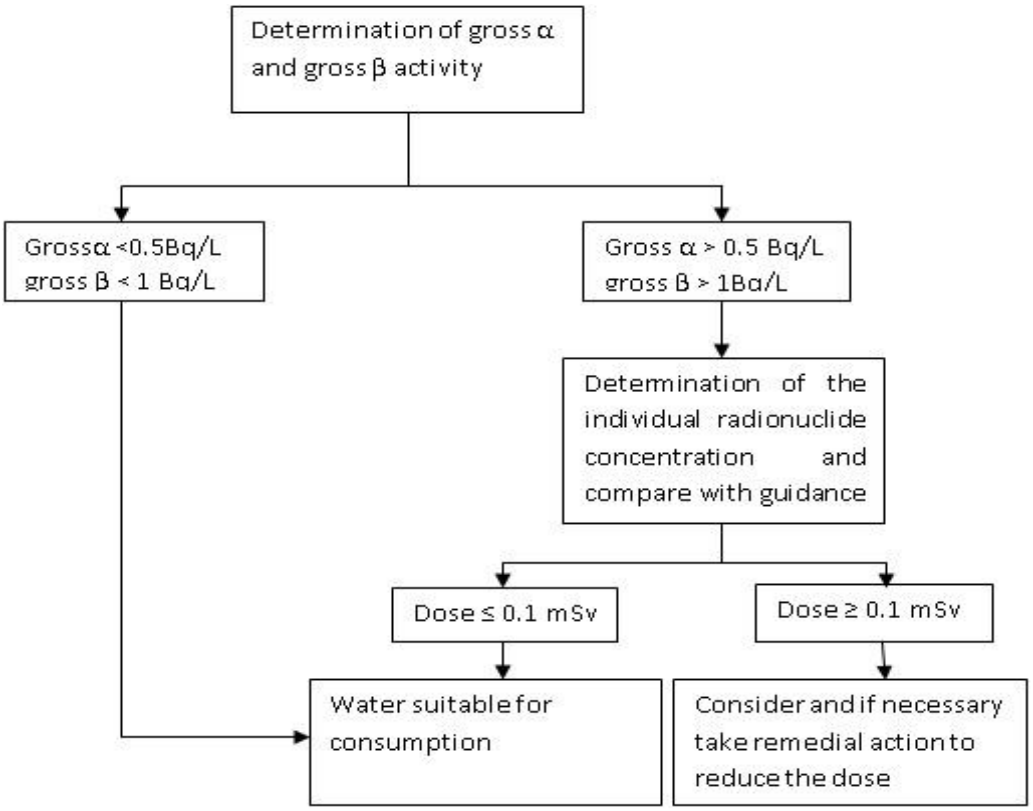

Figure 2.2: Outline of the screening process to determine the suitability of water for drinking, in terms of radioactivity (WHO, 2011)

The first step before determining the concentration of individual radionuclides in water is to determine the gross alpha and gross beta activity of the water. If the gross alpha and beta are less than 0.5 Bq/L and 1 Bq/L respectively, the water will be suitable for drinking in terms of radioactivity (WHO, 2011). On the other hand, if the gross alpha and beta activities are greater than 0.5 and 1 Bq/L, respectively, then the concentration of the individual radionuclide should be measured and compared to the World Health Organization (WHO) guidelines. If the dose is at most 0.1 mSv, the water is suitable for drinking. If the dose is greater than 0.1 mSv then remedial action should be undertaken. A dose of at most 0.1 mSv is achieved if the following formula is satisfied:

$$\sum_i \frac{C_i}{GL_i} \leq 1 \quad \text{.....2.3}$$

Where, C_i= measured activity of radionuclide *i*, and GL_i is the guideline concentration of radionuclide at an intake of 2 litres per day for one year. This will result in an effective dose of 0.1 mSv per year (WHO, 2011).

2.7 MODELLING

The Geochemist's Workbench (GWB) is a software program comprising various programs to manipulate chemical reactions, calculate stability diagrams and the equilibrium states of natural waters, trace reaction processes, model reactive transport, plot the results of these calculations, and store the related data (Bethke and Yeakel, 2010). The software is constantly upgraded. In this study, SpecE8 and Act2 programs of the GWB 8.0 essential software were used.

SpecE8 is capable of calculating species distribution in aqueous solutions, mineral saturation indices and gas fugacities. SpecE8 can also account for sorption of species onto mineral surfaces according to a variety of methods, including surface complexation and ion exchange. The Act2 program calculates and plots activity-activity diagrams. These diagrams show the stability of minerals and predominance of aqueous species in chemical systems. Variables of the axes of the stability diagrams include species activity, gas fugacity, activity or fugacity ratio, pH, or redox potential (Bethke and Yeakel, 2010).

2.7.1 **Species distribution**

Speciation, as defined here, is the chemical form in which ions exist in aqueous solutions or natural waters. Speciation is extremely important as the bioavailability of an ion or element, as a required nutrient or toxicant, depends on its chemical form. The toxicology of some elements is very complex, because some elements are toxic in one form while in another they may be an essential nutrient (Jain and Ali, 2000; Florence et al., 1992; Allen et al., 1980). Mostly hydrated metal ions are considered to be toxic, while complexed species are usually deemed less toxic (Russeva, 1995). Different analytical protocols and models have been used to elucidate the different forms of ions in natural water. In this study, GWB software was used to speciate the ions that were detected in mine water from two mines, i.e. Matla and Rand Uranium, using inductively-coupled plasma-optical emission spectroscopy (ICP-OES) and ion chromatography (IC).

2.7.2 **Prediction of the mineral phases**

During treatment of mine water with alkaline ameliorants such as fly ash and/or lime, potentially toxic constituents are mainly removed through precipitation. The Act2 program of the GWB software was used to predict the aqueous species distribution in Matla mine water and any stable mineral phases that may form during precipitation of potentially toxic elements/ions from Rand Uranium and Matla mine water. The prediction was done using the analytical and physical results determined by IC, ICP-OES, a pH/EC/TDS meter and an autotitrator. The independent variable was chosen as $\log_a Ca^{2+}$ and the dependent variable was the pH. These values were chosen based on the fact that treatment of mine water with coal is based on the neutralisation of the pH due to the dissolution of the lime fraction in coal FA.

2.8 SUMMARY

Mine water is an environmental liability produced during mining activities. Mine water usually comes from pumping underground water in order for miners to access the minerals; alternatively, it leaches from mine tailings or acid-impacted geologies exposed to air and water. The composition of mine water differs from mine to mine depending on the exploited geology. Types of mine water are classified according to their chemical composition. Mine water composition depends on the mined ore and the chemical additives used

in the mineral processing and hydrometallurgical processing. This means that there is no typical composition of mine waters and as a result, the classification of mine water based on its composition is very complex.

Mine water is mainly composed of Fe, Al, and Mn (for AMD) or Ca and Mg (for NMD) cations together with other potential pollutants depending on the geology that is mined. Sulphate is the major anion found in mine water and ranges from around 1 000 to 30 000 mg/L. Due to vast differences in the chemistry of mine waters and the variety of physical, chemical and biological methods to separate metals from mine water, there is a wide range of treatment technologies for mine water treatment. Treatment of mine drainage can be achieved through passive or active processes (Neculita et al., 2007).

Passive treatment schemes take advantage of naturally occurring geochemical and biological processes in order to improve the quality of the influent waters with minimal operation and maintenance requirements. Passive treatment can be broadly classified as chemical or biological systems depending on the processes that are occurring to ameliorate the mine water (Neculita et al., 2007). Passive treatment of mine water is limited by the unavailability of enough space to set up the proper facility. Also the quality of the product water is not guaranteed and the passive system loses its buffering capacity over time.

Active treatment technologies improve the water quality by processes which require continuous input of artificial energy, biochemical or chemical reagents. Active treatment methods are recognised by the presence of a water treatment plant that is being monitored regularly by a skilled workforce who operate and maintain the equipment. Active treatment technologies are broadly classified as biological, chemical and membrane methods. Biological methods involve the use of sulphate reducing bacteria (Johnson, 2000). Chemical treatment include the precipitation of contaminants from the mine water using chemicals such as lime/limestone, $BaCO_3$, BaS, $Ba(OH)_2$, $Mg(OH)_2$, $MgCO_3$ and $Al(OH)_3$ (Geldenhuys et al., 2001; Bosman, 1983, Smit, 1999, Adlem, 1997; Bosman et al., 1990). Membrane methods for the treatment of mine water include nano filtration (Kentish and Stevens, 2001), reverse osmosis (Del Pino and Durham, 1999; Kentish and Stevens, 2001; Matsuura, 2001), electro dialysis (Valerdi-Perez et al., 2001; Del Pino and Durham, 1999; Schoeman and Steyn, 2001; Kentish and Stevens, 2001) and ion exchange (Kitchener, 1957).

The major advantage of active treatment is the capability to respond to changes in mine water quality and quantity. This is because of the precise process control possible in response to these changes. Also active treatment is a preferred technique to passive treatment if the land availability is a limiting factor. The major disadvantages of the active treatment method are the brines and sludges that are produced as wastes which are more expensive to handle and dispose than the water purification process itself. Also the continuous input of energy, reagents and the need for manpower to run and maintain the treatment plant makes the technique expensive.

The choice of a suitable treatment technology depends on the mine water quality, the mine water quantity, the treated water quality, the storage options for any sludge produced and the cost of the treatment technique. In reality, there is no technical limit to the quality of the water which can be achieved using current existing techniques; cost is the limiting factor. Therefore, the selection of treatment technique comes down to an economic-environment cost-benefit analysis. New, cheaper methods to remove contaminants from mine water

are constantly sought. One method is the use of FA from coal power stations (Gitari et al., 2008). The advantage of this method is that FA is a waste material from coal combustion found close to coal mines. This means that FA treatment of mine water can be sustainable since FA is a waste material. Approximately 80% of South African electricity is produced from coal and large amounts of FA are generated in the process. Disposing of FA has proved to be an environmental concern, and therefore recycling of FA for mine drainage treatment is important to achieve zero effluent discharge.

PRIOR WORK

Full references can be found in the section titled 'Prior work by the authors', on page xiii of the preliminary pages. Large volumes of AMD are formed during coal and gold mining, and AMD contains radionuclides, high levels of sulphate and numerous other toxic elements, as well as being highly acidic (Madzivire et al., 2013; 2014). Radioactivity in mine water from a gold mine in South Africa has been reported (Madzivire et al., 2013). Removal of sulphates from South African mine water using coal FA has been shown to be effective (Petrik et al, 2005; Misheer et al., 2010). FA was used to neutralise and treat AMD from coal and gold mining, reducing major inorganic contaminants in the water to within water quality specifications, and FA treatment can be applied in passive or active systems (Gitari et al., 2006; 2008; 2013). These studies have shown that FA presents a promising route to treating AMD. FA actively or passively neutralised and improved the quality of AMD at large scale (80 L) achieving sulphate removal in a one-step process (Petrik, 2005; Surender et al., 2010; Misheer et al., 2010; Gitari et al., 2010a&b). Partitioning of major and trace inorganic contaminants in solid residues derived from fly ash-acid mine drainage has been studied in a passive column study (Gitari et al.,2010). Much mine water is rich in Ca and Mg, and poor in Al and Fe, but still contains a high load of sulphate. The application of coal FA to circumneutral mine waters for the removal of sulphates as gypsum and ettringite has been demonstrated (Madzivire et al., 2010) and the fate of sulphate removed during the treatment of circumneutral mine water, as well as AMD with coal FA, has been shown using a modelling and experimental approach (Madzivire et al., 2011). The fate of the naturally occurring radioactive materials during treatment of AMD with coal FA and aluminium hydroxide has been determined (Madzivire et al., 2014). Use of FA to treat AMD, followed by use of the resulting solid residues in backfill operations, has been demonstrated (Fester et al., 2008). Neutralisation of AMD using FA, and strength development of the resulting solid residues has been shown (Vadapalli et al., 2008), and the effect of FA size fraction on the potential to neutralise AMD, and upon the rheological properties of the residual sludge, was further investigated (Vadapalli et al., 2013). The degree of dewatering and particle size could be used to control the rheological properties making it possible to backfill underground voids. The residues remaining after AMD treatment were thus found suitable for backfilling of mine voids and developed sufficient strength, once placed, to prevent collapse and would seal the ingress of air and water, thus could prevent the formation of AMD, offering a cradle-to-cradle solution for mine closure (Vadapalli et al.,2008; 2012; Gitari et al., 2013; 2016). The removal of sulphates from mine water using coal FA depends on the amount of FA used, the final pH achieved and the composition of the mine water (Madzivire et al., 2009; 2011; 2012; 2015). Studies of the chemistry and speciation of potentially toxic and radioactive elements during AMD treatment proved that mine waters of very different qualities can be treated successfully with coal FA, lime and $Al(OH)_3$ to obtain product water that meets target water quality range (TWQR) guidelines for irrigation or drinking water. After the AMD is treated, the remaining solids can thus be used to refill mine voids after a mine is no longer in use to prevent the formation of AMD because sealing the mine voids ensures that air and water are excluded. The study by Petrik et al. (2005; 2006; 2007a) assessed the feasibility of large-

scale treatment of AMD from coal mines and recovery of water, including the preliminary planning and consultation for large-scale studies, including neutralisation, backfill, ash walling, ash lining, water recovery and mineralogical studies. An evaluation of historical ash placement studies was provided, to gain access and determine the mineralogical and other environmental impacts and changes associated with historical placements of ash previously used as fill materials, and determination of the overall suitability of solid residues for extending the life of coal mines and increasing the amount of extractable coal from each mine was shown. The potential was shown for control of surface AMD by employment of FA as ash walls within coal mine spoil heaps to establish an in-situ barrier for passive treatment of AMD flows. The impact of microbiology on FA-AMD co-disposal and remediation systems was also evaluated (Cowan et al., 2010). Thus, our previous studies have shown that South African fly ash is a low-cost and competitive technology for the treatment of AMD, and offers a route to stop the formation of AMD by backfill of mine voids.

In terms of producing value-added products from FA, the conversion of FA, or its waste residues after AMD treatment, into zeolites or geopolymer concretes is promising. The alkaline hydrothermal conversion of FA precipitates into various zeolites was demonstrated (Somerset et al., 2003; Gitari et al., 2016b). Zeolites are commercially applied as high-value, high-volume porous minerals that are useful for numerous applications in gas separation, hydrocarbon processing, adsorption, slow release fertilisers, and moisture and odour control, to name a few applications. Zeolite Na-P1 was successfully synthesised from coal FA, and Hg, Pb and other toxic metals could be removed from polluted water with zeolite Na-P made from FA (Petrik et al., 2007; Somerset et al., 2003; 2005a,b,c; 2008). A synthesis of zeolite-P from coal FA derivatives was utilised in mine water remediation (Vadapalli et al., 2010).

CHAPTER 3: CHARACTERISATION OF FLY ASH AND ACID MINE DRAINAGE

3.1 INTRODUCTION

In this chapter, the experimental and analytical procedures used to characterize the fly ash (FA) and mine waters are presented. The results, showing the physical and chemical characteristics of the raw materials, FA, $Al(OH)_3$, aluminium chlorohydrate (ACH) and mine water are also presented and explained, based on the data obtained from the analytical protocols.

3.2 EXPERIMENTAL AND ANALYTICAL TECHNIQUES

FA samples were analysed using quantitative X-ray diffraction (XRD) and laser ablation inductively-coupled plasma mass spectroscopy (LA-ICP-MS), for mineralogy, and for elemental composition of minor elements, respectively. Radioactivity analysis of coal FA was done using gamma spectroscopy. The mine water used in this study was characterized using ion chromatography (IC) and inductively-coupled plasma-optical emission spectroscopy (ICP-OES). The physical parameters such as pH, electrical conductivity (EC) and total dissolved solids (TDS) were measured on site. The mine water was also filtered through a 0.45 µm filter paper, and the acidity or alkalinity was determined using a Metrohm Autotitrator. Mine water samples that were to be analysed for radioactivity were first filtered sequentially through 8 µm and 0.45 µm filter papers to remove coarse materials and suspended solids. The samples were then acidified to ensure radionuclides were not adsorbed on container walls.

3.2.1 **X-ray diffraction spectroscopy**

Qualitative XRD was performed to evaluate any mineralogical changes between the fresh coal FA and the solid residues after mixing with mine water. This was performed using a Philips X-ray diffractometer and Cu-K_α radiation with a PW3011 (Miniprop) detector. The instrument settings are as shown in Table 3.1.

Table 3.1 The XRD settings during analysis of coal FA and the solid residues

Radiation source	Cu-K_α
Radiation wavelength (λ)	1.541
Voltage	40 Kv
Current	25 Ma
2θ	$4^o<2\theta<65^o$
Step size	0.02
Anti-scatter slit	1^o

The mineral phases were identified by search and match technique using the powder diffraction data file. This identification was achieved by matching with Joint Committee of Powder Diffraction Standards (JCPDS) files for inorganic compounds.

3.2.2 **Quantitative x-ray diffraction spectroscopy**

Quantitative XRD was performed to evaluate the amount of minerals in fresh coal FA. Coal FA was mixed with 20% Si (Aldrich 99% pure) for determination of amorphous content and then milled in a McCrone micronizing mill. The samples were prepared for XRD analysis using a back-loading preparation method and were analysed with a PANalytical X'Pert Pro powder diffractometer with X'Celerator detector, variable divergence and receiving slits with Fe filtered Co-Kα radiation. The phases were identified using X'Pert Highscore Plus software. The relative phase amounts (weight %) were estimated using the Rietveld method (Autoquan Program).This was performed using a Philips X-ray diffractometer and Cu-K_α radiation with a PW3011 (Miniprop) detector.

3.2.3 **Scanning electron microscopy**

Matla FA was analysed using a HITACHI X-650 Scanning Electron Microanalyser. The samples were prepared by fixing the powder form samples on aluminium stubs using carbon adhesive. The carbon adhesive was attached to the top part of the aluminium stub and then the powder was sprinkled on the carbon adhesive with great precaution to avoid forming a thick layer that would absorb the incident light. Since the samples that were analysed were poor electromagnetic conductors, they were gold-coated using argon gas on Sputter Coater S150B. The gold coating was done under vacuum.

3.2.4 **X-Ray fluorescence spectroscopy (XRF)**

Matla FA samples were crushed into a fine powder (particle size < 100 µm) with a jaw crusher and milled in a tungsten zib mill, to prevent trace and rare earth element (REE) contamination, prior to the preparation of a fused disc for major and trace element analysis. The jaw crusher and mill were cleaned with uncontaminated quartz after analysing each sample to avoid cross contamination. Pressed powder pellets were prepared for XRF analysis using 8 g of the sample, and a few drops of MOVIOL binder were added for binding.

The composition was then determined by XRF spectrometry on a Philips 1404 Wavelength Dispersive spectrometer. The spectrometer was fitted with an Rh tube and with the following analysing crystals: LIF200, LIF220, LIF420, PE, TLAP and PX1. The instrument is fitted with a gas-flow proportional counter and a scintillation detector. The gas-flow proportional counter uses a 90% argon and 10% methane gas mixture. Trace elements were analysed on a pressed powder pellet at various kV and mA tube operating conditions, depending on the analysed element. Matrix effects in the samples were corrected for by applying theoretical alpha factors and measured line overlap factors to the raw intensities measured with SuperQ Philips software. Control standards that were used in the calibration procedures were NIM-G (Granite from the Council for Mineral Technology, South Africa) and BHVO-1 (Basalt from the United States Geological Survey (USGS), Reston).

3.2.5 **Laser ablation inductively coupled plasma-mass spectrometry**

The instrument was set by connecting a 213 nm laser ablation system to an Agilent 7500ce ICP-MS. The FA sample was coarsely crushed and fusion disks were made by an automatic Claisse M4 Gas Fusion instrument and ultrapure Claisse Flux. A chip of sample was mounted in a 2.4 cm, round resin disk. The mounted sample was then polished for analysis. The sample was ablated using He gas and then mixed with Ar after coming out of the ablation cell. The sample was then passed through a mixing chamber before being introduced into the ICP-MS.

Trace elements were quantified using NIST 612 for calibration method and 29Si as internal standard. Three replicate measurements were taken on each sample. The calibration standard was run after every 12 samples. A quality control standard was run at the beginning of the sequence as well as with the calibration standards throughout. Both basaltic glasses, BCR-2 or BHVO 2G, were used as certified reference standards, as produced by USGS (Dr Steve Wilson, Denver, CO 80225). A fusion control standard from certified basaltic reference material (BCR-2, also from USGS) was also analysed at the beginning of a sequence, to verify ablation on fused material. Data was processed using Glitter software.

3.2.6 **Radioactive analysis of Matla fly ash**

Matla FA samples were dried overnight in an oven at 105˚C. The samples were then milled to obtain a homogeneous powder so that representative portions could be sampled for the various analyses. The homogenised sample (500 g) was placed in Marinelli beakers and analysed by gamma spectroscopy for gross alpha and beta to obtain a first-order estimate of the total activity of the sample. After determination of the gross alpha and beta, the samples were analysed for various radioisotopes using low-energy gamma analysis and high-energy gamma analysis, according to a method used by Newman et al. (2008), and Radium-226 was determined by measuring its decay products. A three-week waiting period was allowed to establish radioactive equilibrium between radium and its decay products.

3.2.7 **Radioactive analysis of fly ash using gamma spectrometry**

Two high-resolution ERL gamma-ray spectrometers with p-type coaxial hyper-pure germanium (HPGe) detectors were used for the determination of ^{210}Pb, ^{238}U, ^{235}U, ^{234}U, ^{228}Ra, ^{226}Ra, ^{232}Th, ^{228}Th, ^{40}K, and other products in the thorium-232 and uranium-235 decay series, in Matla fly ash. One of the HPGe detectors had a relative efficiency of 45% and an energy resolution of 2 keV at 1.33 MeV. The other detector had a relative efficiency of 110% and an energy resolution of 2.1 keV. To avoid background radiation, both detectors were shielded from background radiation. Gamma reference materials were used to determine the absolute efficiency of the gamma spectrometers. Measurement of the sample was done at the same conditions with background measurements and subtracted from the sample measurement. Several gamma-ray peaks at various energies obtained in Table 2.1 were averaged, assuming secular equilibrium in ^{238}U and ^{232}Th decay series, as follows:

- Uranium-238 activity concentration was determined by using the gamma-ray peaks of the 351.9 keV from ^{214}Pb and the 609.3 keV from ^{214}Bi.
- Radium-226 was determined using the gamma ray with energy of 186 keV.
- To determine the activity concentration of ^{232}Th, the gamma-ray peaks of the 911.2 keV from ^{228}Ac and the 583.2 keV from ^{208}Tl were used.
- Activity concentration of ^{40}K was determined from its own gamma-ray peak at 1460.8 keV.

3.2.8 **Ion chromatography**

Ion chromatography (IC) was used to determine the concentration of anions in the mine water. The samples were filtered through a 0.45 µm nucleopore membrane filter paper and preserved at 4˚C until analysis was conducted. A Dionex DX-120 Ion Chromatograph, with an AS40 automated sampler, ASRS-300 suppresser, AS14 analytical column, AG14 guard column and a conductivity detector, was used for the analysis. The eluant used was a mixture of 3.5 mM $NaHCO_3$ and 1.0 mM Na_2CO_3. A Dionex SEVEN ANION standard was used to check the accuracy of the IC machine. The SEVEN ANION was made up of the composition as shown in Table 3.2 below.

Table 3.2: Composition of the Dionex SEVEN ANION standard

Anion	Concentration (mg/L)
F^-	20
Cl^-	30
NO_2^-	100
Br^-	100
NO_3^-	100
PO_4^{3-}	150
SO_4^{2-}	150

3.2.9 **Inductively coupled plasma-optical emission spectroscopy**

Cation concentrations were analysed using inductively coupled plasma-optical emission spectrometry (ICP-OES) to follow the changes in the composition of the mine water during treatment. The ICP-OES instrument

was calibrated before analysis. The ICP-OES instrument used was a Varian 710-ES series spectrometer equipped with a CCD detector, axially-viewed plasma, a cooled cone interface, and ICP Expert II software.

3.2.10 **Determination of acidity or alkalinity**

The alkalinity of the mine water used in experiments was determined, to gain an understanding of the acid-neutralising potential. This parameter is very important for cation/anion balance in GWB geochemical modelling. The alkalinity was determined by titrating circumneutral mine water (20 mL) with 0.1 M HCl to an end point of pH 4 (Eaton et al., 1995). The alkalinity was calculated as follows (equation 3.1):

$$mg \cdot L^{-1}(HCO_3^-) = \frac{1000 \times 61.02 \times V(acid) \times [HCl]}{V(sample)} \text{ ; where V = ml and [ ] = mol/L}\ldots\ldots\ldots\ldots\ldots\ldots 3.1$$

Acidity was determined by titrating an AMD (20 mL) sample with 0.1 M NaOH to an end point of 8.3. The acidity was calculated as follows (equation 3.2):

$$mg \cdot L^{-1}(CaCO_3) = \frac{V(NaOH) \times [NaOH] \times 1000}{V(sample)} \text{ ; where V = ml and [ ] = mol/L}\ldots\ldots\ldots\ldots\ldots\ldots 3.2$$

3.2.11 **Analysis of mine water**

Three mine waters were characterised, namely, mine waters sourced from Rand Uranium mine, Matla mine and Lancaster dam. Lancaster dam water was sourced at site from a decant site in the Krugersdorp area, and Rand Uranium water was collected before the river enters the Hippo dam in Randfontein in the Western Rand basin in Witwatersrand Goldfields. These waters might vary but not that much since they come from the same geological area. The Matla mine water sample was collected from underground water pumping during coal mining at Matla coal mine.

The mine water samples were filtered, acidified and then stored at 4°C before analysis. Before the samples were analysed using alpha spectrometry, they were first pre-treated and prepared specifically for analysis of a specific element. The following steps cover how the samples were prepared and analysed using alpha spectrometry.

3.2.11.1 Sample preparation for uranium determination by alpha spectrometry

The method was based on solid phase extraction of uranium from water samples, with detection of the uranium isotopes by alpha spectrometry. An aliquot (200 mL) of the sample was measured into a beaker and uranium-232 internal tracer was added for recovery determination. The sample was evaporated to a volume of 10 mL, and acidified using 2 drops of 2 M HNO_3. The sample was loaded on a TruSpec (Eichrom resins) column to absorb uranium. A mixture of HCl and HF acid was added to the column to elute uranium. The separated

uranium was loaded on a cation exchange column to further purify uranium. Uranium was eluted with concentrated 2 M HCl and collected on a filter paper by lanthanum fluoride micro co-precipitation.

3.2.11.2 Sample preparation for thorium determination by alpha spectrometry

The method was based on solid phase extraction of Th from water samples, with detection of the different Th isotopes by alpha spectrometry. Thorium^{-229} was added as an internal tracer to a 200 mL aliquot of the sample. Sample volume was reduced to a volume of 10 mL by evaporation, and acidified using 2 M HNO_3. The sample was loaded on a TruSpec column (Eichrom resins) to absorb Th and other nuclides. Th was eluted with a mixture of HCl and HF. The collected eluent was loaded on a cation column for further purification. Th was finally eluted with 2 M H_2SO_4 solution and collected on a filter paper by lanthanum fluoride micro co-precipitation.

3.2.11.3 Sample preparation for radium determination by alpha spectrometry

Barium^{-131} was added as an internal tracer to the sample. Ra was separated from the bulk of the sample material by adding Pb and Ba carriers to the sample, followed by precipitating these elements and Ra present as sulphates. The precipitate was purified from other ions by washing, and then dissolved again by adding a complexing agent. Ba (and Ra) was again precipitated and filtered as sulphate, while Pb was kept in solution by careful adjustment of the pH. Barium^{-131} in the separated fraction was measured for on a radiation detector for yield determination.

3.2.11.4 Sample preparation for lead and polonium determination by alpha spectrometry

Polonium^{-209} was added as an internal tracer for recovery determination. The sample was acidified with 2 M HCl and heated to a temperature of 90˚C. A silver disk was added to the sample and the solution was stirred for several hours to induce spontaneous deposition of polonium^{-210}. A reducing agent was added at the start of the process to prevent iron from plating on the silver disk. The disk was removed, washed and air-dried to prepare it for measurement on the alpha spectrometer.

3.2.11.5 Alpha spectrometry analysis of the prepared samples

Prepared samples were counted on Canberra Alpha Analyst or Alpha Apex systems. These systems consist of 12 vacuum chambers each hosting an alpha PIPS detector. Samples were counted for a period of 24 hours to reach the required detection limits. The acquired spectra were analysed for counts collected in the respective alpha peak positions shown in Table 3.3.

Table 3.3: Peaks position used for identification of nuclides using alpha spectrometry

Nuclide	Peaks position energy (MeV)
^{238}U	4.72
^{235}U	4.40
^{234}U	4.77
^{232}Th	4.01
^{230}Th	4.69
^{227}Th	5.76, 5.93 and 6.04
^{228}Th	5.42
^{226}Ra	4.78
^{224}Ra	5.68
^{210}Po	5.30

The peak positions were chosen based on the highest intensities of the alpha energy of the respective decay of the nuclide (Bonotto et al., 2009). These counts were entered into data reduction programs to calculate nuclide activities, associated uncertainties and minimum detectable activity concentrations. A control sample, containing known amounts of the analyte nuclides, was used to calibrate the machine for each batch of samples. Measured activities must lie within prescribed limits for the results of the batch to be accepted. The yield for a sample must also be within range. Background, energy, peak-width and efficiency checks were performed on a weekly basis to ensure correct operation of detectors.

3.3 RESULTS AND DISCUSSION

The results, showing the physical and chemical characteristics of the raw materials, i.e. fly ash, $Al(OH)_3$ and aluminium chlorohydrate (ACH), and the mine water, are presented and explained, based on the data obtained from the analytical protocols.

3.3.1 **Matla coal fly ash**

3.3.1.1 Scanning electron microscopy (SEM) and X-ray diffraction

The FA used in this study was collected from Matla coal-fired power station, in the Mpumalanga province of South Africa. The morphological characteristics of the FA were visualised on a scanning electron microscope (SEM). The results in Figure 3.1a show that the FA is made up of mainly smooth spherical particles of less than 40 µm. Energy dispersive x-ray spectroscopy (EDX) showed that the FA particles were made of mainly Si and Al atoms. Other atoms such as O, Ca, K, Fe and Cu were available in small proportions, as shown in Figure 3.1b.

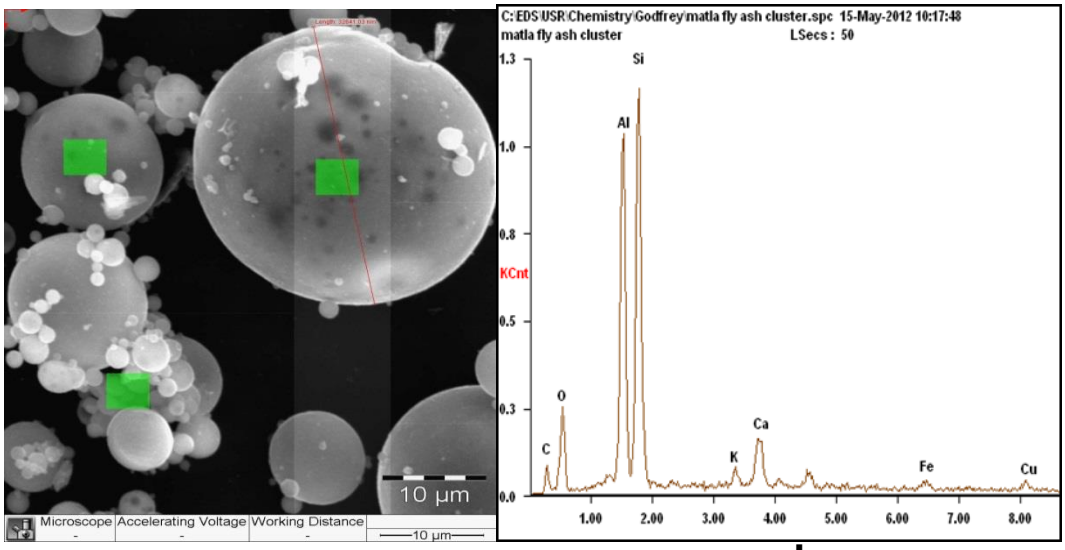

Figure 3.1: The morphology of Matla fly ash, captured using a scanning electron microscope at magnification x1000 (a), and the EDS analysis (b)

Matla FA was further characterised using XRD for the mineralogical composition, and the results are as shown in Figure 3.2 below.

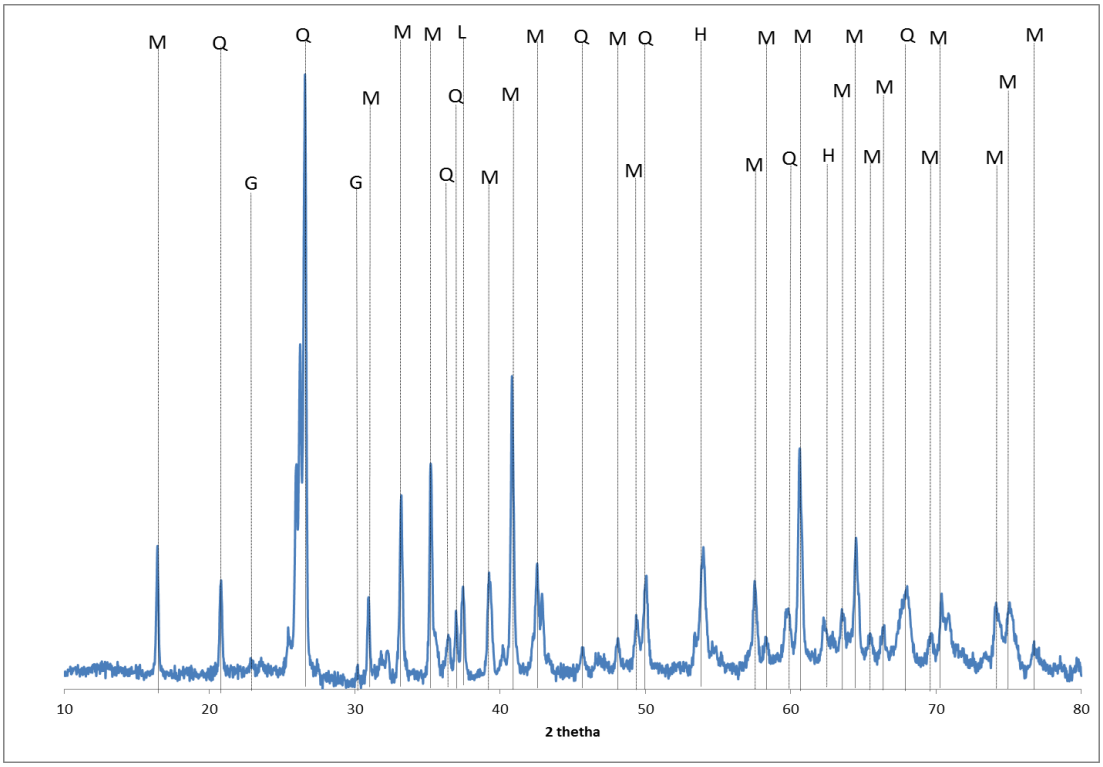

Figure 3.2: **The XRD spectrum showing the mineralogical composition of Matla coal FA (M-mullite; Q-quartz; G-gypsum; L-lime; H-hematite)**

From the XRD spectrum above, the identified crystalline phases that make up Matla coal FA are mullite ($Al_2Si_2O_{13}$), quartz (SiO_2), hematite (Fe_2O_3), gypsum ($CaSO_4.2H_2O$) and lime (CaO). These minerals phases

were formed through transformation of the inorganic material in the coal that was burnt. The XRD results correlated well with the EDS compositional results.

3.3.1.2 Quantitative XRD

The coal FA used in this study was collected from Matla coal-fired power station in the Mpumalanga province of South Africa. Matla coal FA was also analysed using quantitative XRD to determine the percentage mineral phase composition of the minerals, determined by qualitative XRD as explained above. The mass percentage mineral phase composition of Matla fly ash, measured by quantitative XRD, is shown in Figure 3.3.

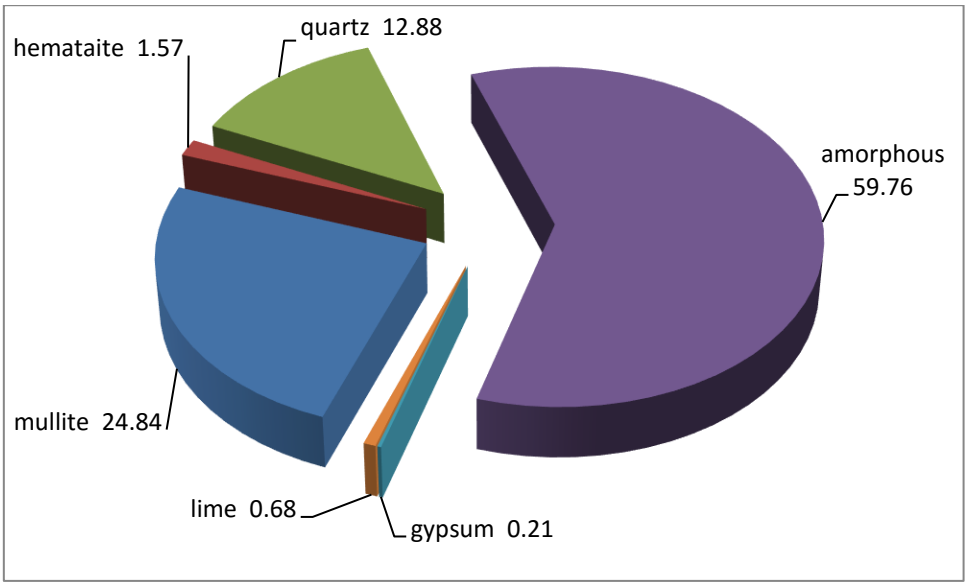

Figure 3.3: Quantitative phase mineralogy of fresh Matla coal FA (mass percent).

The results of quantitative phase mineralogy (by XRD) for Matla coal FA showed that it was mainly composed of amorphous, glassy aluminosilicate phase which made up about 60% of the coal FA. Mullite, quartz, hematite, lime and gypsum constituted about 25%, 13%, 2%, 1% and 0.2%, respectively.

3.3.1.3 Elemental composition using XRF and LA-ICP-MS

The quantitative elemental composition was analysed using XRF, and the results are shown in Table 3.4. The composition shows that it was Class F since the sum of SiO_2, Fe_2O_3 and Al_2O_3 was greater than 70% (ASTM, 1994; McCarthy, 1988). Class F is produced from the burning of bituminous coal and anthracites. Class F FA has pozzolanic properties, that is, it hardens when it reacts with $Ca(OH)_2$ and water (Vassilev and Vassileva, 2007). Matla FA was found to contain CaO (6.71%). Lime imparts alkalinity to FA. It is this alkaline property that was exploited during the treatment of mine water with FA in this study. Loss on ignition is the carbon content that passed through the combustion process of the feed coal.

Matla FA was found to contain potentially toxic elements such as Cr, Pb, Ba, Cu, Zn, V, etc. and radioactive elements such as U and Th that could leach into surface or ground water, if the FA is subjected to conditions that mobilise these elements. Mobilisation of these potentially toxic elements would enhance the bioavailability

of these elements, thereby posing a health risk to the surrounding ecosystem. The trace elements detected in Matla coal FA were limited to the standards that were available. If elements do not appear in Table 3.4, it does not necessarily mean that they are not available in coal FA.

Table 3.4: The elemental composition of Matla coal fly ash, obtained using XRF

Oxide	% RSD	% w/w	Element	% RSD	(mg/kg)
SiO_2	0.09	48.27 ± 0.044	Sr	-65	3495.55 ± 5.63
Al_2O_3	-0.52	30.89 ± 0.22	Ba	-11.67	2079.31 ±
CaO	-0.32	6.71 ± 0.08	Zr	9.00	787.73 ± 3.35
Fe_2O_3	-1.61	2.81 ± 0.03	Ce	1.79	226.02 ± 30.00
MgO	25	2.12 ± 0.04	Cu	-112.5	117.26 ± 3.38
TiO_2	-2.78	1.26 ± 0.02	La	2.75	111.45 ± 6.51
P_2O_5	0.53	0.89 ± 0.01	Y	2.80	103.71 ± 1.46
K_2O	0.15	0.84 ± 0.01	Nd	39.62	100.32 ± 2.45
Na_2O	-4.32	0.55 ± 0.01	Pb	2.50	100.25 ± 4.02
SO_3	NC	0.19 ± 0.002	Cr	NC	89.36 ± 2.29
MnO	12.50	0.02 ± 0.0004	Ni	18.5	88.97 ± 6.41
Loss on ignition	NC	5.24 ± 0	Rb	0.63	72.48 ± 0.89
Sum		99.79 ± 0.07	V	-75	64.91 ± 6.24
			Zn	-14	64.61 ± 4.41
			U	43.33	63.28 ± 2.43
			Ga	1.85	61.87 ± 1.89
			Nb	31.94	51.50 ± 1.80
			Th	3.92	46.60 ± 3.33
			As	26.67	20.07 ± 2.68
			Co	-100	16.08 ± 6.89
			Mo	NC	2.28 ± 0.02

NC = not calculated; % RSD = % relative standard deviation

The minor and trace elements in Matla FA were also analysed using LA-ICP-MS. The results obtained are as depicted in Table 3.5 below.

The results obtained using LA ICP-MS correlate well with the values obtained using XRF (for the minor elements analysed), although the values are not the same. The highest minor elements in Matla FA were found to be Ba and Sr which were in g/kg values, as shown in Tables 3.4 and 3.5. Concentration of other elements determined by LA ICP-MS did not agree with XRF results, but generally the relative abundances of these elements seemed to correlate well.

Minor and trace element analysis of Matla FA has shown that it contained about 34 elements. These elements included 16 (Ce, La, Nd, Y, Sc, Pr, Sm, Gd, Dy, Er, Eu, Ho, Tb, Tm and Lu) of the rare earth elements (REE), excluding promethium (Pm). The concentration of REE was found to be much higher than the normal concentration in the soil (Long et al., 2010). Rare earth elements have found wide applications in catalysis, magnetic resonance imaging and other applications in industry. It would be worthwhile to explore cheap technologies for recovering these elements from FA. Recovering these elements would minimise the release of these elements into the environment and provide a readily available source of these valuable minerals.

Table 3.5: Concentration of trace elements in Matla FA, obtained using LA-ICP-MS

Element	% RSD	mg/kg	Element	% RSD	mg/kg
Ba	8.25	2372.11 ± 32.01	Pr	6.32	18.35 ± 0.60
Sr	5.29	2137.02 ± 81.70	Co	2.35	17.30 ± 0.49
Zr	1.30	313.94 ± 19.57	Cs	1.55	13.64 ± 0.11
Ce	4.76	189.78 ± 4.13	U	7.64	13.38 ± 0.38
Cr	4.48	183.01 ± 2.41	Sm	8.95	11.95 ± 0.56
V	1.41	154.31 ± 3.49	Mo	8.26	10.45 ± 0.33
La	9.46	81.66 ± 4.31	Gd	6.36	10.40 ± 0.82
Pb	5.68	69.00 ± 1.78	Dy	5.42	9.50 ± 0.56
Nd	8.21	63.50 ± 1.78	Hf	7.03	8.63 ± 0.57
Cu	0.25	61.84 ± 0.96	Er	3.12	5.38 ± 0.28
Rb	3.87	55.46 ± 2.20	Yb	8.83	5.27 ± 0.47
Y	3.72	52.30 ± 3.47	Ta	4.34	2.69 ± 0.11
Ni	3.86	49.54 ± 1.80	Eu	9.48	2.35 ± 0.13
Zn	8.57	45.25 ± 2.67	Ho	4.81	1.97 ± 0.19
Nb	4.69	42.97 ± 1.35	Tb	7.23	1.60 ± 0.12
Th	10.56	35.44 ± 1.53	Tm	1.51	0.77 ± 0.06
Sc	1.71	24.94 ± 1.46	Lu	2.22	0.72 ± 0.04

% RSD = percentage relative standard deviation.

The radioactivity of Matla FA was assessed using gamma spectrometric analysis and the results are as shown in Table 3.6. There were no anthropogenic (man-made) radionuclides found in Matla coal FA. Only naturally occurring radionuclide materials (NORM) were detected, which were U, Th, Ra, Pb and K. The activities (Bq.kg^{-1}) were converted to mg/L using the relationship shown in equation 3.3 (Debertin, 1996):

$$1\text{Bq} = \frac{m}{Ar} \times N \times \frac{\ln 2}{t_{\frac{1}{2}}} \qquad \text{.....3.3}$$

$$where\ m = mass\ in\ g, Ar = atomic\ mass\ in\ g.mol^{-1},$$

$$N = Avogadro's\ number\ and\ t_{\frac{1}{2}} = half\ life\ in\ sec$$

Table 3.6: Gross alpha and beta radioactivity and the activity of the different radioisotopes in Matla coal FA

Nuclide	Activity ($Bq.kg^{-1}$)	Concentration (mg/kg)
^{238}U	186 ± 2	14.95 ± 0.0002
^{234}U	188 ± 2	$8.14 \times 10^{-4} \pm 8.68 \times 10^{-9}$
^{235}U	8.58 ± 0.009	$0.11 \pm 1.12 \times 10^{-7}$
^{232}Th	156 ± 3	$1.13 \times 10^{-6} \pm 1.07 \times 10^{-10}$
^{228}Th	184 ± 10	$38.42 \pm 7.4 \times 10^{-4}$
^{228}Ra	182 ± 13	$1.82 \times 10^{-8} \pm 2.46 \times 10^{-12}$
^{226}Ra	161 ± 9	$4.4 \times 10^{-6} \pm 1.3 \times 10^{-10}$
^{210}Pb	320 ± 32	$1.07 \times 10^{-6} \pm 1.07 \times 10^{-10}$
^{40}K	330 ± 39	$1.24 \pm 1.47 \times 10^{-4}$
Gross alpha	3440 ± 210	
Gross beta	1200 ± 20	

The results in Table 3.6 showed that Matla coal FA was much more radioactive than average radioactivity in soil. The radioactivity was found to be attributed to mainly ^{238}U, ^{234}U, ^{235}U, ^{232}Th, ^{228}Th, ^{228}Ra, ^{226}Ra, ^{210}Pb, and ^{40}K. The Th concentration in Matla coal FA was almost ten times greater than the concentration of ^{232}Th in soil samples collected from a gold mine dump in the Witwatersrand Goldfields, South Africa. The ^{238}U and ^{40}K concentration was comparable to a soil sample collected from a gold mine dump (Newman et al., 2008). The ^{232}Th activity of Matla coal FA was slightly greater than the average activity concentration of ^{232}Th in Greece. The activity concentration of ^{238}U and ^{40}K in Matla FA was within the range of the activity concentration found in Greek FA (Papastefanou, 2010; Baykal and Saygili, 2011; Turhan et al., 2010; USGS, 1997). Exposing the FA to aqueous conditions, such as in the remediation of AMD, might cause the mobilisation of these radioisotopes, thereby contaminating the treated water. So, it is necessary to find out if these radioisotopes are mobilised when Matla coal FA is mixed with AMD.

The total concentrations of Th obtained using XRF, LA ICP-MS and gamma analysis were close to each other. Th concentration obtained using LA-ICP-MS (35.44 mg/kg) was closer to that obtained using gamma spectrometry analysis (38.42 mg/kg) than that obtained using XRF (46.60 mg/kg). Scheid et al (2009) found that gamma spectrometry analysis and LA-ICP-MS gave Th results that were in agreement with each other when a brick clay was analysed using the two techniques. On the other hand, it was not possible to detect Th in brick clay at a concentration of less than 14 mg/kg of Th.

Uranium concentration obtained using XRF (63 mg/kg) was well above the values obtained using LA-ICP-MS (13.38 mg/kg), and the values using gamma spectrometry (14.95 mg/L). Thus, XRF analysis of radioactive elements such as U and Th was not deemed that accurate. In effect, XRF produced values that were higher than the more sensitive techniques such as gamma spectrometry and LA-ICP-MS. The accuracy of XRF analysis of U and other trace elements was not reliable because of the higher percentage relative standard

deviation of most trace elements, as shown in Table 3.2. Percentage relative standard deviation was calculated as follows:

$$\frac{Expected\ value - Analytical\ Value}{Expected\ value} \times 100 \quad \text{.....3.4}$$

where expected value is the value on the certified standard and analytical value is the value obtained when the certified was analysed

The total concentration of Pb in Matla coal FA, obtained using XRF and LA ICP-MS, was 100 mg/kg and 69 mg/kg respectively. Gamma spectrometry analysis of Pb showed that 1.07 x 10^{-6} mg/kg was the radioactive ^{210}Pb. Also, the gamma spectrometry analysis showed that 1.24 mg/kg of K was ^{40}K out of 6973 mg/L detected by XRF in Matla FA.

Fly ash has found significant application in the construction industry, but the limit of the activity concentration index for building materials (***I***) is 0.3-1 mSv per annum, which is calculated as follows (Risica, 1998; Somlai et al., 2008):

$$I = \frac{C_{Ra}}{300\,Bq \cdot kg^{-1}} + \frac{C_{Th}}{200\,Bq \cdot kg^{-1}} + \frac{C_{K}}{3000\,Bq \cdot kg^{-1}}, \quad \text{.....3.5}$$

where C_{Ra}, C_{Th}, C_K are activity concentrations in Bq.kg^{-1} for *Ra, Th* and *K* respectively.

The activity concentration index for Matla coal FA (according to Equation 4) was 2.96 mSv. This activity concentration index was three times the building materials upper limit of 1 mSv. This means that building materials containing coal FA from power stations in South Africa should be evaluated for a final activity concentration index prior to use in commercial applications.

The Matla coal FA analysed was made up of 59.76%, 24.84%, 12.88%, 1.57%, 0.68% and 0.21% of amorphous material, mullite, quartz, hematite, lime and gypsum respectively. It was also made up of potentially toxic elements such as Th, U, Ba, Pb, etc. This means that these elements could leach into mine water when coal FA is used for neutralisation of AMD. Therefore, the fate of these, potentially toxic, elements needs to be studied. Since coal FA contained radioactive elements such as Th and U, the radioactivity of the coal FA, before and after treatment of mine water, needs to be examined and removed if present, so that recovered water does not retain high radioactivity.

3.3.2 **Aluminium chlorohydrate**

The composition of aluminium chlorohydrate (ACH) was determined using ICP-OES and IC and the results are as shown in Table 3.7 below. From Table 3.7, ACH was acidic and comprised Al and Cl ions in its structure.

Table 3.7: The composition of aluminium chlorohydrate

Element	Concentration (mg/L) – except pH
pH	3.38
Al	135769
Cl	170578

The speciation of ACH was elucidated using GWB software, to determine how the Al and Cl are associated in the ACH gel. It was shown that Al existed as Al^{3+}, $Al_{13}O_4(OH)_{24}^{7+}$, $Al_3(OH)_4^{5+}$, $Al_2(OH)_2^{4+}$, $AlOH^{2+}$, $Al(OH)_2^{+}$, $Al(OH)_3$ and $Al(OH)_4^{-}$, as shown in Figure 3.4 below. Free Al^{3+} ions make up about 61% of the total Al concentration in ACH. Oligomeric Al species, such as $Al_{13}O_4(OH)_{24}^{7+}$, $Al_3(OH)_4^{5+}$and $Al_2(OH)_2^{4+}$, make up about 30, 6 and 2%, respectively, of the total Al concentration in ACH. Mononuclear species such as $AlOH^{2+}$, $Al(OH)_2^{+}$, $Al(OH)_3$ and $Al(OH)_4^{-}$ were in very low abundances in ACH.

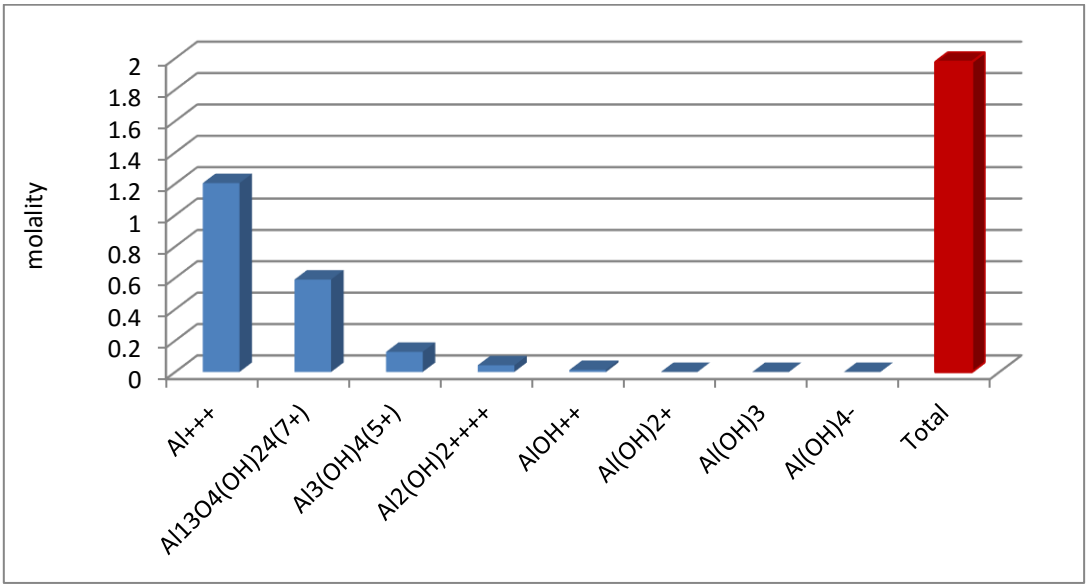

Figure 3.4: The Al species in aluminium chlorohydrate

The Cl species in ACH was determined using GWB software and are as shown in Figure 3.5 below. It was found that the Cl mainly existed as free Cl^- ions, with very low amounts of HCl species in ACH.

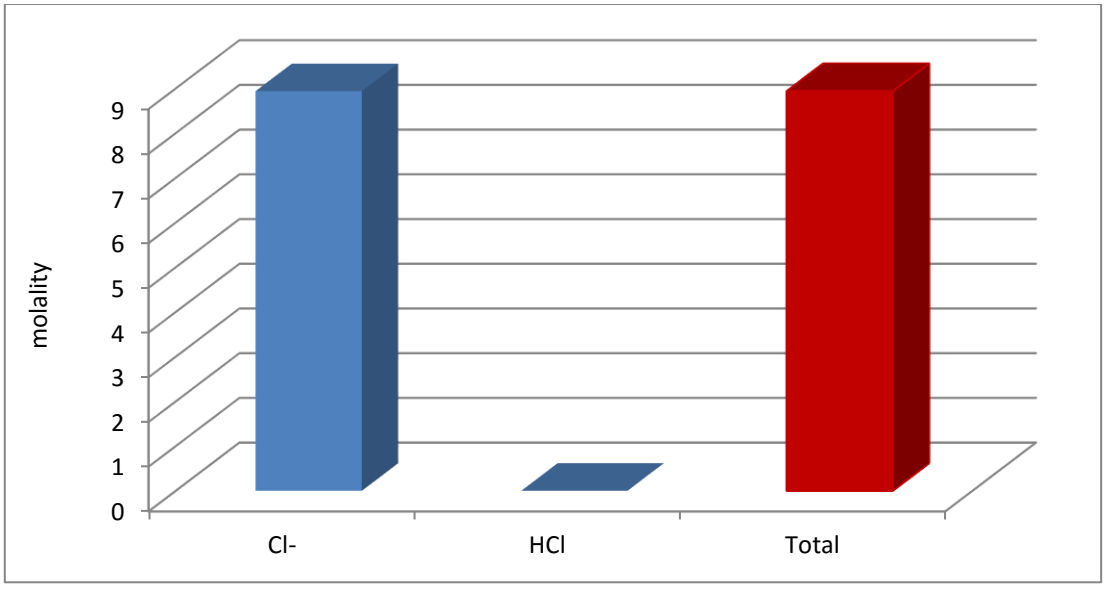

Figure 3.5: The Cl species in aluminium chlorohydrate

3.3.3 **Aluminium hydroxide**

Aluminium hydroxide was analysed using SEM to establish the morphological make up. It was established that $Al(OH)_3$ was made up of spherical particles with rough surfaces as shown in Figure 3.6a. The energy dispersive X-ray spectroscopy (EDS) spot analysis on selected areas in the microgram revealed that $Al(OH)_3$ was made up of mainly Al and O atoms, as shown in Figure 3.6b. The C atoms that are pronounced in the spectra were due to the C-coating of the sample before analysis.

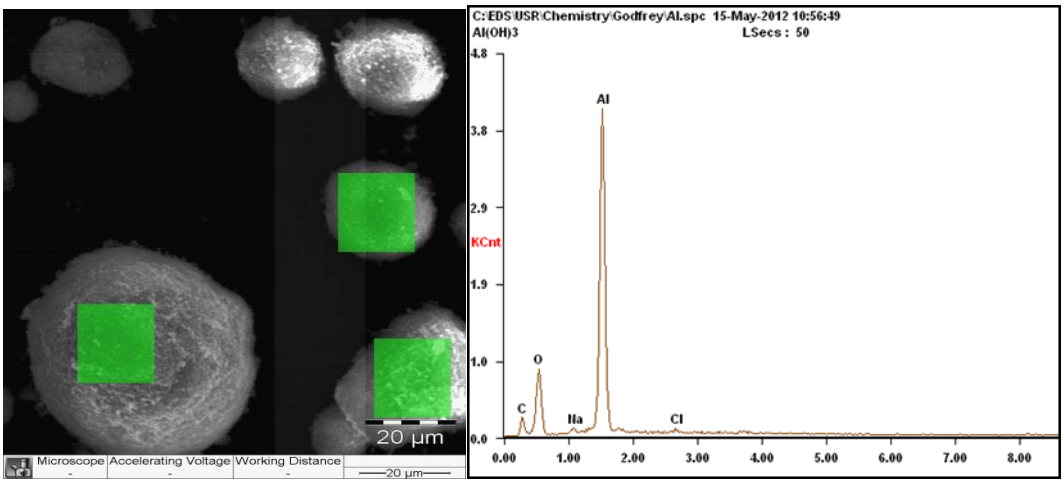

a **b**

Figure 3.6: The SEM microgram (a) and the EDS spot analysis (b) of $Al(OH)_3$

The mineral phases of $Al(OH)_3$ were determined using XRD, and the spectrum is shown in Figure 3.7 below. $Al(OH)_3$ was made of bayerite ($Al_2O_3.3H_2O$) and boehmite (AlOOH) mineral phases. These results correlated well with the EDS composition obtained, which showed that $Al(OH)_3$ was made of almost exclusively Al and O atoms (Figure 3.6b).

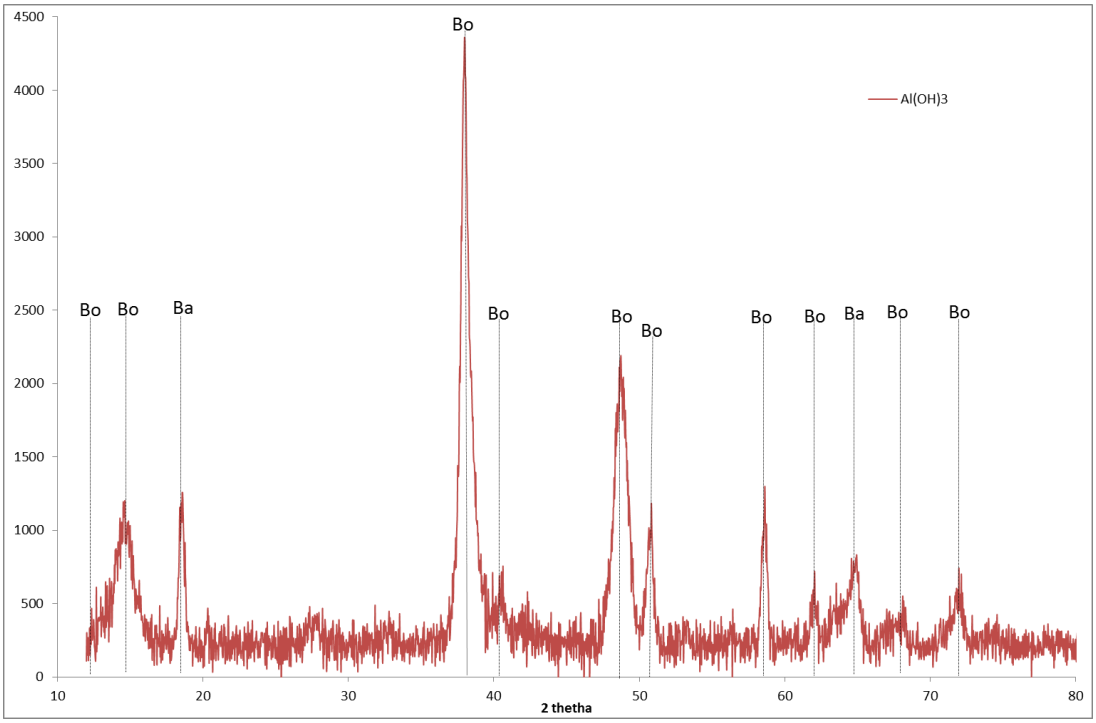

Figure 3.7: XRD spectrum of $Al(OH)_3$ (Bo =boehmite; Ba =bayerite)

3.3.4 **Lime**

Lime was analysed using SEM to determine its structure, as shown in Figure 3.8a. Figure 3.8b shows the EDS compositional spot analysis results of lime. It was observed that lime was made of agglomerated irregular particles which were mainly made up of Ca and O atoms.

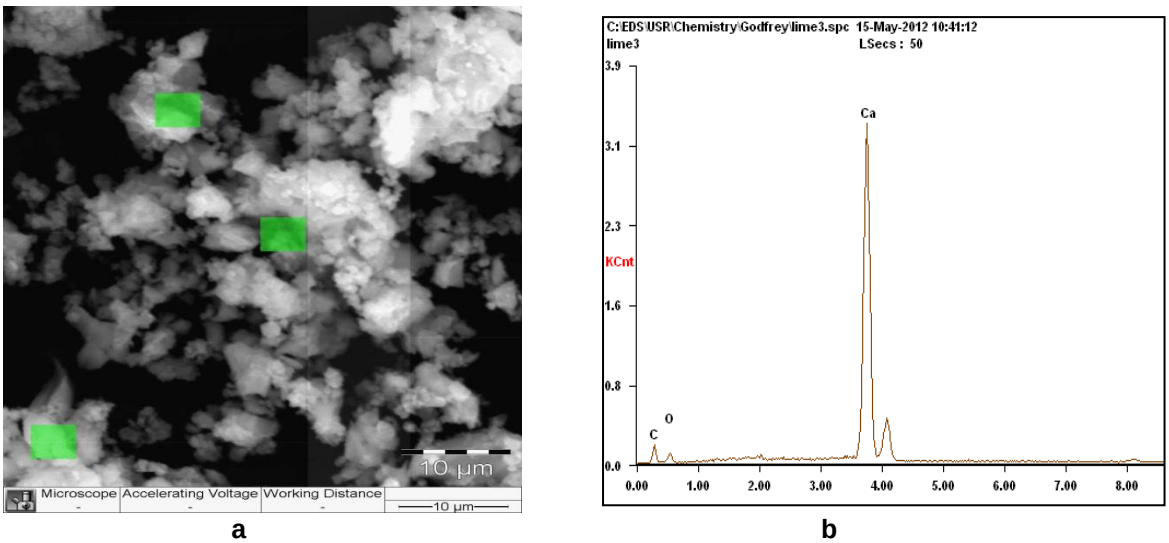

a **b**

Figure 3.8: SEM (a) and the EDS (b) analysis of lime

Quantification of lime composition was conducted using XRF. According to the XRF results, the lime was found to be mainly composed of CaO, which made up about 72%, as shown in Table 3.8. The other major component of the lime was loss on ignition (LOI), which made up about 27%. The LOI in this case can be attributed to moisture content. This correlates well with the EDS results.

Table 3.8: Elemental composition of lime

Oxide	Composition (% w/w)
CaO	72.19
MgO	0.72
Na_2O	0.23
SiO_2	0.12
Al_2O_3	0.09
Fe_2O_3	0.06
K_2O	0.02
MnO	0.02
P_2O_5	0.01
TiO_2	0.01
Loss on ignition	26.65
Total	**100.12**

Mineralogical analysis of the lime, using XRD, showed that it is indeed made up of mainly lime (CaO) and calcite ($CaCO_3$) minerals, as shown in Figure 3.9. Calcite could have resulted from the interaction of CaO with CO_2 from the atmosphere.

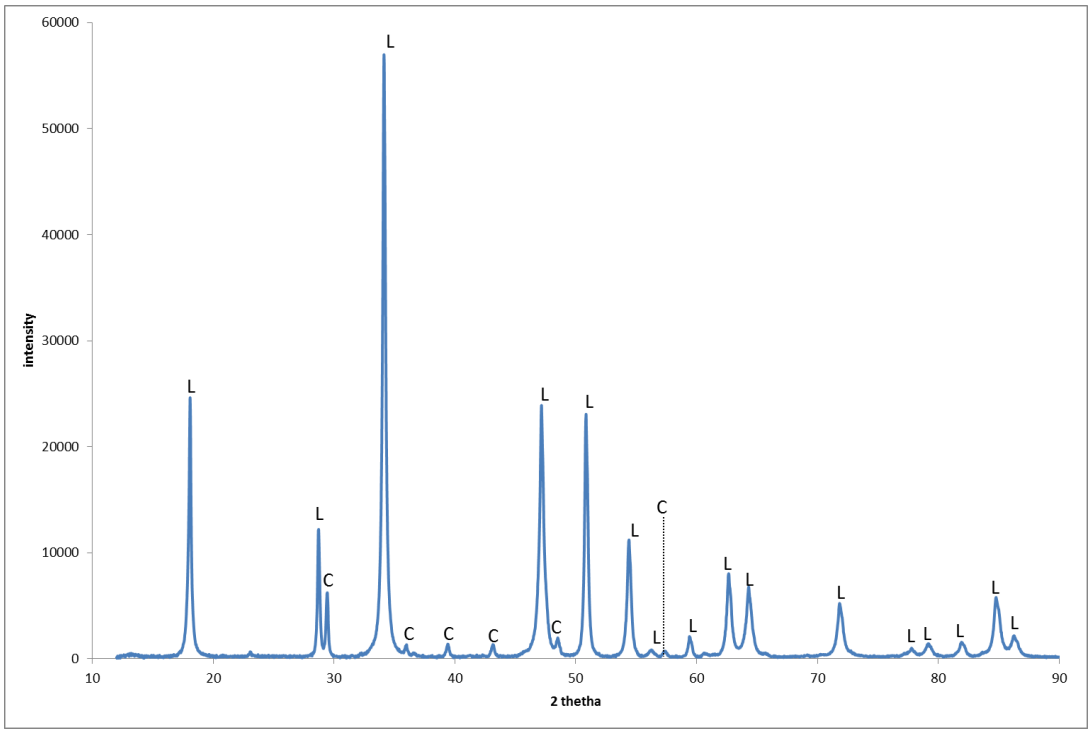

Figure 3.9: XRD spectrum of lime (L-lime and C-calcite)

3.3.5 **Matla mine water**

Matla mine water was collected from the Matla coal mine in Mpumalanga province. The composition of the mine water was determined using ICP-OES and IC. The results are shown in Table 3.9. Matla mine water was

formed from the oxidation of pyrite, followed by *in situ* neutralisation by the acid-neutralising mineral NaOH (equation 3.6). This resulted in water with a pH near neutral, containing elevated concentrations of Na and sulphate ions.

$$FeS_2 + 3NaOH + H_2O + \tfrac{13}{2}O_2 \rightarrow Fe(OH)_3 + 3Na^+ + 2CO_2 + 2SO_4^{2-} + 2OH^- \quad \text{.....3.6}$$

From Table 3.9, the mine water from Matla coal mine is neutral mine drainage (NMD) because the pH lies between 6 and 8 (Morin and Hutt, 1997; Younger et al., 2002).

Table 3.9: The physiochemical parameters of Matla mine water

pH	-	8.00
Electrical conductivity (EC)	uS/cm	3371
Alkalinity	mg/L of $CaCO_3$	561.6
TDS	mg/L	1955
Sulphate	mg/L	1475
Na	mg/L	886.6
Ca	mg/L	70.35
Mg	mg/L	39.54
B	mg/L	14.93
K	mg/L	10.08
Hg	mg/L	2.43
Sr	mg/L	2.05
Se	mg/L	1.12
Zn	mg/L	0.41
Ba	mg/L	0.2
Cu	mg/L	0.19
Fe	mg/L	0.06
Al	mg/L	0.056
Mn	mg/L	0.0094
As	mg/L	0.0027
Cr	mg/L	nd
Pb	mg/L	nd
Rb	mg/L	nd
Ni	mg/L	nd
Co	mg/L	nd
Th	mg/L	nd
U	mg/L	nd

The water contained very low concentrations of Fe, Al and Mn. This was because at a pH greater than 6, Fe and Al precipitate out as hydroxides, while Mn is known to precipitate out at pH values greater than 9 (Gitari

et al., 2008, Petrik et al., 2006). Elevated concentrations of sulphate ions cause water to have a taste. The extent of the taste varies with the cation associated with the sulphate ion. For water containing sulphate ions associated with Na ions such as Matla mine water, the taste threshold is 250 mg/L. If the sulphate ions are associated with Ca, the taste threshold is approximately 1000 mg/L (WHO, 2004). Water containing a sulphate concentration of greater than 1000 mg/L can have a laxative effect on individuals who have not adapted to the water (WHO, 2004). This means that Matla mine water can have a noticeable taste and can also have a laxative effect on individuals who are not used to the water.

3.3.6 **Rand Uranium mine water**

Rand Uranium mine water was collected from the West Rand basin in the Witwatersrand Gold Fields, South Africa. The mine is a semi-abandoned mine, since only tailings are mined and no underground mining is taking place anymore. The pH, EC and TDS were measured on-site. The chemical composition of the samples was analysed using IC and ICP-OES and the results are as shown in Table 3.10.

Rand Uranium mine water was AMD, because the pH is below 5 (Morin and Hutt, 1997; Younger et al., 2002). Rand Uranium mine water has high concentrations of Fe and Al. Typically, AMD contains more of the combined concentrations of Fe, Al and Mn than the combined concentrations of Ca, Mg and Na. and the converse is true for NMD (Cravotta et al, 1990; Lottermoser, 2007; Younger et al., 2002).

Table 3.10: The physiochemical parameters of Rand Uranium mine water

pH		2.65
Electrical conductivity (EC)	uS/cm	2000
Acidity	mg/L of $CaCO_3$	266.34
TDS	mg/L	1076
Sulphate	mg/L	2562
Fe	mg/L	201.10
Ca	mg/L	360.1
Mn	mg/L	60.16
Mg	mg/L	153
Na	mg/L	89.44
Cl	mg/L	26.89
B	mg/L	0.231
Al	mg/L	26.63
Cr	mg/L	0.023
Pb	mg/L	0.0075
K	mg/L	6.47
Cu	mg/L	0.28
U	mg/L	0.27
Sr	mg/L	0.45
Zn	mg/L	1.93

Th	mg/L	0.018
P	mg/L	0.024
Ba	mg/L	0.026
Li	mg/L	0.069
Hg	mg/L	3.93×10^{-6}
As	mg/L	0.0058
Se	mg/L	0.061

In the West Rand basin, Au occurs in association with FeS_2. Pyrite makes up about 3% of the Au mineral (Durand, 2012). Therefore, Rand Uranium mine water was formed by oxidation of the acid-producing mineral FeS_2 (Equation 3.7), containing insufficient proportions of acid-neutralising minerals such as dolomite and limestone, resulting in acidic water. The acidity generated from FeS_2 caused the weathering of surrounding rocks, causing the leaching of potentially toxic elements into the water.

$$FeS_2 + \tfrac{7}{2}O_2 + H_2O \rightarrow Fe^{3+} + 2H^+ + 2SO_4^{2-} \quad \text{.....3.7}$$

Rand Uranium mine water contained elevated concentrations of Fe, Mn, Al, Pb and sulphate, which were above the limit for potable, industrial and agricultural purposes (DWAF, 1996; WHO, 2004). Also, the U concentration was well above the limit for potable water. The concentrations of Ca and Mg were also above the limit for potable water. The pH of Rand Uranium mine water makes it unsuitable for domestic, agricultural and industrial use (DWAF, 1996; WHO, 2004) and other parameters make it unsuited for potable use.

3.3.7 **Radioactivity of Rand Uranium mine water**

The geology of the West Rand basin is made of more U minerals than Au-bearing minerals (Cole, 1998). Analysis of the Rand Uranium mine water for radioactivity was carried out using alpha and gamma spectrometry. The results obtained indicated that the gross alpha and beta radioactivity of the mine water was 12 and 6 times more than the required limit for potable water respectively, as shown in Table 3.11. The maximum gross alpha and beta radioactivity for potable water is 0.5 $Bq.L^{-1}$ and 1 $Bq.L^{-1}$ respectively (WHO, 2011).

Table 3.11: Alpha, beta and isotope activities of Rand Uranium mine water

Isotope	Activity ($Bq.L^{-1}$)	Concentration (µg/L)	WHO, 2011 ($Bq.L^{-1}$)
^{238}U	3.16 ± 0.04	253.99 ± 3.22	10
^{234}U	4.71 ± 0.05	$0.020 \pm 2.17 \times 10^{-4}$	1
^{230}Th	0.69 ± 0.11	$9.59 \times 10^{-4} \pm 1.47 \times 10^{-4}$	1
^{226}Ra	0.36 ± 0.01	$9.87 \times 10^{-6} \pm 2.74 \times 10^{-7}$	1
^{210}Po	0.02 ± 0.0037	$4.47 \times 10^{-8} \pm 8.10 \times 10^{-9}$	0.1
^{235}U	0.145 ± 0.002	1.81 ± 0.025	1
^{227}Th	0.202 ± 0.016	$1.77 \times 10^{-10} \pm 1.41 \times 10^{-11}$	10
^{229}Ra	0.101 ± 0.01	$1.33 \times 10^{-14} \pm 1.32 \times 10^{-15}$	-
^{232}Th	0.0619 ± 0.071	15.24 ± 1.75	1
^{228}Th	0.124 ± 0.01	$4.23 \times 10^{-9} \pm 3.41 \times 10^{-10}$	1
^{224}Ra	0.0306 ± 0.045	$5.11 \times 10^{-12} \pm 7.51 \times 10^{-13}$	1
gross alpha	6.01 ± 0.93		0.5
gross beta	6.05 ± 0.41		1

Radioisotopes that contributed to the radioactivity of Rand Uranium mine water were; ^{238}U, ^{234}U, ^{230}Th, ^{226}Ra, ^{235}U, ^{227}Th, ^{229}Ra, ^{232}Th, ^{228}Th, and ^{224}Ra. The activities of radioisotopes that were greater than the allowed limit for potable water were ^{234}U, ^{235}U and ^{228Th}, as shown in Table 3.11. If U accumulates in the kidneys, it causes kidney failure (WHO, 2011). Total U concentration that was determined in Rand Uranium mine water was about 256 µg/L. This was well above the allowed limit for total U concentration set by the WHO in 2011, which is 30 µg/L. Analysis of Rand Uranium mine water with ICP-OES showed that the water contained 290 µg/L of U and 18 µg/L of Th, as shown in Table 3.11. These results were close to those obtained using alpha and gamma spectrometry which found that the concentrations of U and Th were about 256 µg/L and 15 µg/L, respectively. This showed that ICP-OES can be used to analyse radioactive elements such as Th and U (in aqueous solutions), as an alternative to sophisticated, rigorous and expensive analytical techniques such as alpha and gamma spectrometry. There were no radioactive isotopes for K and Pb detected in Rand Uranium mine water using alpha and gamma spectrometry.

The radioactivity detected in the mine water is attributed to the fact that U is mined in addition to Au mining at Rand Uranium mine. The exposure of FeS_2 to oxidizing conditions results in formation of AMD. The strong acidity of the water enhances the dissolution of the associated U-containing minerals, resulting in AMD which is radioactive. Since the radioactivity of Rand Uranium mine water was much greater than the required limit for potable water, the treated water was evaluated for radioactivity as well and the activity was found to be significantly reduced, as is shown in Chapter 7.

CHAPTER 4: MODELLING OF MINE WATER AND FLY ASH/MINE WATER

4.1 INTRODUCTION

The Geochemist's Workbench (GWB) is a software package comprising different programmes to manipulate chemical reactions, calculate stability diagrams and the equilibrium states of natural waters, trace reaction processes, model reactive transport, plot the results of these calculations, and store the related data (Bethke and Yeakel, 2010). In this study, SpecE8 and Act2 programs of the GWB 8.0 essential software were used. SpecE8 is capable of calculating species distribution in aqueous solutions, mineral saturation indices and gas fugacity. SpecE8 can also account for sorption of species onto mineral surfaces according to a variety of methods, including surface complexation and ion exchange. The Act2 program calculates and plots activity-activity diagrams. These diagrams show the stability of minerals and predominance of aqueous species in chemical systems. Variables of the axes of the stability diagrams include species activity, gas fugacity, activity or fugacity ratio, pH, and redox potential (Bethke and Yeakel, 2010).

4.1.1 SPECIES DISTRIBUTION

Speciation, as defined here, is the chemical form in which ions exist in aqueous or natural waters. Speciation is extremely important as the bioavailability of an ion or element as a required nutrient or toxicant depends on its chemical form. The toxicology of some elements is very complex because some elements can be toxic in one form and in another be an essential nutrient (Jain and Ali, 2000; Florence et al., 1992; Allen et al., 1980). Mostly hydrated metal ions are considered to be toxic, whilst complexed species are usually deemed less toxic (Russeva, 1995). Different analytical protocols and models have been used to elucidate the different forms of ions in natural water. In this study, GWB software was used to speciate the ions that were detected in Matla mine water and Rand Uranium mine water using ICP-OES and IC. The Act2 program of the GWB software was used to calculate the species distribution and the saturation indices of the different minerals in Rand Uranium mine water and Matla mine water. The Rand Uranium mine water sample was taken from a decant site in Krugersdorp and the Matla mine water sample was collected from the underground water pumping during coal mining. The mine waters samples were characterized by their pH, EC, alkalinity and acidity and the concentration of individual ions. The pH and EC of the mine water was measured in the field. Alkalinity was determined using a Metrohm Autotitrator. The elemental composition of Rand Uranium and Matla mine water was obtained using ICP-OES and IC and was presented in Chapter 3.

4.2 RESULTS AND DISCUSSION

The results of modelling carried out on the mine water before and after interaction with Matla FA are presented in this section. The modelling was carried out to predict the distribution of species in Matla mine water and the mineral phases formed after interaction with FA.

4.3 PREDICTION OF THE MINERAL PHASES IN MINE WATER

During treatment of mine water with alkaline ameliorants such as fly ash and/or lime, potentially toxic constituents are mainly removed through precipitation. The Act2 program of the GWB software was used to predict the aqueous species distribution in Matla mine water and any stable mineral phases that may form during precipitation of potentially toxic elements/ions from Rand Uranium and Matla mine water. The prediction was done using the analytical and physical results determined by IC, ICP-OES, pH/EC/TDS meter and the autotitrator. The independent variable was chosen as $\log_a Ca^{2+}$ and the dependent variable was the pH. These values were chosen based on the fact that treatment of mine water with coal is based on the neutralisation of pH due to the dissolution of the lime fraction in coal FA.

4.3.1 Aqueous distribution of major elements in Matla mine water

The physiochemical properties of Matla mine water were used for modelling the aqueous species distribution in Matla mine water. Matla mine water was speciated using the SpecE8 sub program of the GWB software. Matla mine water was found to be a Na-SO_4 type of water. This means that the main cation for Matla mine water was Na and the water contained sulphate ions as the main anion. The predicted distribution of Mg species in Matla mine water, obtained using the GWB SpecE8 program, is shown in Figure 4.1 below.

From Figure 4.1, the Mg species in Matla mine water were found to be mainly free Mg^{2+} ions and $MgSO_4$ which made up 65% and 31% respectively of the total Mg content in Matla mine water. $MgHCO_3^-$ species contributed about 4% of the total Mg content. Other species, such as $MgCl^+$, $MgCO_3$, $MgB(OH)_4^+$, $MgOH^+$, $Mg_2CO_3^{2+}$, Mg_2OH^{3+} and $Mg_4(OH)_4^{4+}$, contributed less than 0.05% of the total Mg content in Matla mine water.

Sulphate species in Matla mine water that were predicted using the GWB SpecE8 program are depicted in Figure 4.2. The program predicted that sulphate existed mainly as free SO_4^{2-} ions, which constituted about 86% of the total sulphate ions. About 7%, 4% and 3% of the sulphate ions comprised $NaSO_4^-$, $CaSO_4$ and $MgSO_4$ species, respectively. Less than 0.1% of the sulphate content in Matla mine water was comprised of KSO_4^-, $SrSO_4$, $ZnSO_4$, $BaSO_4$, HSO_4^-, $MnSO_4$, $AlSO_4^+$, $Al(SO_4)_2^-$, $CuSO_4$, $Al_{13}O_4(OH)_{24}^{7+}$, $FeSO_4^+$, $Fe(SO_4)_2^-$, H_2SO_4 and $FeHSO_4^{2+}$.

There was an appreciable amount of sulphate predicted to be associated with Na in Matla mine water (7%). This was because the Na concentration in Matla mine water was very high. The amount of Mg and Ca associated with sulphate in Matla mine water was similar to each other because the molar concentration of Ca

and Mg in Matla mine water was almost identical. The sulphate species associated with Fe was insignificant in Matla mine water. This was because the Fe concentration in Matla mine water was very low.

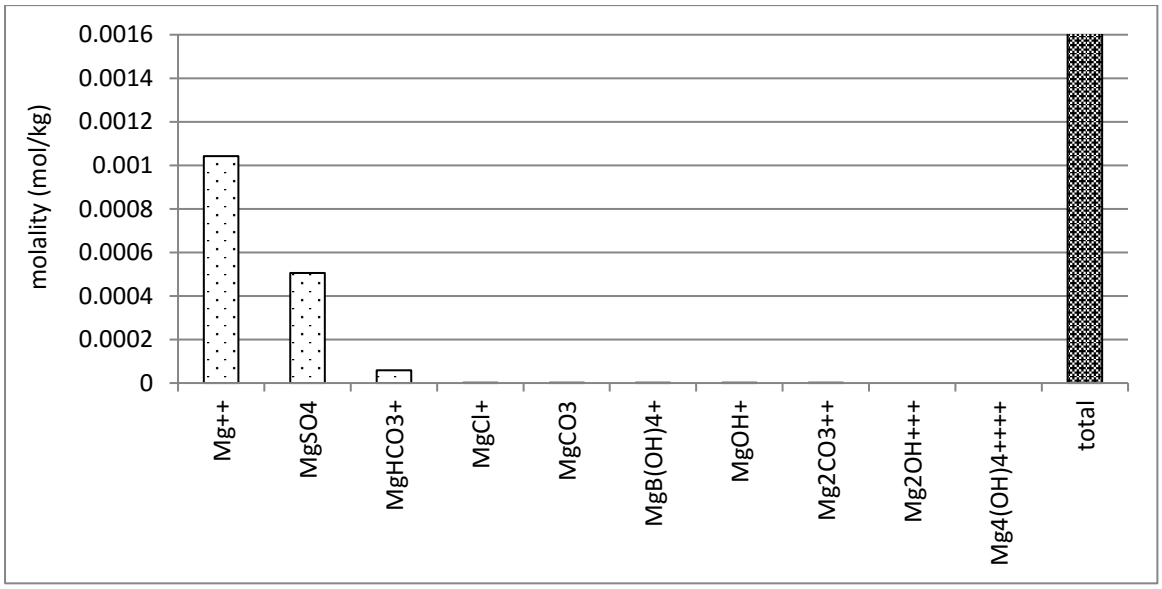

Figure 4.1: Magnesium aqueous species distribution in Matla mine water

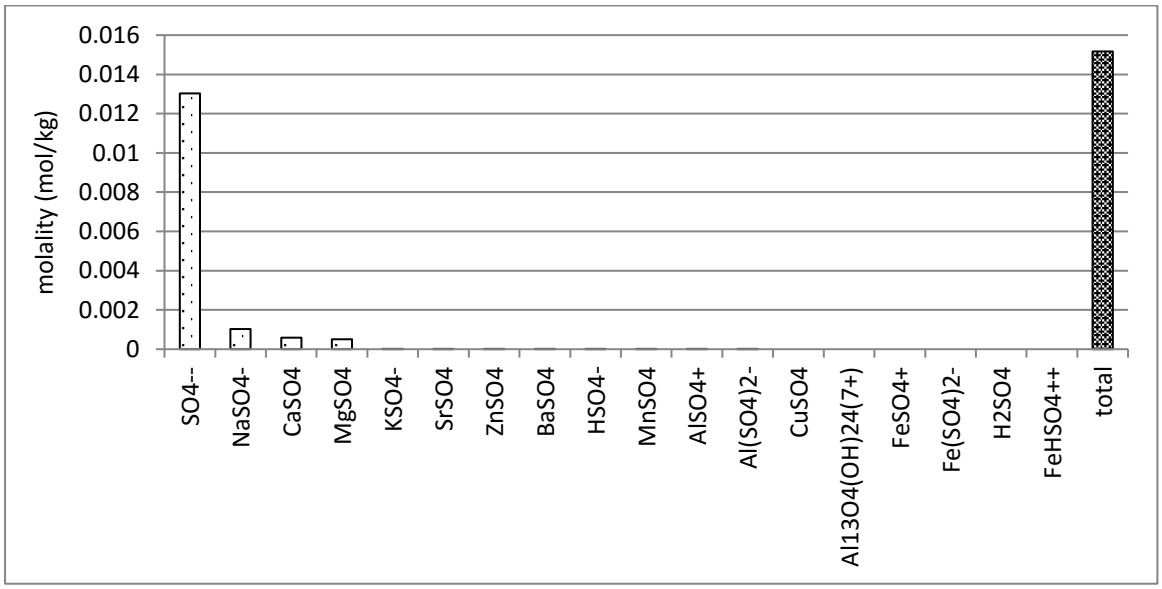

Figure 4.2: Sulphate aqueous species distribution in Matla mine water

The speciation of aluminium in Matla mine water is shown in Figure 4.3. Most of the Al species in Matla mine water (Figure 4.3) were associated with hydroxyl ions, which make up about 99% of the total Al concentration. These hydroxyl Al species were $Al(OH)_4^-$, $Al(OH)_3$, $Al(OH)_2^+$ and $AlOH^{2+}$. The Al species that were associated with sulphate ions; $AlSO_4^+$ and $Al(SO_4)_2^-$, made up less than 1% of the total Al content. Free Al^{3+} in Matla mine water was less than 0.5%. The oligomeric species of Al, i.e. $Al_{13}O_4(OH)_{24}^{7+}$, $Al_2(OH)_2^{4+}$ and $Al_3(OH)_4^{5+}$, were negligible.

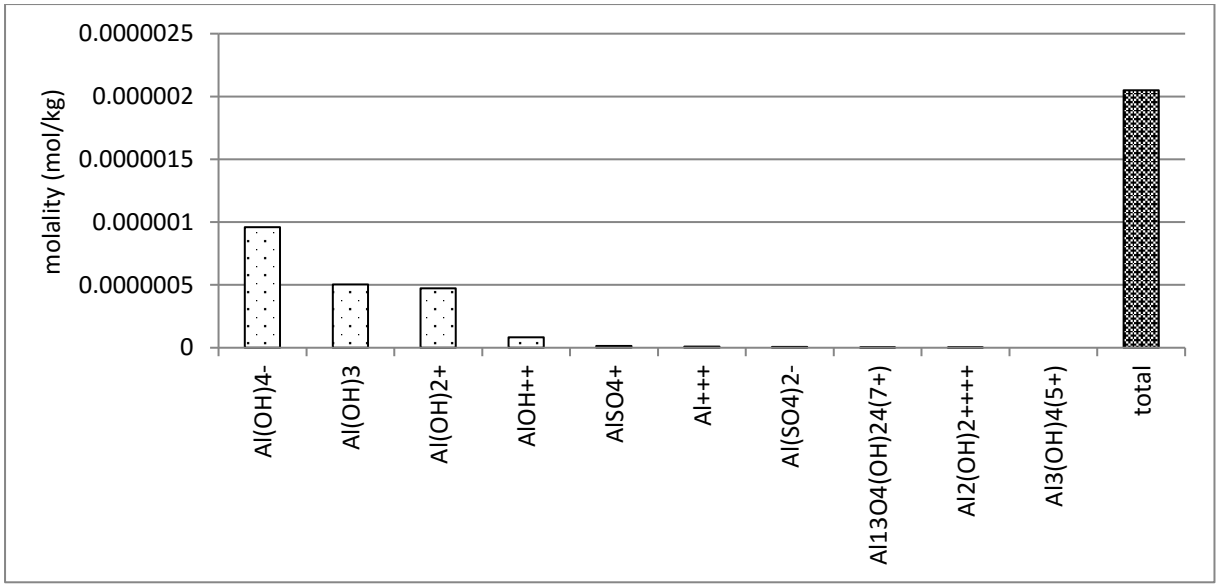

Figure 4.3: Aluminium aqueous species distribution in Matla mine water

The speciation of Fe in Matla mine water is shown in Figure 4.4. The GWB SpecE8 program showed that Fe mainly existed in the form of hydroxyl species. The species were 64% $Fe(OH)_2^+$ and 35% $Fe(OH)_3$.

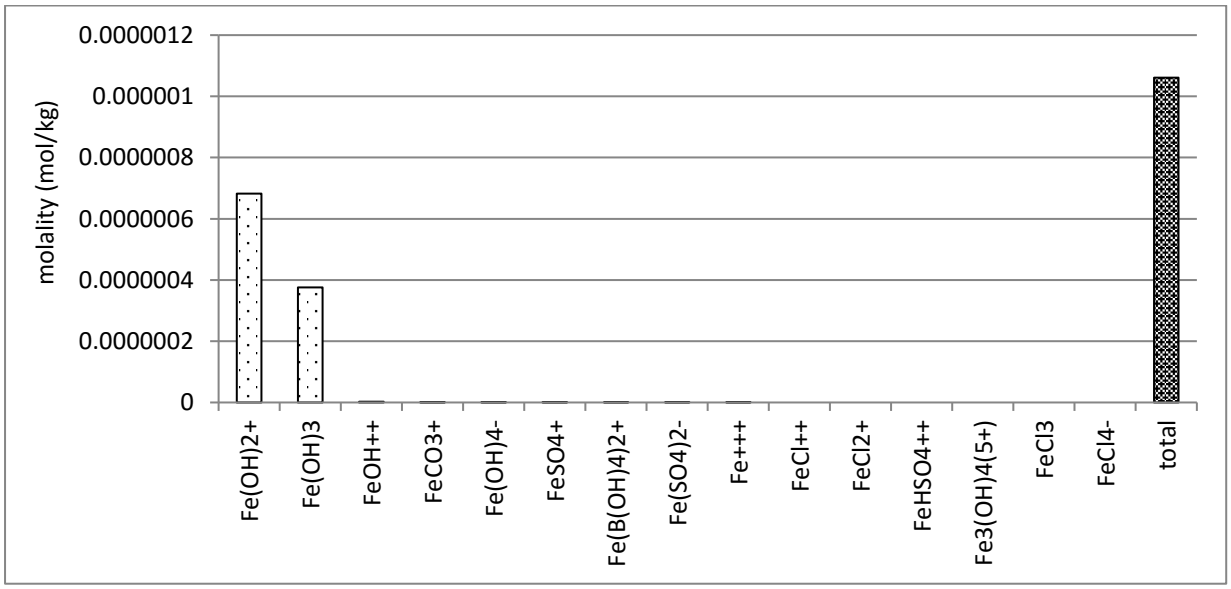

Figure 4.4: Iron aqueous species distribution in Matla mine water

The other Fe species predicted by GWB software comprised less than 1% of the total Fe content in Matla mine water. These species were $FeOH^{2+}$, $FeCO_3^+$, $Fe(OH)_4$, $FeSO_4^+$, $Fe(B(OH)_4)_2^+$, $Fe(SO_4)_2^-$, Fe^{3+}, $FeCl^{2+}$, $FeCl_2^+$, $FeHSO_4^{2+}$, $Fe_3(OH)_4^{5+}$, $FeCl_3$ and $FeCl_4^-$.

In the case of Ca, the predicted species in Matla mine water were mainly free Ca^{2+} and $CaSO_4$ species, as shown in Figure 4.5. These species contributed respectively about 61% and 34% of the total Ca content. $CaHCO_3^+$ species made up about 5% of the total Ca content. The other aqueous species, such as; $CaCl^+$, $CaCO_3$, $CaB(OH)_4^+$ and $CaOH^+$, were negligible in Matla mine water.

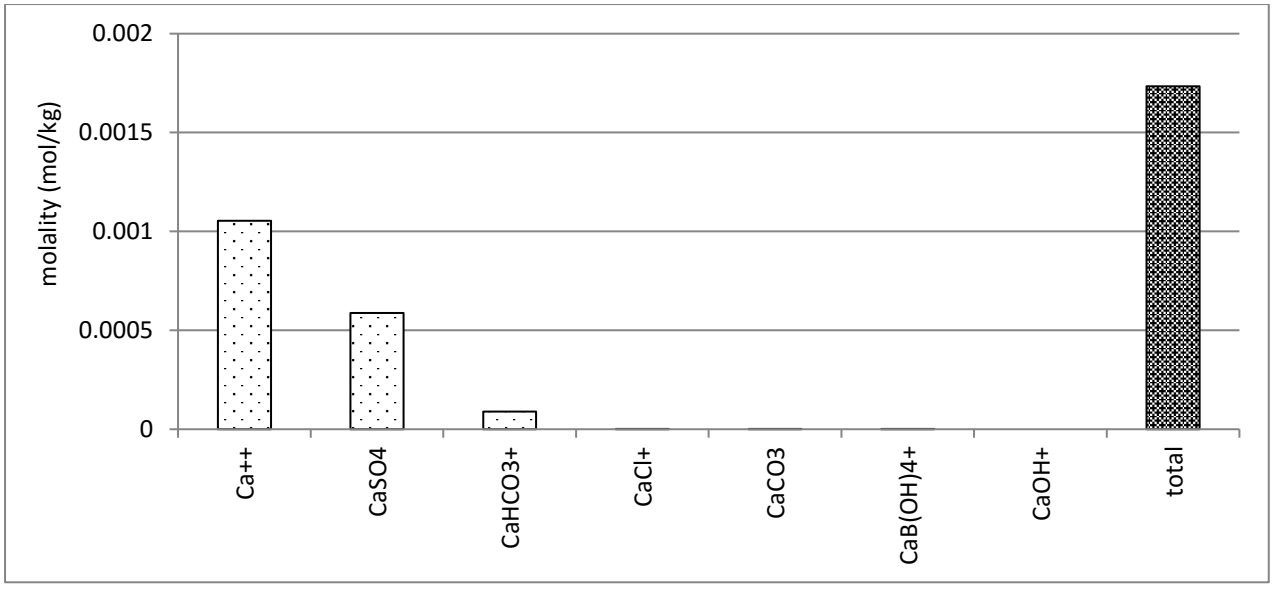

Figure 4.5: Calcium aqueous species distribution in Matla mine water

The Mn present in Matla mine water was predicted to be distributed mainly between Mn^{2+} ions and $MnSO_4$ which contributed about 62% and 32% respectively, as shown in Figure 4.6. About 6% of Mn present in Matla mine water was predicted to be in the form of $MnHCO_3^+$. The other species; $MnCO_3$, $MnOH^+$, $MnCl_2$, $Mn(OH)_2$, Mn_2OH^{3+}, $Mn_2(OH)_3^+$, $Mn(OH)_3^-$ and $Mn(OH)_4^{2-}$, constituted less than 0.07% of the total Mn content in Matla mine water.

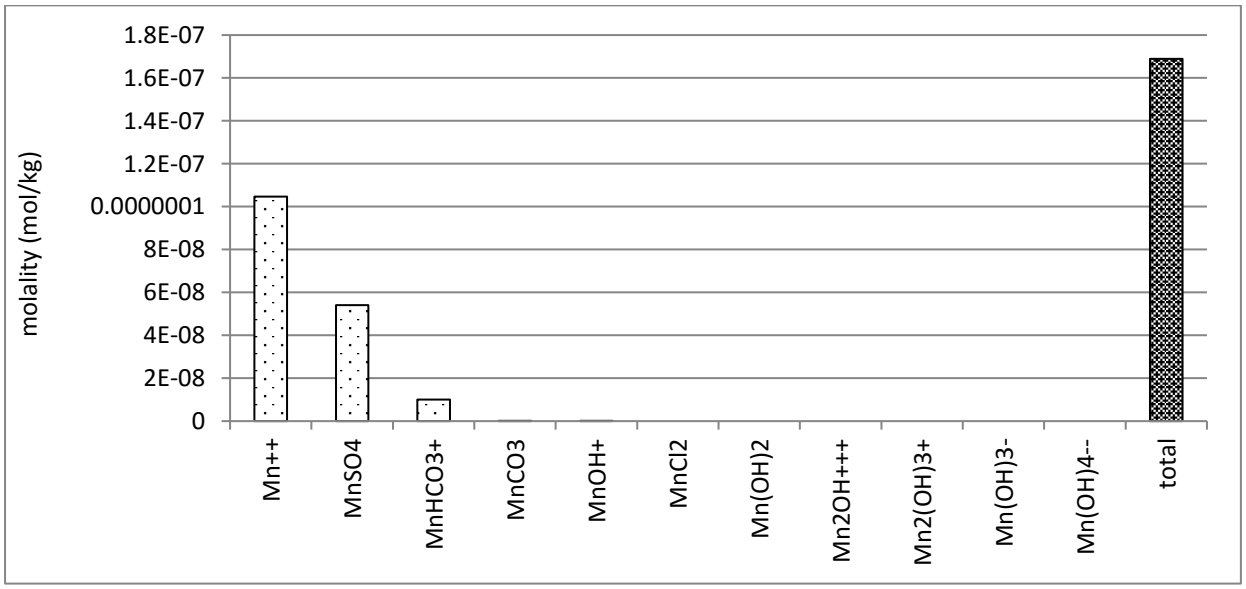

Figure 4.6: Manganese aqueous species distribution in Matla mine water

Sodium species in Matla mine water were comprised of free Na^+ ions which constituted about 96.2% of the total Na content, as shown in Figure 4.7. The other Na species were comprised of $NaSO_4^-$ which constituted about 3% in Matla mine water.

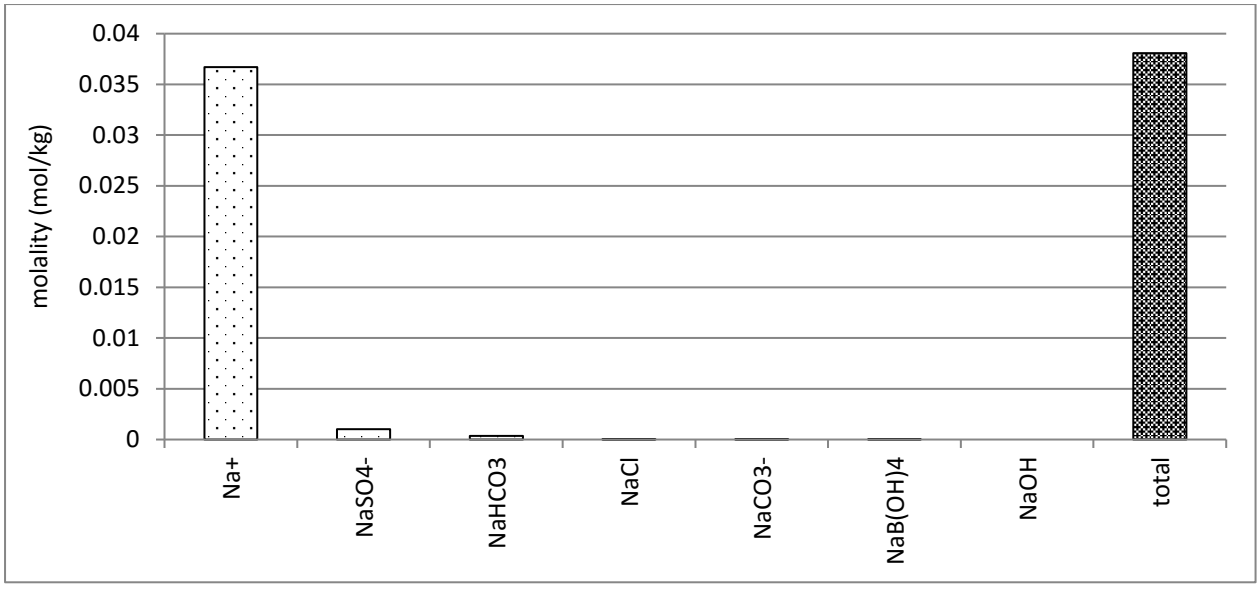

Figure 4.7: Sodium aqueous species distribution in Matla mine water

Other Na species in Matla mine water, as predicted using GWB software, were $NaHCO_3$, NaCl, $NaCO_3^-$, $NaB(OH)_4$ and NaOH. These species contributed an insignificant percentage to the total Na content in Matla mine water. This shows that Na is a very conservative element that exists mainly as free ions in the aqueous media. This was because Na mainly existed as a free ion in Matla mine water.

The K concentration was predicted to be mainly free K^+ species, which constituted about 96%, as shown in Figure 4.8. The KSO_4^- species in Matla mine water contributed about 4% of the total K content.

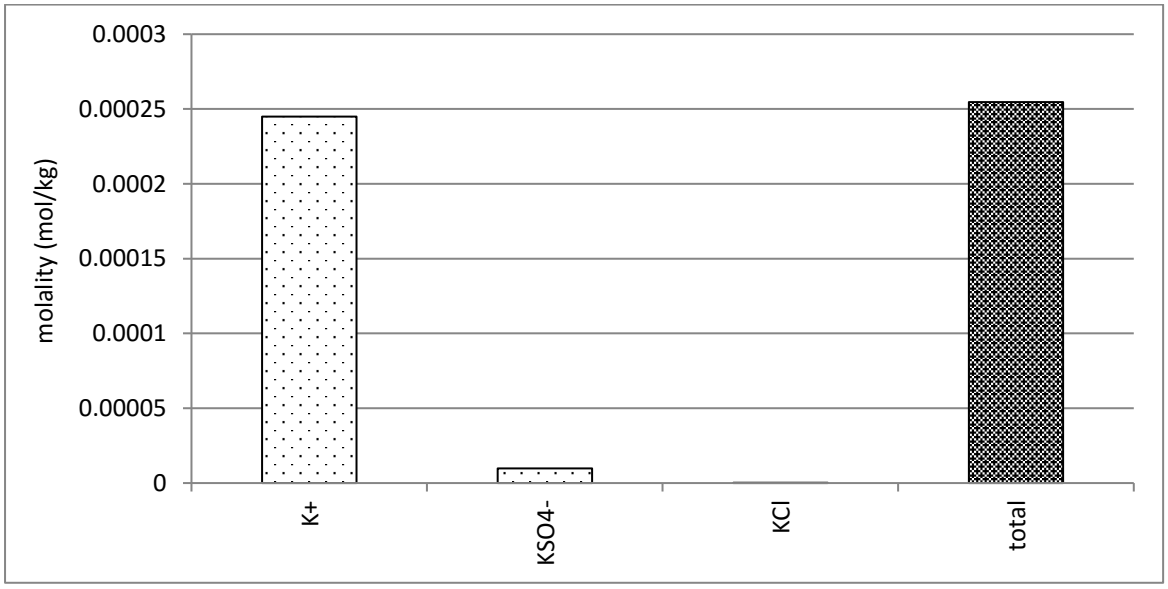

Figure 4.8: Potassium aqueous species distribution in Matla mine water

The KCl species were negligible in terms of the total K content in Matla mine water. Just like Na, K is also a conservative mineral because it mainly exists as free K^+ ions in aqueous media.

4.3.2 **Aqueous distribution of major elements in Rand Uranium mine water**

The physicochemical properties of Rand Uranium mine water, speciated using the GBW Spec8 program, are shown in Table 3.10. The predicted distribution of the Mg species in Rand Uranium mine water is shown in Figure 4.9 below. The Mg species in Rand Uranium mine water existed mainly as free Mg^{2+} and $MgSO_4$ species which constituted about 61% and 39%, respectively, of the total Mg species distribution. Other species; $MgCl^+$, $MgH_2PO_4^+$, $MgB(OH)_4^+$, $Mg(OH)^+$, $MgHPO_4$, Mg_2OH^{3+}, $MgPO_4^-$ and $Mg(OH)4^{4+}$, constituted less than 0.07% of the total Mg species distribution in Rand Uranium mine water, as shown in Figure 4.9.

Sulphate species distribution in Rand Uranium mine water is as shown in Figure 4.10. The distribution of sulphate species was mainly comprised of free SO_4^{2-} ions. Figure 4.10 shows that free sulphate ions in Rand Uranium mine water amounted to about 57% of the total sulphate species. About 19%, 9%, 4%, 4% and 3% of the total sulphate species comprised of $FeSO_4^+$, $CaSO_4$, $MgSO_4$, $MnSO_4$, $Fe(SO_4)_2^-$ respectively. Less than 0.1% of the total sulphate species in Rand Uranium mine water was comprised of HSO_4^-, $NaSO_4^-$, $AlSO_4^+$, $Al(SO_4)_2^-$, $FeHSO_4^{2+}$, $ZnSO_4$, $SrSO_4$, KSO_4^-, $Th(SO_4)_2$, $U(SO_4)_2$, $BaSO_4$, $Th(SO_4)_3^{2-}$, $ThSO_4^{2+}$, USO_4^{2+}, H_2SO_4, $CuSO_4$.

Aluminium aqueous species in Rand Uranium mine water are as shown in Figure 4.11. Most of the Al species were predicted to be associated with sulphate, as $Al(SO_4)^-$ and free Al^{3+} species, which make up about 66% and 33% of the total species distribution of Al, respectively. Less than 1% of the total species predicted for Al in Rand Uranium mine water were $AlOH^{2+}$, $Al(OH)_2^+$, $AlHPO_4^+$, $AlH_2PO_4^{2+}$, $Al_2(OH)_2^{4+}$, $Al(OH)_3$, $Al(OH)_4^-$ and $Al_3(OH)_4^{5+}$ species, as shown in Figure 4.11.

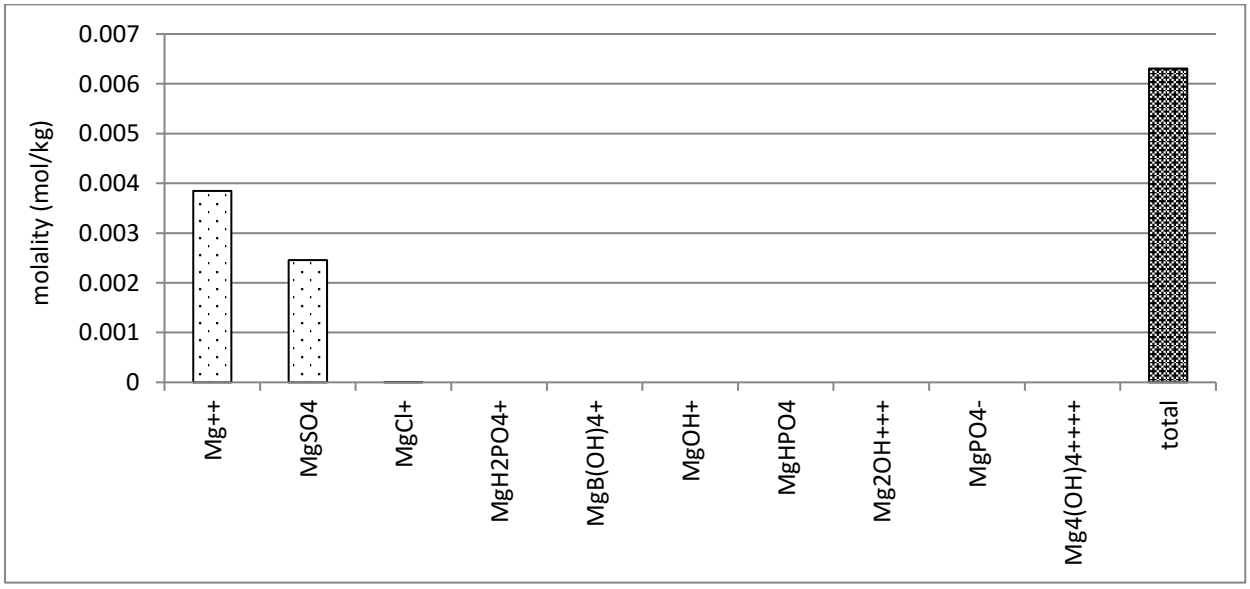

Figure 4.9: Magnesium aqueous species distribution in Rand Uranium mine water

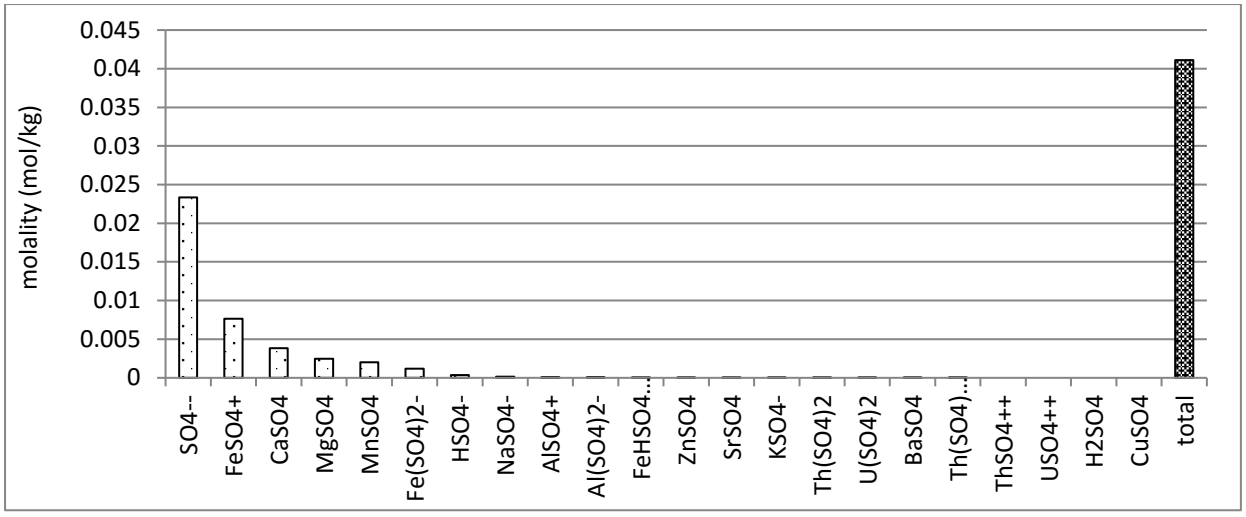

Figure 4.10: Sulphate aqueous species distribution in Rand Uranium mine water

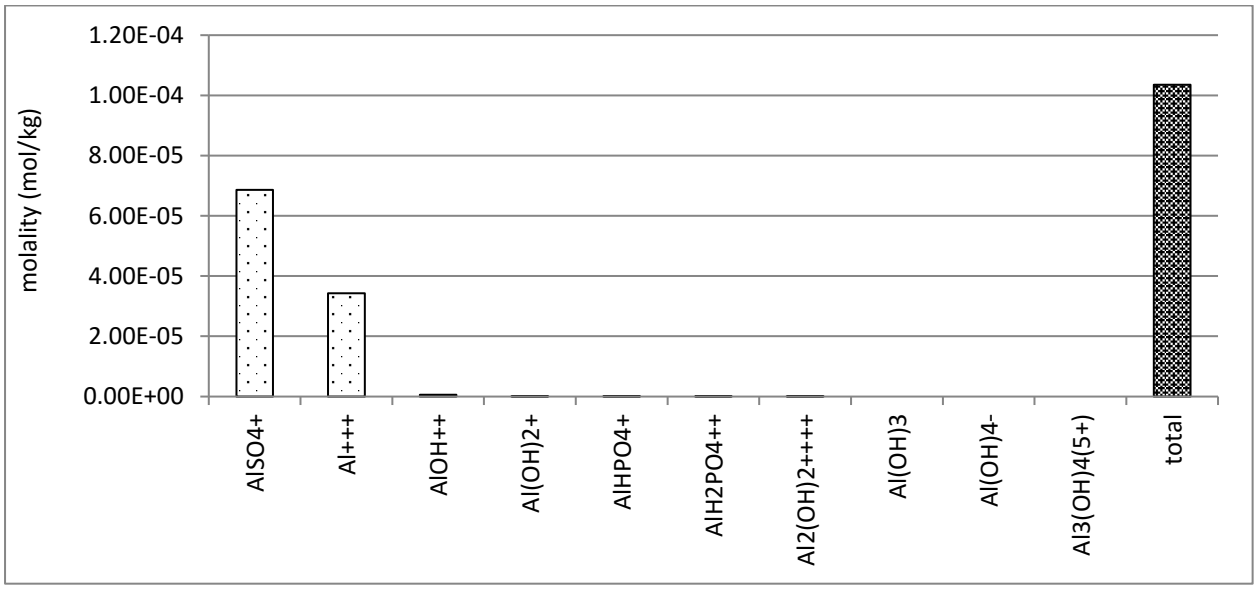

Figure 4.11: Aluminium aqueous species distribution in Rand Uranium mine water

The predicted distribution of Fe species in Rand Uranium mine water is shown in Figure 4.12. Iron species occurred mainly in association with sulphate ions. The species in Rand Uranium mine water included about 53% $FeSO_4^+$ and about 8% $Fe(SO_4)^{2-}$. Other predominant species for Fe were associated with hydroxyl ions, such as $FeOH^{2+}$, $Fe(OH)_2^+$, $Fe_3(OH)_4^{5+}$ and $Fe_2(OH)_2^{4+}$ which constituted about 19%, 10%, 3.5% and 3.5%, respectively, of the total Fe species distribution in Rand uranium mine water as shown in Figure 4.12. Free Fe^{3+} ions constituted about 2% of the total Fe species. Other ions such as $FeCl^{2+}$, $FeHSO_4^{2+}$, $Fe(OH)_3$, $FeB(OH)_4^{2+}$, $FeHPO_4^+$, $FeH_2PO_4^{2+}$, $FeCl_2^+$, $Fe(B(OH)_4)_2^+$, $FeCl_3$, $Fe(OH)_4^-$ and $FeCl_4^-$ constituted about 3.5% of the total Fe species.

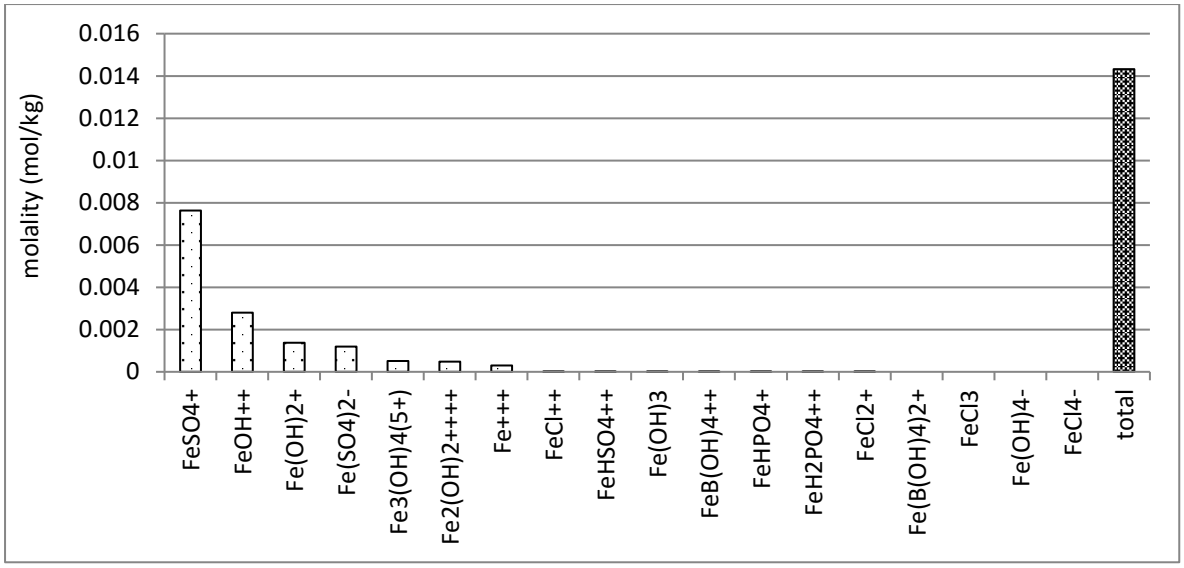

Figure 4.12: Iron aqueous species distribution in Rand Uranium mine water

The predicted aqueous calcium distribution in Rand Uranium mine waters is depicted in Figure 4.13.

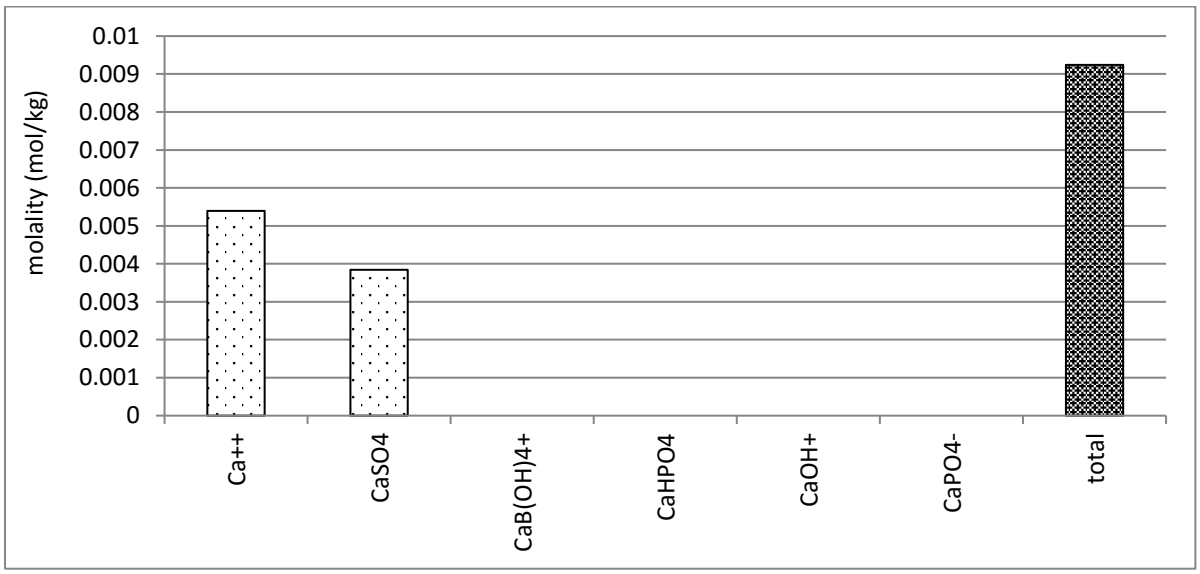

Figure 4.13: Calcium aqueous species distribution in Rand Uranium mine water

Calcium species in Rand Uranium mine water (Figure 4.13) were predicted to exist mainly as free Ca^{2+} and $CaSO_4$ species, which constituted about 58% and 42% of the total Ca species, respectively. Other Ca aqueous species in Rand Uranium mine water included $CaB(OH)_4^+$, $CaHPO_4$, $CaOH^+$ and $CaPO_4^-$, which together contributed only 1% of the total Ca species.

The predicted species distribution of Mn in Rand Uranium mine water is depicted in Figure 4.14. Free Mn^{2+} and $MnSO_4$ species constituted about 60% and 40% respectively of the total Mn species. The distribution of Mn between other species such as $MnCl^+$, $MnCl_2$, $MnH_2PO_4^+$, $MnOH^+$, $MnHPO_4$, $MnCl_3^-$, Mn_2OH^{+++}, $MnPO_4^-$, $Mn(OH)_2$, $Mn_2(OH)_3^+$, $Mn(OH)_3^-$ and $Mn(OH)_4^{2-}$ was negligible in Rand Uranium mine water.

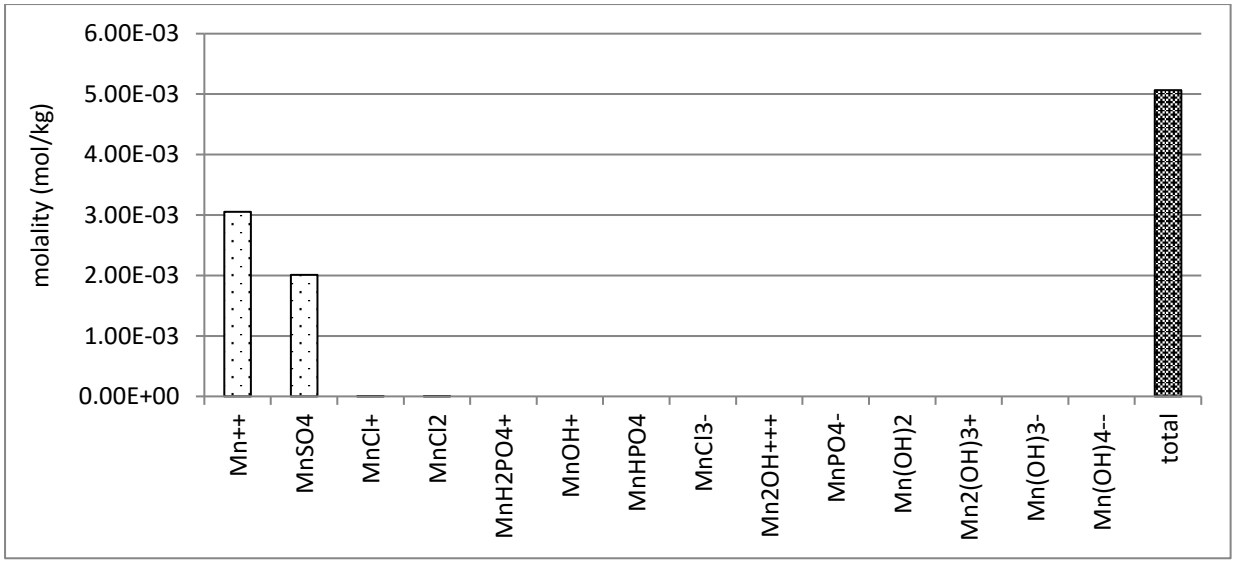

Figure 4.14: Manganese aqueous species distribution in Rand Uranium mine water

The predicted Na species in Rand Uranium mine water are as shown in Figure 4.15. Sodium species were mainly free Na^+ ions which contributed about 96%. The other Na species was $NaSO_4$, which was predicted to contribute about 4% of the total Na in Rand Uranium mine water in both cases. This shows that Na is an element that does not form many complexes, compared to other elements modelled such as Fe, Al and Mn. The other Na-containing species predicted by the model were negligible such as NaCl, $NaHPO_4^-$ and $NaOH^-$.

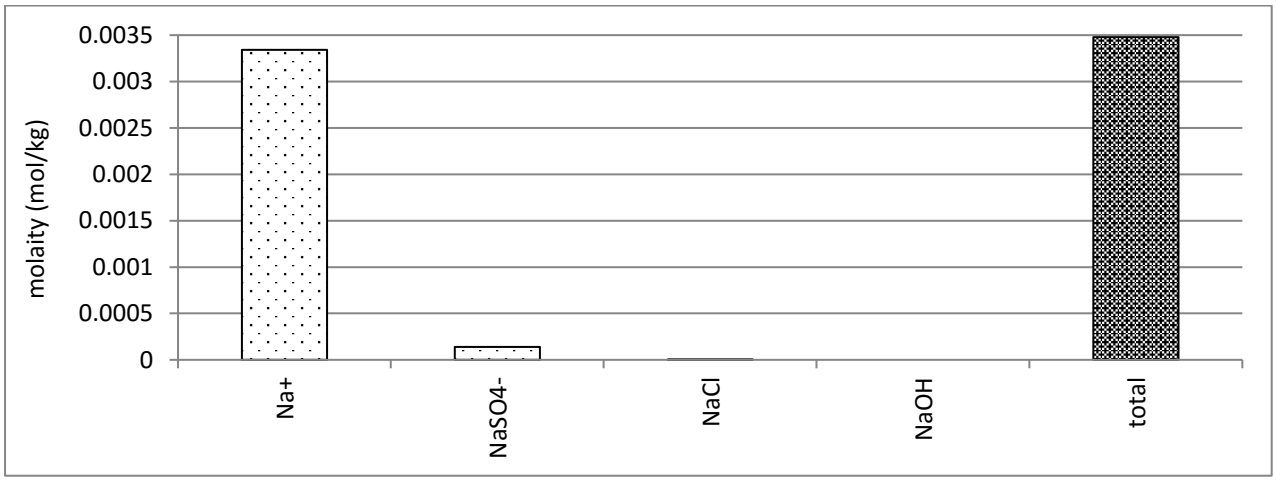

Figure 4.15: Sodium aqueous species distribution in Rand Uranium mine water

Potassium in Rand Uranium mine water was found to be distributed mainly as free K^+ ions (94%) and as KSO_4^- (6%) in aqueous media, as shown in Figure 4.16. The other, negligible, species of K predicted in Rand Uranium mine water were KCl, $KHPO_4^-$ and KOH. Potassium is also a conservative element, similar to Na, and does not readily form complexes with other ions in aqueous media.

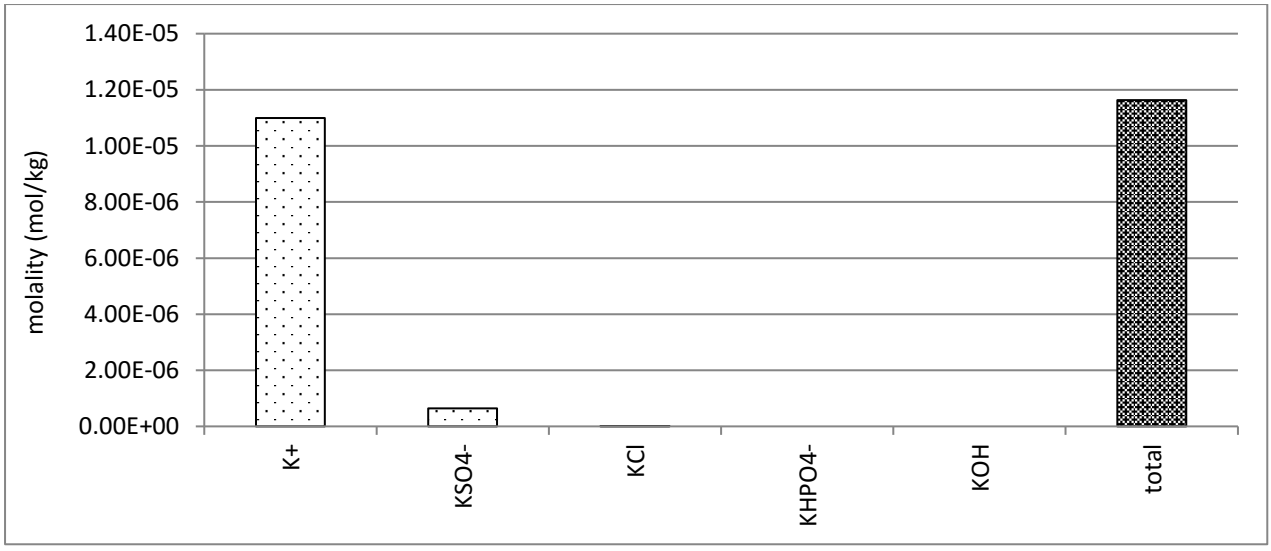

Figure 4.16: Potassium aqueous species distribution in Rand Uranium mine water

4.3.3 **Aqueous distribution of naturally occurring radionuclide materials**

Two of the naturally occurring radionuclide materials (NORMs) identified in Rand Uranium mine water were U and Th. The distribution of these NORMs were modelled using the GWB SpecE8 program. The predicted distribution of U species in Rand Uranium mine water is shown in Figure 4.17.

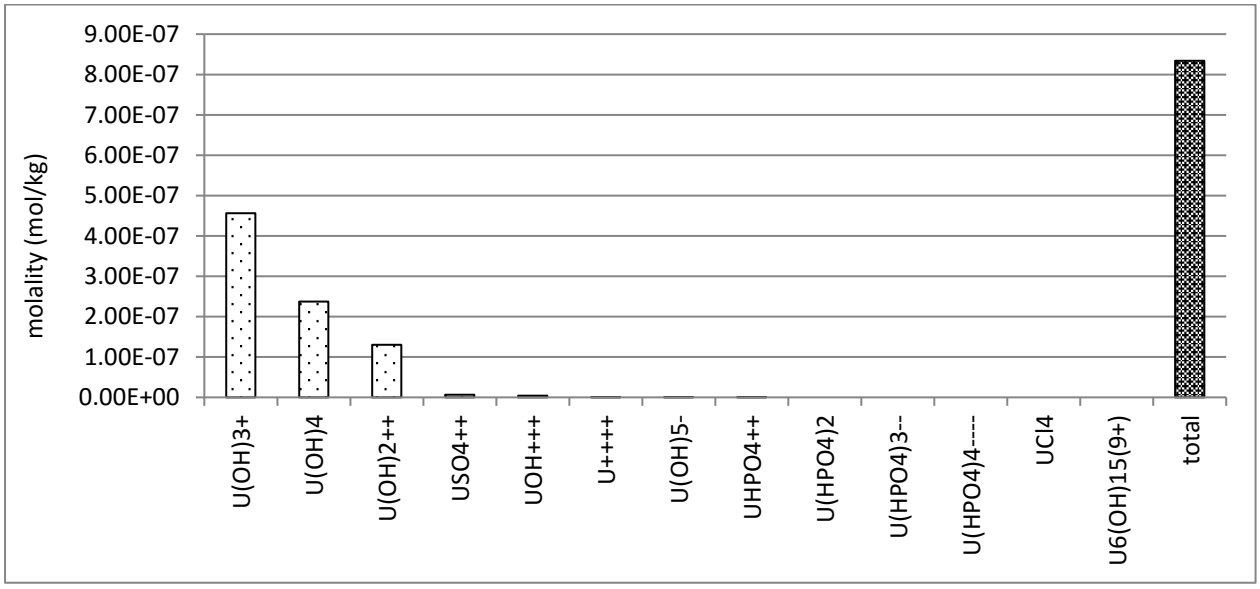

Figure 4.17: Uranium aqueous distribution in Rand Uranium mine water

The modelled results show that U species in Rand Uranium mine water were predicted to be mainly comprised of species associated with hydroxyl ions such as $U(OH)_3^+$, $U(OH)_4$ and $U(OH)_2^{2+}$, which made up about 57, 28 and 16% of the total U species, respectively, as shown in Figure 4.17.

The modelling results produced by GWB software of Th species in Rand Uranium mine water are shown in Figure 4.18.

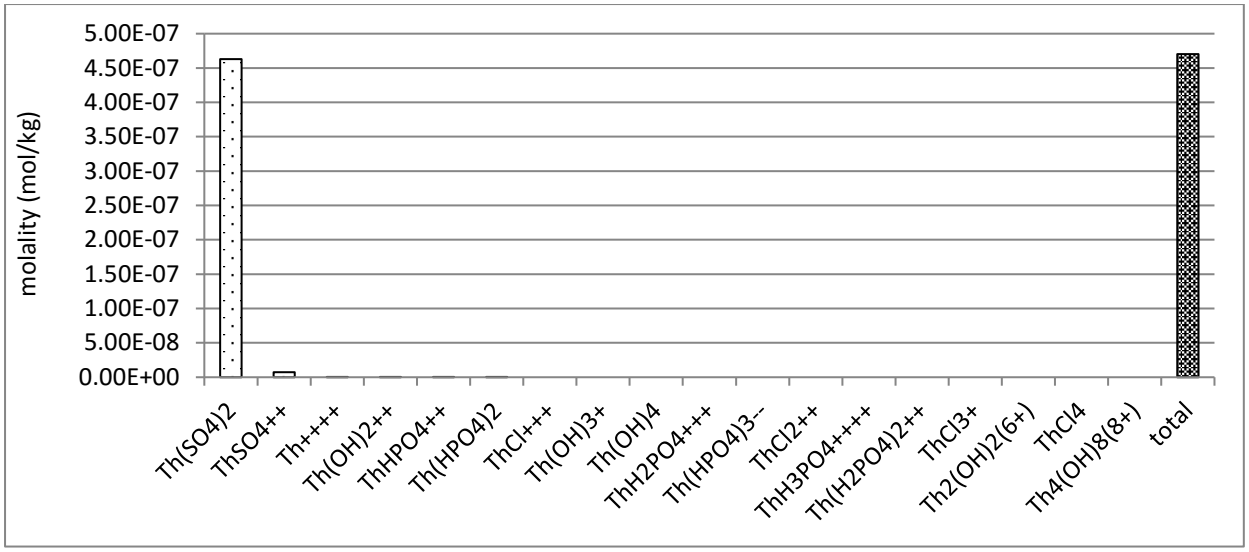

Figure 4.18: Thorium aqueous distribution in Rand Uranium mine water

According to the GWB SpecE8 program, the main species of Th in Rand Uranium mine water were $Th(SO_4)_2$ and $ThSO_4^{2+}$ which comprised about 98% and 2%, respectively, of the total Th species, as shown in Figure 4.18.

4.3.4 **Conclusions**

Matla mine water can be classified as NMD because the pH was 8. Rand Uranium mine water can be classified as AMD because the pH was less than 5, and the water contained elevated concentrations of Fe, Al and Mn. The sulphate concentration of Rand Uranium water was much greater than that of Matla mine water. This indicates that *in situ* natural buffering by minerals, such as dolomite, occurs, and that the buffering of the acidity produced from pyrite oxidation was lower in Rand Uranium mine water compared with Matla mine water. Analysis of Matla mine water using ICP-OES and IC showed that the concentrations of Na and sulphate were very high, rendering the water unsuitable for irrigation or domestic and industrial purposes. Rand Uranium mine water was unsuitable for any purpose (drinking, irrigation or industrial) because of its low pH and elevated concentrations of Fe, Al, Mn, Pb and sulphate ions, as well as the high radionuclide content of the water.

The GWB specE8 program showed that major elements (or ions) in Matla mine water and Rand Uranium mine water, such as Mg, sulphate, Mn, Na and K ions, mainly exist in aqueous media as free ions, i.e. they are non-associated or not complexed with ligands or other ions. This increases their mobility in the ecosystem, thereby enhancing bioavailability and toxicity. On the other hand, Fe and Al were found to occur in association with hydroxyl ions. It is known that complexed species are less mobile, and thereby have reduced bioavailability and toxicity. The NORMS, such as Th and U, were found to exist in association with sulphate ions in Rand Uranium mine water. This means that these ions are less bioavailable as their mobility was reduced because of their nature.

4.4 PROBABLE MINERAL PHASES DURING TREATMENT OF MINE WATER WITH FLY ASH

The GWB Act2 program was used to predict the different mineral phases that could form if Matla mine water or Rand Uranium mine water was treated with Matla coal FA. The minerals that were investigated and predicted were those containing the major elements (Fe, Al, Mn, Na, K and sulphate ions) and radioactive elements (Th and U) in Matla mine water or Rand Uranium mine water. The following assumptions were made to obtain these modelling results:

- Treatment of mine water with Matla coal FA is effected by dissolution of the CaO fraction in coal FA, resulting in the increase in concentration of Ca^{2+} and in the pH of the mine water.
- The percentage of CaO determined by XRF was assumed to be equivalent to the percentage of lime in Matla coal FA.

During treatment of mine water with Matla coal FA, the increase in pH depended on the amount of lime that dissolved into the water. Therefore, the independent variable chosen in this modelling was the concentration of Ca^{2+} added to the mixture in terms of log activity of the Ca^{2+} ($\log_a Ca^{2+}$). The dependent variable was pH.

4.4.1 Probable minerals predicted during Matla mine water treatment with coal fly ash

Treatment of Matla mine water with Matla coal FA was modelled using the GWB Act2 program, to predict the probable sulphate and Mg phases that could form at various $\log_a Ca^{2+}$ and pH points. The predicted sulphate and Mg phases that could form when Matla mine water was treated with Matla coal FA at various $\log_a Ca^{2+}$ and pH end values is shown in Figure 4.19.

From Figure 4.19a, it is seen that the sulphate ions exist mainly as free ions, as Matla water has a pH of 8 (Table 3.9). As the $\log_a Ca^{2+}$Ca ions were increased to greater than -2.4, the Act2 program showed that the sulphate ions in Matla mine water would form $CaSO_4$ aqueous species. Although the solution will be supersaturated with respect to gypsum at $\log_a Ca^{2+}$ of -2 and greater, no gypsum was predicted to form by the Act2 program. This can be attributed to the fact that the high concentration of Na^+ in Matla mine water could inhibit the formation of gypsum by inhibiting the growth rate of gypsum crystals (Reznik et al., 2009; Zhang & Nancollas, 1992).

The Act2 program showed that Mg ions existed mainly as free ions in Matla mine water, as shown in Figure 4.19b. If Matla mine water was to be treated with Matla coal FA, the Act2 program showed that the Mg ions in Matla mine water would start precipitating, at pH values greater than 10, as brucite ($Mg(OH)_2$). The formation of brucite was shown by the Act2 program to be pH dependent but Ca independent. Below pH 10, Mg was predicted to remain in Matla mine water as free Mg^{2+} ions, regardless of the amount of Ca^{2+} added to the mixture. The modelled results for K and Na phases obtained using the Act2 program, for the treatment of Matla mine water with Matla coal FA, are shown in Figure 4.20. From the results, K and Na would remain as free ions in aqueous solution at various pH and $\log_a Ca^{2+}$ values (Figure 4.20).

The GWB has shown that if Matla mine water was to be treated with just Matla coal FA, only Mg ions can be removed if, and only if, the pH could be increased to greater than 10. No mineral phases were predicted by the Act2 program to precipitate out sulphate, Na and K from Matla mine water when treated with Matla coal FA alone.

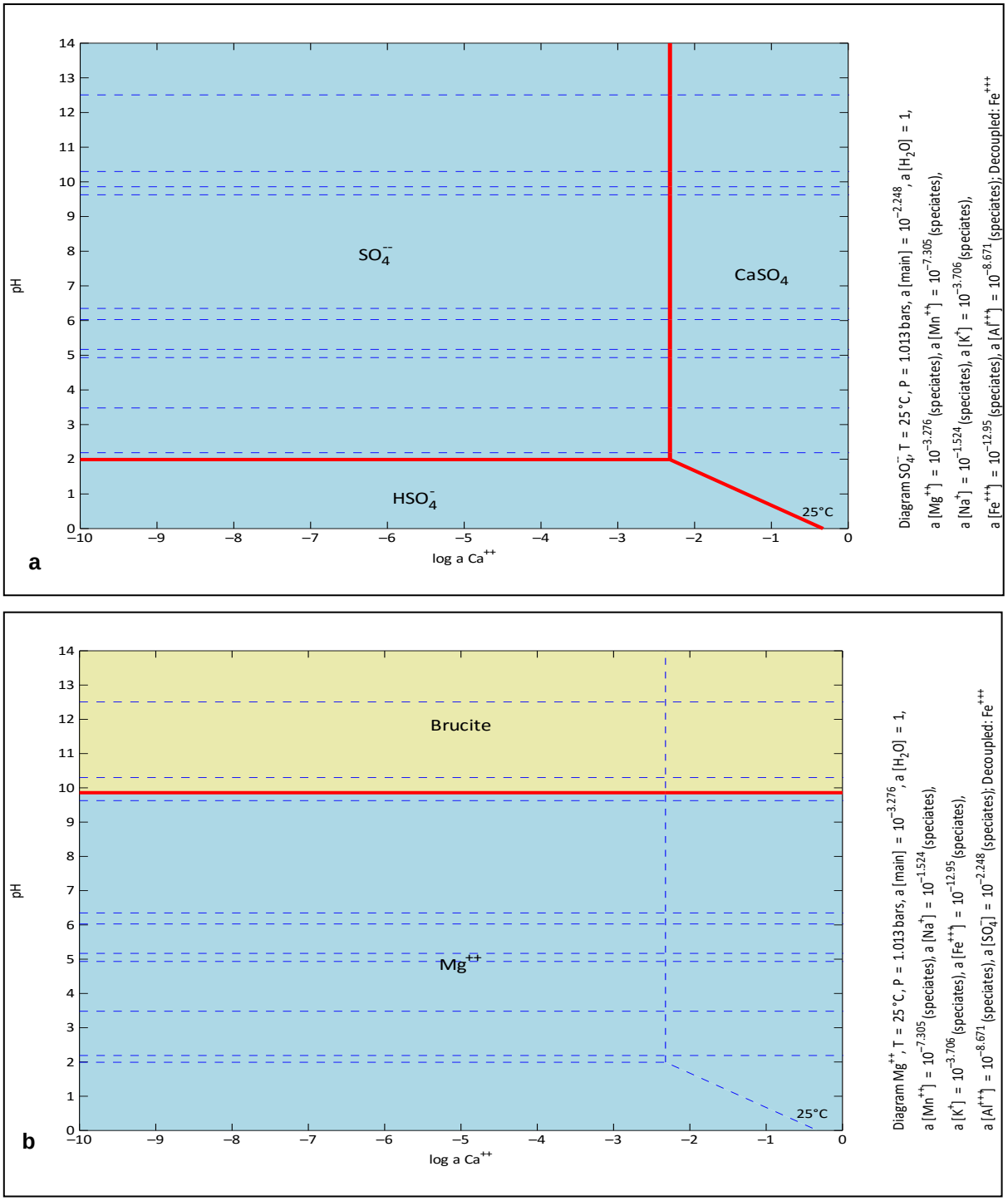

Figure 4.19: Sulphate (a) and magnesium (b) phases that were predicted to form by the GWB Act2 program, when Matla mine water was treated with Matla coal FA to various $\log_a Ca^{2+}$ and pH values *(the yellow colour shows mineral phases and the blue colour represents aqueous phases)*

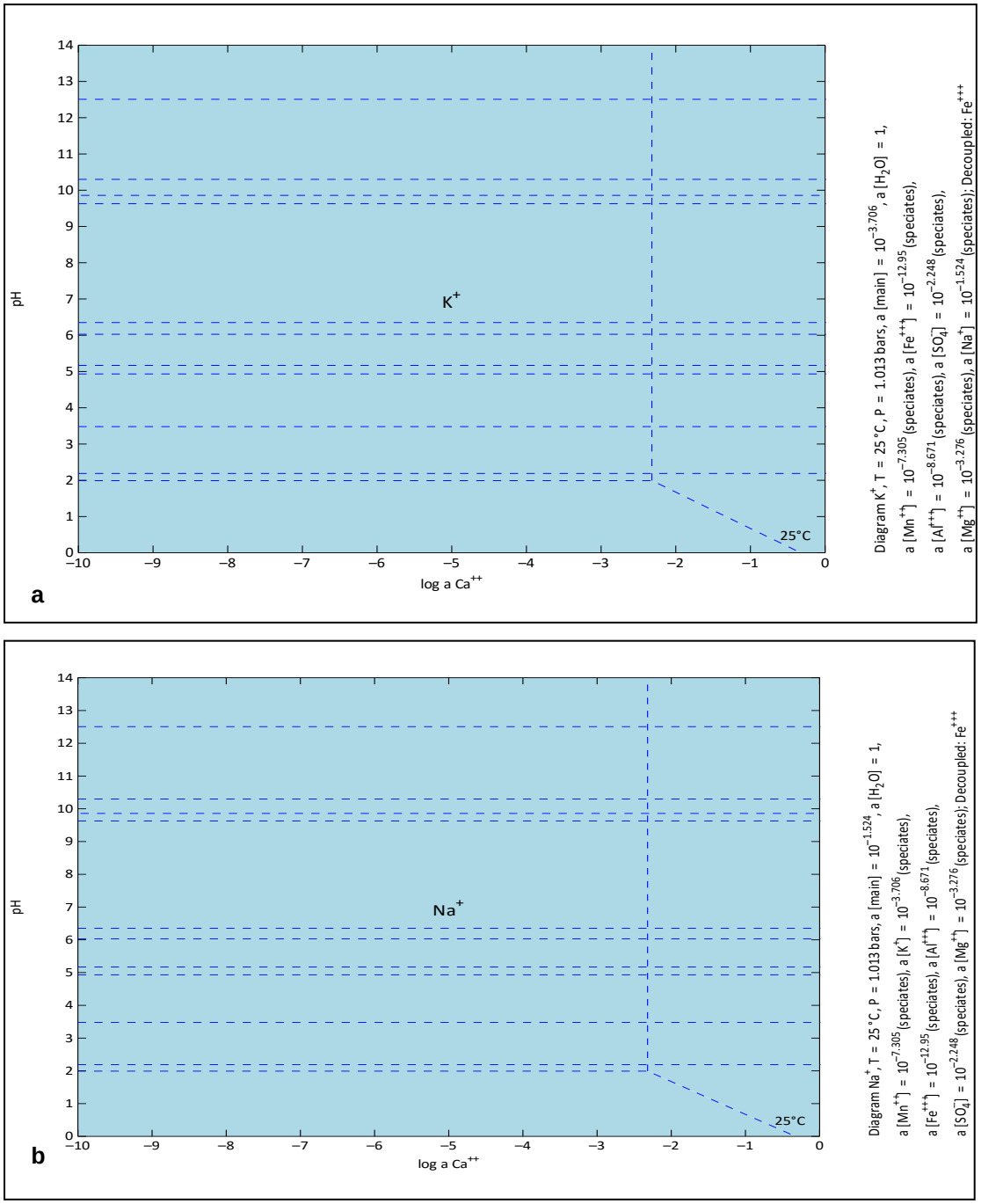

Figure 4.20: Potassium (a) and sodium (b) phases predicted to form by the GWB Act2 program, when Matla mine water was treated with Matla coal FA to various $\log_a Ca^{2+}$ and pH values *(yellow colour shows mineral phases and blue colour represents aqueous phases)*

4.4.2 **Probable minerals predicted during Rand Uranium mine water treatment with coal fly ash**

The probable mineral phases that could form when Rand Uranium mine water was mixed with Matla coal FA were predicted using the GWB Act2 program. The composition of Rand Uranium mine waters is shown in Table 3.10.

4.4.2.1 Probable minerals phases for major elements

The GWB Act2 program was used to predict the phases of Fe, Al, Mn, Mg and sulphate ions that could form if Rand Uranium mine waters were treated with Matla coal FA. It was assumed that the addition of Matla coal FA resulted in the dissolution of CaO, causing the concentration of Ca^{2+} in the mine water to increase. The dissolution of lime was assumed to cause the pH of the mine water to increase. Therefore, the increase in pH was dependent on the amount of CaO that dissolved into the mine water. Removal of sulphate ions from Rand Uranium mine waters, when treated with Matla coal FA, was modelled using the GWB Act2 program. Rand Uranium mine water contained elevated concentrations of sulphate, Fe, Al, Mn, Mg and Ca ions, as shown in Table 3.10. The predicted sulphate phases at various $\log_a Ca^{2+}$ and pH values are shown in Figure 4.21.

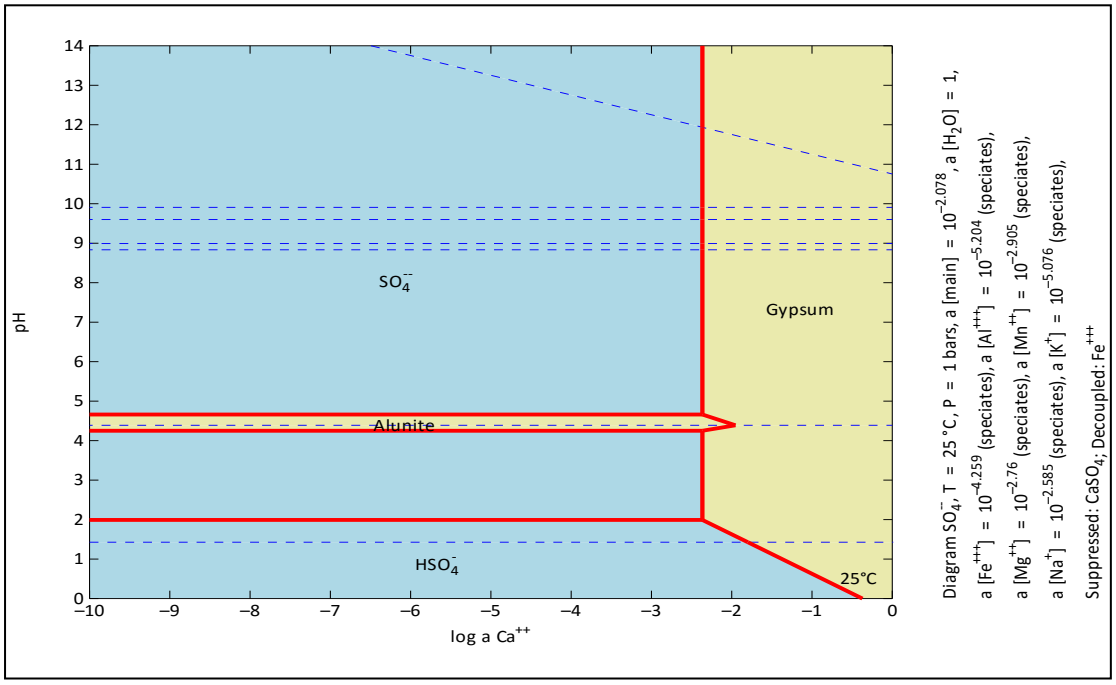

Figure 4.21: Sulphate phases that were predicted to form by the GWB Act2 program when Rand Uranium mine water was treated with Matla coal FA to various pH end points *(yellow colour shows mineral phases and blue colour represents aqueous phases)*

The Act2 program showed that similar sulphate phases would form if Rand Uranium mine waters were treated with Matla coal FA to specific pH end points. The program showed that if Rand Uranium mine water was to be treated with Matla coal FA, sulphate could precipitate as alunite ($KAl_3(SO_4)_2(OH)_6$) or gypsum ($CaSO_4.2H_2O$), as shown in Figure 4.21. Formation of gypsum in Rand Uranium mine water was predicted to be mainly dependent upon the amount of Ca ions added to the mine water. Gypsum precipitation could occur when

$log_a Ca^{2+}$ was greater than -2.5 as, at this concentration, the mixture was supersaturated with respect to gypsum. Since the pH of Rand Uranium mine water was greater than 2, the formation of gypsum was independent of the pH of the mixture. From Figure 4.21, the formation of gypsum is affected only when the pH is less than 2.

The formation of alunite in Rand Uranium mine waters was found to be mainly dependent on pH. The concentration of Ca ions added to Rand Uranium mine water would tend to affect the pH at which alunite is stable. When $log_a Ca^{2+}$ is greater than -2, the formation of alunite tends to decrease in favour of the formation of gypsum, a more stable mineral, as shown in Figure 4.21. Usually, sulphate ions are removed from acid mine water by gypsum precipitation to a concentration between 1500 mg/L and 2000 mg/L (Madzivire, 2010; Geldenhuys et al., 2001). This amount of sulphate ions is still above the required limit for domestic purposes; thus treatment would be required to reduce the sulphate concentration to less than 500 mg/L.

According to the GWB Act2 program, the probable Al mineral phases that are predicted to form when Rand Uranium mine water is treated using Matla coal FA are shown in Figure 4.22. Aluminium could be removed as gibbsite ($Al(OH)_3$), according to the Act2 program, as shown in Figure 4.22.

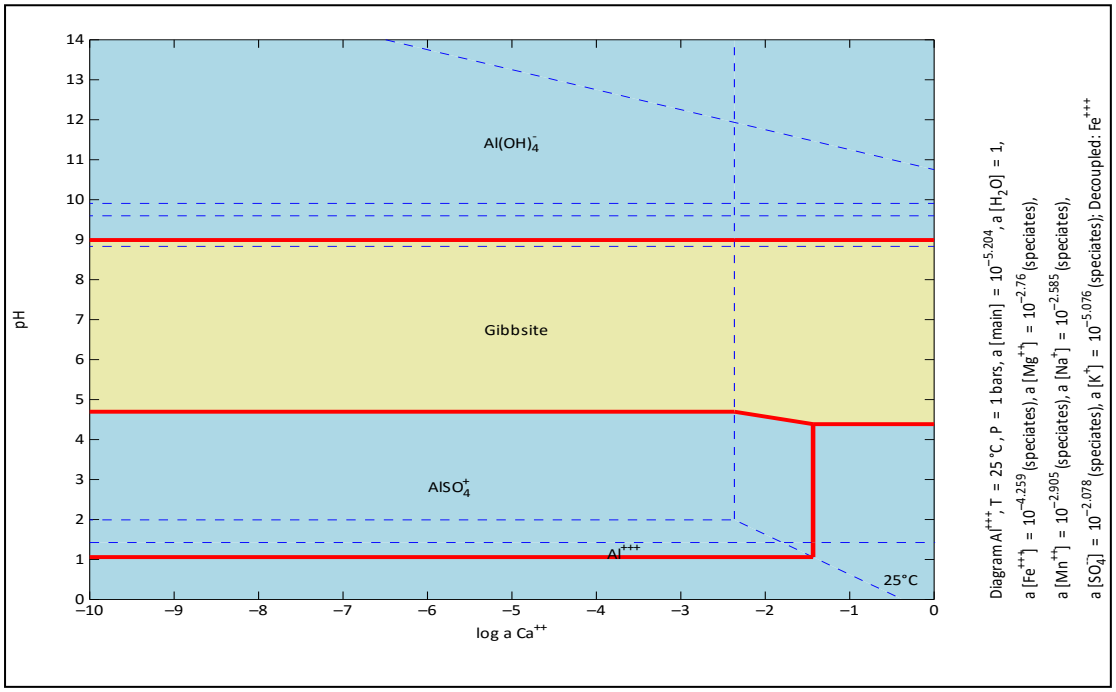

Figure 4.22: Aluminium phases that were predicted to form by the GWB Act2 program when Rand Uranium mine water was treated with Matla coal FA to various $log_a Ca^{2+}$ and pH values *(yellow shows mineral phases and blue represents aqueous phases)*

Precipitation of gibbsite was found to depend on pH and $log_a Ca^{2+}$. Gibbsite formation would occur if the pH of the mixture was between 4.7 and 9 when $log_a Ca^{2+}$ was less than -2.5 in Rand Uranium mine water, as shown in Figure 4.22. When $log_a Ca^{2+}$ was increased to -2.5 and greater, the formation of gibbsite would start occurring at pH 4 in both Rand Uranium mine water, as shown in Figure 4.22. Increasing the pH of Rand Uranium mine water to greater than 10, $Al(OH)_4^-$ phase would be formed, according to the Act2 program. This phase was expected to react with Ca^{2+} and sulphate ions to form ettringite mineral phase (Madzivire, 2010). The ettringite mineral phase was not predicted by the GWB Act2 program because the databases contained in the GWB

software did not have the thermodynamic parameters for ettringite. The probable Fe mineral phases that were predicted to form by the Act2 program, when Rand Uranium mine water was treated with Matla coal FA to various $\log_a Ca^{2+}$ and pH values, are shown in Figure 4.23. The GWB software has shown that the mineral phases that could form were similar when Matla coal FA was to be added to both mine waters. The Fe minerals that were predicted using the GWB were jarosite-K ($KFe_3(SO_4)_2(OH)_6$) and $Fe(OH)_3$.

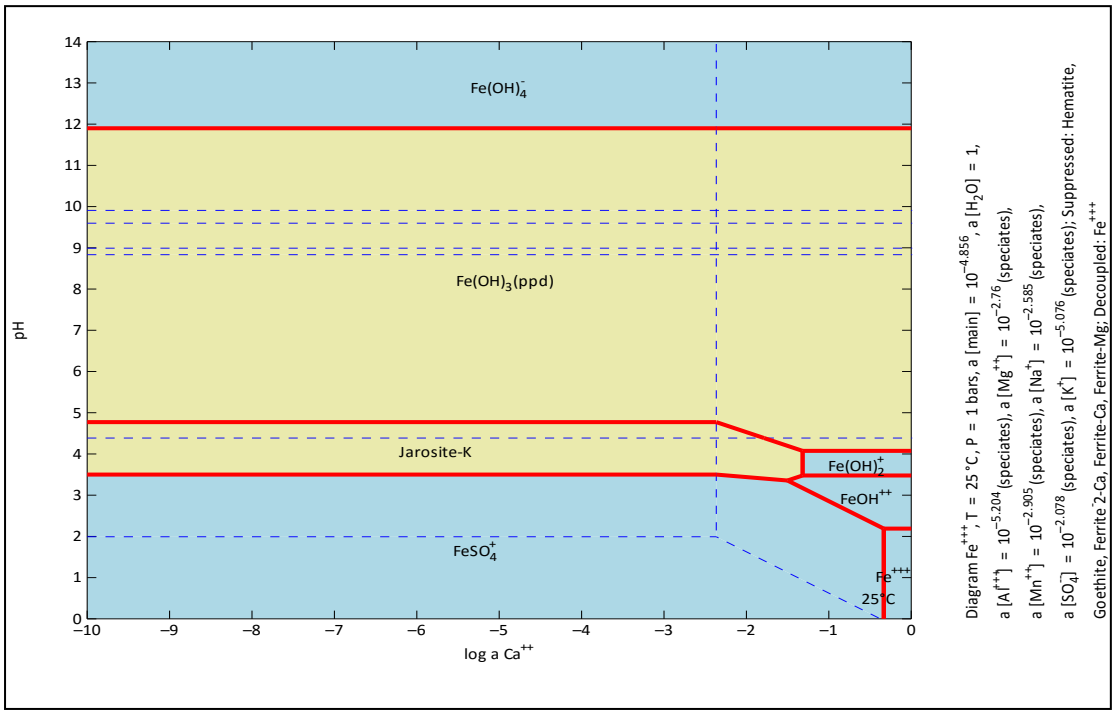

Figure 4.23: Iron phases that were predicted to form by the GWB Act2 program when Rand Uranium mine water was treated with Matla coal FA to various $\log_a Ca^{2+}$ and pH values *(yellow shows mineral phases and blue represents aqueous phases)*

The formation of these minerals was dependent on both pH and $\log_a Ca^{2+}$ according to the Act2 program. The formation of jarosite-K was predicted to occur at pH 3.5 to 4.5 when $\log_a Ca^{2+}$ was -10. In Rand Uranium mine water, jarosite-K was predicted to form between pH 3 and 5 when $\log_a Ca^{2+}$was less than -2.5 (Figure 4.23). At $\log_a Ca^{2+}$ greater than -2.5, the pH range at which jarosite-K may form narrowed gradually. No jarosite-K formation will form if $\log_a Ca^{2+}$ is greater than -1, as shown in Figure 4.23. Precipitation of $Fe(OH)_3$ when $\log_a Ca^{2+}$ was between -10 and -2.5, $Fe(OH)_3$ occurred at pH between 5 and 12 in Rand Uranium mine water when $\log_a Ca^{2+}$ was less than -2.5 as shown in Figure 4.23. If the $\log_a Ca^{2+}$ was to be increased to greater than -2.5, the lower limit pH for $Fe(OH)_3$ decreased gradually to 4. The upper limit of $Fe(OH)_3$ was not affected by $\log_a Ca^{2+}$ in Rand Uranium mine water.

The GWB model showed that if Rand Uranium mine water was to be treated with Matla coal FA, Mn ions could be removed from mine water as amorphous $Mn(OH)_2$. The formation of $Mn(OH)_2$ was found to be pH dependent and independent of the concentration of Ca ions added to the mine water, as is shown in Figure 4.24.

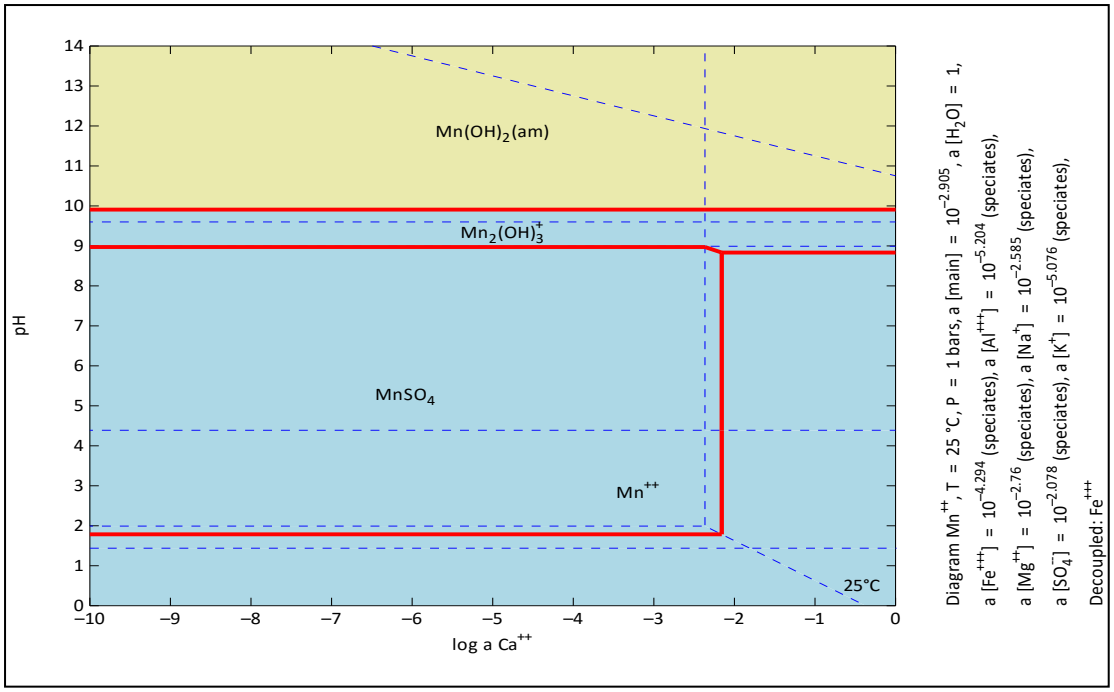

Figure 4.24: Manganese phases that were predicted to form by the GWB Act2 program when Rand Uranium mine water was treated with Matla coal FA to various $\log_a Ca^{2+}$ and pH values *(yellow shows mineral phases and blue represents aqueous phases)*

Keeping the pH of the mine water less than 9 would result in the Mn existing as free Mn^{2+} and $MnSO_4$ species. If the pH of the mine water was to be increased to between 9 and 10, Mn would exist in aqueous solution as $Mn_2(OH)_3^+$. In Rand Uranium mine water, amorphous $Mn(OH)_2$ was predicted to start precipitating at pH 10 (Figure 4.24).

Magnesium was predicted to be removed from Rand Uranium mine water as brucite ($Mg(OH)_2$) when Rand Uranium mine water was treated with Matla coal FA, as shown in Figure 4.25. According to the Act2 program, the formation of brucite was dependent on pH but independent of the amount of Ca ions added to the mine water. The formation of brucite was predicted to occur when the pH of Rand Uranium mine water was increased to greater than 9.5 with alkalinity generated by the dissolution of lime from Matla coal FA. The potassium phases predicted by the Act2 program are shown in Figure 4.26.

The Act2 program predicted that when Rand Uranium mine water was treated with Matla Coal FA, K can only precipitate in the form of alunite ($KAl_3(SO_4)_2(OH)_6$) at a specific pH and Ca concentration. Alunite could only form at pH values between 4.3 and 4.8 when $\log_a Ca^{2+}$was less than -2, as shown in Figure 4.26. At all other pH and $\log_a Ca^{2+}$ conditions, K was predicted by the Act2 program to exist as free K^+ ions.

According to the GWB Act2 program, if Rand Uranium mine water was to be treated with Matla coal to various pH and $\log_a Ca^{2+}$ values, Na would remain in aqueous solution as free Na^+ ions, as shown in Figure 4.27.

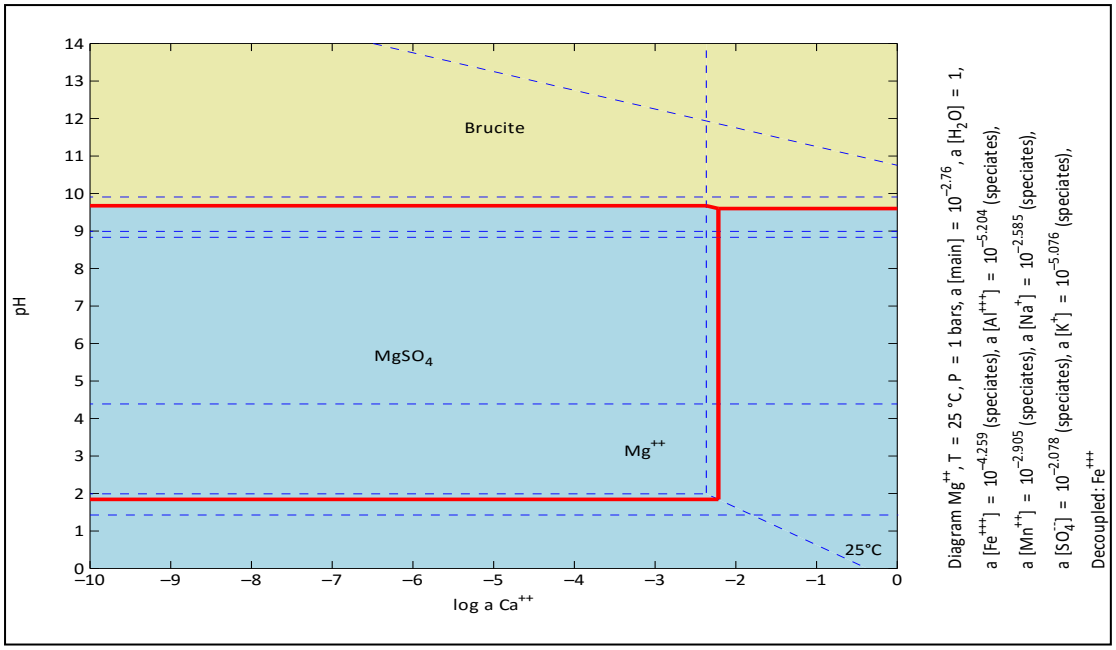

Figure 4.25: Magnesium phases that were predicted to form by the GWB Act2 program when Rand Uranium mine water was treated with Matla coal FA to various log_aCa^{2+} and pH values *(yellow shows mineral phases and blue represents aqueous phases)*

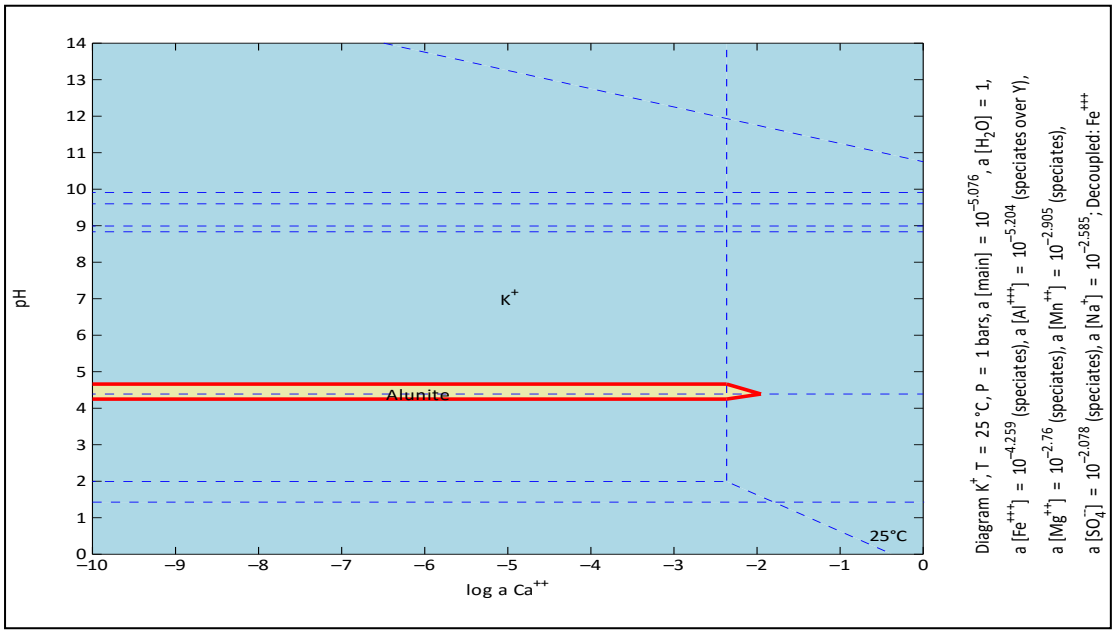

Figure 4.26: Potassium phases that were predicted to form by the GWB Act2 program when Rand Uranium mine water was treated with Matla coal FA to various log_aCa^{2+} and pH values *(yellow shows mineral phases and blue represents aqueous phases)*

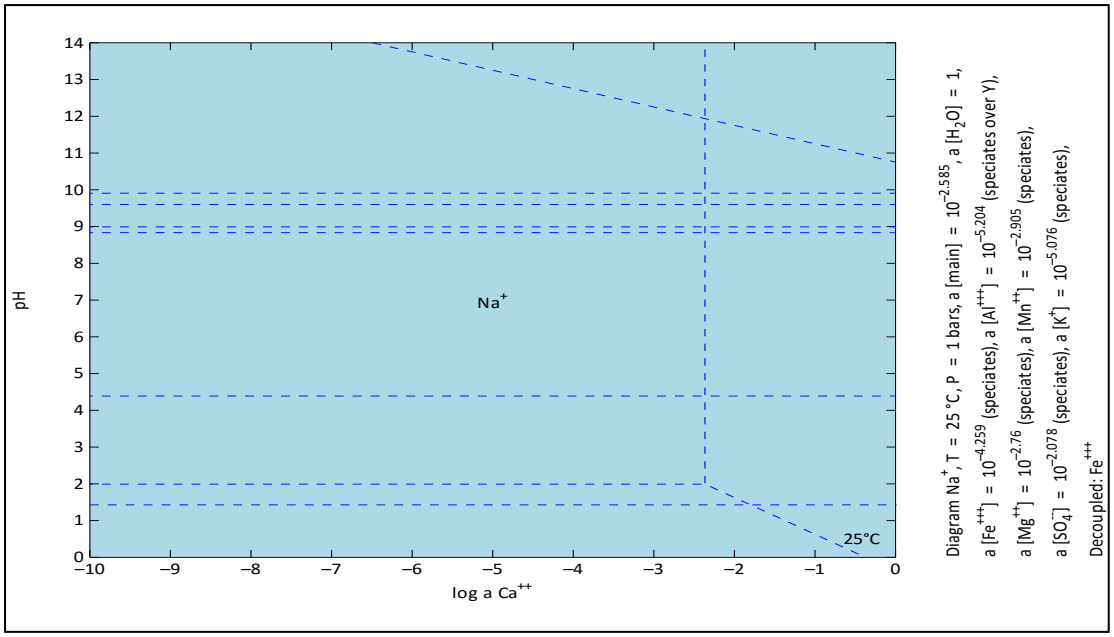

Figure 4.27: Sodium phases that were predicted to form by the GWB Act2 program when Rand Uranium mine water was treated with Matla coal FA to various log_aCa^{2+} and pH values *(yellow shows mineral phases and blue represents aqueous phases).*

If Rand Uranium mine water was to be treated with FA, it was predicted that no Na ions would be removed from the mine water by precipitation in any mineral form.

4.4.3 **Probable mineral phases associated with natural radioactive elements**

Naturally occurring radioactive elements that were found to be above the required limit for potable water in Rand Uranium mine water were Th and U as shown in Table 3.10. The probable phases of Th and U that could form when Rand Uranium mine water was to be treated with Matla coal FA were modelled using the GWB Act2 program. The probable phases of U that were predicted to form are shown in Figure 4.28. From the Act2 results, if Rand Uranium mine water was to be treated with Matla coal FA, U could precipitate in the form of uraninite (UO_2). The formation of UO_2 was found to be pH dependent if the log_aCa^{2+} was less than -2.7. When log_aCa^{2+} was less than -2.7, precipitation of UO_2 would occur when the pH of mine water was increased to greater than 3. If the log_aCa^{2+} of the mine water was to be increased from -2.7 to 0, the pH at which UO_2 could start precipitating would decrease from 3 to 2 as more Ca ions were added to the mixture. At pH less than 3 and log_aCa^{2+} less than about -0.3, U will exist as $U(SO_4)_2$ in solution. If log_aCa^{2+} was increased to greater than about -0.3 and the pH kept below 3, U will exist as USO_4^{2+}, UOH^{3+} and $U(OH)_2^{2+}$ as shown in Figure 4.28.

The Act2 program predicted that if Rand Uranium mine water was to be treated with Matla coal FA, Th could be removed as thorianite (ThO_2), as shown in Figure 4.29. The formation of ThO_2 was found to be pH dependent, when log_aCa^{2+} was less than -2.3. When log_aCa^{2+} was less than -2.3, ThO_2 could form if the pH of the mine water was increased to greater than 5. Increasing log_aCa^{2+} from -2.3 to 0 would result in a decrease in the pH at which ThO_2 would precipitate from about 5 to about 4, as shown in Figure 4.29. At pH less than 5 and log_aCa^{2+} less than about -0.2, Th would exist as $Th(SO_4)_2$. If the log_aCa^{2+} was to be increased to greater than -0.2 and the pH kept less than 4, Th would exist as $ThSO_4^{2+}$ and $Th(OH)_2^{2+}$.

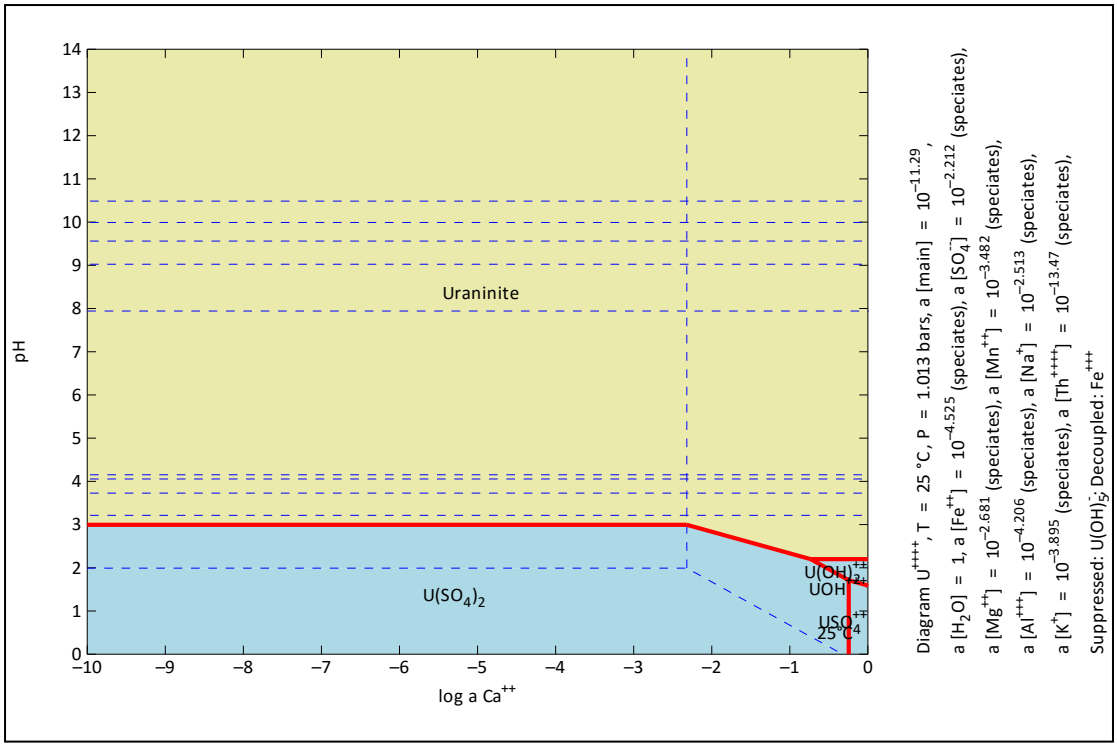

Figure 4.28: Uranium phases that were predicted to form by the GWB Act2 program when Rand Uranium mine water was treated with Matla coal FA to various $\log_a Ca^{2+}$ and pH values *(yellow shows mineral phases and blue represents aqueous phases)*

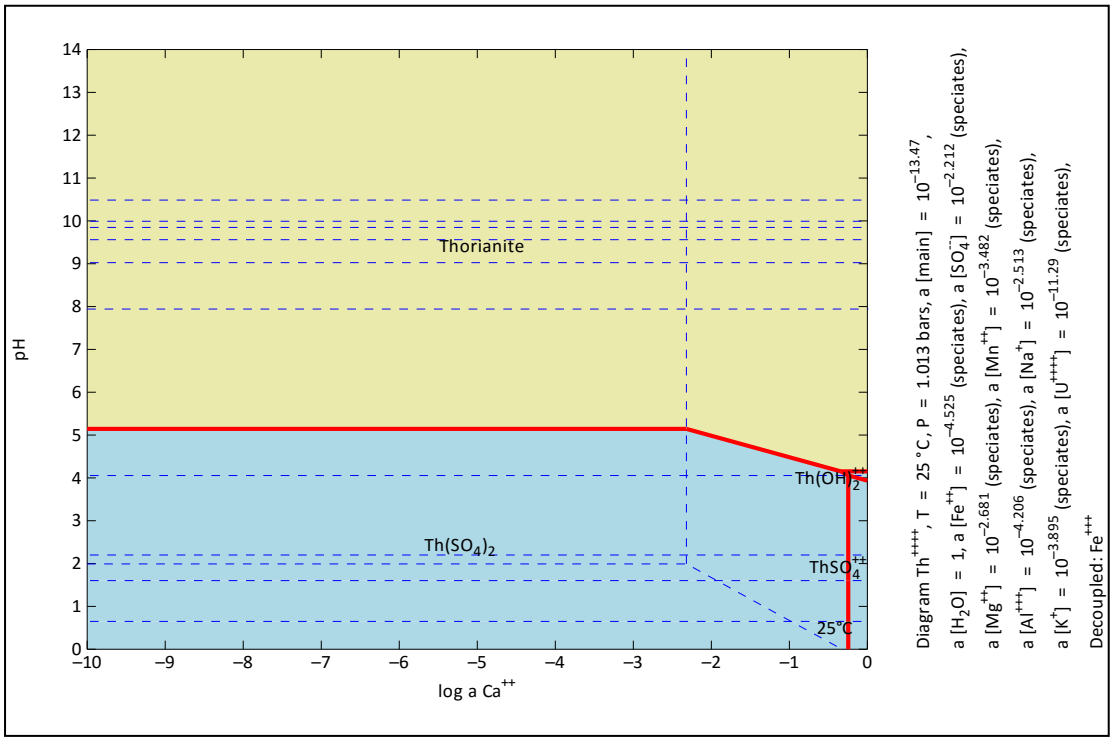

Figure 4.29: Thorium phases that were predicted to form by the GWB Act2 program when Rand Uranium mine water was treated with Matla coal FA to various $\log_a Ca^{2+}$ and pH values *(yellow shows mineral phases and blue represents aqueous phases)*

4.5 CONCLUSIONS

The GWB Act2 program predicted that if Matla water mine water or Rand Uranium mine water was to be treated with coal FA, the removal of potentially toxic elements depended on the pH end point of the treatment process and the concentration of Ca ions added to the mine water. The results are very helpful, especially to determine the amount of coal FA or alkaline chemicals that would be required to treat a particular composition of the mine water. It was predicted by the Act2 program that the removal of Mg ions from Matla mine water was pH dependent. It was found that increasing the pH of Matla mine water to greater than 10 would result in the precipitation of Mg as brucite. No removal of sulphate, K and Na ions from Matla mine water was predicted even if the concentration of Ca ions was increased such that $\log_a Ca^{2+}$ was to be increased from -10 to 0 and pH was increased to 14. The Act2 program predicted that treatment of Rand Uranium mine water with coal FA could remove sulphate ions as alunite or gypsum. Removal of alunite and gypsum from Rand Uranium mine water was found to be $\log_a Ca^{2+}$ and/or pH dependent. If sulphate ions were to be removed in the form of alunite, the pH of the mixture would need to be maintained between 3.5 and 5 and $\log_a Ca^{2+}$ less than -1. If the sulphate ions were to be removed in the form of gypsum, the $\log_a Ca^{2+}$ of the mixture would have to be increased to greater than -2.5. Removal of Al ions from Rand Uranium mine water was predicted to take place through alunite or gibbsite precipitation. Formation of alunite and gibbsite was found to be dependent upon pH and the concentration of Ca ions of the mine water. The conditions for the removal of Al as alunite are the same as the conditions for the removal of sulphate ions as alunite. Removal of Al ions as gibbsite would occur when the pH of the mine water was increased to between 4.5 and 10. The probable Fe-containing mineral phases that were predicted to form when Rand Uranium water was treated with coal FA were jarosite-K and $Fe(OH)_3$. The formation of these minerals was found to be pH and $\log_a Ca^{2+}$ dependent. Jarosite-K was predicted to form at a pH between 3.5 and 5 if $\log_a Ca^{2+}$ was between -10 and -2.5. As $\log_a Ca^{2+}$ was increased from -2.5 to -1, the range of stability of jarosite-K decreased. As $\log_a Ca^{2+}$ was increased to greater than -1, no jarosite would form in Rand Uranium mine water. Formation of $Fe(OH)_3$ could only form if the pH of the mine water was to be between 5 and 12. Modelling results using the GWB model have shown that if Rand Uranium mine water was to be treated with coal FA, Mn and Mg ions would be removed as $Mn(OH)_2$ and $Mg(OH)_2$ respectively. The formation of $Mn(OH)_2$ and $Mg(OH)_2$ depends on the final pH attained during treatment and is independent of the amount of Ca^{2+} ions added into the mixture. $Mn(OH)_2$ and $Mg(OH)_2$ were found to precipitate at pH 10 and 9.5, respectively.

Removal of K ions from Rand Uranium mine water was found to be through the precipitation of alunite, according to the GWB. On the other hand, the GWB model showed that if Rand Uranium mine water was to be treated with FA, there is no expected Na-mineral phase that would form. Therefore, if Rand Uranium water is to be treated with FA, Na concentration would remain the same if there is no leaching of Na from FA or adsorption or absorption of Na ions by the FA particles.

These results are very important in planning the treatment of mine water during exploration or mining. The information can be used in deciding on the treatment technology and budgeting for the treatment process. It is advisable to employ software packages such as GWB so that scientists can reduce the amount of time and the number of experiments during research and development of treatment technologies and remediation techniques at a particular mine.

CHAPTER 5: RHEOLOGY

5.1 INTRODUCTION

This section presents the results of the rheology study carried out on the FA/mine water slurry. The rheology study was a preparatory step in designing the pilot plant. The objectives of this investigation were to prepare residual FA suspensions at various concentrations in order to perform standard tube viscometer tests, determine the rheological behaviour of the slurries and provide details to suppliers regarding specifications of pumps and mixers. A brief comparison was drawn with the rheology of Arnot and Lethabo ashes tested previously.

5.2 RHEOLOGY STUDIES

The rheology of the FA/mine water mixture was studied to determine the right specifications for the pump required to handle the FA/AMD slurries which are abrasive and corrosive. Subject to neutralisation, the residual solids have to be pumped away to a disposal site for further processing or for backfill operations to close mine voids. Correct pipe and pumping design is imperative to prevent abrasion and solidification of slurries in full-scale operations. Previous studies showed that particle size distribution had a significant effect on the rheology and the hydraulic gradient of these FA slurries. The rheology of FA and normal water slurry is significantly different to FA slurries used for neutralisation of AMD. The rheological behaviour of FA from different power stations is also markedly different in FA slurries. Additives are introduced during the neutralisation tests and the effect of these additives on the rheology of the residual solids of Matla FA was investigated. These initial results were used to estimate pumping conditions at the pilot plant and for further processing of solid residues as a backfill material.

5.3 EXPERIMENTAL APPARATUS

5.3.1 **The pipe rig**

A unique portable pipe rig was constructed at the Flow Process and Rheology Centre, Cape Peninsula University of Technology (CPUT). The pipe rig consists of a progressive cavity positive displacement pump with variable speed drive which feeds through a damper to three PVC tubes and one stainless steel pipe. The three PVC tubes were used as an in-line pipe viscometer. The stainless steel pipe (inner diameter 16 mm), fitted with housing adapters for ultrasound transducers, was also used to measure rheological parameters in-line by using the UVP-PD method. The PVC tubes were in parallel and had 16 mm, 9 mm and 13 mm inner diameters respectively. All the pipes were linked to one in-line mass-flow meter from Danfoss Instrumentation, which could also measure fluid temperature and density. The mixing tank had a capacity of 50 L and was fitted with an electrically driven mixer that ran continuously during the tests. All the outputs of the pressure

transducers and the mass-flow meter were connected to a data acquisition unit linked to a personal computer (PC). The schematic layout is depicted in Figure 5.1. The clear water test results indicated that the combined error from the mass-flow meter and the point pressure sensors was less than 5%, over the velocity range tested.

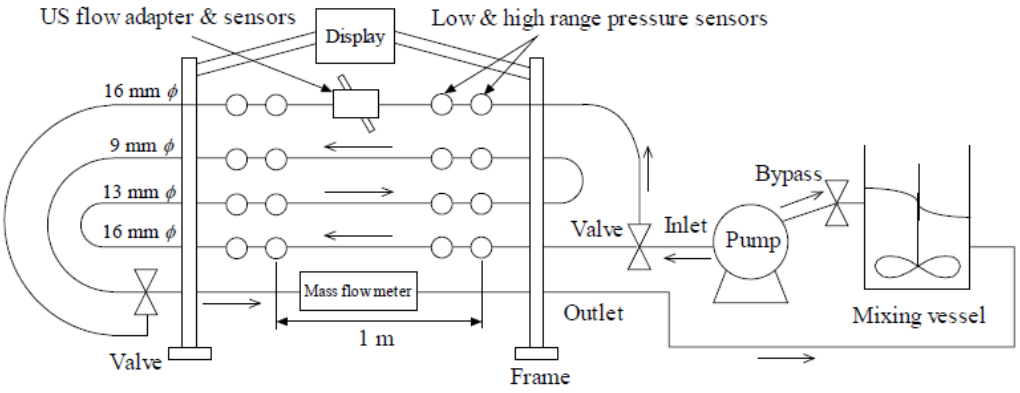

Figure 5.1: Schematic drawing of pipe rig

The FA/AMD slurries recovered after the neutralisation experiments were allowed to settle. The bulk of the water was removed and the settled slurry was then tested at the maximum concentration achieved, and diluted to two more concentrations. Since the slurries could only be prepared by settling and removal of water, it was difficult to prepare slurries with exactly the same densities for comparison. The maximum solids concentration that could be obtained from allowing slurries to settle over time was ~36% by weight. The pressure drop was measured at various flow rates. The shear stress and shear rate were calculated to obtain the rheological behaviour of the slurries.

5.3.2 Pipe flow models

Laminar pipe flow for Herschel-Bulkley fluids can be predicted from Govier & Aziz, (1972)

$$\frac{32Q}{\prod D^3} = \frac{8V}{D} = \frac{4n}{K^{1/n}\tau_0^3}(\tau_0 - \tau_y)^{\frac{1+n}{n}}\left[\frac{(\tau_0 - \tau_y)^2}{1+3n} + \frac{2\tau_y(\tau_0 - \tau_y)}{1+2n} + \frac{\tau_{y^2}}{1+n}\right] \quad \text{.....(5.1)}$$

where $\tau_0 = \frac{D\Delta p}{4L}$ *and* $V = \frac{Q}{A}$

This model is very useful as it can accommodate Newtonian, power-law, Bingham and yield pseudoplastic behaviour.

5.4 RESULTS AND DISCUSSION

This section presents the results of the rheology tests carried out on the FA/mine water slurries, at three concentrations, in order to determine the right specifications for the pump required to handle the slurries which are abrasive and corrosive.

5.4.1 **Pipe tests**

The rheological data can be extracted from pressure drop data and the velocity measured as the fluid flows through the straight pipe. Tests should be carried out in not less than two tube diameters to establish the no-slip condition. This is indicated by the fact that the data from different pipe diameters coincide on the shear stress versus shear rate plot. Although testing slurries in pipes has the advantage of measuring the transitional and turbulent flow over rotational rheometers, it is essential that only laminar data be used in the analysis of the rheological behaviour of the fluid. Figure 5.2 gives a typical pseudo-shear diagram obtained on the test rig.

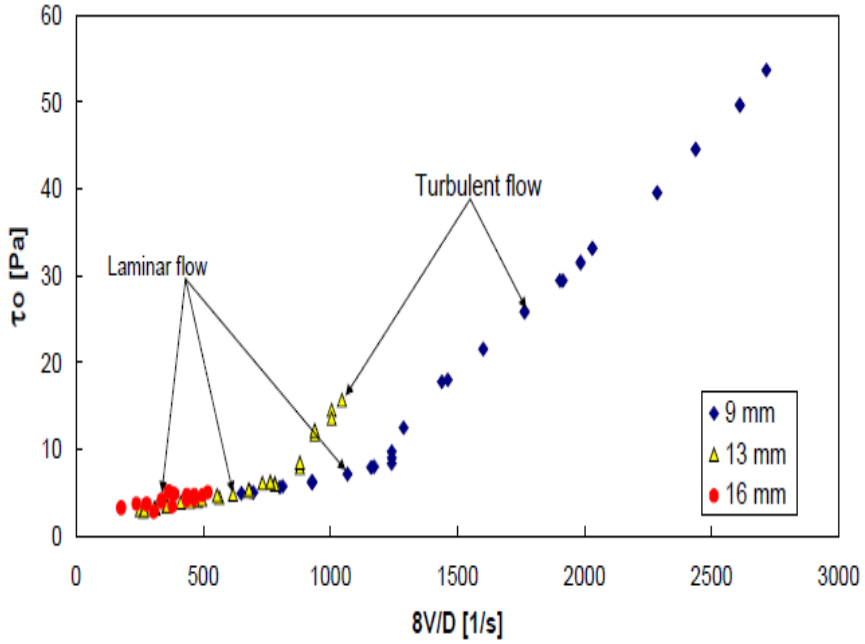

Figure 5.2: Typical pseudo-shear diagram data obtained using three different diameter pipes, in the pipe rig with FA/AMD slurries

5.4.2 **Matla fly ash residual solid slurry**

A slurry obtained from the FA/AMD experiments as reported previously was used for preliminary testing. Several concentrations of the slurry were prepared and it was possible to obtain relative densities of 1.347 with this slurry. This slurry showed typical Bingham plastic behaviour. The yield stress for the maximum concentration was ~9 Pa. The pseudo-shear diagram and rheological parameter results are given in Table 5.1 and Figure 5.3.

Table 5.1: Matla fly ash properties obtained from different slurry concentrations

Property	**Concentration**			
	1	2	3	4
Density	1171	1273	1312	1342
Ty (Pa)	0	30509	50955	90337
K (Pa.S^n)	0.004	0.005	0.006	0.007
n	1	1	1	1

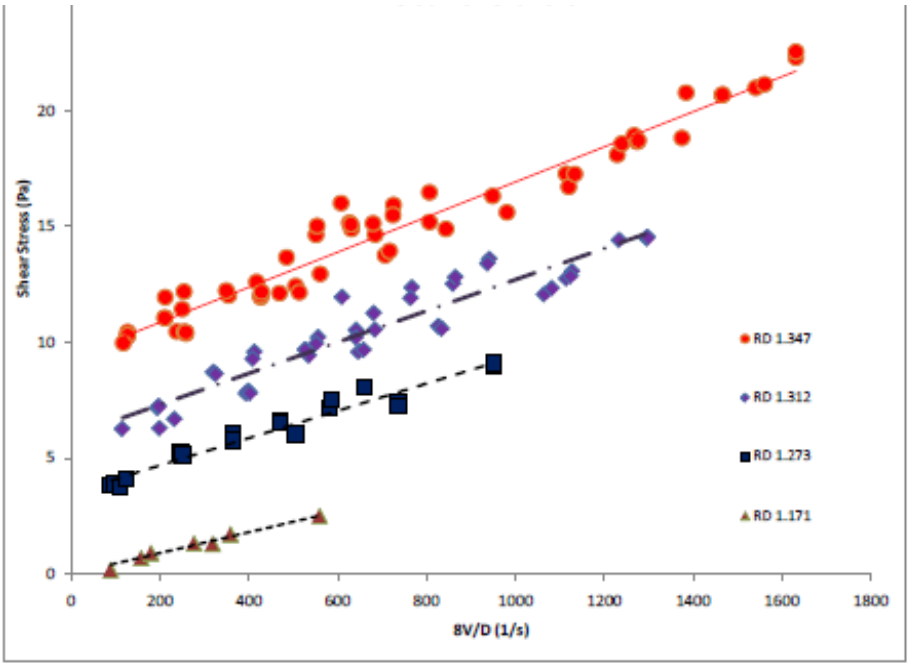

Figure 5.3: **Pseudo-shear diagram for Matla fly ash slurries of different densities**

5.4.3 Matla fly ash residual solid slurry

The particle size distribution, moisture and rheological properties of the Matla FA residual solid slurry is provided in Table 5.2. The slurries were collected after treatment of mine water with FA, lime and $Al(OH)_3$, followed by bubbling CO_2 into the mixture of mine water and FA (labelled AMD + lime + FA + $Al(OH)_3$ + CO_2). The other slurries were obtained after treating mine water with FA, lime and $Al(OH)_3$ (labelled AMD + lime + FA +$Al(OH)_3$). The sample labelled AMD + lime + FA + $Al(OH)_3$+CO_2, was tested at relative densities of 1.237 and 1.270. Two concentrations of relative densities of 1.198 and 1.222 were prepared for the sample labelled AMD + lime + FA + $Al(OH)_3$.

5.4.4 Particle size distribution

The particle size distribution of the various slurries is given in Table 5.2 and Figure 5.4. Previous trials with Lethabo ash showed that it was the intermediate range of particles, between 20 and 100 µm, that affected the rheological parameters most (Vadapalli et al., 2013).

Table 5.2: **Summary of particle distribution of slurries**

Sample name	d(0.1)	d(0.5)	d(0.9)	D[3,2]	D[4,3]	span
AMD + lime + FA + $Al(OH)_3$ + CO_2	0.114	11.467	96.352	0.453	31.997	8.392
AMD + lime + FA + $Al(OH)_3$ + CO_2	0.114	10.984	94.216	0.452	31.672	8.567
AMD + lime + FA + $Al(OH)_3$	0.117	10.996	91.488	0.478	30.395	8.309
AMD + lime + FA + $Al(OH)_3$	0.117	11.282	93.21	0.477	30.797	8.252

Figure 5.4 shows the particle size distribution of the different slurries tested.

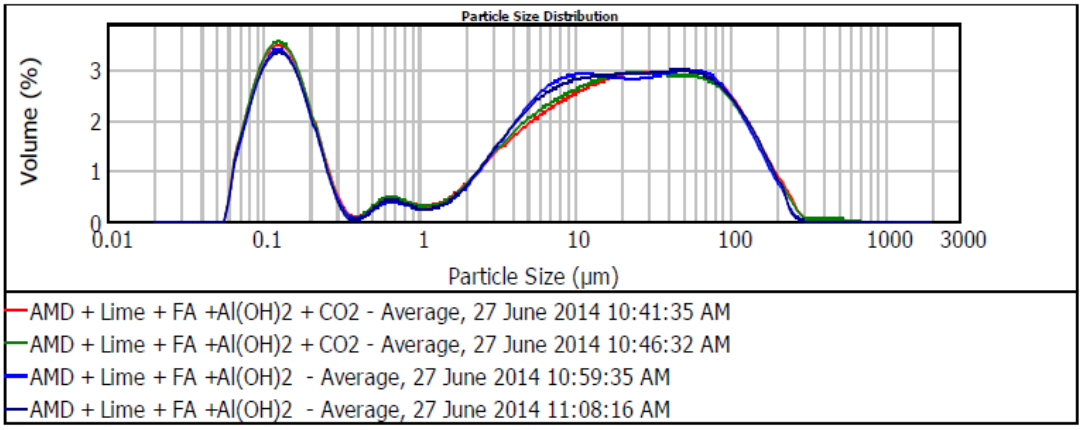

Figure 5.4: Particle size distribution results for slurries tested

The bimodal particle size distribution observed in the 1 to 100 micron particle size range was reduced in the case where the slurry was treated with CO_2 for pH correction and Ca removal after the AMD neutralization experiment using FA, $Al(OH)_2$ and lime. This could be due to calcite formation after sparging with CO_2.

5.4.5 **Pipe test results**

The pipe test result for the residual slurries, prepared in the absence and presence of CO_2, is given in this section. Laminar and turbulent flows were tested as far as could be obtained. The pressure drop per meter length was measured over a range of velocities from 0.2 to 5 m/s. The pressure drop in the 13.16 mm pipe did not exceed 4 kPa/m at approximately 2 m/s, after which turbulent flow ensued. At approximately 5 m/s the pressure drop increased to ~20 kPa. These results are shown in Figures 5.5–5.8.

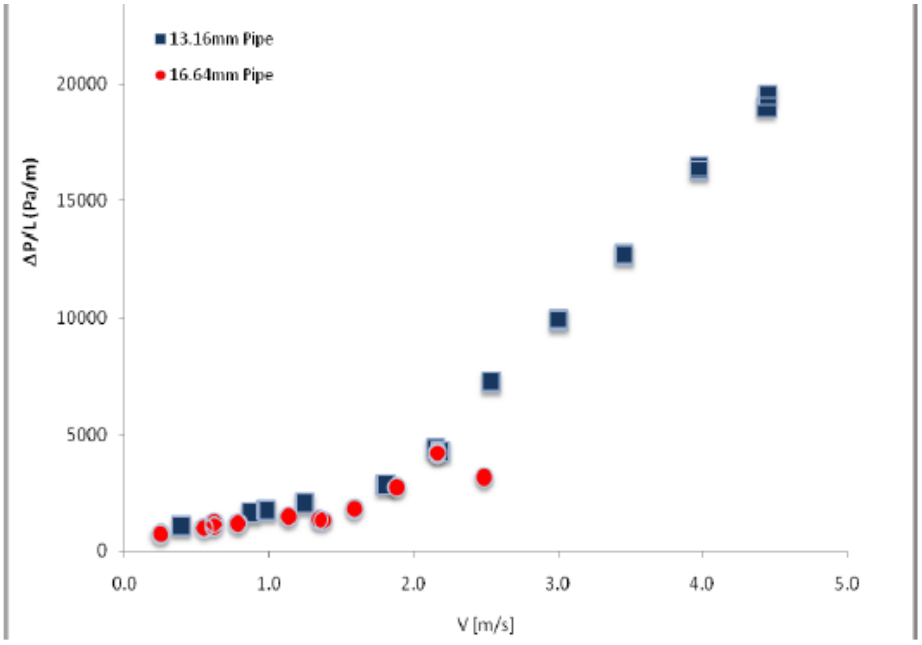

Figure 5.5: Pipe test results for FA + AMD + lime + $Al(OH)_3$ at RD 1.198

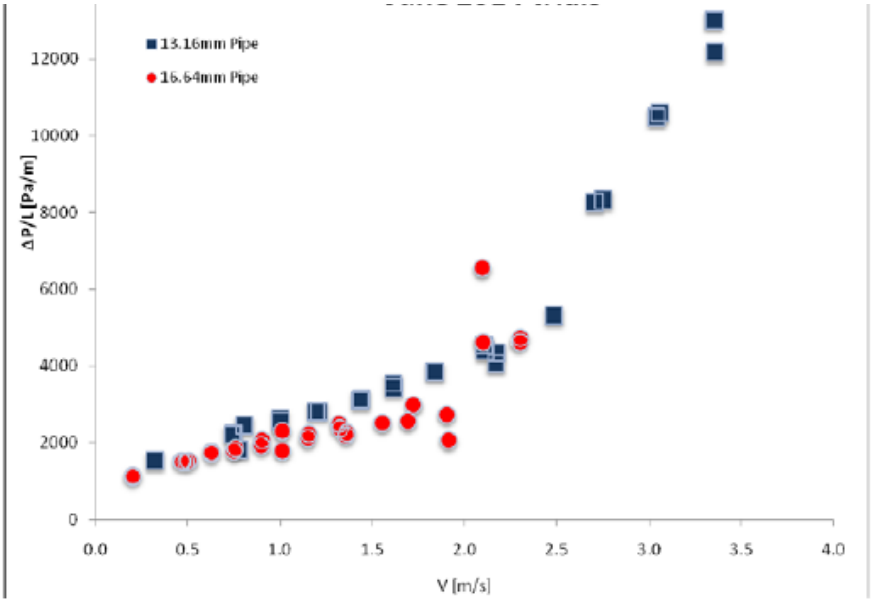

Figure 5.6: Pipe test results for FA + AMD + lime + $Al(OH)_3$ at RD 1.222

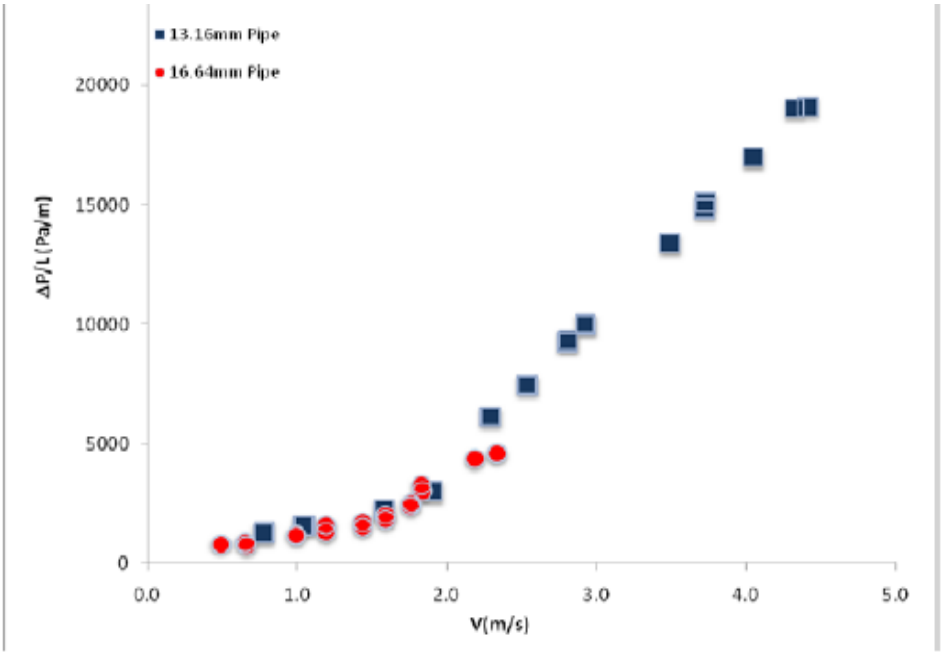

Figure 5.7: Pipe test results for FA + AMD + lime + $Al(OH)_3$ + CO_2 at RD 1.237

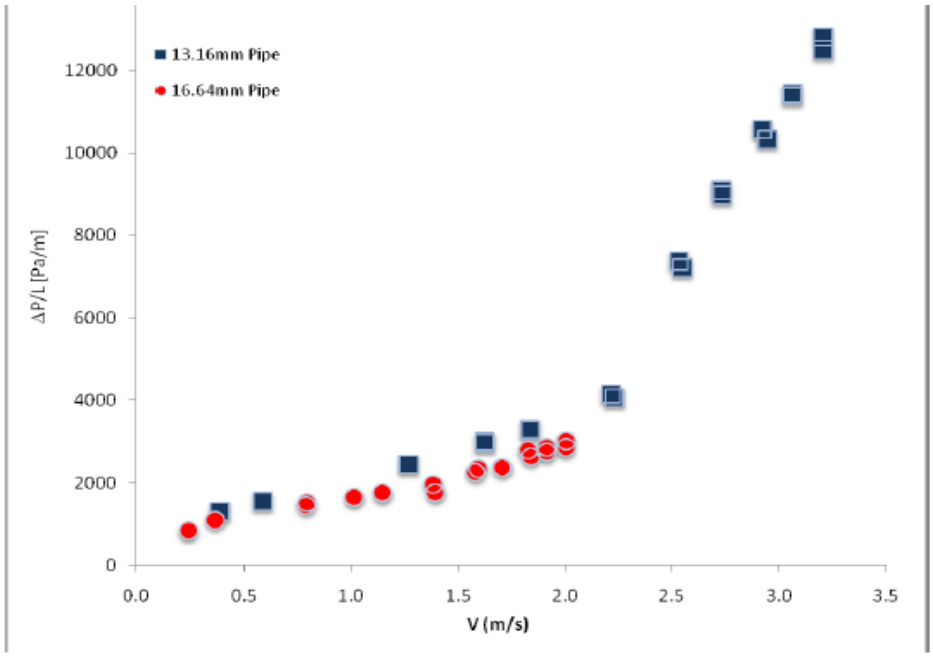

Figure 5.8: Pipe test results for FA + AMD + lime + $Al(OH)_3$ + CO_2 at RD 1.270

5.5 RHEOLOGICAL PROPERTIES

To obtain the viscous properties of the slurries, the shear stresses were calculated at various pseudo-shear rates. The laminar data obtained in both pipes (which coincided) was used to plot the pseudo-shear diagrams. Equation 5.1 was used to determine the rheological properties of each slurry. The density, moisture content, concentration of solids and rheological properties of the samples are provided in Table 5.3. A comparison of

the pseudo-shear diagrams for the slurries resulting after CO_2 sparging are given in Figure 5.9 and for those prepared in the absence of CO_2 are given in Figure 5.10. In both cases, the shear stresses increased for each slurry with increasing density of the slurry. Figure 5.11 shows a comparison of all slurries. Since the slurries could only be prepared by settling and removal of water, it was difficult to prepare slurries with exactly the same densities for comparison. The maximum solids concentration that could be obtained from allowing slurries to settle over time was ~36% by weight.

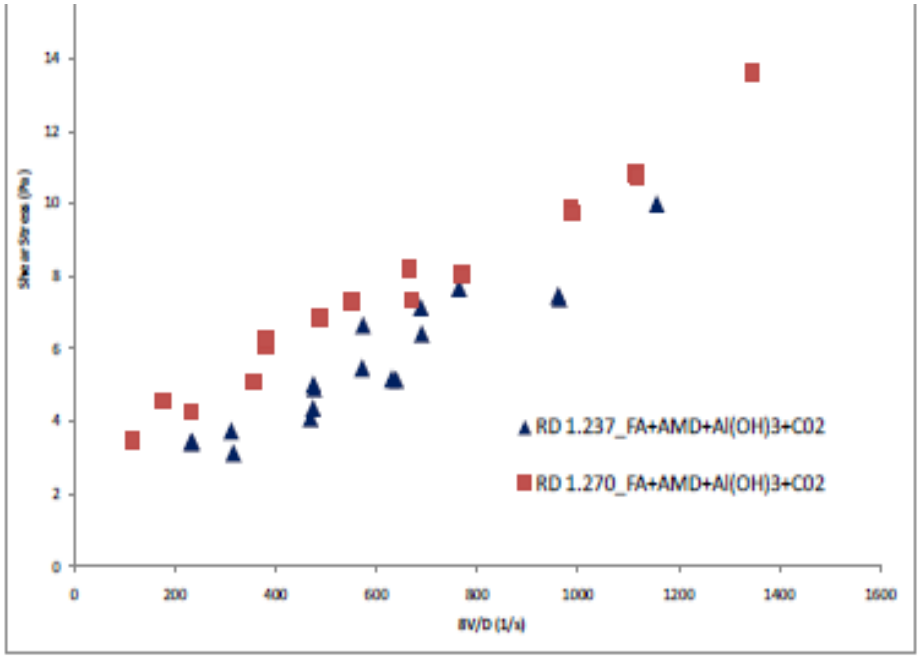

Figure 5.9: Pseudo-shear diagram for samples prepared in the presence of CO_2

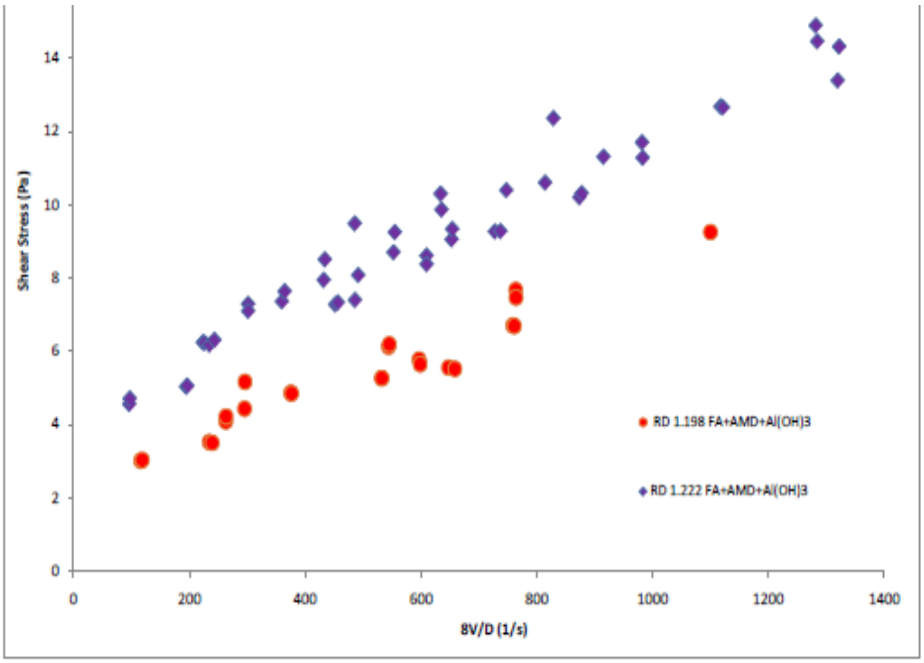

Figure 5.10: Pseudo-shear diagram for samples prepared in the absence of CO_2

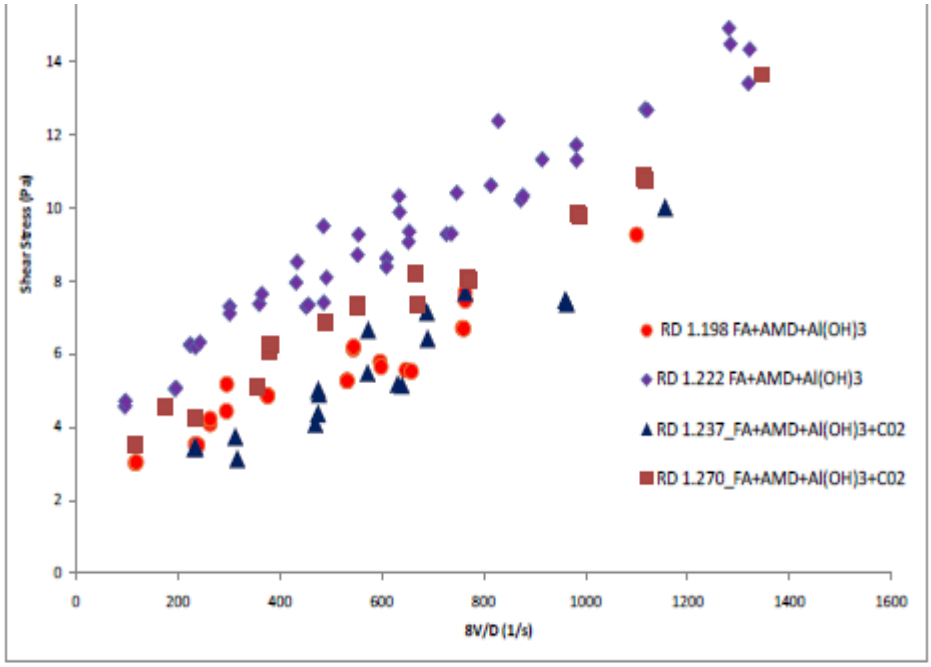

Figure 5.11: Comparison of viscous properties of slurries prepared in presence and absence of CO_2

Table 5.3: Summary of particle distribution of slurries

	RD	Moisture (%)	(%w/w)	Ty [Pa]	K [Pas^n]	n [-]
AMD+ LIME+ FA+ Al(OH)3 + CO2	1.237	67.32	32.68	0.0941	0.0076	1
AMD+ LIME+ FA+ Al(OH)3 + CO2	1.270	63.29	36.71	2.726	0.0065	1
AMD+ LIME+ FA+ Al(OH)3	1.198	73.21	26.79	1.764	0.0067	1
AMD+ LIME+ FA+ Al(OH)3	1.222	67.86	32.14	3.223	0.0078	1
AMD+ LIME+ FA+ Al(OH)3 (Repeat after 1 month later)	1.218	69.27	30.73	3.682	0.0076	1

Interestingly, Figure 5.11 shows that the viscous properties of slurries prepared in the absence of CO_2 sparging, after neutralisation are higher than those prepared in the presence of CO_2. The slurries showed Bingham plastic behaviour. The yield stresses ranged from 0.94 to 3.6 Pa.

5.6 PUMP SPECIFICATIONS

From the above results, the best pump specifications for the recirculation tests of the neutralisation rig are as follows: 1.5 to1 inch centrifugal pump, with a 6 Bar delivery system and a 15 kW motor having a variable speed drive (VSD) and pulley system.

5.7 SUMMARY

Separate pipe tests were performed to determine the slurry densities and pipe diameters most suited to pumping the partially dewatered slurry to the placement site. Previous trials with Lethabo ash showed that the intermediate range of particles, between 20 and 100 µm, affected the rheological parameters most (Vadapalli et al., 2013). In this study, pseudo-shear data were obtained using 9 mm, 13 mm and 16 mm diameter pipe tests. Several concentrations of the slurry were prepared and it was possible to obtain relative densities of 1.347 RD with this slurry. The slurries showed typical Bingham plastic behaviour. The yield stress for the maximum concentration was ~9 Pa. Laminar and turbulent flows were tested. The pressure drop per meter length was measured over a range of velocities from 0.2 to 5 m/s. The pressure drop in the 13.16 mm pipe did not exceed 4 kPa/m at approximately 2 m/s, after which turbulent flow ensued. At a velocity of approximately 5 m/s, the pressure drop increased to ~20 kPa. To obtain the viscous properties of the slurries, the shear stresses were calculated at various pseudo-shear rates. The shear stresses increased for each slurry with increasing density of the slurry. The viscous properties of slurries tested prior to CO_2 sparging were higher than those tested after CO_2 sparging for pH correction and Ca removal. The yield stresses ranged from 0.94 to 3.6 Pa. The pumping tests provided an insight into the conditions to be applied for placement of the backfill after the neutralisation.

CHAPTER 6: PILOT PLANT DESIGN

6.1 INTRODUCTION

In this section, the pilot plant design and treatment of AMD with FA, lime and Al $(OH)_3$ in a jet loop reactor is presented, at 1 000 L scale. As shown in Figure 6.1 below, the design of the pilot is made up of storage tanks for fly ash (5 000 L) and AMD (35 000 L). The AMD storage comprised three 1 2000 L tanks connected to the mixing and clarification tanks by a pump. The FA was conveyed from storage to the mixing/clarification tank using a chain block pulley system. After the FA and mine water was mixed, the mixture was clarified and separated by pumping the water to a carbonation tank (unit 7). The remaining residue was pumped in slurry form to the storage tank (unit 9). The treated water was mixed with carbon dioxide to bring the pH down to between 6 and 9. The calcium carbonate that forms was filtered from the water using the in-line filter.

The plant lay out is shown in Figure 6.2. The fly ash storage (Unit 1) was a 5 000 L capacity storage tank. The AMD (3 5000 L) was stored in three 1 2000 L tanks (together comprising Unit 2). Likewise, the storage tank for the treated water (Unit 8) comprised three tanks of similar size.

During the operation of the pilot plant, the main investigations undertaken were: the energy consumption of the plant; the optimum circulation of the water through the jet reactor; the quality of the incoming water and the treated water.

Based on these results, the energy costs of the plant could be deduced. Various stakeholders were invited to see the pilot plant in operation.

6.2 PLANT MONITORING AND CONTROLLING

The process will be monitored and controlled from a control room, using a supervisory control and data acquisition system (SCADA). The SCADA system will consist of pH, EC and temperature sensors connected to various tanks. Most of the external analytical techniques, such as ion chromatography (IC), and ICP-OES will be applied, for analysis of samples taken during the process, in order to provide feedback on the efficiency of the process, but are not part of the monitoring system of the plant. The engineering designs, drawn for the 1 000 L pilot, are shown in Figures 6.1–6.3. The major sensors in the plant were pH and EC sensors, as indicated in these figures. These sensors were connected to the control box system, where the pH and EC at each stage was monitored and controlled accordingly. The programmable logic controller (PLC) for the monitoring of the pilot plant is shown in Figure 6.4.

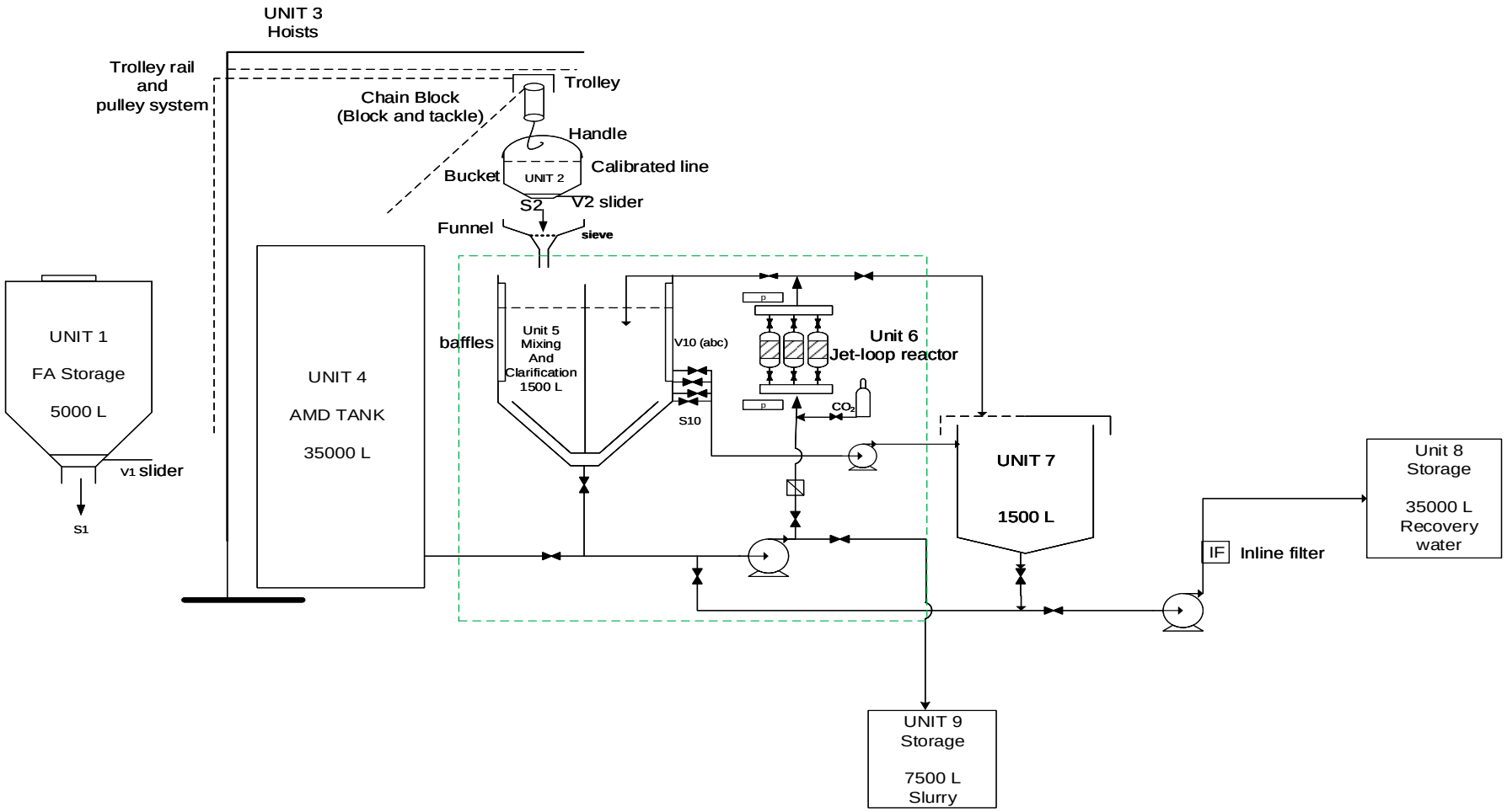

Figure 6.1: Detailed pilot plant design for the treatment of mine water using coal fly ash, lime and aluminium hydroxide

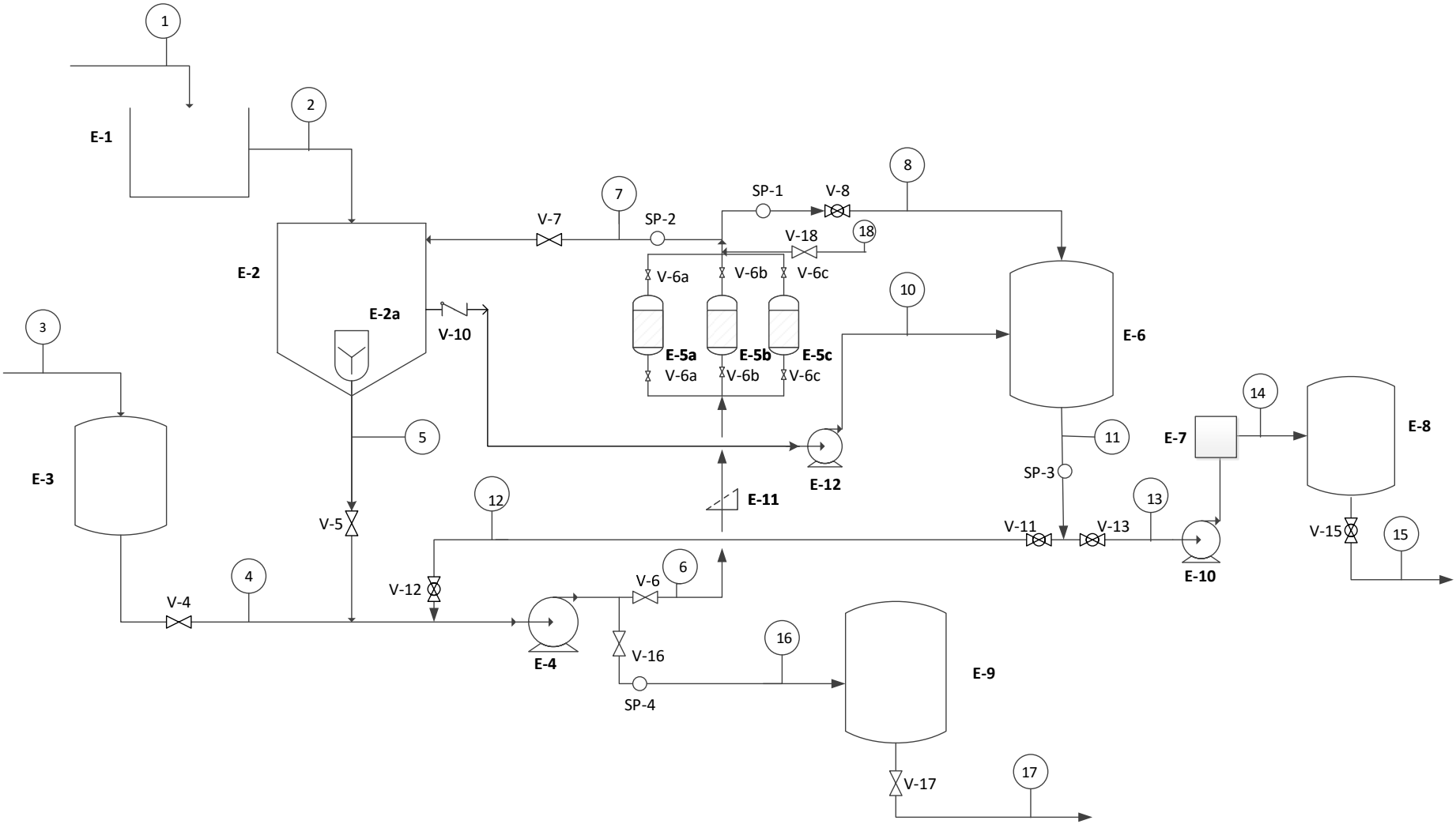

Figure 6.2: Block flow diagram of the pilot plant

PLANT LAYOUT

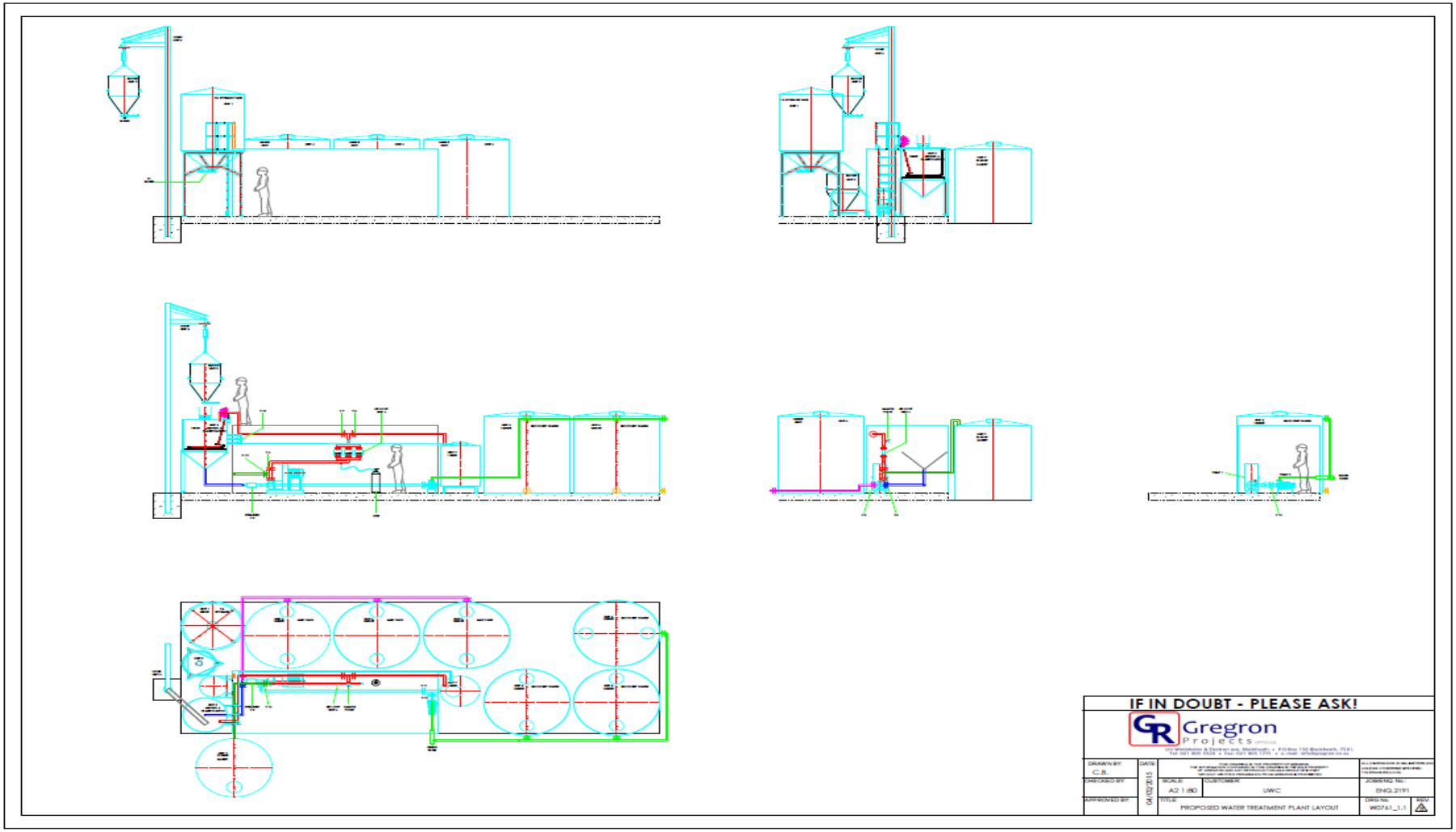

Figure 6.3: The layout of the pilot plant

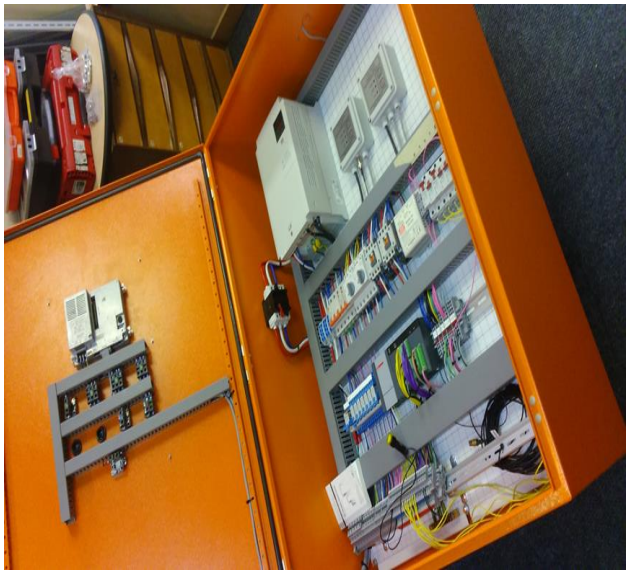

Figure 6.4: The PLC for the pilot plant

6.3 OPERATION MANUAL

Table 6.1 Unit operations

Unit number	Equipment
E-1	FA storage
E-2	Mixer & clarifier
E-2a	Agitator
E-3	AMD storage
E-4, 10 and 12	Centrifugal pumps
E-5 (a, b, c)	Jet loop reactors
E-6	Plug flow tank
E-7	In-line filter
E-8	Water storage
E-9	Slurry storage
E-10	Centrifugal pump 2
E-11	Strainer
SP-1-4	Sampling point

Table 6.2: Stream compositions

Stream number and valve	Composition
1;	FA
2;	Manual transfer of FA, lime & aluminium hydroxide
3;	AMD
4; V-4	Same as 3
5; V-5	AMD, FA, lime and aluminium hydroxide
6; V-6	Same as 5
7; V-7	Same as 5
8; V-8	Carbonation (water)
9; V-9	Sample point
10; V-10	Clear water
11; V-11	Same as 8
12; V-12	Same as 8
13; V-13	Treated water
14;	Same as 13
15;	Same as 13 (to sewer or recovery for reuse)
16; V-16	Slurry
17; V-17	Same as 16 (to waste or pumped to backfill)
18; V-18	Carbon dioxide

6.3.1 Process description (Plant start-up, operation, monitoring and controlling)

Monitoring and controlling are valuable tools for ensuring reliable product quality in the process industry. The software installed for this scale-up process was SCADA. This software was chosen based on its primary drivers which are to increase efficiency, reduce costs, enhance decision making and simplify operations. The process is operated from a control room, where operators engage the system from one or more human-machine interface (HMI) workstations. When equipment starts or stops, sensors measure the change at field level and transmit a signal to the PLC which communicates to the HMI system, where graphical elements change colour to reflect current conditions. When an anomaly occurs, the same process was repeated, and the HMI system alerts operations staff.

6.3.2 Process description and start-up

Regarding assembly of the raw materials, AMD was collected from Lancaster dam, FA was obtained from Matla power station, and lime and aluminium hydroxide were supplied by Sigma Aldrich, Kimix or Merck.

The treatment of AMD will be carried out as follow:

Cycle 1: Neutralisation and clarification

Ensure that all valves are closed. Open valve 4, valve 6, valve 7 and jet loop valves (V-6abc), depending on the number of jet loops you want to use, to allow 1000 L of AMD to flow within the system through the jet loop, then press the pump start button on the control box (in the control room) to run pump P1 (E-4) to fill unit E-2 with 1 000 L AMD to the calibrated line (using a level probe); press the pump P1 (E-4) to stop on the control box then close valve 4.
Fill up the bucket (Figure 1 unit 2) with coal FA to the calibrated line by opening unit 1 (slider 1), allowing the coal FA out of unit 1 into the bucket. Close unit 1 (slider 1) when the bucket is filled to the calibrated line that represents 167 kg. Use the chain block on unit 3 (hoists) to hook on to the handle on unit 2 and then lift and convey unit 2 to position it directly on the funnel above unit E-2 using the pulley system. The funnel is mounted on top of the roof of the container housing unit E-2, it protrudes through the container roof and enters unit E-2, the mixing tank. Its role is to channel the coal FA into the mixing tank (unit E-2).

Note: Add 167 kg coal FA to unit 5 only if the filling of unit 5 with 1000 L AMD has been completed.

Open valve 5 and press the pump start button on the control box to run pump P1 (E-4) to allow the AMD to circulate through the jet loop. Open unit 2 (slider 2), add 167 kg of coal fly ash through the funnel whilst the AMD is circulating through the jet loop and simultaneously press the agitator (E-2a) start button on the control box to run the agitator (E-2a) to ensure thorough mixing. Only run pump P1 (E-4) for a required time, stop and then use agitator (E-2a) for mixing.

Use the scale to weigh 2.1 kg of lime and 3.6 kg of aluminium hydroxide, separately, into separate bags. Following mixing of AMD and FA, immediately add 2.1 kg of the pre-weighed lime to the AMD+FA mixture through the funnel into unit E-2. From the display screen, monitor the pH. When the pH is greater than 11, add the pre-weighed 3.6 kg of aluminium hydroxide. Circulate the AMD + FA + lime + Al $(0H)_3$ mixture through the jet loop for a required period of time (according to the experimental procedure). Press pump P1 (E-4) stop button on the control box to stop the pump; then, immediately close valve 5 (this is to avoid the slurry from settling in the pipes). Close valve 6, 6abc and 7 after stopping the pump; at this time you would have to switch to use the agitator (E-2a) in unit E-2 for mixing.

Stop the agitator E-2a in unit E-2 after 180 minutes mixing time has elapsed. Leave the slurry to settle whilst clarification of water takes place. After approximately 30 minutes, clarification should be completed; use valve 10 either a, b, c or d; then press pump P3 (E-12) start button on the control box to start pumping the clarified solution into unit E-6. From the sight glass on the pipeline, monitor the colour of the water. When the colour of the water changes, immediately close valve 10, either a, b, c or d. Thereafter, stop pump P3 (E-12).

Cycle 2: Carbonation

Open valves 11, 12, 6, 8 and the jet valves (inlet and outlet jet loop reactors' valves) preparing for carbonation. Press pump P1 (E-4) start button for circulating the clarified solution (water) in unit E-6 through the jet loop for carbonation. Press the gas regulator button on the HMI and allow carbonation to take place through the jet loop, monitoring the pH. In the CO_2 stream, there is a one-way valve (V-18). Stop carbonating when the pH is between 6 and 9; simultaneously, stop the pump. Close valve 11 first, then valve 12 and allow the solution (water) within pipes to go into unit E-6. Close valves 6 and 8 after pumping water back into unit E-6. Open valve 13, allow the solution (water) to flow through pump 2 (E-10) and press pump P2 start button allowing the water to flow through the in-line filter in stream 14 into unit E-8 (recovered water). Not all the water will be pumped to unit E-8; some of it will be used to clean the pipe and pump P1 after the final step.

Final step

Open valve 5 and valve 16, and then press pump P1 (E-4) start button, pumping the slurry from unit E-2 to unit E-9 (slurry storage). The slurry remaining in the system will be cleaned with the water in unit E-8.
Ensure that all valves are closed. Open valves 11, 12, and 16, allow the water to flow through pump P1 (E-4) and press pump P1 start button, allowing the water to flow from E-6 to E-9.

Repeat the cycle of operation as required. Prepare for the next run, cycle 1, by opening valves 4, 6 and 7, allowing the AMD to flow through the jet loop. Press pump 1 start button and fill unit 5 to the calibrated line which represents 1000 L AMD, and close the valves, etc.

6.4 PIPING AND INSTRUMENTATION DIAGRAM

The scaled-up jet loop reactor process (1000 L) for AMD treatment is monitored and controlled using an automatic system. The control industry (especially the chemical and process industry) describes its plants and their instrumentation by a piping and instrumentation diagram (P&ID). The P&ID shows the flows in a plant (in the chemical or process industry) and the corresponding sensors or actors. At the same time, the P&ID gives a name ("tag") to each sensor and actor, along with additional parameters. This tag identifies a "point" not only on the screens and controllers, but also on the objects in the field (AA, 2008). Tag "numbers" are letters and numbers placed within or near the instrument to identify the type and function of the devices (AA, 2008). The P&ID for the pilot plant is depicted in Figure 6.5 below.

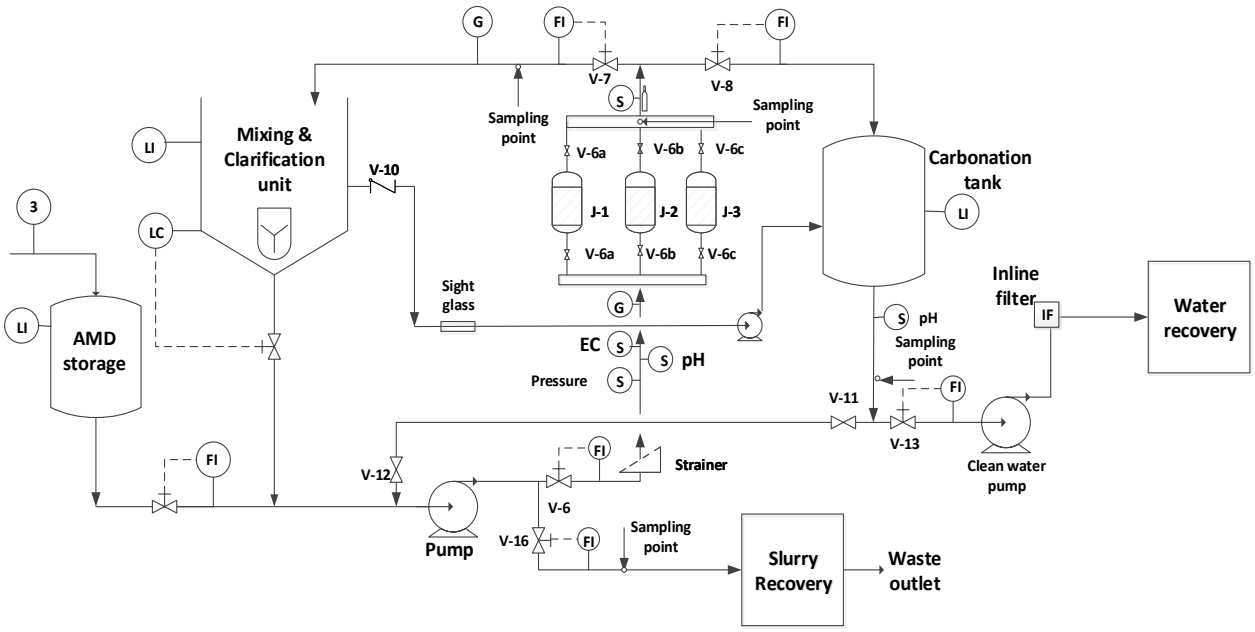

Figure 6.5: P&ID block diagram

Table 6.3 P&ID symbols and description

Symbol	Description
FI	Flow indicator
FIC	Flow indicator controller
FT	Flow transmitter
G	Pressure gauge
LI	Level indicator
LC	Level controller
TIC	Temperature indicator controller
S	socket

Monitoring and controlling are valuable tools for ensuring reliable product quality in the industry. Table 6.3 highlighted different sensors or automation devices which are incorporated in the pilot plant; all the valves have a sensor which enables the operations staff to control the system. The software installed in the automation of the process is SCADA. This software was chosen based on its primary drivers which are to increase efficiency, reduce costs, enhanced decision making and simplify operations.

The automation of the pilot plant simplified operations; when equipment starts or stops, the sensors measure the change at field level and transmit a signal to the programmable logic controllers (PLC), which then communicates to the human-machine interface (HMI) system, where the graphical elements change colour to reflect current conditions. When an anomaly occurs the same process is repeated, and the HMI system alerts operations staff in the control room.

6.5 MATERIAL BALANCE

The investigations carried out to date in this project have proven that AMD can be treated using FA and chemical reagents (see associated publications output list). The products are good quality water (that can be used for irrigation) and a solid residual material can be used for mine backfilling or zeolite synthesis, thereby producing zero effluent and a cradle to cradle solution. In order to quantify the amount of mine water and chemical reagents fed, and the amount of treated water and slurry recovered at the end of the process; the concepts of material balance were used.

Material balances are nothing more than the application of the law of conservation of mass, which states that mass can neither be created nor destroyed. Material balances are an important first step when designing a new process or analysing an existing one**.** They are almost always a prerequisite for all other calculations in the solution of process engineering problems (Felder & Rousseau, 1986). A process is any operation or series of operations by which a particular objective is accomplished. Those mentioned operations involve a physical or chemical change in a substance or mixture of substances. The material that enters a process is referred to as the input or feed, and that which leaves is the output or product (Noor, 2010).

Let us suppose that lime is a component of both the input and output streams of the continuous process unit shown below, and that the flow rates of the input and output are measured and found to be different.

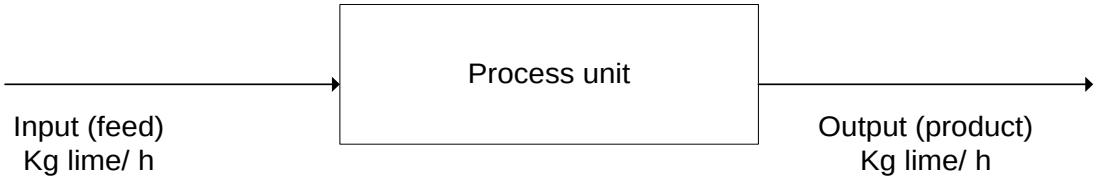

Figure 6.6: Material balance representation

If there are no leaks and the measurements are correct, then the other possibilities that can account for this difference are that lime is either being generated, consumed, or accumulated within the process unit. A balance (or inventory) on a material in a system (a single process unit, a collection of units, or an entire process) may be written in the following general equation:

ACCUMULATION = IN - OUT + GENERATION – CONSUMPTION

where,

Accumulation: builds up within system

Input: enters through system boundary

Generation: produced within system

Output: leaves through system boundary

Consumption: consumed within system

A material balance is an accounting for material. Thus, material balances are often compared to the balancing of current accounts. They are used in industry to calculate mass-flow rates of different streams entering or leaving chemical or physical processes (Felder & Rousseau, 1986). The process boundary of AMD treatment is shown in figure 6.7 below.

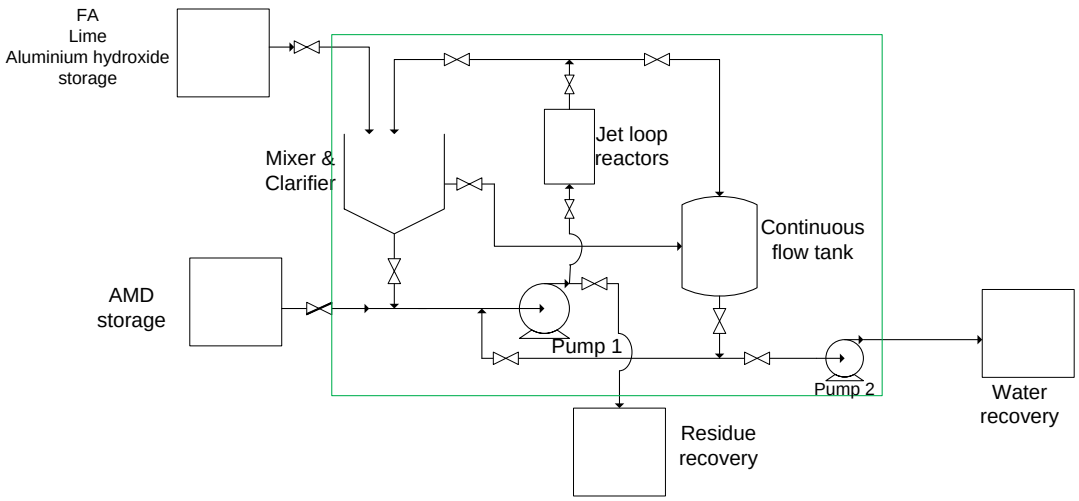

Figure 6.7: Process boundary for AMD treatment

Treatment of AMD with FA, using the 1000 L pilot plant (Figure 6.7), was carried out as described here.
The first step was to assemble the raw materials, consisting of AMD, FA, lime and aluminium hydroxide. Neutralisation, clarification, carbonation, and recovery of water and sludge are the main steps that constitute the operation of the pilot plant (as shown in Figure 6.7). In the mixing unit (E-2), 1000 L of AMD was mixed with 200 kg of FA and 2.5 kg of lime. The mixture was circulated through jet loop reactors (E-5) in order to enhance the homogeneity of the solution and reduce the residence time of the reaction, which resulted in an increase in pH to greater than 11, and improved the quality of the water. After every 30 minutes, throughout the experiment, samples were collected for analysis. At 166 minutes, the pH got to 11.2, then 3.6 kg of $Al(OH)_3$ was added to the solution of AMD+FA+lime. Eight minutes later, the pH dropped to 8.9, till 180 minutes was completed. Thereafter, the solution was allowed to settle for 60 minutes in unit E-2. However, the clear water was decanted to the continuous tank (E-6). The pH of the clear water was 8.9.
Thereafter, the water was pumped from E-6 to unit E-8 for storage (Figure 3). Finally, the sludge was pumped from E-2 to the E-9 residue recovery tank. The slurry remaining in the piping system was cleaned with the remaining water in unit E-8.
In this section of the study, the unknown masses of components (water recovered, sludge recovered, mass of water and solid in the sludge) of all the inputs and outputs of the process units were determined using material balance concepts.

AMD mass calculation

Assuming that the density of acid mine drainage, $\rho_{AMD} = 1094\ \frac{kg}{m^3}$

$V_{AMD} = 1000\ L = 1\ m^3$

$\rho = \frac{m}{v} \rightarrow m_{AMD} = \rho \times v = 1094 \times 1 = 1094\ kg$

The following is the general material balance equation:
Accumulation = input– output + generation - consumption
The calculations were done using the following assumptions:

- A system is at steady state, accumulation = 0

  Input + Generation = Output + Consumption

- The balanced quantity is total, generation = 0 and consumption = 0

Input = Output

Table 6.4. Feed streams composition

Input stream	
Elements	**Mass (kg)**
Acid mine drainage	1094
Coal fly ash	200
Aluminium hydroxide	3.6
Lime	2.5
Total = 1300.1 kg	

Since mass is a more practical property to measure than moles, flow rates are often given as mass flow rates rather than molar flow rates. When this occurs, it is convenient to express concentrations in terms of mass fractions, defined similarly to mole fractions:

$$X_a = \frac{m_a}{m_t}$$

where:

X_a: the mass fraction of component A

m_a: the mass of component A (kg)

m_t: the total mass of all components in the system (kg) for fly ash, aluminium hydroxide, and lime.

Therefore, the mass fractions were determined as follows:

$$X_{FA} = \frac{m_{FA}}{m_t} = \frac{200}{206.1} = 0.970$$

$$X_{lime} = \frac{m_{lime}}{m_t} = \frac{2.5}{206.1} = 0.012$$

$$X_{Al(OH)_3} = \frac{m_{Al(OH)_3}}{m_t} = \frac{3.6}{206.1} = 0.017$$

$$X_{AMD} = \frac{m_{AMD}}{m_t} = \frac{1094}{1094} = 1$$

An initial representation of the mass and mass fractions of different streams that constitute the AMD treatment process is shown below:

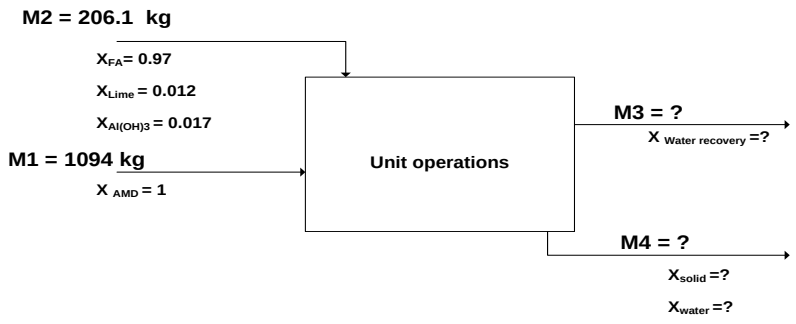

Figure 6.8 Initial block diagram of AMD treatment process

where:

M_1: the mass of AMD fed to the process (kg)

M_2: the total mass of FA, lime, and aluminium hydroxide fed to the process (kg)

M_3: the mass of water recovered from the process (kg)

M_4: the mass of sludge recovered from the process (kg)

X: the mass fraction of a component.

The unknowns are M_3, M_4, $X_{Water\ recovery}$, and components for the residue (X_{solid}, and X_{water}). The experiment was carried out for 180 minutes with a pH of 8.9.

Experimentally, the amount of water recovered was 728.56 kg (666 L) after a settling time of 60 minutes, the percentage of water recovery was calculated as follow:

$$\text{Percentage of water recovery} = \left[\left(\frac{\text{M}_{\text{water recovery}}}{\text{M}_{\text{acid mine drainage}}}\right) \times 100\right] = \left[\left(\frac{728.56}{1094}\right) \times 100\right] = 66.6\%$$

Different assumptions were made from the general material balance equation; the mass of sludge was determined, as follows:

Inputs = Outputs

$$\text{M}_1 + \text{M}_2 = \text{M}_3 + \text{M}_4 \quad \rightarrow \text{M}_4 = \text{M}_4 + \text{M}_2 - \text{M}_3 \quad \rightarrow \text{M}_4 = 1094 + 206.1 - 728.56$$

M_4 = 571.54 kg

One of the objectives of running this pilot plant to treat AMD is to recover as much water as possible. When 1000 L of AMD was fed to the process for treatment, at the end of the experiment, 728.56 kg of water was recovered, which represents 66.6% of the mine water that was fed to the process. The assumption made from the general material balance equation is that inputs equal outputs. This should be applied to all the components involved in the AMD treatment process. The law of conservation of mass states that mass can neither be created nor destroyed (Felder, 1986). That means that 33.4% of the remaining water is retained in the sludge. and can be determined to finally have 1094 kg of mine water fed to be equal to 1094 kg of water exiting the process.

The sludge is made of solid materials, which separated from clear water after settling, and decanting of the water. In addition to solids, sludge contains a high percentage of water. At the end of the experiment, 571.54 kg of sludge was recovered; the amount of water and solid in the sludge can be determined using the method of moisture content

6.6 DETERMINATION OF MOISTURE CONTENT

Three sludge samples were collected after 60 minutes settling, weighed immediately and recorded as the wet weight of sample (9 grams). These wet samples were dried to a constant weight at a temperature of 100ºC, using an oven, for 24 hours. The samples were allowed to cool. The cooled samples were weighed again, and recorded as the dry weight of sample, as shown in Table 6.5 below.

Table 6.5 Moisture content: Wet and dry samples

	Mass (g)		
	Sample 1	Sample 2	Sample 3
Wet weight samples	9.503	9.500	9.502
Dry weight samples	3.441	3.423	3.416

The moisture content of the sample is calculated using the following equation:

$$\%W = \left(\frac{A - B}{A}\right) \times 100$$

Where,

%W: Percentage of moisture in the sample

A: Weight of wet sample (grams)

B: Weight of dry sample (grams)

The moisture content of the sludge was determined as follows:

Sample 1

$$\%W = \left(\frac{A - B}{A}\right) \times 100 = \frac{9.503 - 3.441}{9.503} \times 100 = \mathbf{63.79}\%$$

Sample 2

$$\%W = \left(\frac{A - B}{A}\right) \times 100 = \frac{9.500 - 3.423}{9.500} \times 100 = \mathbf{63.97}\ \%$$

Samples 3

$$\%W = \left(\frac{A - B}{A}\right) \times 100 = \frac{9.502 - 3.416}{9.502} \times 100 = \mathbf{64.05}\ \%$$

$$\text{Average \% moiture content} = \frac{63.79 + 63.97 + 64.05}{3} = \mathbf{63.94}\ \% \sim \mathbf{64}\%$$

The moisture content in the sludge recovered at the end of the AMD treatment process was found to be 63.94%. The amount of water in the sludge was calculated as follows:

$$\text{Amount of water in sludge} = \text{average moisture content of sludge} \times \text{mass of sludge}$$

$$\text{Amount of water in sludge} = 0.6394 \times 571.54\ \text{kg} = 365.44\ \text{kg}$$

At the end of the AMD treatment process, water retained in the sludge was found to be 365.54 kg; which means a significant amount of water could be recovered if the process could be improved by adding a dewatering unit operation to this pilot plant so that the dry solid can be discarded and the water can be recycled into the process. 66.6% (728.56 kg) of water was recovered as main product; the remaining 33.4% is equivalent to 365.44 kg of water that was retained in the sludge. From the results obtained, it could be said that most of the water was recovered.

The sludge is a combination of water and solid material. In this study, the amount of sludge and water in the sludge recovered were found to be 571.54 kg and 365.44 kg, respectively. The following material balance equation was used to determine the amount of solid in the sludge:

$$\text{Mass of sludge} = \text{mass of water in the sludge} + \text{mass of solid in the sludge}$$

$571.54 = 365.44 + \text{mass of solid in the sludge}$

Mass of solids in the sludge = 206.1 kg

The amount of solids fed to the AMD treatment process was 206.1 kg (FA, lime, and aluminum hydroxide) and 206.1 kg of solid was recovered.

The following figure is the overall material balance block flow diagram of the pilot plant.

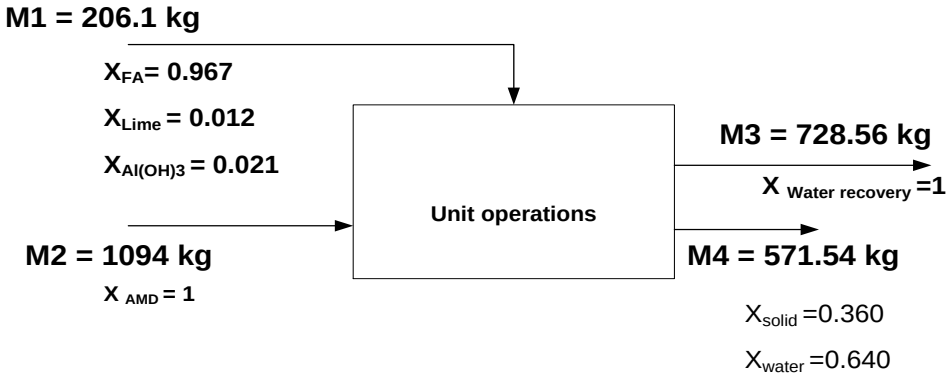

Figure 6.9 Material balance block flow diagram

The amount of material fed into the AMD treatment process was found to be almost equal to that produced, in terms of masses of solids and liquids. The water produced met the standard for irrigation according to TWQR and this was possible due to chemical reactions accelerated by the energy produced during the AMD treatment process.

6.7 ENERGY BALANCE

The pilot plant was designed, constructed and implemented to use less expensive chemicals, equipment, and then lower operating cost by minimizing the amount of energy consumption. This pilot plant is a fluid system. This fluid system was designed to transport the mixture of AMD, FA, lime, and aluminium hydroxide from one tank to another at a specified flow rate, velocity, and elevation difference. The system can consume mechanical energy in the centrifugal pump during the mine water treatment process. In addition to the mass balance, the other important quantity to be considered in the analysis of fluid flow is the energy balance or conservation of energy, as shown in the equation below

Accumulation = energy in – energy out + generation – consumption

The First Law of Thermodynamics expresses a fundamental law of physics: energy is conserved. Energy can neither be created nor destroyed (just like mass and momentum), but energy can move across the boundaries of a system. By increasing or decreasing the total system energy, energy can cross system boundaries in a variety of ways. One is in the form of heat, and another is in the form of work. A third way energy enters or leaves a system is when it is carried along by material entering or leaving the system, a mechanism known as convection (Morrison, 2005). The AMD treatment process consisted of three pumps which are involved in the

transfer of fluid from one location to another, depending on the procedure and stage of the experiment. These pumps are highlighted in Figure 6.10.

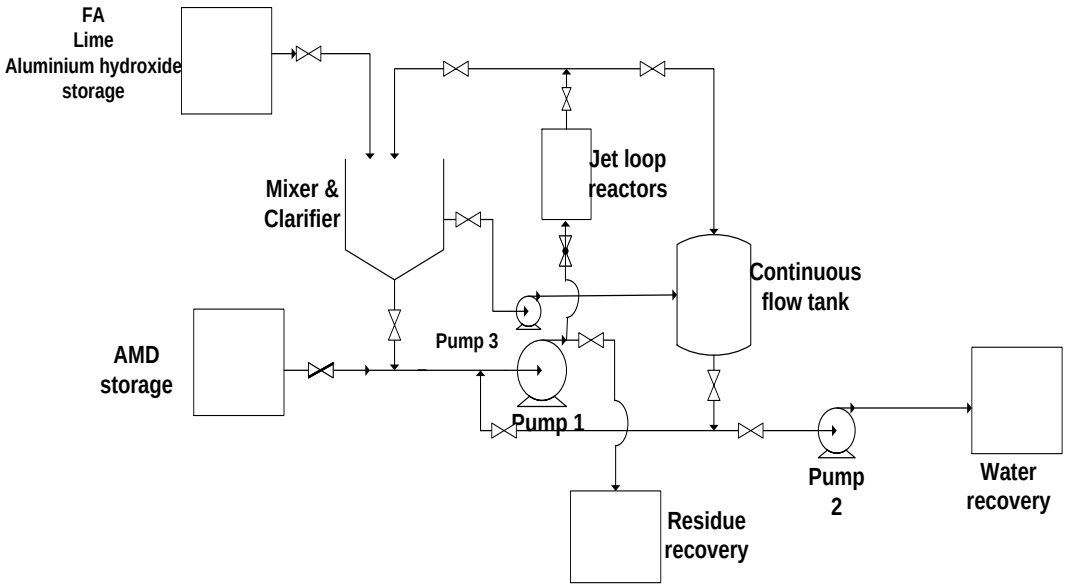

Figure 6.10: Location of pumps in the AMD process

Although three pumps were used, as shown in Figure 6.10, the conservation of energy was calculated for pump 1 only, because pump 1 was mostly used throughout the treatment, whereas pumps 2 and 3 are merely used to pump the recovered water to storage and the clear water to the carbonation tank, respectively. It is simple and easy to use the relation between the pressure, velocity and elevation in a moving fluid by applying the Engineering Bernoulli Equation to determine the energy created by the pump. When the Engineering Bernoulli Equation is applied to fluid contained in a control volume fixed in space, typically the control volume has impenetrable boundaries, with the exception of one or more inlets and one or more outlets through which fluid enters and leaves the control volume. During passage of fluid through the control volume, mechanical work is irreversibly transformed by fluid friction into heat, leading to losses. Also, the fluid work may be performed on the fluid by a pump. This leads to shaft work, assumed by convention to be positive when performed by the fluid, and negative when performed on the fluid. Both losses and shaft work are included in the energy form of the Engineering Bernoulli Equation on the basis of unit mass of fluid flowing through (Subramanian, 2014). The two most common forms of the resulting equation, assuming a single inlet and a single exit, are presented next.

Energy form of the Engineering Bernoulli Equation.

Each term has dimensions of energy per unit mass of fluid.

$$\frac{\mathbf{P_{out}}}{\boldsymbol{\rho}} + \frac{\mathbf{V_{out}^2}}{\mathbf{2}} + \mathbf{g z_{out}} = \frac{\mathbf{P_{in}}}{\boldsymbol{\rho}} + \frac{\mathbf{V_{in}^2}}{\mathbf{2}} + \mathbf{g z_{in}} + \mathbf{loss} - \mathbf{W_s}$$

In the above equation,

P: is pressure, which can be either absolute or gage, but should be in the same basis on both sides, represents the density of the fluid, assumed constant (Pa),

V: is the velocity of the fluid at the inlet/outlet (m/s), and

Z: is the elevation about a datum that is specified. Note that it is only differences in elevation that matter, so that the choice of the datum is arbitrary (m).

g: This letter stands for the magnitude of the acceleration due to gravity (m^2/s).

Loss: stands for losses per unit mass flowing through (m), while

$\mathbf{W_s}$: represents the shaft work done by the fluid per unit mass flowing through (W).

The form given above assumes flat velocity profiles across the inlet and exit, which is a reasonable approximation in turbulent flow. In laminar flow, the velocity distribution across the cross-section must be accommodated in the kinetic energy calculation.

The head form of the Engineering Bernoulli Equation is obtained by dividing the energy form throughout by the magnitude of the acceleration due to gravity, *g:*

$$\frac{\mathbf{P_{out}}}{\boldsymbol{\rho g}} + \frac{\mathbf{V_{out}^2}}{\mathbf{2g}} + \mathbf{z_{out}} = \frac{\mathbf{P_{in}}}{\boldsymbol{\rho g}} + \frac{\mathbf{V_{in}^2}}{\mathbf{2g}} + \mathbf{z_{in}} + \frac{\boldsymbol{loss}}{\boldsymbol{g}} - \frac{\boldsymbol{W_s}}{\boldsymbol{g}}$$

Head developed by a pump is defined as $\mathrm{H_S} = -\frac{\mathrm{W_s}}{\mathrm{g}}$; because the work done, term $\mathrm{W_s}$, is negative for a pump, the head developed by a pump H_S is always positive.

Loss is always positive, head loss is defined as $\frac{\mathrm{loss}}{\mathrm{g}} = \mathrm{H_L}$

Therefore, the head form of the Engineering Bernoulli Equation can be written as:

$$\frac{\mathbf{P_{out}}}{\boldsymbol{\rho g}} + \frac{\mathbf{V_{out}^2}}{\mathbf{2g}} + \mathbf{z_{out}} = \frac{\mathbf{P_{in}}}{\boldsymbol{\rho g}} + \frac{\mathbf{V_{in}^2}}{\mathbf{2g}} + \mathbf{z_{in}} + \boldsymbol{H_L} - \boldsymbol{H_S}$$

The head loss in pipes is symbolized by $\mathrm{H_L}$ and can be expressed as

$$\mathbf{H_L} = \mathbf{f} \times \frac{\mathbf{L}}{\mathbf{D}} \times \frac{\mathbf{V^2}}{\mathbf{2g}}$$

where

f: friction factor

L: length of pipe (m)

D: diameter of pipe (m)

V: velocity of the flow (m/s)

Friction losses in pipes vary with laminar $(\mathrm{Re} < 2000)$ or turbulent flow $(\mathrm{Re} > 4000)$. When the pipe flow is laminar, it can be shown that $\mathrm{f} = \frac{64\mu}{\mathrm{vD}\rho}$; by recognizing that $Re = \frac{\rho \mathrm{vD}}{\mu}$**,** as Reynold number; therefore, $\mathrm{f} = \frac{64}{\mathrm{Re}}$, frictional factor is a function of the Reynold number similarly for a turbulent flow, f is a function of a Reynold number also, $\mathrm{f} = \mathrm{F}\,(\mathrm{Re})$. Another parameter that influences friction is the surface roughness relative to the pipe diameter $\frac{\varepsilon}{\mathrm{D}}$. Such that $\mathrm{f} = \mathrm{F}(\mathrm{Re}, \frac{\varepsilon}{\mathrm{D}})$ pipe friction factor is a function of pipe Reynold number and the relative roughness of pipes. Major losses due to friction, significant head loss is associated with the straight portions of pipe flows. This loss can be calculated using the Moody chart.

The friction factor is a dimensionless term in the Darcy-Weisbach equations, as shown below:

$$\boldsymbol{f_f} = \mathbf{f_D}\left(\frac{\mathbf{L}}{\mathbf{D}} \times \frac{\mathbf{V^2}}{\mathbf{2g}}\right)$$

$$\mathbf{f_f} = \mathbf{4f_F}\left(\frac{\mathbf{L}}{\mathbf{D}} \times \frac{\mathbf{V^2}}{\mathbf{2g}}\right)$$

A concise history of the Darcy-Weisbach equation has been written by Brown. Two variants of the friction factor are in common use: the Darcy friction factor $\mathbf{f_D}$; which Moody plotted, and the fanning friction f_F; which equals one quarter of the Darcy factor, as expressed below. Versions of the diagram for both friction factors have been prepared in Appendix A.

$$\mathbf{f_F = \frac{f_D}{4}}$$

The energy use in a pumping installation is determined by the flow required, the height lifted and the length and friction characteristics of the pipeline.

In this investigation, the following types of powers of the pump were determined:

- **Fluid power** of a pump is the energy per second carried in the fluid in the form of pressure and quantity. Fluid power is expressed as

$$\mathbf{Power_{Fluid} = Q \times \rho \times H_S \times g}$$

- **Shaft power** of a pump is the mechanical power transmitted to it by the shaft. Shaft power is expressed as

$$\mathbf{Power_{Shaft} = \frac{Power_{Fluid}}{Efficiency_{Pump}}}$$

- **Electrical power** of a pump is the amount of energy supplied to the pump unit by the motor. Electrical power is expressed as

$$\mathbf{Power_{Electrical} = \frac{Power_{Shaft}}{Efficiency_{Motor}}}$$

The AMD experiment was carried out for 180 minutes using the scaled-up pilot plant (1000 L) newly implemented. This pilot plant is equipped with devices which require energy for them to do work, among which an agitator and a big and small centrifugal pump. The agitator was used for a certain period of time before carbonation (cycle 2 from the experimental procedure). The small centrifugal pump (1.5 kW) was only used to transfer the treated water from a tank to the storage unit. The big centrifugal pump (15 kW) was used throughout the experiment; that is why, in this report, the conservation of energy calculation was only done for the big centrifugal pump.

Table 6.6 Parameters used in energy balance calculation

Parameters	
Height	3.155 m
Inner diameter	0.05 m
Length	5.8 m
Volumetric flow rate	0.01 m^3/s
Density	1094 kg/m^3
Viscosity	0.003958 Pa.s
Suction pressure	101 325 Pa
Discharge pressure	480000 Pa

The parameters in Table 6.6 were used to determine different unknowns, as detailed below.

- Area of the pipe calculation

$$\mathrm{A} = \frac{\pi \mathrm{d}^2}{4} = \frac{\pi(0.05)^2}{4} = 1.963 \times 10^{-3} m^2$$

The area of the pipe was found to be 0.001963 m^2.

- Velocity of the fluid calculation

$$V = \frac{\mathrm{Q}}{\mathrm{A}} = \frac{0{,}01}{1.963 \times 10^{-3}} = 5.093\ \mathrm{m/s}$$

The velocity of the fluid was calculated to determine the Reynold number.

- Reynold number calculation

$$\mathrm{R}e = \frac{\rho \mathrm{v} \mathrm{D}}{\mu} = \frac{1094 \times 5.093 \times 0.05}{0.003958} = 70\ 385$$

The Reynold number was greater than 4100 which meant the flow was turbulent.

- Friction factor calculation

Material of construction of the pipe is steel structure ($\varepsilon = 2.5 \times 10^{-5}$)

$$\epsilon = \frac{\varepsilon}{d} = \frac{2.5 \times 10^{-5}}{0.05} = 5 \times 10^{-4}$$

Using the Moody chart to obtain the Darcy friction factor, the value found was 0.0158; fanning friction is equal to one quarter of the Darcy factor; therefore, the fanning friction was calculated as follows:

$$\mathrm{f_F} = \frac{\mathrm{f_D}}{4} = \frac{0.0158}{4} = 3.95 \times 10^{-3}.$$

- Head loss calculation

$$\mathrm{H_L} = \mathrm{f} \times \frac{\mathrm{L}}{\mathrm{D}} \times \frac{\mathrm{V}^2}{2\mathrm{g}} = 3.95 \times 10^{-3} \times \frac{5.8}{0.05} \times \frac{(5.093)^2}{2 \times 9.8} = 0.606\, m$$

- Head developed by the pump or head system calculation

$\mathrm{V_{in}^2}$ was assumed to be negligible, and $\mathrm{z_{in}}$ is equal to zero.

$$\frac{\mathrm{P_{out}}}{\rho \mathrm{g}} + \frac{\mathrm{V_{out}^2}}{2\mathrm{g}} + \mathrm{z_{out}} = \frac{\mathrm{P_{in}}}{\rho \mathrm{g}} + \frac{\mathrm{V_{in}^2}}{2\mathrm{g}} + \mathrm{z_{in}} + H_L - H_S$$

$$H_S = \frac{\mathrm{P_{out}} - \mathrm{P_{in}}}{\rho \mathrm{g}} + \frac{\mathrm{V_{out}^2} - \mathrm{V_{in}^2}}{2\mathrm{g}} + (\mathrm{z_{out}} - \mathrm{z_{in}}) + H_L$$

$$\mathrm{H_S} = \frac{480000 - 101325}{1094 \times 9.8} + \frac{(5.093)^2 - (0)^2}{2 \times 9.8} + (3.155 - 0) + 0.606 = 40.402\ \mathrm{m}$$

- Fluid power calculation

$$\mathrm{Power_{Fluid}} = \mathrm{Q} \times \rho \times \mathrm{H_S} \times \mathrm{g} = 0.01 \times 1094 \times 40.402 \times 9.8 = 4\ 331..579\ \mathrm{w} = 4.3\ \mathrm{kw}$$

The energy imparted by the pump to the fluid in the treatment of AMD with FA was found to be 4.3 kW at a flow rate of 0.01 m^3/s.

- Shaft power calculation

The shaft power, at a flow rate of 0.01 m^3/s resulting in a pump efficiency of 29%, is

$$\text{Power}_{\text{Shaft}} = \frac{\text{Power}_{\text{Fluid}}}{\text{Efficiency}_{\text{Pump}}} = \frac{4\,331.579}{0.29} = 14\,936.48\ \text{w} = 14.9\ \text{kw}$$

The amount of energy released by the shaft was found to be 14.9 kW; however, the energy empower to the flow of the fluid is 4.3 kW. Most of the energy released by the pump in the treatment of AMD with FA using a jet loop reactor is transformed. The energy lost can be the reason for the increase in the temperature of the mixture during the treatment. The mechanical energy of the shaft might have been transformed into heat because the energy balance principle states that energy is conserved.

- Electrical power calculation

The efficiency of the motor is 89.2%; this figure was obtained from the pump supplier.

$$\text{Power}_{\text{Electrical}} = \frac{\text{Power}_{\text{ Shaft}}}{\text{Efficiency}_{\text{Motor}}} = \frac{14\,936.48}{0.892} = 16\,744.933\ \text{w} = 16.7\ \text{kw}$$

The scaled-up pilot plant was designed to use as little energy as possible in treating AMD and recovering water of a quality that meets the TWQR standard in South Africa. The energy balance calculation was done specifically for the big centrifugal pump; this device was used more than the small pumps and the agitator during the experiment. The energy required to treat 1000 L of AMD with 200 kg of coal FA using a jet loop reactor pilot plant at a flow rate of 0.01 m^3/s is 16.7 kW. Most of the energy input is unused and might have been transformed into heat, resulting in the rise in the temperature of the mixture. Considering the equipment that constitutes the pilot plant such as pumps, jet loop reactors, etc.; the thermal energy generated during the treatment was found to be very high. The temperature increased from 25˚C to 80˚C throughout the process.

The conservation of energy, however, differs from that of mass in that energy can be generated (or consumed) in a chemical process. A chemical reaction can evolve energy (exothermic) or consume energy (endothermic). In plant operation, an energy balance (energy audit) of the plant will show the pattern of energy usage and evolution, and suggest areas for conservation and savings. Energy is transferred either as heat or work. A system does not contain “heat”, but the transfer of heat or work to a system changes its internal energy (Sinnott, 2005).

It is simple and easy to use the relation between the pressure, velocity and elevation in a moving fluid by applying the principle of the Engineering Bernoulli Equation to determine the energy created or evolved by the pump. When the Engineering Bernoulli Equation is applied to fluid contained in a control volume fixed in space, typically the control volume has impenetrable boundaries, with the exception of one or more inlets and one or more outlets through which fluid enters and leaves the control volume. During passage of fluid through the control volume, mechanical work is irreversibly transformed by fluid friction into heat, leading to higher temperatures as was observed and energy losses if the heat is not recovered. Also, the fluid work may be performed on the fluid by a pump. This leads to shaft work, assumed by convention to be positive when performed by the fluid, and negative when performed on the fluid. Both losses and shaft work are included in the energy form of the Engineering Bernoulli Equation on the basis of unit mass of fluid flowing through (Morrison, 2005).

The energy use in a pumping installation is determined by the flow required, the height lifted, the length and friction characteristics of the pipeline, the time required to run a process and the energy generated in the chemical reaction; these variables should be considered as well when it comes to reducing the energy consumption of a process. In the jet loop system, the mechanical work of the pump is transformed into heat which can be recovered.

6.8 HEAT TRANSFER

The quality of the water recovered from AMD treatment was enhanced not only by the mixing of AMD with coal FA, lime, and aluminium hydroxide, but also by the movement or speed at which this mixture was pumped, was mixed by the jet loop, and was flowing in the pipes throughout the process. The speed of the water generated heat, and this heat was flowing during the experiment inside the pipes creating three types of mechanical heat transfer, namely conduction, convection, and radiation. All three types may occur at the same time, and it is advisable to consider the heat transfer by each type in any particular case as discussed below.

6.8.1 **Conduction**

Conduction is the transfer of heat from one part of a body to another part of the same body, or from one body to another in physical contact with it, without appreciable displacement of the particles of the body (Knudsen, 1998). In this investigation, the fluid was mixed by jet looping and pumped, and it flowed at a very high pressure and velocity. The speed at which the fluid was flowing inside the pipe generated heat. This heat was transferred by conduction from the inner to the outer body of the pipe, as shown in Figure 6.11 below.

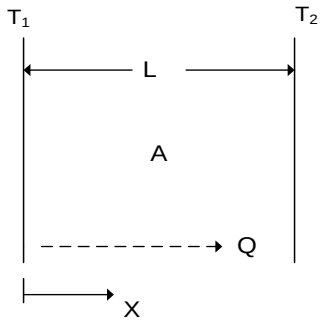

Figure 6.11: Heat transfer by conduction block diagram

The direction of heat flow is designated as x, since heat flows from a higher to a lower temperature region; it follows that T_1 (℃) is greater than T_2(℃); $\frac{dT}{dX}$ is the temperature gradient, A (m^2) is the area through which heat flows, Q (W) is used for the rate of heat transfer and L (m) is the thickness of the pipe. These quantities are related by Fourier's law, as shown in the following equation

$$\mathbf{Q = -kA\frac{dT}{dX}}$$

A significant feature of this equation is the negative sign. This recognises that the natural direction for the flow of heat is from high temperature to low temperature, and hence down the temperature gradient. The additional

quantity that appears in this relationship is k, the thermal conductivity (w/mk) of the material through which the heat flows. This is a property of the particular heat-conduction substance and, like other properties, depends on the state of the material, which is usually specified by its temperature and its pressure (Lienhard, 2008).

6.8.2 **Convection**

Convection is the transfer of heat from one point to another within a fluid, gas or liquid, by the mixing of one portion of the fluid with another. In natural convection, the motion of the fluid is entirely the result of differences in density resulting from temperature differences; in forced convection, the motion is produced by mechanical means. When the forced velocity is relatively low, it should be realised that “free-convection” factors, such as density and temperature difference, may have an important influence (Knudsen, 1998).

The pilot plant consists of three major unit operations (pumps, agitator, and jet loop reactors) which generate heat in the course of the experiment, and heat can be transferred by convection in all three units. For example, the agitator consists of impellers which rotate to enhance the mixing of the fluid for about three hours during the experimental procedure for AMD treatment. Inside the mixer, convection occurs when a warmer area of the liquid rises to cooler areas in the liquid. Cool liquid then takes the place of the warmer areas which has risen higher. This results in a continuous circulation pattern as shown in Figure 6.12 below.

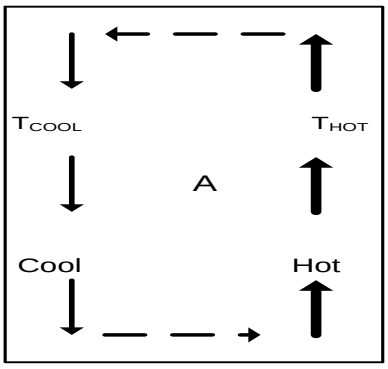

Figure 6.12: Heat transfer by convection block diagram

It is warmer at RHS and cooler at LHS of the convection block, so this warmer liquid rises up to the cooler side. The process of carrying heat away by moving fluid is known as convection. The heat transfer by convection can be expressed as:

$$\mathbf{q = h_c A dT}$$

Where,

q: heat transfer per unit time (w)

A: heat transfer area of the surface (m^2)

$\mathbf{h_c}$: Convective heat transfer coefficient of the process ($\mathrm{w/m^2k}$) or ($\mathrm{w/m^2{}^\circ C}$)

dT: temperature difference between the surface and the bulk fluid ($\mathrm{k\ or\ {}^\circ C}$)

In reality, convection is a combination of diffusion and bulk motion of molecules. Near the surface, the fluid velocity is low, and diffusion dominates. Away from the surface, bulk motion increases in influence and dominates.

6.8.3 **Radiation**

Radiation is the transfer of heat from one body to another, not in contact with it, by means of wave motion through space (Knudsen, 1998). If something radiates, then it protrudes or spreads outward from the origin. The transfer of heat by radiation involves the carrying of energy from an origin to the space surrounding it. The AMD treatment consists of several units of equipment which are carrying fluid during the experiment, and this fluid has undertaken heat transfer by conduction and convection. Heat transfer by radiation occurred between the items of equipment and between the pipes and the surroundings. During heat transfer by radiation, energy is carried by electromagnetic waves, i.e. heat transfer does not involve the movement or the interaction of matter. Thermal radiation can occur through matter or through a region of space that is void of matter. Heat transfer by radiation can be described as shown in Figure 6.13 below

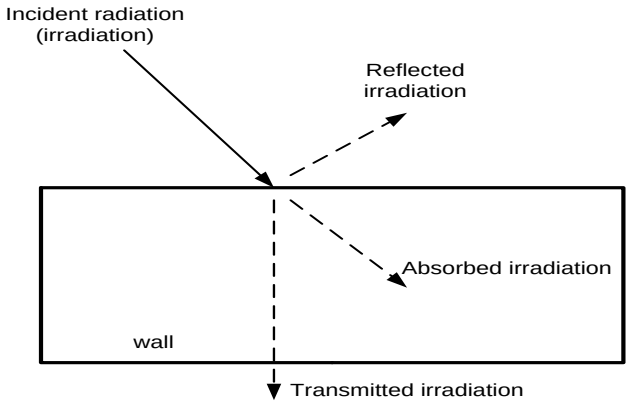

Figure 6.13: Heat transfer by radiation block diagram

All objects radiate energy in the form of electromagnetic waves. Based on experimental data by Stefan (1879) and theoretical derivation by Boltzmann (1884), the rate at which the energy is released is proportional to the Kelvin temperature (T) raised to the fourth power as shown in the following equation:

$$\textbf{Radiation rate} = \boldsymbol{\sigma} \times \mathbf{T^4}$$

The energy radiated from an object is usually a collection or range of wavelengths. This is usually referred to as an emission spectrum. As the temperature of an object increases, the wavelengths within the spectra of the emitted radiation decrease. Hotter objects tend to emit shorter wavelengths and higher frequency radiation.

The heat transferred into or out of an object by thermal radiation is a function of several components. These include its surface reflectivity, emissivity, surface area, temperature, and geometric orientation with respect to other thermally participating objects. In turn, an object's surface reflectivity and emissivity is a function of its surface conditions (roughness, finish, etc.) and composition. The heat transfer by radiation equation can be expressed as follows:

$$\mathbf{q} = \boldsymbol{\varepsilon\sigma A}(\Delta \mathbf{T^4})$$

where,

$\mathbf{q}$: is the heat transfer by radiation (W)

$\boldsymbol{\varepsilon}$: is the emissivity of the system

$\boldsymbol{\sigma}$: is the constant of Stephan-Boltzmann ($5{,}6697 \times 10^{-8} \mathrm{w/m^2k^4}$)

A: is the area involved in the heat transfer by radiation (m^2)

$\Delta \boldsymbol{T^4}$: is the temperature difference between two system to the fourth or higher power (k^4)

Having ascertained the different types of heat transfer, the maximum heat flux used to raise the temperature from 25˚C to 80˚C was calculated in two ways as follows: Heat flux was determined using the following assumptions:

- Mine water was treated using coal FA only
- Heat capacity of mine water and coal FA is 4.2 and 0.72 j/g˚C respectively
- Mole fraction of FA and mine water is 17% and 83%, respectively

Heat capacity of the mixture ($\mathrm{Cp_m}$) calculation

$\mathrm{Cp_m} = \mathrm{X_w Cp_w} + \mathrm{X_{FA} Cp_{FA}}$

where,

$\mathbf{X_w}$**:** is the molar fraction of mine water (mole)

$\mathbf{Cp_w}$**:** is the heat capacity of mine water ($\mathbf{j/g}$℃)

$\mathbf{X_{FA}}$**:** is the molar fraction of fly ash (mole)

$\mathbf{Cp_{FA}}$: is the heat capacity of fly ash ($\mathbf{j/g}$℃)

$\mathrm{Cp_m} = \mathrm{X_w Cp_w} + \mathrm{X_{FA} Cp_{FA}} = (0.83 \times 4.2) + (0.17 \times 0.72) = \mathbf{3.608\ j/g}$℃

Therefore, maximum heat flux was determined as follows:

$$q = mCp\frac{dT}{dt} = 96000 \times 3.608 \times \frac{(80-25)}{12600} = 1511.924\ W = \boldsymbol{1.5\ kW}$$

The temperature was raised from 25˚C to 80˚C by the amount of heat evolved of 1.5 kW. The mine water was treated using chemical flocculants and coal FA. The above assumptions can be true if only FA was used in the treatment of AMD. Theoretically, the heat flux that raised the temperature from 25˚C to 80˚C could be said to be equal to the difference between the energy of the shaft and that of the fluid. This statement was used to determine the heat flux that raised the temperature of the mixture, as shown below:

$$\mathrm{q} = \text{energy of shalt} - \text{energy of fluid} = 14.9 - 4.3 = 10.6\ \mathrm{kW}$$

Using the law of conservation of energy, 10.6 kW could be said to be the amount of heat flux transferred. The thermal energy evolved during the experiment was very high, considering the different equipment and their functions that constitute the pilot plant. Evaporation of liquid was observed. The liquid evaporated can also be accounted for by the mass of the liquid lost during mass balance calculations. Heat transfer caused the increased temperature of the mixture which resulted in the evaporation of the liquid. In many engineering applications, if the surface temperature is high enough, then the heat transfer from a surface may take place simultaneously by convection and radiation to the surroundings. In many technical applications, heat transfer processes occur simultaneously with mass transfer processes. The heat evolved in this jet loop system can easily be recovered.

6.9 MASS TRANSFER

Mass transfer phenomena impact upon all facets of chemical technology (Yusuf, 2007). Mass transfer is the transport of components under a chemical potential gradient. The component moves in the direction of reducing concentration gradient. The transport occurs from a region of higher concentration to lower concentration. Equilibrium is reached when the gradient is zero. The transport or migration of a constituent from a region of higher concentration to that of lower concentration is known as mass transfer (Geankoplis, 2005). Mass transfer always involves mixtures. When a system contains three or more components, as many industrial fluid streams do, the problem becomes unwieldy very quickly. The conventional engineering approach to problems of multicomponent systems is to attempt to reduce them to representative binary (i.e. two-component) systems. The AMD treatment involved the mixture of liquid, solid and gas phases; after using the mechanical equipment that constitutes the pilot plant, these phases were reduced to two phases (solid and liquid). A group of operations for separating the components of mixtures is based on the transfer of material from one homogeneous phase to another. These methods are covered by the term mass transfer operations which include techniques like gas absorption and stripping, liquid-liquid extraction, leaching, distillation, humidification, drying, crystallisation and a number of other separation techniques (Geankoplis, 2005). During the treatment of AMD, transfer of material by adsorption and precipitation was occurring. For example, the formation of ettringite precipitate was a result of calcium sulphate being brought into contact with an aluminium-containing agent. Another by-product was calcite; the carbonate fraction was precipitated by CO_2 sparging of the recovered water that had high calcium content to form calcite.

In mass transfer operations, the concentration gradient is the driving force when other driving forces (temperature, pressure gradients, etc.) are kept constant. The actual driving force for mass transfer to occur is a gradient of chemical potential (between two points), which is a function of all external forces. Concentration gradients are generally expressed in terms of mass concentration of component, molar concentration of component and mass or mole fraction of species (Geankoplis, 2005) and can be expressed as $\mathbf{C_A}$.

Mass transfer operations depend on molecules diffusing from one distinct phase to another, and are based upon differences in the physico-chemical properties of molecules, such as vapour pressure or solubility. For interphase mass transfer there is a concentration gradient between bulk and interface; however, under steady state, at interface equilibrium is assumed (Geankoplis, 2005). Just as momentum and energy (heat) transfers have two mechanisms for transport (molecular and convective), so does mass transfer. However, there are convective fluxes in mass transfer, even on a molecular level. The reason for this is that in mass transfer, whenever there is a driving force, there is always a net movement of the mass of a particular species which results in bulk motion of molecules. Of course, there can also be convective mass transport due to macroscopic fluid motion. The mass (or molar) flux of a given species is a vector quantity denoting the amount of the particular species, in either mass or molar units, that passes per given increment of time through a unit area normal to the vector.

The flux of species defined with reference to fixed spatial coordinates, N_A is

$$\mathbf{N_A} = \mathbf{C_A} \times \mathbf{V_A}$$

where,

$\mathbf{N_A}$ *or* $\boldsymbol{J_A}$**:** Flux of diffusion relative to the molar average velocity mole.$S^{-1}\mathrm{m}^{-2}$

$\mathbf{C_A}$**:** Concentration of component A mole.m^{-3}

$\mathbf{V_A}$**:** Velocity of component A m.S^{-1}

An empirical relation for the diffusional molar flux, first postulated by Fick and, accordingly, often referred to as Fick's first law, defines the diffusion of component A in an isothermal, isobaric system. For diffusion in only the Z direction, the Fick's rate equation is

$$\mathbf{J_A} = -\mathbf{D_{AB}}\frac{\mathbf{dC_A}}{\mathbf{dZ}}$$

Where,

$\mathbf{D_{AB}}$**:** is diffusivity or diffusion coefficient for component A diffusing through component B (m^2/s)

$\frac{\mathbf{dC_A}}{\mathbf{dZ}}$: is the concentration gradient in the $\mathrm{Z}-$ direction

Table 6.7: Analysed results for Lancaster mine water and mass transfer

Parameters		Raw mine water (mg/L)	Product water (mg/L)	Mass transfer	
				mg/L	mg/1000 L
Major elements	pH	3.12 +- 0.32	9.98+-0.51		
	EC(uS/cm)	6720 +- 7.5	4450+-140		
	Sulphate	5680.33	87.27	5593.06	5593060
	Al	1862.51	13.37	1849.14	1849140
	Ca	1694.55	242.77	1451.77	1451770
	Fe	1377.74	0.54	1377.2	1377200
	Mg	765.62	0.05	765.57	765570
	Na	463.35	86.46	376.88	376880
	Mn	224.44	0.05	224.39	224390
	K	51.27	BDL	51.27	51270
	Si	482.22	16.60	465.61	465610
Minor elements	Zn	154.59	BDL	154.59	154590
	Ni	79.62	BDL	79.62	79620
	Co	30.55	BDL	30.55	30550
	Cu	23.74	BDL	23.74	23740
	Cr	1.03	1.27	-0.23	-230
	Pb	16.55	1.49	15.06	15060
	P	BDL	0.66	-660	-660
	Mo	BDL	0.84	-0.84	-840
	Ti	4.80	BDL	4.80	4800
	As	BDL	0.55	-0.55	-550

EC=mS/cm; pH is dimensionless; BDL= below detection limit; - means concentration increased from raw water to product water.

The process of treating AMD using coal FA and chemical flocculants was a success. Throughout the treatment, components of different concentrations were mixed together to finally recover a quality of water that met the TWQR standard.

Samples of calculation

Mass transfer= C_i - C_f

where: $\mathbf{C_i}$ and $\mathbf{C_f}$ are the initial and final concentration (mg/L) respectively.

- Sulphate

Mass transfer= C_i - C_f = 5680.33 - 87.27 = 5593.06 mg/L

- Al

Mass transfer= C_i - C_f = 1862.51 - 13.37 = 1849.14 mg/L

In many chemical engineering processes, the concentration is the main concern, as it is the basis for calculating the mass transfer efficiency (Yuan, 2014). The process of mass transfer is realised by the mass transport from interface to the bulk fluid. This phenomenon occurred during the treatment of AMD. When FA, lime, and $Al(OH)_3$ were added to AMD, this mass transfer was due to random molecular motion of solid and liquid. The insoluble solid species in the liquid, hence downward motion by diffusion, were balanced by upward bulk motion (advection) such that absolute flux was everywhere zero. Basically, the production of alkalinity is the main process in the treatment of AMD (Madzivire, 2009). Therefore, the water recovered at the end of the treatment contained fewer impurities.

CHAPTER 7: PILOT PLANT TEST

7.1 INTRODUCTION

This chapter presents and discusses the results from analysis of both the raw AMD feedstock, and the treated water recovered after the treatment of AMD with coal FA and chemical flocculants, on the scaled-up 1000 L capacity pilot plant. The status of the environmental impact assessment licence, water use licence and waste licence, with respect to the treatment of AMD using FA, is also presented. Licensing procedures associated with the use of FA in industrial applications are presented at the end of this chapter.

7.2 EXPERIMENTAL AND ANALYTICAL METHODS

This section outlines the experimental and analytical methods employed in analysis of the feedstock FA obtained from Matla coal power station, the raw AMD feedstock and the treated water recovered. The feedstock for the experiment constituted 1000 L of raw AMD, 200 kg of FA, 2.5 kg of lime and 3.6 kg of aluminium hydroxide. The 200 kg of coal FA was added while the AMD was circulating through the jet loop, and, simultaneously, the agitator was activated to ensure thorough mixing. Following AMD and FA mixing, 2.5 kg of lime was added to the AMD + FA mixture. The pH of the mixture was constantly monitored from the electronic display of the automated system for controlling and monitoring the AMD treatment process. When the pH of the solution increased to above 11 (after 150 minutes of mixing), 3.6 kg of aluminium hydroxide was added to the AMD + fly ash + lime mixture. The subsequent AMD + FA + lime + Al $(OH)_3$ mixture was circulated through the jet loop for 180 minutes and the mixture was allowed to settle before the clear solution was decanted to another tank for carbonation to correct the pH and precipitate calcite. The carbonation step was stopped when the pH was between 6 and 9, and the treated water was then recovered. At the end of the experiment, the calculated amount of the treated water recovered was 666 L (66.6% of the initial raw AMD feedstock). The mass of the sludge recovered after settling for one hour and then decanting the clear water was found to be 571.54 kg, of which 64% was the sludge moisture content, while 365.44 kg and 206.01 kg were found to be the masses of water and solids in the sludge respectively.

7.2.1 **Pore water analysis**

This analytical procedure was performed on the feedstock Matla FA, to determine the pH of the pore water extracted from the ash. The pore water was extracted using a solid: water ratio of 1:10 in which 5 grams of the FA sample was weighed and put in a sample bottle. An amount of 50 mL of ultra-pure water was added and the mixture was then thoroughly agitated for 1 hour using a mechanical shaker, and allowed to settle for 15 minutes. The pH of the supernatant was recorded at room temperature. A portable, waterproof Hanna pH meter series HI 991301N was used. pH calibration was done in accordance with the instruction manual, using buffer solutions of pH 4 and 7 before the measurements were taken.

7.2.2 **pH and electrical conductivity**

During the 1000 L trial, the pH and electrical conductivity (EC) of the raw AMD feedstock and the treated water were taken from the readings on the electronic display of the automated system for controlling and monitoring the AMD treatment process (Figure 7.5).

7.2.3 **Cation and anion analysis**

The cations present in the AMD before and after treatments were identified using inductively coupled plasma-optical emission spectroscopy (ICP-OES). The aqueous AMD samples were filtered through a 0.45 µm pore membrane to remove suspended solids and then acidified to stabilize the cations. 1000x dilution factor was used in diluting the aqueous samples prior to ICP-OES analysis where 0.01 mL of aqueous sample was diluted with 9.99 mL of 2% HNO_3. The analysis was done using a Varian 710-ES series spectrometer equipped with a CCD detector, axially-viewed plasma, a cooled cone interface, and ICP Expert II software. Ion chromatography (IC) was used in the identification and quantification of the anions present in the AMD before and after treatment. The samples were analysed using a Dionex DX-120 ion chromatograph with an Ion Pac AS14A column and AG14-4 mm guard column.

Figures 7.1 – 7.5 show the initial commissioned, working module of the 1000 L pilot plant at Blackheath, Cape Town.

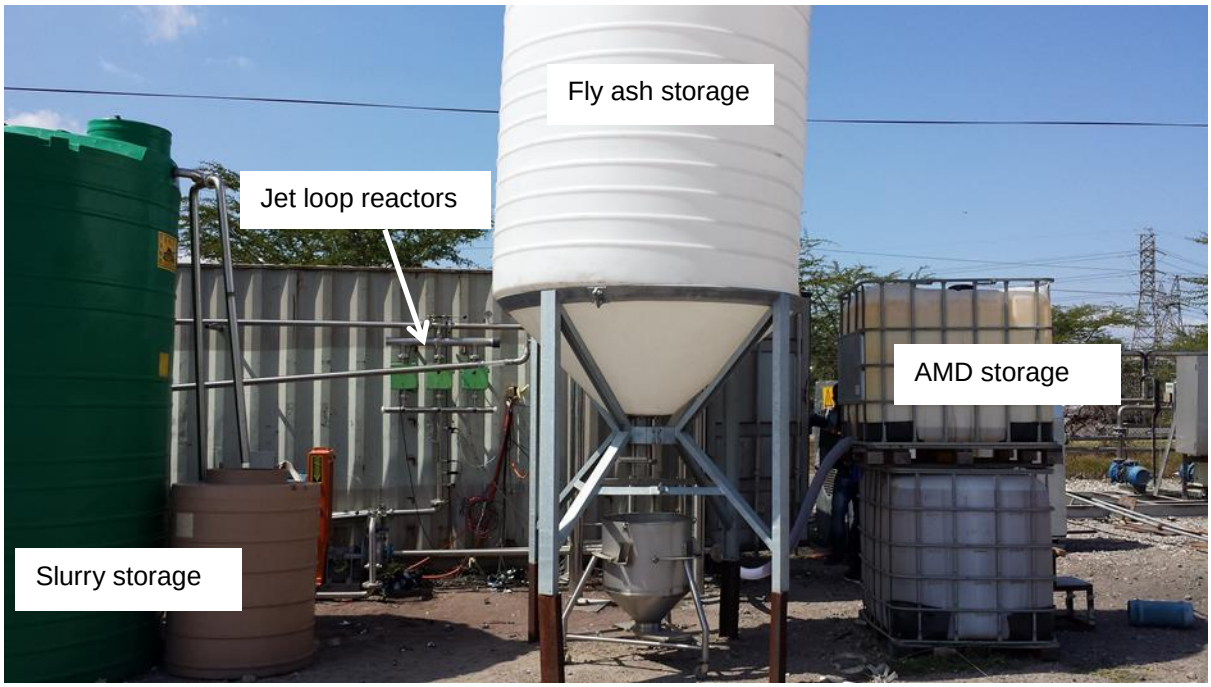

Figure 7.1: Pilot plant for AMD treatment

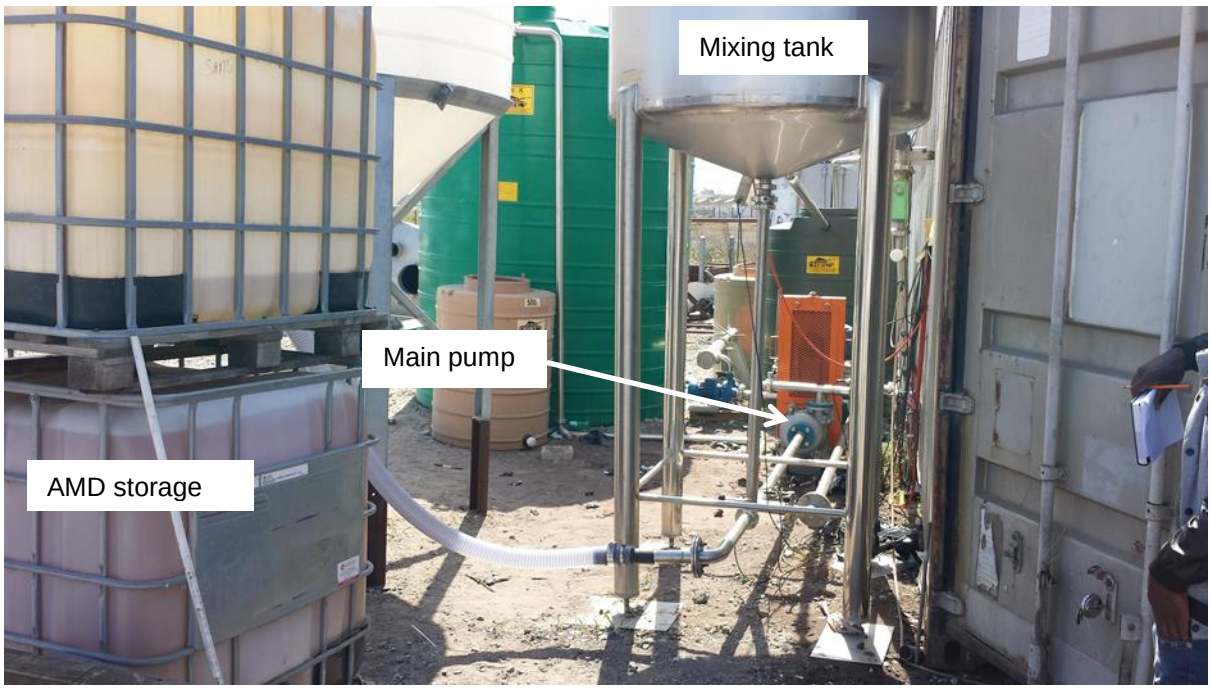

Figure 7.2: Pilot plant for AMD treatment

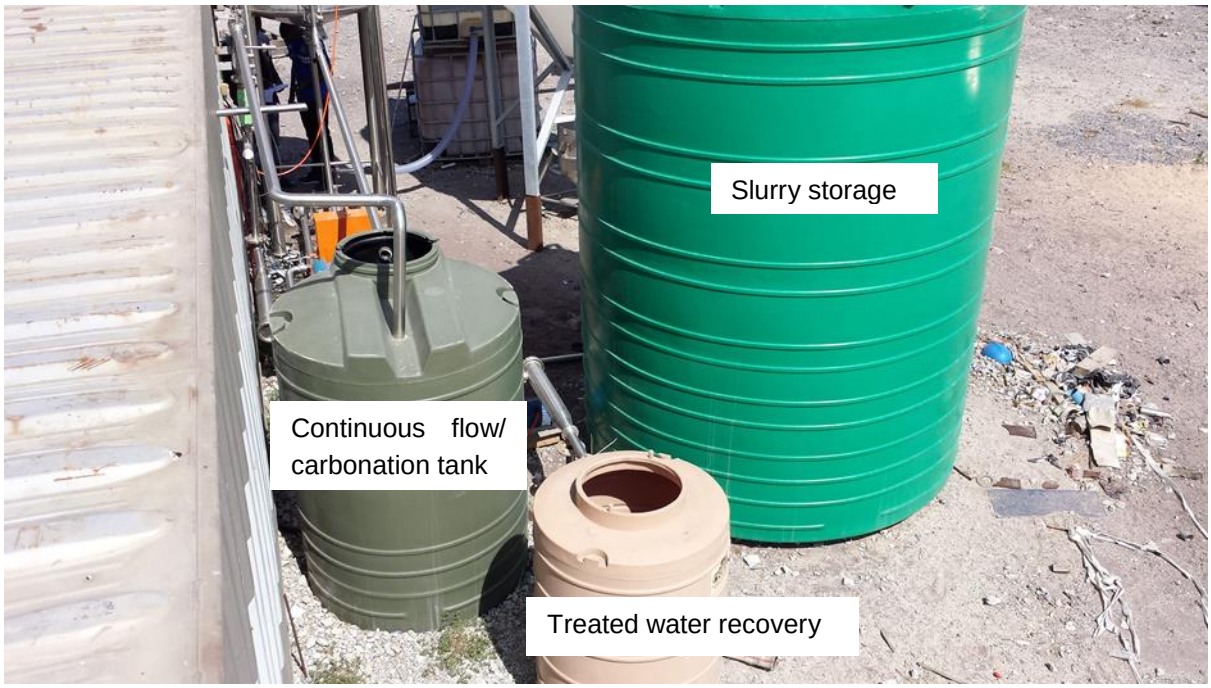

Figure 7.3: Pilot plant for AMD treatment

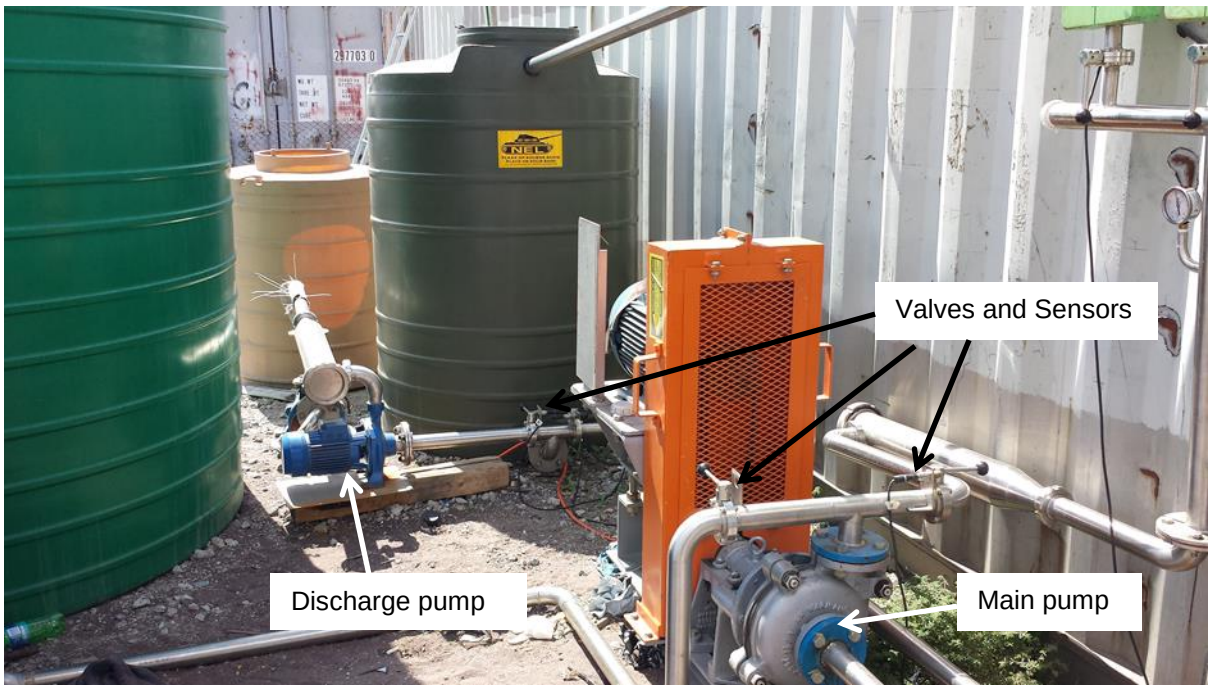

Figure 7.4: Pilot plant for AMD treatment

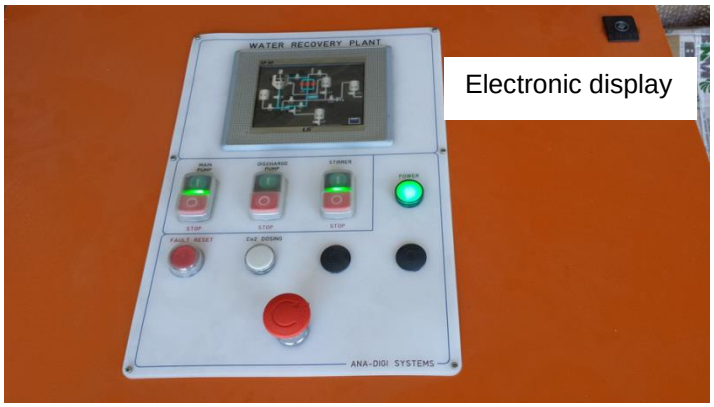

Figure 7.5: Automated system for controlling and monitoring the AMD treatment process

7.3 RESULTS AND DISCUSSION

This section presents and discusses the results obtained from the analysis of Matla FA, the raw AMD feedstock and the treated water, after neutralisation at 1000 L pilot plant scale. The composition of Lancaster dam AMD before and after treatment is shown in Table 7.1.

Table 7.1 Composition of the raw Lancaster dam AMD and the treated AMD (treatment at 1000 L capacity with 167 kg of Matla coal fly ash, 2.1 kg of lime and 3.6 kg of aluminium hydroxide, for 30–180 min)

Parameter	Raw AMD	Treated AMD						Guidelines	
		30 mins	60 mins	90 mins	120 mins	150 mins	180 mins	Potable	Irrigation
pH	2.26	10.1	9.9	9.9	9.7	10.5	8.8	6 - 9	6.5-8.4
EC (µS/cm)	6880.00	14	14	14	14	14	14		
Element (mg/L)	**Raw AMD**	**30 mins**	**60 mins**	**90 mins**	**120 mins**	**150 mins**	**180 mins**		
Sulphate	5680.33	92.77	90.99	85.01	92.28	83.37	87.27	0-200	
Al	1862.51	26.07	21.20	10.18	2.68	1.30	13.37	0-0.15	0-5
Ca	1694.55	305.13	250.56	228.48	253.02	248.77	242.77	0-32	
Fe	1377.74	1.38	0.43	0.77	0.11	0.08	0.54	0-0.1	0-5
Ta	1013.41	34.07	67.91	7.73	nd	30.66	54.60		
Mg	765.62	0.33	0.04	0.07	0.07	0.27	0.05	0-30	
Si	482.22	16.96	17.03	17.53	17.54	21.26	16.60		
Na	463.35	73.07	70.02	71.46	71.94	71.26	86.46	0-100	70.00
Mn	224.44	0.01	nd	0.01	0.06	0.07	0.05	0-0.05	0-0.2
Zn	154.59	0.57	0.08	0.18	nd	nd	nd	0-3	0-1
Ni	79.62	0.64	0.47	0.48	0.89	0.39	nd		0-0.20
K	51.27	3.49	nd	nd	nd	nd	nd	0-50	
Co	30.55	nd	nd	nd	nd	nd	nd		0-0.05
Cu	23.74	nd	nd	nd	nd	nd	nd	0-1	0-0.2
Pb	16.55	1.18	0.70	1.07	0.34	1.66	1.49	0-0.01	0-0.2
Ti	4.80	nd	nd	nd	nd	nd	nd	0-0.01	
Sr	3.43	4.90	4.08	6.33	7.52	9.04	7.16		
U	2.36	0.23	0.37	0.38	0.37	0.30	nd		
Cd	1.50	0.07	0.06	0.08	0.04	0.08	0.03	0-5	0-10
Cr	1.03	1.01	1.78	0.98	1.28	1.12	1.27	0-0.05	0-0.1
Th	0.23	0.01	nd	nd	nd	0.01	nd		
As	nd	0.36	0.48	1.41	0.11	0.93	0.55		0-0.1
Mo	nd	1.26	0.35	0.63	1.31	1.16	0.84		
Se	nd	nd	nd	nd	nd	0.80	nd	0-0.02	0-0.20
P	nd	1.39	1.16	0.36	0.46	0.01	0.66		
Li	nd	0.82	0.61	0.67	0.69	0.56	nd		0-2.5
Be	nd	0.00	nd	nd	nd	nd	nd		0-0.1

**pH of as-received (feedstock) fly ash obtained from Matla coal power station = 11.93*

The results in Table 7.1 show that the raw Lancaster AMD had a pH of 2.26 and an EC of 6880 µS/cm. The feedstock FA obtained from Matla coal power station had a pH of 11.93, as revealed by analysis of the pore water extracted from the fly ash. The concentration of elements present in the AMD before and after treatment was determined using the ICP-OES analytical technique. The concentration of sulphate, Al, Ca, Fe, Ta, Mg, Si, Na, Mn, Zn, Ni and K ions in the raw AMD was 5680.33, 1862.51, 1694.55, 1377.74, 1013.41, 765.62,

482.22, 463.35, 224.44, 154.59, 79.62 and 51.27 mg/L respectively, while the concentration of sulphate, Al, Ca, Fe, Ta, Mg, Si, Na Mn, Zn, Ni and K ions in the treated AMD, after 30 minutes of treatment, was 92.77, 26.07, 305.13, 1.38, 34.07, 0.33, 16.96, 73.07, 0.01, 0.57, 0.64 and 3.49 mg/L respectively. Figure 7.6 shows the major element removal trends over time.

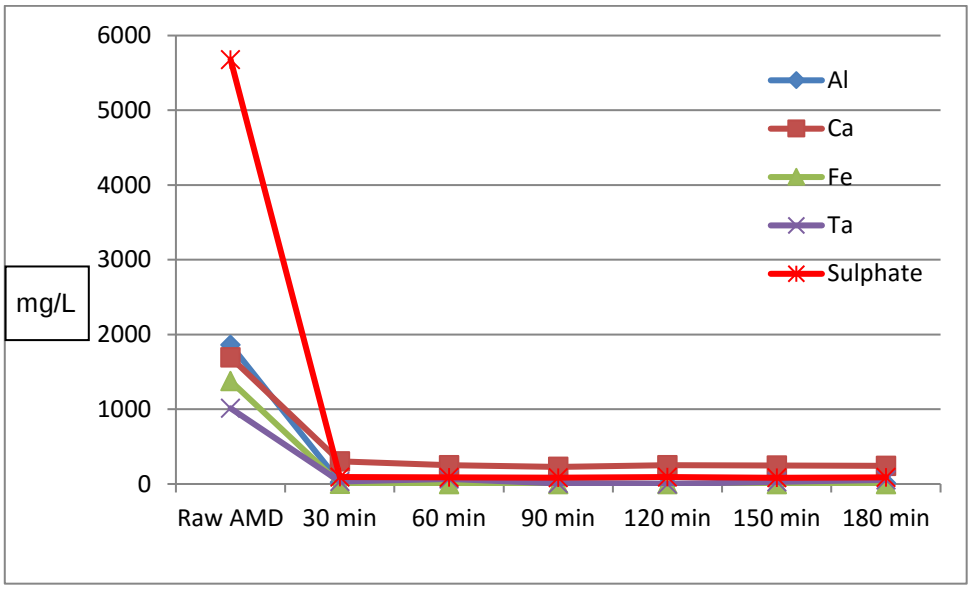

Figure 7.6 Concentration of major elements in raw AMD compared with treated AMD at various times

The concentration of sulphate, Al, Ca, Fe, and Ta was reduced to well below that of the raw AMD after 30 minutes, prior to the addition of $Al(OH)_3$. The concentration of Al, Ca, Fe, Ta, Mg, Si, Na and Mn ions in the treated AMD, after 180 minutes of treatment, was 87.27, 13.37, 242.77, 0.54, 54.60, 0.05, 16.60, 86.46 and 0.05 mg/L respectively. Zn, Ni, Co, Cu, Ti and K were not detected in the treated water after 180 minutes of treatment. It is noteworthy that after only 30 minutes of treatment, prior to the addition of $Al(OH)_3$, the concentration of most elements, including U and Th, in the treated AMD was significantly lower compared to the raw AMD.

Table 7.2. Activity of mine water before and after treatment (determined by gamma spectroscopy)

Sample	^{238}U	^{232}Th	^{40}K
	A (Bq/l)	**A (Bq/l)**	**A (Bq/l)**
AMD before treatment	33 ± 5	5 ± 3	32 ± 6
30 min treatment	6 ± 4	6 ± 5	31 ± 5
90 min treatment	10 ± 5	6 ± 3	35 ± 6
120 min treatment	11 ± 2	5 ± 4	35 ± 6
150 min treatment	5 ± 4	5 ± 4	29 ± 5
180 min treatment	4 ± 3	5 ± 2	18 ± 5

Uncertainties are at 1σ

The activity of the water after treatment was found to be significantly lower, even after only 30 minutes, in the case of ^{238}U and ^{232}Th but ^{40}K levels remained unchanged until 150 min. Hence the treatment with FA significantly reduced the activity of the treated water.

Ions such as Cu, Co, Be and Ti showed approximately 100% removal since they were only detected in the raw AMD and not in the treated AMD. Low traces of Sr (7.16 mg/L), As (0.55 mg/L) and Mo (0.84 mg/L) were detected in the treated water. These elements leached from the FA during treatment of AMD, since they were only detected in the treated AMD and not in the raw AMD. Overall, 180 minutes of treatment resulted in removal of the highest tally of elements that either had the lowest concentration (Si and Cd) or were not detected at all (Cu, Zn, Co, Ni, Se, Li, Be, K and Ti), therefore the addition of $Al(OH)_3$ assisted to further reduce the concentration of these elements.

However, the lowest concentrations of Ca, Mo, Cr, Pb, Al, Mg, Fe, Na and sulphate were recorded after 90, 60, 90, 120, 150, 60, 150, 60 and 150 minutes of treatment respectively, before $Al(OH)_3$ addition, thus $Al(OH)_3$ addition is not strictly necessary depending upon the target water quality.

The pilot plant has been reconfigured to fit with industry specifications, as shown in Figure 7.7, and is currently being prepared for transport, commissioning and operation at ESKOM, Rocherville, for further trials and demonstration at 1000 L scale.

Figure 7.7: Reconfigured 1000 L pilot plant

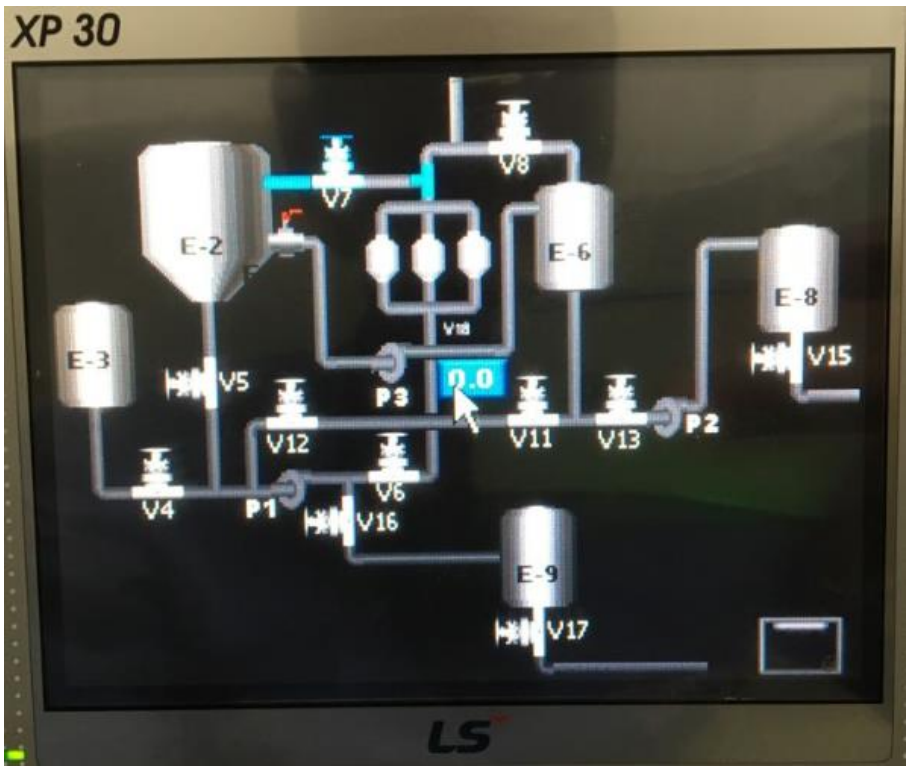

Figure 7.8: Automated digital control panel layout

7.4 ENVIRONMENTAL IMPACT ASSESSMENT LICENCE, WATER USE LICENCE AND WASTE LICENCE

This section discusses the licencing procedures associated with the use of FA in industrial applications.

7.4.1 Beneficial use of ash and exemption of waste management activities in terms of NEM:WA GN R.634

Currently, a consortium, drawn from the coal mining industry, Eskom, academia and other parties, is in the process of clarifying the legislative process to obtain an exemption of waste management activities in terms of National Environmental Management: Waste Act (Act No. 59 of 2008) (NEM:WA GN R.634). A “bulk” exclusion process is required – individual applications are costly and not beneficial to the industry. A blanket exclusion from government is unlikely. The legal application was made under the Eskom name although focus was on industry-wide applications. Eskom was willing to do this for the benefit of industry. Industry and key stakeholders have been requested to support the Eskom effort through provision of information, knowledge, support and advice. The focus was on completing Regulation 9 requirements. The main aims are to demonstrate that the use of coal FA is safe for human health and the environment in applications such as brick and block making, road construction, mine back-filling and agriculture. The intention is to demonstrate this through a motivation, which will be submitted to the Minister of the Department of Environmental Affairs (DEA), to exempt specific waste management activities from the requirements of a waste management licence, in terms of section 19 of NEM:WA, as well as the associated regulations, including a detailed analysis of

Regulation 9 requirements, the potential requirements in terms of the Water Act, and the requirements in terms of SANS 10234. The consolidated requirements dictate the scope of the information to be provided in the application. The above defines the scope of the research to be conducted to assess the environmental and health impact per application, rather than for ash specifically. Meetings were conducted with DEA to understand the process to obtain exclusions from the requirements for a waste management licence. Timelines and tasks are shown in Table 7.2 and the preliminary motivation document was presented to DEA in April, 2016. Regulation 9(1) requirements are extensive in terms of information to be provided. Currently, engagement with DEA on providing the missing information is ongoing.

Table 7.2: Gantt chart of the tasks and timelines envisaged in developing the motivation for exemption of fly ash for specified applications

LEGISLATIVE ACTIONS	2015		2016													Status
	7-Dec	14-Dec	11-Jan	18-Jan	25-Jan	1-Feb	8-Feb	15-Feb	22-Feb	29-Feb	7-Mar	14-Mar	21-Mar	28-Mar	4-Apr	
Obtain Funding																
Clarify DEA Requirements							Δ			Δ				Δ		
Appoint Environmental Consultants																
Develop detailed scope statement																
Evaluate Proposals																
Appoint Consultants																
Create Governance Structures																
Mine Backfilling Steering Committee							Δ		Δ		Δ		Δ		Δ	
Other Applications Steering Committee					Δ		Δ		Δ		Δ		Δ		Δ	
Source Regulation 9 information																
Tracker in place																
Map available information to requirements																
Close the gaps (4 weeks thereafter)																
Research																
Source information																
Initiate literature studies																
Scoping of Research Requirments																
Compile Application to DEA																N/A
Submit to DEA																N/A

The purpose of the motivation document was to:

- Provide a national approach to the management and storage of coal combustion products for the beneficial uses of brick making, road construction, soil remediation and mine backfilling;
- Ensure best practice with reference to transport, storage facilities and use;
- Provide details regarding the requirements of transport, storage facilities and use;
- Provide monitoring and measurement requirements associated with the uses; and
- Provide details for the decommissioning phase of these facilities.

Environmental legislation in South Africa was promulgated with the aim of, at the very least, minimising, and at the most, preventing environmental degradation. The Acts and Regulations directly applicable to the proposed applications are discussed below.

7.4.2 Constitution of the Republic of South Africa, 1996

The Constitution provides a foundation for environmental regulation and policy. Section 24 of the Constitution makes provision for environmental protection for the benefit of present and future generations, and the right to

an environment that is not harmful to health and well being. This can only be achieved through a reasonable legislative framework and other measures that prevent pollution and ecological degradation, promote conservation, and secure ecologically sustainable development and the sustainable use of resources.

7.4.3 **National Environmental Management: Waste Act, 2008 (Act No. 59 of 2008)**

The purpose of the Act:

- To reform the law regulating waste management in order to protect health and the environment by providing reasonable measures for the prevention of pollution and ecological degradation and for securing ecologically sustainable development;
- To provide for institutional arrangements and planning matters;
- To provide for national norms and standards for regulating the management of waste by all spheres of government;
- To provide for specific waste management measures;
- To provide for the licensing and control of waste management activities;
- To provide for the remediation of contaminated land;
- To provide for the national waste information system;
- To provide for compliance and enforcement; and
- To provide for matters connected therewith.

The scope of work is underpinned by the legal provisions as reflected in the NEM:WA. The waste management activity in question relates to the reuse and recycling of hazardous waste in excess of 1 ton per day as per Regulation 4(2) (Category B) of GN 921 of 29 November, 2013.

7.4.4 **Waste Classification and Management Regulations of 23 August 2013 (GN R.634)**

The purpose of the above regulations is to:

- Regulate the classification and management of waste in a manner which supports and implements the provisions of the Act;
- Establish a mechanism and procedure for the listing of waste management activities that do not require a Waste Management Licence;
- Prescribe requirements for the disposal of waste to landfill;
- Prescribe requirements and timeframes for the management of certain wastes; and
- Prescribe general duties of waste generators, transporters and managers.

7.4.5 **National Norms and Standards for Disposal of Waste to Landfill of 23 August 2013 (GN R.636)**

The purpose of the above regulations is to:

- Determine the requirements for the disposal of waste to landfill with reference to the required liner system for classified waste.

7.4.6 **National Norms and Standards for the Storage of Waste, 29 November 2013 (GN R.926)**

The purpose of the above regulations is to:

- Provide a uniform national approach to the management of waste storage facilities;
- Ensure best practice in the management of waste storage facilities; and
- Provide minimum standards for the design and operation of new and existing storage facilities.

7.4.7 **The National Water Act, 1998 (Act No. 36 of 1998)**

In terms of the National Water Act (NWA), (Act No. 36 of 1998), the National Government, acting through the Minister of the Department of Water and Sanitation, is the public trustee of South Africa's water resources, and must ensure that water is protected, used, developed, conserved, managed and controlled in a sustainable and equitable manner for the benefit of all persons. The Minister is responsible for ensuring that water is allocated equitably and used beneficially in the public interest, while promoting environmental values. Government, acting through the Minister, has the power to regulate the use, flow and control of all water in South Africa. Water uses are defined in Section 21 (S21) of the NWA.

7.4.8 **Occupational Health and Safety Act (Act No.85 of 1993) Regulation 1179, dated August, 1995**

FA is considered a hazardous chemical and all manufacturers and sellers of the products must provide an appropriate Material Safety Data Sheet (MSDS) to users and other potentially affected parties, as stipulated in SANS 10234 and SANS/ISO 11014.

7.5 EXEMPTION FROM WASTE MANAGEMENT ACTIVITY LICENCES FOR SPECIFIC USES OF PULVERISED COAL-FIRED BOILER ASH IN TERMS OF GN R 634

The motivation document discussed in 7.4.1, that has been submitted to DEA, presents information required for Section 9 of GN R.634 of 23 August, 2013, to acquire exemption from waste management licences. The motivation relates to activities for the downstream use of coal combustion products in soil amelioration, road construction, brick making and mine backfilling. The motivation formally invited guidance from the DEA in successfully executing the motivation process for obtaining the relevant legal exemptions. The purpose of this exemption application is to provide a motivation for DEA to exempt proposed beneficial uses of pulverised coal-fired ash from requiring a waste management licence in terms of the National Environmental Management: Waste Act (Act 59 of 2004). It was anticipated that this application would facilitate engagement of the applicant with the competent and commenting authorities. It was envisaged that this collaboration will enable the promulgation of norms and standards to regulate beneficial use of pulverised coal-fired boiler ash within South Africa.

Environmental legislation in South Africa is based on, amongst others, the "precautionary principle", a "cradle-to-grave" approach and an integrated environmental management approach. This has resulted in ponderous

regulation of all activities that may have a detrimental impact on the environment. A comparison with international legislation indicates that the use of coal combustion products is permitted, under certain controls, for beneficial uses in several countries, including Australia, USA, United Kingdom and India.

The legislation of these countries has allowed for beneficial use of coal-fired ash, and even stipulates that coal-fired ash be used to a specified percentage for certain construction operations, within certain radii of the source power station. In particular, the uses include brick making and road construction. The legislation includes control and mitigation measures to minimise impact to the environment or to human health.

South Africa classifies coal-fired ash as a Type 3 waste, which stipulates specific handling and disposal requirements. In comparison, the USA, Australia, Canada, the European Union, Israel, Japan and Russia all classify their ash as non-hazardous waste, allowing that ash be utilised within industries, under controls for minimisation of potential impact. In terms of South African legislation, the NWA (Act 36 of 1998, as amended) and the NEM: WA (Act 59 of 2004) requires that the handling or disposal of hazardous waste be licensed. Various other Acts are also relevant to hazardous waste handling or disposal, and may require additional authorisations.

Environmental legislation in South Africa manages substances identified in terms of NEM:WA and GN R.634 and SANS 10234:2008 in terms of the definitions of general or hazardous waste. Although the NEM:WA and National Waste Management Strategy (NWMS) have made some strides in bringing about a paradigm shift towards recovery and recycling of waste in how South Africa views waste, more will have to be done to change historical views on substances defined as waste, especially hazardous waste.

In terms of the NWMS, stakeholders are obligated to implement the principles of the waste management hierarchy, and therefore must develop and implement strategies to reduce the disposal of coal combustion products to landfill, and increase the recycling and beneficial reuse and recovery of these products that will reduce waste and stimulate economic opportunities at the same time.

It is evident that environmental legislation needs to evolve or be reformed to facilitate implementation of the objectives of the NWMS. Such evolution has been seen in several countries, including the USA and Australia. The Indian government, for example, enacted enabling legislation to drive greater utilisation of ash, particularly in brick making, while reducing ash to landfill in the process. Furthermore, South Africa still doesn't have a national strategy or dedicated regulations (norms and standards) for coal combustion product reuse and beneficiation. This national strategy should be driven and developed by the DEA.

Commenting authorities such as the Department of Water and Sanitation and Department of Mineral Resources have been identified for future engagement regarding beneficial use of pulverised coal-fired ash. Two steering committees have been formed to provide input and advice in terms of the proposed beneficial uses of pulverised coal ash in the South African context. These committees include academics, researchers, the South African Coal Ash Association, a state-owned entity, Eskom, with experience in technical experimentation and testing of ash, and mining houses and mining associations that may benefit from the use of ash.

Power generation in South Africa largely depends on coal. Coal can be defined as an inhomogeneous mixture of numerous types of metamorphosed plant material. The major coal-bearing strata in South Africa are associated with the Karoo Basin and occur primarily on the southern and eastern flanks of the Kaapvaal Craton. Most South African coal has been found to be of low quality with a low heat value and to contain a significant amount of inorganic (incombustible) contaminants, i.e. yielding high ash content as a result of the coal combustion process. Generally, all the inorganic material is not removed from the coal and becomes an integral part of the carbonaceous fuel fed to the boiler during the power generation process. The inorganic materials result in the ash volume for disposal.

Eskom operates 15 coal-fired power stations within Mpumalanga, the Free State and Limpopo provinces. Based on the results obtained from the distilled water leach, and analyses performed on the leach solution, Eskom pulverised coal-fired ash is assessed as a Type 3 waste (low hazard waste) requiring disposal on a waste disposal facility with a Class C barrier system, provided there are no site-specific risks that require a more conservative barrier system.

Eskom currently utilises a conveyance system and trucks to transport coal combustion product from the power generation plant to an ash disposal facility site. During the process of selection and licensing of a suitable ash disposal facility, minimisation of the site footprint is considered. Beneficial use of coal combustion products would reduce the required footprint for permanent disposal of pulverised coal-fired ash from Eskom power stations.

7.6 BENEFICIAL USE OF COAL COMBUSTION PRODUCTS

The following management measures should be implemented for the storage of coal combustion products before utilisation in any process:

- The storage area must have bund walls and a hard surface with a lining;
- The storage area must have a drainage system for collection of leachate;
- The bund wall height must be adequate to contain any spills of coal combustion product;
- Any dedicated area where pulverised coal ash is temporarily stored must be covered;
- All trucks transporting pulverised coal ash must be covered with tarpaulins;
- Leachate must be collected and managed as dirty water;
- Dust suppression methods must be employed.

Human health risks are identified as dermal contact, eye contact and inhalation. To mitigate these potential health risks, it is recommended that:

- Workers should wear personal protective clothing when handling coal combustion products;
- Dust generation should be avoided and workers should wear protective eyewear during handling of coal combustion products;
- Dust generation should be avoided and workers should wear dust masks when handling coal combustion products.

According to the American Coal Ash Association (American Coal Ash Association, 2003) utilisation of ash in road construction includes the following: stabilized base courses, flowable fill, structural fills/embankments, asphalt pavements, and grouts for pavement sub-sealing. In India, the use of coal combustion products in National Highway road construction reduced construction costs by between 10 and 20%. The findings of case studies in the USA showed negligible environmental impact but a sustainable high performance. The South African National Roads Agency (SANRAL) maintains that pulverised coal ash is a valuable bulk fill material for road construction. USA and Australia have identified the following management and mitigation measures for the effective use of coal-fired ash:

- Assess the hydrogeological characteristics of the project site;
- Mitigate leaching through engineering and design practices, and follow proper construction techniques;
- Un-encapsulated coal combustion products may be used when an assessment indicates they will not affect ground or surface water;
- Materials should be kept moist and drained to avoid erosion;
- Materials should be compacted as soon as practical after placement; and
- Where materials are not being stabilised, they should be capped with a soil cover.

However, it must be noted that studies have shown that while leaching may be possible from un-encapsulated uses, it does not occur in practice at high concentrations and has not been shown to migrate far from the site when appropriate engineering practices are followed. When coal combustion products are encapsulated, it is unlikely that there would be any leachate from the finished surface.

According to SANRAL, the following should be taken into consideration when using the material for road construction (South African National Roads Agency SOC Limited, 2013): Grain shape and particle size make the upper layers of pulverised coal-fired boiler ash difficult to compact. Freshly placed coal combustion product behaves in a similar manner to silt and, if not protected, may liquefy under wet conditions. Capping and sub-base layers tend to be relatively permeable and a layer of general fill over FA is considered desirable to add some protection. FA has a relatively low density compared with other natural fill materials and is usually compacted to an end-product specification. FA may possess self-cementing properties when compacted. Should hardening occur, settlement within the FA fill will be less than with other materials. The composition and properties of PFA from different power stations may vary significantly, and FA is not suitable for selected or sub-base layers.

7.7 BENEFICIAL USE OF COAL-FIRED ASH FOR MINE-RECLAIMED LAND

Benefits of using pulverised coal-fired ash in soil amelioration or on mine-reclaimed land include:

- Diversion of waste from land placement (ash dumps/dams);
- Substitution for, and hence conservation of, raw (virgin) lime materials normally used in soil amelioration or on mine-reclaimed land;
- Creation of a green economy that contributes to stable employment prospects;

- The development of norms and standards for downstream use of coal combustion product which will advance source conservation and the integrated waste management hierarchy, as provisioned in the relevant environmental legislation in South Africa.

Considering international trends in the beneficial use of coal combustion products in mine backfilling, the following objectives for their use in coal mine backfilling have been identified:

- Void infilling, spoil pile re-contouring or high wall reclamation in active or previously abandoned open-cut mines;
- Grouting or infilling of active or abandoned underground openings to control subsidence, ground movement or water flow;
- Amelioration and treatment of unfavourable water quality associated with surface or underground exposures, mine overburden or preparation refuse emplacements;
- Provision of base, sub-base or embankment fills for construction of mine access and haulage roads;
- Stabilisation or cementing of soil cover or overburden emplacements to prevent wind or water erosion;
- Provision of a sealing medium to control water seepage or contaminant migration, or to deal with underground fires and spontaneous combustion problems;
- Improvement of water retention and fertility of natural or artificial soils, to enhance plant cover or assist crop growth as part of mine-site rehabilitation programs; and
- Underground recovery of coal resources.

The advantages of this beneficial use include:

- Diversion of coal combustion products directly from the coal combustion units to Eskom tied collieries;
- Reduction in coal combustion product to land disposal, especially beneficial for power stations that are running out of capacity at their disposal facilities;
- Conditioning of coal combustion products at the colliery with acid mine water to activate pozzolanic properties and prepare for emplacement; (this step deals with the treatment of AMD);
- Emplacement of mine wall in mining voids with coal combustion products to prevent further AMD development;
- No liner is required as the mine wall simulates an impermeable layer due to its pozzolanic properties activated through AMD treatment;
- Subsequent phases of mine wall placement can continue until mining voids are filled. This will prevent further AMD leaching and prevent subsidence issues in these mines; and
- Mine backfilling results in beneficial use of large volumes of coal combustion product.

General mitigation and monitoring measures that must be considered for implementation of mine backfilling with coal combustion product include:

- Incorporate engineering norms and standards during the planning and implementation of the mine backfill procedures.
- Continuous monitoring would serve as a means of minimising impact on the environment (Vidya and Snigdha, 2006, as cited by Petrik & Kruger, 2011). Therefore, general management measures must

involve continuous monitoring of groundwater, surface water and wetland systems potentially affected by the backfilling activities. Biomonitoring must also be undertaken at regular intervals.

- Reporting of monitoring results, and measures implemented to mitigate any observed impacts, will be critical.
- Utilisation of FA as an ameliorant in itself serves as a very effective mitigation measure to eliminate AMD. Neutralisation of AMD rich in sulphate, iron and aluminium has proved to be feasible and practical in the South African context. The free alkalinity imparted by CaO and other ash components, and the fact that FA has a very high surface area and small particle size, make South African FA a good neutralisation agent and thus an AMD ameliorant.

The exemption application for beneficial use of pulverised coal-fired ash provides an opportunity to compile effective norms and standards for managing downstream uses of coal combustion products, in this instance, brickmaking, road construction, mine backfilling and soil amelioration. The environmental benefits of utilising this ash in the methods discussed within this application are extensive and significant. By exempting these uses from NEM:WA licensing requirements, and enforcing norms and standards, the DEA will be encouraging reduced disposal of coal combustion product within South Africa. Moreover, the spinoffs of these applications include social, economic and environmental improvements for local communities, the national economy and receiving environments.

The exemption of these beneficial uses, to be regulated by norms and standards, will enhance local small businesses facilitate the treatment and prevention of AMD in a cost-effective manner on a large scale. These beneficial uses furthermore potentially provide:

- Improved safety of mined-out areas;
- Reduced impact from coal combustion product disposal facilities;
- Business opportunities for local, small businesses;
- Treatment and prevention of water contamination (AMD);
- Rehabilitation of mining land for secondary use.

The exemption application provides the first step in assessment of these beneficial uses. In the way forward the following steps are envisaged:

1. Engagement between Eskom, the DEA and associated authorities for each beneficial use;
2. Identification of beneficial uses for immediate exemption;
3. Highlighting of additional information required for beneficial uses that cannot be exempted at this stage;
4. Compilation of norms and standards to control the implementation of beneficial use of pulverised coal-fired boiler ash;
5. Initiation of pilot studies of beneficial uses that are not yet exempted.

CHAPTER 8: CONCLUSIONS AND RECOMMENDATIONS

8.1 CONCLUSIONS

This study built on prior work and demonstrated the neutralisation of AMD in a jet loop reactor system at 1000 L scale.

Rand Uranium mine water can be classified as AMD because the pH was less than 5 and it contained an elevated concentration of Fe, Al, Mn and sulphate ions. Untreated Rand Uranium mine water was unsuitable for any purpose (drinking, irrigation or industrial) because of the low pH and the elevated concentration of Fe, Al, Mn, Pb and sulphate ions in the water. The radioactivity of Rand Uranium mine water was found to be well above the required limit for potable water. The gross alpha and beta radio activities of the water were 12 and 6 times above the potable limit respectively. The radioactivity was mainly due to U, Th, K and Ra radioisotopes. After treatment with FA, the activity of the Rand Uranium mine water was significantly reduced. Treatment of mine water therefore requires evaluation of the radioactivity of the product water.

The radioactivity of coal fly ash from Matla power station in Mpumalanga Province was within the range of the radioactivity of some ashes in the world, but was well above the average radioactivity of soil. The activity concentration index of Matla FA was 2.96 mSv. This activity concentration index was three times the upper limit of the activity concentration index for building materials, which is 0.3–1 mSv per annum. Since coal FA and the mine waters contained radioactive elements such as Th and U, the radioactivity of the coal FA, and mine water, before and after treatment, needs to be examined and radionuclides removed if present, so that recovered water does not retain high radioactivity. Both the modelling and the pilot study affirmed that the use of FA for treating mine water contaminated with radionuclides would reduce the concentration of Th and U in the recovered water to nearly undetectable limits.

In this study, the SpecE8 and Act2 programs of GWB 8.0 essential software were used to model mine water quality, and showed that major elements (or ions) in Matla mine water and Rand Uranium mine water such as Mg, sulphate, Mn, Na and K ions mainly exist in aqueous media as free ions, i.e. they are unassociated or not complexed with ligands or other ions. This increases their mobility in the ecosystem, thereby enhancing bioavailability and toxicity. On the other hand, Fe and Al were found to occur in association with hydroxyl ions. It is known that complexed species are less mobile, and thereby have reduced bioavailability and toxicity. The NORMs, such as Th and U, were found to exist in association with sulphate ions in Rand Uranium mine water. This means that these ions are less bioavailable as their mobility was reduced because of their nature.

The GWB Act2 program predicted that removal of the potentially toxic elements from Matla mine water or Rand Uranium mine water, when it was treated with FA, depended on the pH end point of the treatment process and the concentration of Ca ions added to the mine water. For instance, from the Act2 results, if Rand

Uranium mine water were to be treated with Matla coal FA, it was predicted that U could precipitate in the form of uraninite (UO_2). The formation of UO_2 was found to be pH dependent if the $\log_a Ca^{2+}$ was less than -2.7. When $\log_a Ca^{2+}$ was less than -2.7, precipitation of UO_2 would occur when the pH of mine water was increased to greater than 3. If $\log_a Ca^{2+}$ of the mine water was to be increased from -2.7 to 0, the pH at which UO_2 could start precipitating would decrease from 3 to 2 as more Ca ions were added to the mixture. At pH less than 3 and $\log_a Ca^{2+}$ less than about -0.3, U will exist as $U(SO_4)_2$ in solution. If $\log_a Ca^{2+}$ was increased to greater than about -0.3 and the pH kept below 3, U will exist as USO_4^{2+}, UOH^{3+} and $U(OH)_2^{2+}$. The Act2 program predicted that if Rand Uranium mine water was to be treated with Matla coal FA, Th could be removed as thorianite (ThO_2). The formation of ThO_2 was found to be pH dependent, when $\log_a Ca^{2+}$ was less than -2.3. When $\log_a Ca^{2+}$ was less than -2.3, ThO_2 could form if the pH of the mine water was increased to greater than 5. Increasing $\log_a Ca^{2+}$ from -2.3 to 0 would result in a decrease in the pH at which ThO_2 would precipitate, from about 5 to about 4.

The modelling results are very helpful, especially to determine the amount of coal FA or alkaline chemicals that might be required to treat a particular composition of mine water. It was demonstrated that adsorption of contaminants occurred during the formation of several mineral phases as found in the solid residues, among which were ettringite and calcite. This mineral formation occurs due to the pH and transient concentration gradient that evolves during jet loop mixing of mine water with FA which causes supersaturated conditions to arise for a limited period during which minerals precipitate that sequester the problem elements.

In designing the pilot plant, several engineering concepts, including mass and energy balance, heat and mass transfer, and P&ID were applied. The amount of materials fed into the process was found to be almost equal to the materials produced in terms of mass of solids and liquids. When an amount of 1094 kg of AMD was fed to the process, the treated water recovered was found to be 728.56 kg or 66.6% of the mine water fed; 571.54 kg was the mass of the sludge; 64% was the sludge moisture content. With regard to the sludge, 365.44 kg was found to be the mass of water and 206.01 kg was found to be the mass of solid in the sludge. The energy balance was calculated specifically for the big centrifugal pump, as this device was used the most during the experiment, compared to the small pump and the agitator. At the end of the experiment; 4.3 kW, 14.9 kW, and 16.7 kW were found to be the fluid, shaft, and electrical power consumed by the pump respectively over the test period. Heat generated was transferred simultaneously by conduction, convection, and radiation during the treatment. The temperature was raised from 25˚C to 80˚C by heat flux. The amount of heat flux transferred was determined using two assumptions: firstly, 1.5 kW was determined to be the heat flux, assuming that AMD was treated using only FA; secondly, 10.6 kW was found to be the heat flux by determining the difference between the energy of the shaft and of the fluid. Energy in the form of heat can be recovered.

In order to simplify operations, enhance decision making, reduce costs, and increase efficiency, the scaled-up pilot plant was equipped with an automation system for controlling and monitoring the process. Determination of the engineering concepts was successfully achieved because of assumptions made in some of the calculations; these included physical properties such as specific heat capacity, and the molecular weight of the complex materials that were used, in order to determine the heat flux transferred to raise the temperature of the mixture. These parameters need to be known accurately in order to have exact results.

After the design and construction of the pilot plant, the test treatment of mine water from Lancaster dam was successfully conducted in Blackheath, Cape Town, using the constructed and commissioned prototype 1000 L AMD treatment pilot plant. Analysis of samples of the treated mine water showed that the concentration of elements in the treated AMD was significantly lower compared to the raw AMD, after the test run. In fact, the results showed that even after only 30 minutes of treatment, the concentration of most major (sulphate, Al, Fe, Ca, Mg), minor (Na, Mn, Zn) and trace elements in the treated AMD had reduced significantly (between one and four orders of magnitude lower). Elements such as Cu, Co, Be and Ti showed almost complete removal from the raw AMD after treatment; however, low trace amounts of As, Mo, P and Sr appeared to have leached into the mine water from the FA during treatment. The results further showed that although 180 minutes of treatment was somewhat more efficient in terms of element removal, the addition of $Al(OH)_3$ and extended treatment time was not necessary, as high-quality water could be recovered even after 30 minutes. The costs of additional energy and chemical input should be taken into consideration when deciding on the best process conditions, as 30 minutes of treatment time with only FA and a small aliquot of lime resulted in recovery of a very high quality of water.

The treatment of AMD with FA at 1000 L pilot scale was successful, with 98.5% sulphate removal, and water quality remediated to within DWS guidelines in one simple step, using jet loop reactor equipment with few moving parts. The treated water quality was suitable for agricultural and industrial purposes or can be further treated to be made potable by correcting its pH with CO_2 sparging which removed residual Ca in the form of calcite. The residual sodium and trace elements can be easily removed from the recovered water by ion-exchange resins or zeolite adsorption and this process circumvents the need for expensive membrane processes such as reverse osmosis.

Based on the concepts and assumptions made in this investigation, it could be concluded that the 1000 L scale pilot plant process for AMD treatment is suited to AMD treatment, and many coal and mining companies that are facing the problem of how to dispose of their mine water and coal fly ash may find this system of treatment useful to protect the environment and treat polluted mine water. This treatment technology offers a cradle-to-cradle solution, since after active treatment of AMD with FA, the SR from the primary process can be placed back in the mine void from which it originated and thus stop the generation of AMD. This FA-AMD technology is the only available technology to offer a means to treat and prevent formation of AMD. Hence, it is not an end-of- pipe technology but offers the possibility to treat mine water and prevent its future formation. This process is a serious contender for low-cost mine water treatment and recovery.

In terms of the environmental impact assessment licence, water use licence and waste licence, a consortium drawn from the coal mining industry, Eskom, academia and other relevant parties, is currently in the process of clarifying the legislative process to exempt specific waste management activities from the requirements of a waste management licence in terms of NEM:WA GN R.634. The focus was on completing Regulation 9 requirements. Engagement between ESKOM, the DEA and associated authorities for each beneficial use aims to identify beneficial uses for immediate exemption and to highlight the additional information required for beneficial uses that cannot be exempted at this stage. The process will result in the compilation of norms and standards to control the implementation process for beneficial use of pulverised coal-fired boiler ash.

Moreover, the initiation of pilot studies of beneficial uses that are not yet exempted will be commenced in the near future.

8.2 RECOMMENDATIONS

The alpha and gamma spectrometry study of Rand Uranium mine water showed that the gross alpha and beta radioactivity of the mine water was 12 and 6 times more, respectively, than the required limit for potable water, and that the total U concentration was about 256 µg/L, which was well above the allowed limit for total U concentration set by the WHO in 2011, which is 30 µg/L. These results show that it is imperative that the product water always be tested for activity.

The radioactivity of Matla coal FA was found to be three times the upper limit of the activity concentration index for building materials, which is 0.3–1 mSv per annum. Since coal FA has found wide application in construction and has also been proposed for mine water remediation, it is worthwhile to pay attention to the radioactivity of any products made using fly ash for commercial applications such as cement or brick making or for agricultural applications. It is also recommended that placements of solids resulting from the process are backfilled in areas without active flows of water and that the placements are monitored for toxic elements or radionuclides in leachates that may impact on groundwater or surface waters.

Minor and trace element analysis of Matla FA showed that it contained about 34 elements. These elements included 16 (Ce, La, Nd, Y, Sc, Pr, Sm, Gd, Dy, Er, Eu, Ho, Tb, Tm and Lu) of the rare earth elements (REE), excluding promethium (Pm). The concentration of REE was found to be much higher than the normal concentration in soil (Long et al., 2010). These elements are valuable and represent an already mined and accessible source of these elements.

A significant quantity of water was found in the sludge (residue recovered). In order to reduce the quantity of water in the sludge, further studies need to be undertaken on the AMD and FA ratio, because the greater the quantity of solid that is fed to the process, the more water will remain in the sludge. A dewatering unit can be added to the pilot plant. In preparing the pilot scale design, a rheology test was carried out showed that the maximum concentration obtained after settling the slurries for an hour was 36% by weight. Thickeners will probably be required to increase the concentration to 50% by weight if needed. Further dewatering can take place using either filters or deep tank thickeners to a solids concentration of 65% to 80% by weight. Arnot and Lethabo ash could easily settle to 60% by weight. It is important that settling trials be conducted in order to determine the thickening requirements, should the process be scaled up and integrated for backfill applications. The slurries prepared will be able to be pumped easily with a centrifugal pump. Since the final pumping distances are not known yet, it is advised that a small pump be used to pump the slurry from the settling vessel to another storage place. Weir pumps kindly offered a small piston pump for this purpose in the interim for the pilot study.

The energy evolved during the process was found to be high and could be recovered. Further practical investigation needs to be done to ascertain the optimum time for using the agitator and the correct size of pump, to reduce the energy consumption of the entire process, as the pump used was oversized. Moreover, heat recovery would reduce the loss of energy by convection or evaporation.

FUTURE WORK

The reconfigured pilot plant will be transported to ESKOM Rocherville for further trials and demonstration using different sources of fly ash and different mine waters. (See the appendix for engineering drawings.)

REFERENCES

Adlem, C.J.L., 1997. Treatment of sulphate-rich effluents with the barium sulphide process, M.Sc. thesis, University of Pretoria, South Africa.

Adriano, D.C., Page, A.L., Elseewi, A.A., Chang, A.C. and Straughan, I., 1980. Utilization and disposal of fly ash and other coal residues in terrestrial ecosystems: A review. *Journal of Environmental Quality*, 9, pp. 333–344.

Allen, H.E., Hall, R.H. and Brisbin, T.D., 1980. Metal speciation: Effects on aquatic toxicity. *American Chemical Society,* **14**(4), pp. 441–443.

Arai, A. W., 2012. *Coal mining and the impact on our water.* Limpopo Venda: Venda Campaign. Materials. Coal Water.

ASTM, 1994. Standard specification for fly ash and raw or calcined natural pozzolan for use as mineral admixture in Portland cement concrete. Pennsylvania: American Society for Testing and Materials.

Ayanda, O., Fatoki, O., Adekola, F. and Ximba, B., 2012. Characterization of fly ash generated from Matla power station in Mpumalanga. Cape Town: E-journal of chemistry. Available at: http://www.hindawi.com/journals/jchem/2012/451801/abs/ Accessed on 1 June 2015.

Baykal, G. and Saygili, A., 2011. A new technique to reduce the radioactivity of fly ash utilized in the construction industry. *Fuel*, 90(4), pp. 1612–1617.

Bethke, C.M. and Yeakel, S., 2010. *The Geochemist's Workbench® Release 8.0: GWB Essentials Guide.* Colorado, USA: Hydrogeology Program University of Illinois.

Bonotto, D.M., Bueno, T.O., Tessari, B.W. and Silva, A., 2009. The natural radioactivity in water by gross alpha and beta measurements. *Radiation Measurements*, 44(1), pp. 92–101.

Bosman, D.J., 1983. Lime treatment of acid mine water and associated solids/liquid separation. *Wat. Sci. Tech*., 15, pp. 71–84.

Bosman, D.J., Clayton, J.A., Maree, J.P. and Adlem, C.J.L., 1990. Removal of sulphates from mine water with sulphide, Proceedings of the Lisbon 90 International Symposium: Acidic Mine Water in Pyritic Environments 1990, pp. 16.

Coetzee, H., Hobbs, P.J., Burgess, J.E., Thomas, A. and Keet, M., 2010. Report to the Inter ministerial committee on acid mine drainage: Mine water management in the Witwatersrand gold fields with special emphasis on acid mine drainage. South Africa: Council for Geoscience.

Cole, D.I., 1998. Uranium. In: M.G.C. Wilson and C.R. Anhausser, eds, *The mineral resources of South Africa*. 16th ed. Handbook: Council of Geosciences of South Africa, pp. 642–652.

Cravotta, C.A. and Trahan, M.K., 1999. Limestone drains to increase pH and remove dissolved metals from acidic mine drainage. *Applied Geochemistry*, 14, pp. 581–606.

Cravotta, C.A., Brady, K.B.C., Smith, M.W. and Beam, R.L., 1990. Effectiveness of the addition of alkaline materials at surface coal mines in preventing or abating acid mine drainage- Part 1, Geochemical considerations, Charleston, W.V., ed. In: Proceedings of the 1990 Mining and Reclamation Conference 1990, West Virginia University, pp. 221–223.

CSIR. 2009. *Acid mine drainage in South Africa.* Pretoria: CSIR. Natural resources and the environment. Available at: http://www.csir.co.za/nre/docs/BriefingNote2009_2_AMD_draft.pdf Accessed on 6 June 2015.

Debertin, K., 1996. The art of realizing the Becquerel. *Applied Radiation and Isotopes*, 47(4), pp. 423–431.

Del Pino, M.P. and Durham, B.D., 1999. Wastewater reuse through dual-membrane processes: opportunities for sustainable water resources. *Desalination*, 124(1-3), pp. 271–277.

Depoi, F.S., Pozebon, D. and Kalkreuth, W.D., 2008. Chemical characterization of feed coals and combustion-by-products from Brazilian power plants. *International Journal of Coal Geology*, 76(3), pp. 227–236.

Durand, J.F., 2012. The impact of gold mining on the Witwatersrand on the rivers and karst system of Gauteng and North West Province, South Africa. *Journal of African Earth Sciences*, 68(0), pp. 24–43.

DWAF, 1996. South African Water Quality Guidelines (second edition), Volume 3: Industrial Use. Pretoria, South Africa: CSIR Environmental Services, Department of Water Affairs and Forestry.

DWAF, 1996. South African Water Quality, Guidelines (second edition). Volume 1: Domestic Use. Pretoria, South Africa: CSIR Environmental Services, Department of Water Affairs and Forestry

DWAF, 1996. South African Water Quality, Guidelines (second edition). Volume 4: Agricultural Use: Irrigation. Pretoria, South Africa: CSIR, Department of Water Affairs and Forestry.

Fairbrother, A., Bigham, G., Pietary, J. and Tsuiji, J., 2010. *Coal ash: Hazard, Waste or Resource?* New Orleans: Environmental prospective. Available at:http://www.exponent.com/files/Uploads/Documents/Newsletters/Exponent_Newsletter_Coal_Ash.pdf Accessed on 24 June 2015.

Felder, R.M. and Rousseau, R.W.1986. *Elementary principles of chemical processes.* 2nd ed. New Jersey: John Wiley & Sons.

Florence, T.M., Morrison, G.M. and Stauber, J.L., 1992. Determination of trace element speciation and the role of speciation in aquatic toxicity. *Science of the Total Environment,* **125**(0), pp. 1–13.

Ford, K., 2003. *Passive treatment system for the acid mine drainage.* Colorado: National Science & Technology Center.

Geankoplis, C., 2005. *Transport processes and separation process principles.* New Delhi: Prentice-Hall of India.

Geldenhuys, A.J., Maree, J.P., De Berr, M. and Hlabela, P., 2001. An Integrated limestone/lime process for partial sulphate removal. CSIR.

Gitari, W.M., Petrik, L.F., Etchebers, O., Key, D.L., Iwuoha, E. and Okujeni, C., 2008. Utilization of fly ash for treatment of coal mines waste water: Solubility controls on major inorganic contaminants. *Fuel,* **87**, pp. 2450–2462.

Golber, D. N., 2004. *Strategic framework for National Water Resource Quality Monitoring Programmes.* Pretoria: Department of Water Affairs and Forestry.

Govier, G.W. and Aziz, K., 1972. *The Flow of Complex Mixtures in Pipes*. Van Nostrand Reinhold, New York.

Jain, C.K. and Ali, I., 2000. Arsenic: occurrence, toxicity and speciation techniques. *Water Research,* **34**(17), pp. 4304–4312.

JHB, E., 2009. *Acid mine drainage.* Johannesburg: AMD Working Group. Available: earthlife.org.za/campaigns/acid-minedrainage/.

Johnson, D.B., 2000. Biological removal of sulfurous compounds from inorganic wastewaters In: Lens P, Hulshoff Pol, L., eds. *Environmental Technologies to treat sulphur pollution: Principles and Engineering*, International Association on Water Quality, 2000, pp. 175–206.

Kentish, S.E. and Stevens, G.W., 2001. Innovations in separations technology for the recycling and re-use of liquid waste streams. *Chemical Engineering Journal*, 84(2), pp. 149–159.

Kitchener, J.A., 1957. *Ion-exchange Resins*. Great Brittan: Butler and Tanner Ltd.

Klink, M.J., 2003. The potential use of South African coal fly ash as a neutralization treatment option for acid mine drainage. MSc edn. Cape Town: University of the Western Cape.

Knudsen, J. H., 1998. *Heat and Mass Transfer.* New York: The McGraw-Hill Companies, Inc.

Kovler, K., 2012. Does the utilization of coal fly ash in concrete construction present a radiation hazard? *Construction and Building Materials,* **29**(0), pp. 158–166.

Lienhard, J. H., 2008. *A Heat transfer textbook.* Third ed*.* Massachusetts: Philogiston press.

Long, K.R., Van Gosen, B.S., Foley, N.K. and Cordier, D., 2010-last update, The Geology of Rare Earth Elements: Rare Earth Elements Are Not "Rare" [Homepage of geology.com], [Online]. Available: http://geology.com/usgs/ree-geology/ [June, 6, 2012].

Lottermoser, B.G., 2007. *Mine Wastes: Characterization, Treatment and Environmental Impacts*. 2nd ed. Springer.

Madzivire, G., 2010. *Removal of sulphates from South African mine water using coal fly ash*, MSc Thesis, University of the Western Cape.

Madzivire, G., Petrik, L.F., Gitari, W.M., Ojumu, T.V. and Balfour, G., 2010. Application of coal fly ash to circumneutral mine waters for the removal of sulphates as gypsum and ettringite. *Minerals Engineering,* **23**, pp. 252–257.

Matsuura, T., 2001. Progress in membrane science and technology for seawater desalination: a review. *Desalination*, 134(1-3), pp. 47–54.

Mattigod, S.V., Dhanpat Rai., Eary, L.E. and Ainsworth, C.C., 1990. Geochemical factors controlling the mobilization of inorganic constituents from fossil fuel combustion residues: Review of the major elements. *Journal of Environmental Quality*, 19, pp. 188–201.

McCarthy, G.J., 1988. X-ray powder diffraction for studying the mineralogy of fly ash, in Fly Ash and Coal Conversion By-Products: Characterization, Utilization and Disposal IV. Material Research Society Symposium Proceeding, pp. 75.

Morin, K.A. and Hutt, N.M., 1997. Environmental Geochemistry of Minesite Drainage: Practical, Theory and Case Studies. Vancouver, Canada: MDAG.

Morrison, F. A., 2005. *Mechanical energy balance.* Houghton: Associate Professor of chemical engineering Michigan Technological University.

Neculita, C.M., Zagury, G.J. and Brussie, B., 2007. Passive treatment of acid mine drainage in bioreactors using sulfate-reducing bacteria: critical review and research needs. *Journal of Environmental Quality*, 36, pp. 1–36.

Newman, R.T., Lindsay, R., Maphoto, K.P., Mlwilo, N.A., Mohanty, A.K., Roux, D.G., De Meijer, R.J. and Hlatshwayo, I.N., 2008. Determination of soil, sand and ore primordial radionuclide concentrations by full-spectrum analyses of high-purity germanium detector spectra. *Applied Radiation and Isotopes,* **66**(6–7), pp. 855-859.

Noor, N. M., 2010. *Introduction to engineering calculations.* Perlis: Academia.

Ochieng, G. S., 2010. vol. 5 (22) Impacts of mining on water resources in South Africa. *Scientific Research and Essays*, 3351–3357.

Papastefanou, C., 2010. Escaping radioactivity from coal-fired power plants (CPPs) due to coal burning and the associated hazards: A review. *Journal of Environmental Radioactivity,* **101**(3), pp. 191–200.

Paschoa, A.S. and Steinhäusler, F., 2010. CHAPTER 3: Terrestrial, Atmospheric, and Aquatic Natural Radioactivity. Radioactivity in the Environment. Elsevier, pp. 29–85.

Peppas, T.K., Karfopoulos, K.L., Karangelos, D.J., Rouni, P.K., Anagnostakis, M.J. and Simopoulos, S.E., 2010. Radiological and instrumental neutron activation analysis determined characteristics of size-fractionated fly ash. *Journal of Hazardous Materials*, 181(1–3), pp. 255–262.

Petrik, L.F., Hendricks, N., Ellendt, A. and Burgers, C., 2006. Toxic element removal from water using zeolite adsorbents made from solid residues. WRC Research Report No K1546/1/07, ISBN 978-1-77005-464-6. Water Research Commission, South Africa.

Pinetown, K.L., Ward, C.R. and Van Der Westhuizen, W.A., 2007. Quantitative evaluation of minerals in coal deposits in the Witbank and Highveld Coalfields, and the potential impact on acid mine drainage. *International Journal of Coal Geology*, 70(1-3), pp. 166–183.

Reznik, I.J., Gavrieli, I. and Ganor, J., 2009. Kinetics of gypsum nucleation and crystal growth from Dead Sea brine. *Geochimica et Cosmochimica Acta,* **73**(20), pp. 6218–6230.

Risica, S., 1998. Legislation on radon concentration at home and at work, *Radiat. Prot. Dosimetry*, 78, 15–21.

Roy. D.M., Luke. K., Diamond. S., 1985. Characterization of fly ash and its reactions in concrete. Mater. Res.Soc. Symp. Proc., 43, pp. 3–20.

Russeva, E., 1995. Speciation analysis-peculiarities and requirements. . *Anal. Lab.,* **4**(3), pp. 143–148.

Scheid, N., Becker, S., Ducking, M., Hampel, G., Volker Kratz, J., Watzke, P., Weis, P. and Zauner, S., 2009. Forensic investigation of brick stones using instrumental neutron activation analysis (INAA), laser ablation–inductively coupled plasma–mass spectrometry (LA–ICP–MS) and X-ray fluorescence analysis (XRF). *Applied Radiation and Isotopes*, 67(12), pp. 2128–2132.

Schoeman, J.J. and Steyn, A., 2001. Investigation into alternative water treatment technologies for the treatment of underground mine water discharged by Grootvlei Proprietary Ltd into the Blesbokspruit in South Africa. *Desalination*, 133, pp. 13–30.

Scott, R., 1995. Flooding of Central and East Rand gold mines – an investigation into controls over the inflow rate, water quality and the predicted impacts of flooded mines. Water Research Commission, Pretoria.

Senior, C.L., Zeng, T., Che, J., Ames, M.R., Sarofim, A.F., Olmez, I., Huggins, F.E., Shah, N., Huffman, G.P., Kolker, A., Mroczkowski, S., Palmer, C. and Finkelman, R., 2000. Distribution of trace elements in selected pulverized coals as a function of particle size and density. *Fuel Process Technol.* 63 215–241.

Sinnott, R.T., 2005. 4th Ed. Vol 6. Chemical Engineering Design. Coulson & Richardson's Chemical Engineering. Elsevier Butherworth-Heinnemann: Oxford.

Smit, J.P., 1999. The purification of polluted mine water. International symposium of Mine Water & Environment for the 21st Century.

Somlai, J., Jobbágy, V., Kovács, J., Tarján, S., Kovács, T., 2008. Radiological aspects of the usability of red mud as building material additive, *J. Hazard. Mater*. 150, 541–545.

Subramanian, R. S., 2014. *Engineering Bernoulli Equation.* New York: Clarkson Avalaible: http://web2.clarkson.edu/projects/subramanian/ch330/notes/Engineering%20Bernoulli%20Equation.pdf.

Surender, D., 2009. Active neutralization and amelioration of acid mine drainage with fly ash, University of the Western Cape.

Taylor, J. P., 2005. *A summary of passive and active treatment technology for acid and metalliferous drainage (AMD).* Fremantle: Earth systems.

Turhan, Ş., Parmaksiz, A., Kose, A., Yuksel, A., Arikan, I.H. and Yucel, B., 2010. Radiological characteristics of pulverized fly ashes produced in Turkish coal-burning thermal power plants. *Fuel,* **89**(12), pp. 3892–3900.

TUTORVISTA.COM, 2010. Radioactivity. Available: http://chemistry.tutorvista.com/nuclear-chemistry/radioactivity.html [October 9, 2012].

USGS, October 1997, 1997-last update, Radioactive Elements in Coal and Fly Ash: Abundance, Forms, and Environmental Significance [Homepage of United States Geological Survey], [Online]. Available:http://pubs.usgs.gov/fs/1997/fs163-97/FS-163-97.pdf [November, 2011].

Valerdi-Pérez, R., Lopez-Rodriguez, M. and Ibanez-Mengual, J.A., 2001. Characterizing an electrodialysis reversal pilot plant. *Desalination,* 137(1-3), pp. 199–206.

Vassilev, S.V. and Vassileva, C.G., 2007. A new approach for the classification of coal fly ashes based on their origin, composition, properties, and behaviour. *Fuel*, 86(10–11), pp. 1490–1512.

Viswanath R.K. Vadapalli , V., Fester , L. Petrik & P. Slatter, P., 2013. Effect of fly ash size fraction on the potential to neutralise acid mine drainage and rheological properties of sludge, *Desalination and Water Treatment*, DOI: 10.1080/19443994.2013.823355O.

Williams, G., 2011. *Acid mine drainage in Johannesburg.* Johannesburg: Greenpeace.

Winde, F., 2010. Uranium pollution of the Wonderfonteinspruit, 1997-2008 Part 1: Uranium toxicity, regional background and mining-related sources of uranium pollution. *Water SA*, 36(3), pp. 239–256.

WNA, August, 2011, 2011-last update, Naturally-Occurring Radioactive Materials (NORM) [Homepage of World Nuclear Association], [Online]. Available: http://www.world-nuclear.org/info/inf30.html[June, 2012, 2012].

WHO, 2004. Radiological aspects. Guidelines for Drinking water Quality. Third ed. Geneva: World Health Organization, pp. 197–209.

WHO, 2011. Guidelines for drinking-water quality. Third ed., incorporating first and second addenda Volume 1 - Recommendations. World Health Organization. Geneva: WHO Press.

WHO, 2011. Radiological aspects: Guidelines for Drinking water Quality. Third ed. World Health Organization, Geneva:, pp. 197-209.

Younger, P.L., Banwart, S.A. and Hedin, R.S., 2002. *Mine Water: Hydrology, Pollution, Remediation.* Dordrecht Kluwer Academic Publishers.

Yuan, K.-T. Y., 2014. *Introduction to Computational Mass Transfer with Applications to Chemical Engineering.* Tianjin: Springer.

Yusuf, C., 2007. *Mass Transfer.* Illinois: Kirk-Othmer encyclopedia of Chemical Technology.

Zhang, J. and Nancollas, G.H., 1992. Influence of calcium/sulfate molar ratio on the growth rate of calcium sulfatedihydrate at constant supersaturation. *Journal of Crystal Growth,* **118**(3–4), pp. 287–294.

Zielinski, R.A. and Budahn, J.R., 1998. Radionuclides in fly ash and bottom ash: improved characterization based on radiography and low energy gamma-ray spectrometry. *Fuel*, 77(4), pp. 259–267.

APPENDIX A

Table 8.1: Component and price list for 1000 L plant

Piping and Valves					
Valves	**Name**	**Size (mm)**	**cost R**	**Supplier**	**Contact details**
V 1	Slider	300 × 300		Imvusa	021 905 5324
v 2	Slider	300 × 300			
V 3		50.8			
V 4		72.6			
V 5 (pore size 4 mm)	Strainer valve	72.6			
V 6		72.6			
V 7		72.6			
V 8		72.6			
V 9	Sample point	12.7			
V 10 (X3)	Tap-off point	50.4			
V 11 (X6)	V Jet loop	72.6			
V 12		72.6			
V 13		50.4			
V 14		50.8			
V 15	One way	6.4 (0.25 inch)			
V 16		50.8 mm			
V 17	In-line filter	Pore size			
Pressure gauge	range				
P G 1	0 - 10 kpa				
P G 2	0 - 10 kpa				
Sub-Total			38000		
Tanks		Size (L)		Imvusa	021 905 5324
AMD Storage (X3)	PVC (vertical tank)	12000	68260.86		
FA Storage	PVC (silo tank)	5000	21200		
Mixing and clarification tank	Stainless Steel	1500	37500		
Water recovery and carbonation	PVC (vertical tank)	1500	2365.71		
Slurry storage	PVC (vertical tank)	7500	11094.2		
Recovery water storage (X3)	PVC (vertical tank)	12000	68260.86		
Bucket		200	10260		
Funnel	Stainless Steel	0.625			
	sieve pore size	8mm			
		Subtotal	218941.6		
Item				Supplier	Contact
Agitator				Imvusa	021 905 5324
A 1			7300		
A 2			7300		
CO_2 gas cylinder (x10)			889.20		
CO_2 gas pressure regulator		0 - 10 kpa	1500.00		

		Subtotal	16989.20		

Pumps				WEIR MINERALS AFRICA	0119292600
P 1			donated		
P 2			67531		
Concrete mixer	5.5HP 400 lt drum		20000	TurnerMorris	0215519805
Electronic Controllers	PLC equipment		185584	ANA-DIGI SYSTEMS	
		Subtotal	273115		
Drums					
Calcium Carbonate drum	PVC × 1	500 lt	1585.95	Roto Tank	0224332342
JET LOOP REACTOR		subtotal	30000	BioFuelsON	082538033
Personal Protective Equipment(PPE)	Unit price	Quantity			
Fram 4081 Boot Executive Black STC08	338.1	8	2704.8	Treadsafe CC	0317055338
Sweet-Orr 2-Piece 100% Royal(38)97	271	8	2168		
PPE DP Glove VV750N009 Hercules PVC 09	57	8	456		
PPE Respirator Valueair Mask 1001573	192	8	1536		
PPE DP Spec KILIMBLIN100 Kilimanjaro	19	8	152		
		SubTotal	7016.8		
PARTS COSTS			584658.58		

Table 8.2: Transportation costs to move the plant to Johannesburg

Transportation	**Name of company**	**Costs**	**Contact**
Pilot plant to JHB	Imvusa transport	41100	27219060429
Fly-ash	No info available		
Flights Fare	return tickets x5	12500	
Accommodation			
Self-catering apartment	per month	5000	
Total Transportation Costs		**58 600**	

Total Costs for building of the pilot plant and chemicals = R 643 258.58

Table 8.3: Estimated labour costs during recommissioning in Johannesburg

Description	**Cost (R)**
Rheologists	205, 168
Process controllers	100,000
Project manager	50,000
Mechanical engineers	150,000
Water scientist	100,000
Chemical engineers	100,000
Total labour cost	**705,168**

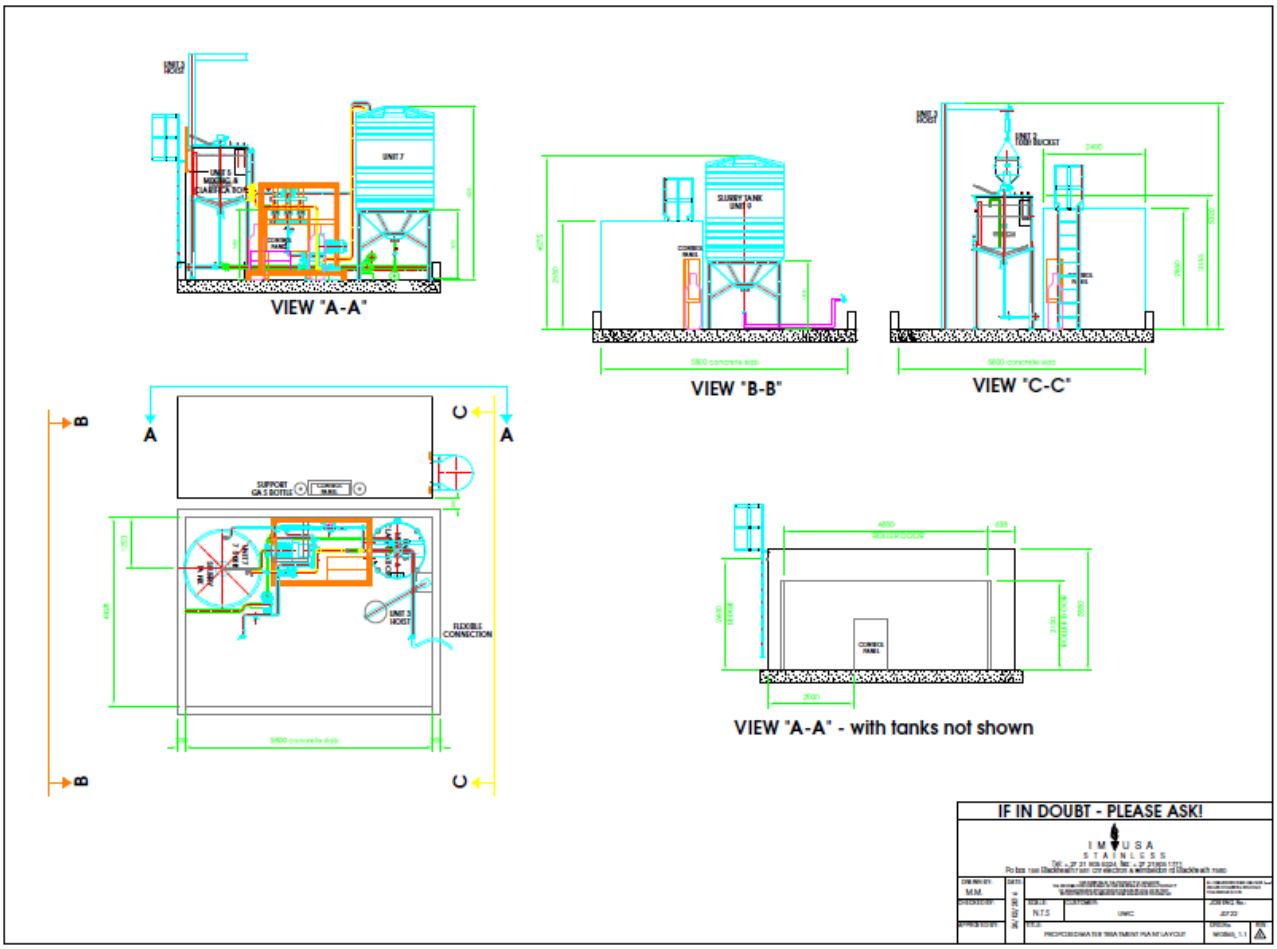

Figure 8.1: The layout of the Eskomised pilot plant

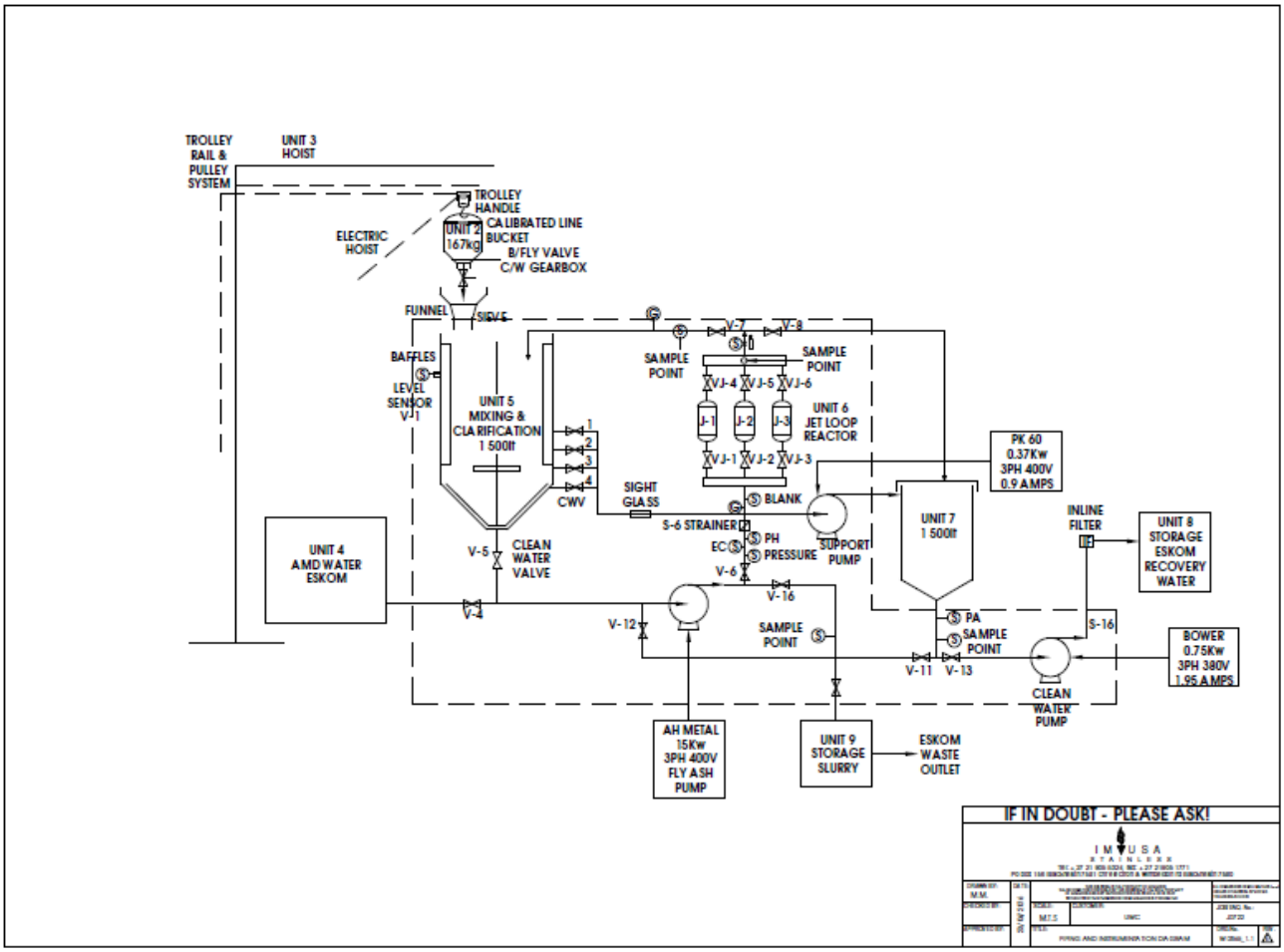

Figure 8.2 Block flow diagram of the reconfigured pilot plant

8.3 MATERIAL BALANCE

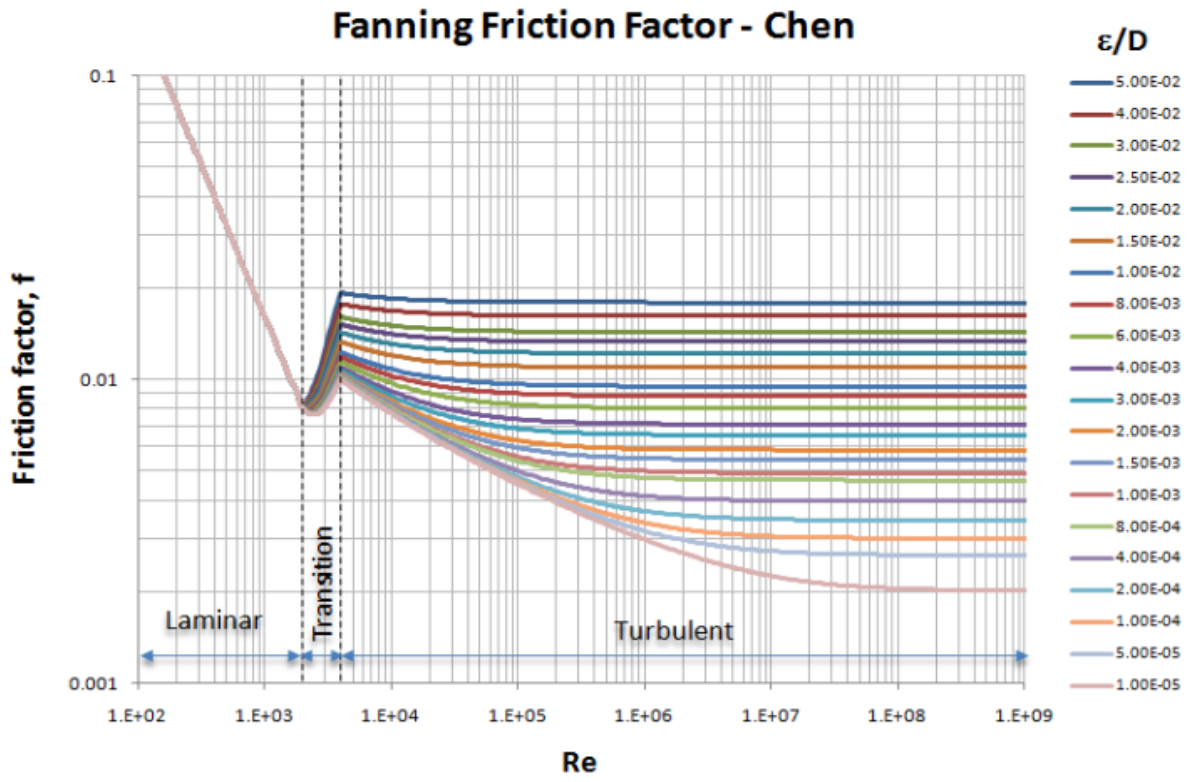

Figure 8.3: Fanning friction factor

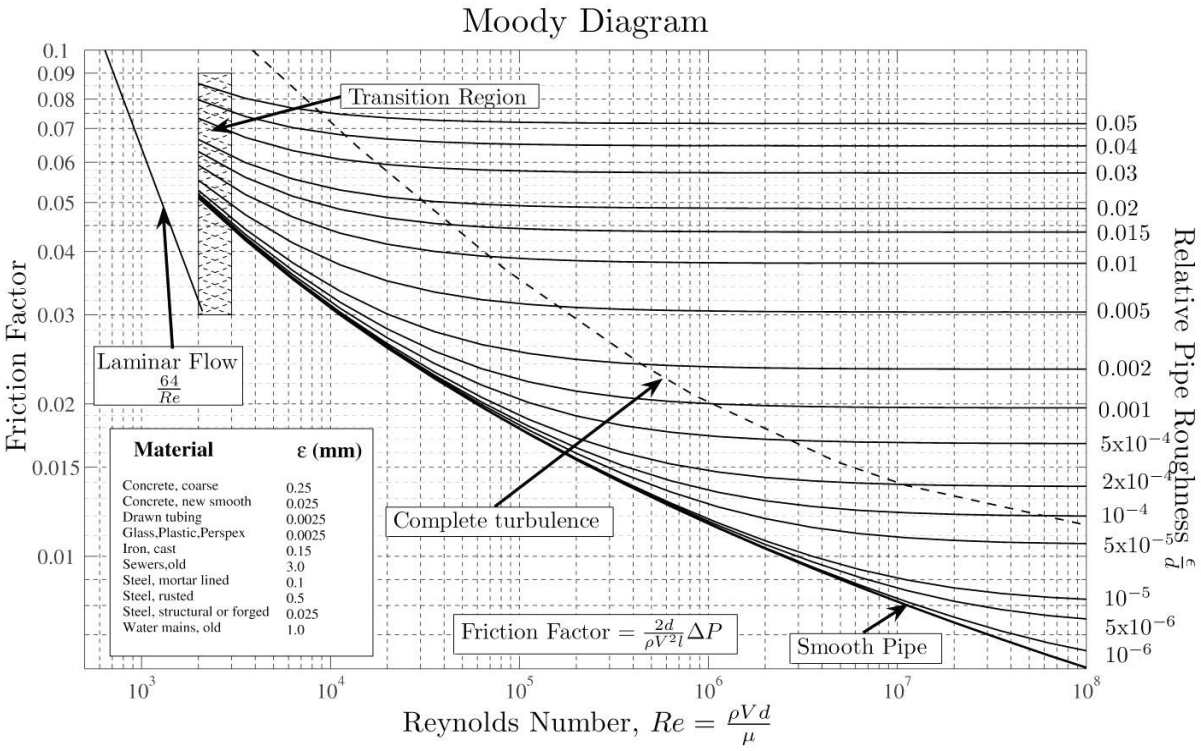

Figure 8.4: Moody diagram